nature portfolio

https://doi.org/10.1038/s41586-021-03335-3

Supplementary information

Initial Upper Palaeolithic humans in Europe had recent Neanderthal ancestry

In the format provided by the authors and unedited

Supplementary Information

Contents:

Supplementary Information 1

Bacho Kiro Cave and human remains

Bacho Kiro Cave is located on the northern slope of the Balkan Mountains and 5 km away from the city of Dryanovo in Bulgaria. First excavated in 1938 by D. Garrod[1] and later in 1970s by a team led by J. Kozłowski[2], Bacho Kiro Cave was recently re-opened and excavated by a research team led by the National Archaeological Institute with Museum in Sofia and the Department of Human Evolution at the Max Planck Institute for Evolutionary Anthropology in Leipzig[3,4]. New excavations focused on two sectors adjacent to the area excavated in 1970s, the Main Sector and the Niche 1 as detailed previously[3,4]. The archaeological sequence of the cave spans the late Middle Palaeolithic (MP) and the early Upper Palaeolithic (UP), with an archaeologically rich assemblage in Layer I[3,4] recognized as a variant of the Initial Upper Palaeolithic (IUP)[5].

Five human specimens from the new excavations were found in a direct association with an IUP assemblage in Bacho Kiro Cave (Fig. 1)[3]. A human lower molar (*F6-620*) was found in the upper part of the Layer J in the Main Sector of the cave and four bone fragments (*AA7-738, BB7-240, CC7-22*89 and *CC7-335*) were found in the Layer I in the Niche 1 sector. These specimens were directly radiocarbon dated to between 45,930 and 42,580 cal. BP[3,4] (re-calibrated with OxCal 4.4.2[6] and IntCal20[7], Tab. S1.1). Their mitochondrial genomes (mtDNA) are attributed to modern humans, suggesting that they are the oldest modern humans in Europe recovered to date[3].

Specimens from Kent's Cavern in United Kingdom[8] and Grotta del Cavallo in Italy[9] have been claimed to represent the earliest evidence of modern humans in western Europe (Fig. 1). However their dates are based on the archaeological context and the exact provenance of these specimens has been extensively debated[10,11]. Modern human remains older than 40,000 cal. BP in Europe are extremely sparse (Fig. 1)[12-14]. Moreover, genome-wide data has been retrieved for only three modern humans from Eurasia that are older than this[15-17] and each of these individuals was found outside of any archaeological context.

The archaeological sites with IUP assemblages span an area from North Africa, southwest Asia, eastern and central Europe to north China[18,19] (Fig. 1, Tab. S1.2), and have been suggested to be associated with the first wave of modern human dispersals out-of-Africa[19]. However, human remains found in the IUP context to date are relatively few[12,20-22], highlighting the relevance of Bacho Kiro Cave IUP human finds[3,4].

Two additional bone fragments were found in Layer B in the Main Sector of Bacho Kiro Cave (*F6-597*) and in the collections of the 1970s excavations in a position corresponding to the interface of Layers B/C (*BK1653*). These two specimens were directly dated to 36,320-35,600 cal. BP and 35,290-34,610 cal. BP[3,4], respectively (re-calibrated with OxCal 4.4.2[6] and IntCal20[7], Tab. S1.1). Although the lithic assemblages from these layers are sparse, they are likely to be Aurignacian[3,4]. Thus, there is ~10,000 years between the two groups of human remains found in the Bacho Kiro Cave. Even though there are more individuals that are older than 30,000 cal. BP and from whom genome-wide data has been retrieved (Fig. 1, Tab. S1.1)[23-26], this genetic record is still quite fragmentary compared to more recent timeperiods (https://reich.hms.harvard.edu/downloadable-genotypes-present-day-and-ancient-dna-data-compiled-published-papers/).

References SI1:

1 Garrod, D. A., Howe, B. & Gaul, J. Excavations in the cave of Bacho Kiro, north-east Bulgaria. *Bulletin of the American School of Prehistoric research* **15**, 46-76 (1939).

2 Kozłowski, J. K. & Ginter, B. Excavation in the Bacho Kiro Cave (Bulgaria): Final Report. *Pańswowe Wydawnictwo Naukowe* (1982).

3 Hublin, J.-J. et al. Initial Upper Palaeolithic Homo sapiens from Bacho Kiro Cave, Bulgaria. *Nature* **581**, 299-302, doi:10.1038/s41586-020-2259-z (2020).

4 Fewlass, H. et al. A 14 C chronology for the Middle to Upper Palaeolithic transition at Bacho Kiro Cave, Bulgaria. *Nat. Ecol. Evol.* **4**, 794-801, doi: 10.1038/s41559-020-1136-3 (2020).

5 Tsanova, T. & Borders, J. The Humanized Mineral World: Towards Social and Symbolic Evaluation of Prehistoric Technologies in South Eastern Europe. *Proceedings of the ESF workshop* Sofia 3-6 September 2003, 1-129 (2003).

6 Ramsey, C. B. Bayesian analysis of radiocarbon dates. *Radiocarbon* **51**, 337-360 (2009).

7 Reimer, P. J. *et al.* The IntCal20 Northern Hemisphere radiocarbon age calibration curve (0–55 cal kBP). *Radiocarbon* **62**, 725-757 (2020).

8 Higham, T. *et al.* The earliest evidence for anatomically modern humans in northwestern Europe. *Nature* **479**, 521-524, doi: 10.1038/nature10484 (2011).

9 Benazzi, S. *et al.* Early dispersal of modern humans in Europe and implications for Neanderthal behaviour. *Nature* **479**, 525-528, doi:10.1038/nature10617 (2011).

10 White, M. & Pettitt, P. Ancient digs and modern myths: The age and context of the Kent's Cavern 4 maxilla and the earliest Homo sapiens specimens in Europe. *European Journal of Archaeology* **15**, 392-420 (2012).

11 Zilhão, J., Banks, W. E., d'Errico, F. & Gioia, P. Analysis of site formation and assemblage integrity does not support attribution of the Uluzzian to modern humans at Grotta del Cavallo. *PLoS One* **10**, e0131181 (2015).

12 Hublin, J.-J. The modern human colonization of western Eurasia: when and where? *Quat. Sci. Rev.* **118**, 194-210, doi:10.1016/j.quascirev.2014.08.011 (2015).

13 Benazzi, S. *et al.* The makers of the Protoaurignacian and implications for Neandertal extinction. *Science* **348**, 793-796, doi:10.1126/science.aaa2773 (2015).

14 Trinkaus, E. *et al.* An early modern human from the Peştera cu Oase, Romania. *Proc. Natl. Acad. Sci. U.S.A.* **100**, 11231-11236, doi: 10.1073/pnas.2035108100 (2003).

15 Fu, Q. *et al.* Genome sequence of a 45,000-year-old modern human from western Siberia. *Nature* **514**, 445-449, doi:10.1038/nature13810 (2014).

16 Fu, Q. *et al.* An early modern human from Romania with a recent Neanderthal ancestor. *Nature* **524**, 216-219, doi:10.1038/nature14558 (2015).

17 Yang, M. A. *et al.* 40,000-Year-Old Individual from Asia Provides Insight into Early Population Structure in Eurasia. *Curr. Biol.* **27**, 3202-3208.e9, doi: 10.1016/j.cub.2017.09.030 (2017).

18 Kuhn, S. L. & Zwyns, N. Rethinking the initial Upper Paleolithic. *Quat. Int.* **347**, 29-38, doi: 10.1016/j.quaint.2014.05.040 (2014).

19 Müller, U. C. *et al.* The role of climate in the spread of modern humans into Europe. *Quat. Sci. Rev.* **30**, 273-279 (2011).

20 Kuhn, S. L. *et al.* The early upper paleolithic occupations at Üçağızlı cave (Hatay, Turkey). *Journal of human evolution* **56**, 87-113 (2009).

21 Copeland, L. & Yazbeck, C. Inventory of stone age sites in Lebanon. Part III, additions and revisions, 1967-2001. *Mélanges de l'Université Saint-Joseph* **55**, 119-325 (1997).

22 Yazbeck, C. Le Paléolithique du Liban: bilan critique. *Paléorient*, 111-126 (2004).

23 Seguin-Orlando, A. *et al.* Genomic structure in Europeans dating back at least 36,200 years. *Science* **346**, 1113-1118, doi:10.1126/science.aaa0114 (2014).

24 Fu, Q. *et al.* The genetic history of Ice Age Europe. *Nature* **534**, 200-205, doi:10.1038/nature17993 (2016).

25 Sikora, M. *et al.* Ancient genomes show social and reproductive behavior of early Upper Paleolithic foragers. *Science* **358**, 659-662, doi: 10.1126/science.aao1807 (2017).

26 Sikora, M. *et al.* The population history of northeastern Siberia since the Pleistocene. *Nature* **570**, 182-188, doi: 10.1038/s41586-019-1279-z (2019).

27 Fu, Q. *et al.* DNA analysis of an early modern human from Tianyuan Cave, China. *Proc. Natl. Acad. Sci. U.S.A.* **110**, 2223-2227, doi:10.1073/pnas.1221359110 (2013).

28 Marom, A., McCullagh, J. S., Higham, T. F., Sinitsyn, A. A. & Hedges, R. E. Single amino acid radiocarbon dating of Upper Paleolithic modern humans. *Proc. Natl. Acad. Sci. U.S.A.* **109**, 6878-6881 (2012).

29 Posth, C. *et al.* Pleistocene Mitochondrial Genomes Suggest a Single Major Dispersal of Non-Africans and a Late Glacial Population Turnover in Europe. *Curr. Biol.* **26**, 827-833, doi:10.1016/j.cub.2016.01.037 (2016).

30 Soficaru, A., Doboş, A. & Trinkaus, E. Early modern humans from the Peştera Muierii, Baia de Fier, Romania. *Proc. Natl. Acad. Sci. U.S.A.* **103**, 17196-17201 (2006).

31 Soficaru, A., Petrea, C., Doboş, A. & Trinkaus, E. The human cranium from the Peştera Cioclovina Uscată, Romania: context, age, taphonomy, morphology, and paleopathology. *Current Anthropology* **48**, 611-619 (2007).

32 Sinitsyn, A. & Hoffecker, J. Radiocarbon dating and chronology of the Early Upper Paleolithic at Kostenki. *Quaternary International* **152**, 164-174 (2006).

33 di Cesnola, A. P. L'Aurignacien et le Gravettien ancien de la grotte Paglicci au Mont Gargano. *L'anthropologie* **110**, 355-370 (2006).

34 Fewlass, H. *et al.* Direct radiocarbon dates of mid Upper Palaeolithic human remains from Dolní Věstonice II and Pavlov I, Czech Republic. *Journal of Archaeological Science: Reports* **27**, 102000 (2019).

35 Simon, U., Händel, M., Einwögerer, T. & Neugebauer-Maresch, C. The archaeological record of the Gravettian open air site Krems-Wachtberg. *Quaternary International* **351**, 5-13 (2014).

36 Richter, D., Tostevin, G. & Škrdla, P. Bohunician technology and thermoluminescence dating of the type locality of Brno-Bohunice (Czech Republic). *Journal of Human evolution* **55**, 871-885 (2008).

37 Richter, D., Tostevin, G., Škrdla, P. & Davies, W. New radiometric ages for the Early Upper Palaeolithic type locality of Brno-Bohunice (Czech Republic): comparison of OSL, IRSL, TL and 14C dating results. *Journal of Archaeological science* **36**, 708-720 (2009).

38 Nejman, L. *et al.* New chronological evidence for the Middle to Upper Palaeolithic transition in the Czech Republic and Slovakia: new optically stimulated luminescence dating results. *Archaeometry* **53**, 1044-1066 (2011).

39 Tsanova, T. Les débuts du Paléolithique supérieur dans l'Est des Balkans. *Réflexion à partir des* (2008).

40 Škrdla, P. & Nikolajev, P. Preliminary comparison of Kulychivka (lower layer) and the Moravian Bohunician. *Матеріали і дослідження з археології Прикарпаття і Волині*, 78-96 (2014).

41 Škrdla, P., Sytnyk, O. & Koropets'kyi, R. New observations concerning Kulychivka site, layer IV. *Матеріали і дослідження з археології Прикарпаття і Волині*, 15-25 (2016).

42 Gladilin, V. & Demidenko, Y. E. Upper Palaeolithic stone tool complexes from Korolevo. *Anthropologie (1962-)*, 143-178 (1989).

43 Koulakovska, L., Usik, V. & Haesaerts, P. Early paleolithic of korolevo site (Transcarpathia, Ukraine). *Quaternary International* **223**, 116-130 (2010).

44 Hoffecker, J. F. *et al.* The dating of a Middle Paleolithic blade industry in southern Russia and its relationship to the Initial Upper Paleolithic. *Journal of Paleolithic Archaeology* **2**, 381-417 (2019).

45 Kuhn, S. L. Questions of complexity and scale in explanations for cultural transitions in the Pleistocene: a case study from the early Upper Paleolithic. *Journal of Archaeological Method and Theory* **20**, 194-211 (2013).

46 Kuhn, S. L., Stiner, M. C. & Güleç, E. Initial Upper Palaeolithic in south-central Turkey and its regional context: a preliminary report. *ANTIQUITY-OXFORD* **73**, 505-517 (1999).

47 Ploux, S. & Soriano, S. Umm el Tlel, une séquence du Paléolithique supérieur en Syrie centrale. Industries lithiques et chronologie culturelle. *Paléorient*, 5-34 (2003).

48 Richter, D., Rink, W., Schwarcz, H., Julig, P. & Schroeder, H. The Middle to Upper Palaeolithic transition in the Levant and new thermoluminescence dates for a Late Mousterian assemblage from Jerf Al-Ajla Cave (Syria). *Paléorient*, 29-46 (2001).

49 Pastoors, A., Weniger, G.-C. & Kegler, J. F. The Middle-Upper Palaeolithic transition at Yabroud II (Syria). A re-evaluation of the lithic material from the Rust excavation. *Paléorient*, 47-65 (2008).

50 Leder, D. Lithic variability and techno-economy of the Initial Upper Palaeolithic in the Levant. *International Journal of Archaeology* **6**, 23-36 (2018).

51 Williams, J. & Bergman, C. The 1937–1938 and 1947–1948 Excavations of Levels XIII-VI at Ksar Akil, Lebanon. *Paléorient* **36**, 117-161 (2010).
52 Garrod, D. A. The Mugharet el-Emireh in Lower Galilee: type-station of the Emiran industry. *The Journal of the Royal Anthropological Institute of Great Britain and Ireland* **85**, 141-162 (1955).
53 Barzilai, O. & Gubenko, N. Rethinking Emireh Cave: the lithic technology perspectives. *Quaternary International* **464**, 92-105 (2018).
54 Garrod, D. A. A transitional industry from the base of the Upper Palaeolithic in Palestine and Syria. *Journal of the Anthropological Institute of Great Britain and Ireland*, 121-130 (1951).
55 Sarel, J. The middle-upper Paleolithic transition in Israel. *BAR International Series* **1229** (2004).
56 Marks, A. E. Reflections on Levantine Upper Palaeolithic studies: past and present. *More than meets the eye: Studies on Upper Palaeolithic diversity in the Near East*, 249-264 (2003).
57 Shunkov, M. V., Fedorchenko, A. Y., Kozlikin, M. B. & Derevianko, A. P. Initial Upper Palaeolithic ornaments and formal bone tools from the East Chamber of Denisova Cave in the Russian Altai. *Quaternary International* (2020).
58 Goebel, T., Derevianko, A. P. & Petrin, V. T. Dating the middle-to-upper-paleolithic transition at Kara-Bom. *Current anthropology* **34**, 452-458 (1993).
59 Slavinskiy, V. Industrii Ranneverhinepaleoliticheskii Ourovney Ovitanya Ctoyanki Ust-Karakol 1 (Early Upper Paleolithic Industry from the occupation levels at Ust-Karakol 1). *Severnaya Evrasia v Anthropologenie. ChelovekPaleolitechnologii, Geoecologia, Ethnografii i Anthropologii*, 197-214 (2007).
60 Derevianko, A. P. *et al.* Paleolithic of the Altai, Richard Liu Foundation. *European Institute of Chinese Studies Occasional Papers* **1** (2001).
61 Goebel, T. & Aksenov, M. Accelerator radiocarbon dating of the initial Upper Palaeolithic in southeast Siberia. *Antiquity* **69**, 349-357 (1995).
62 Orlova, L., Kuzmin, Y. & Lbova, L. Radiocarbon Dates of the Paleolithic and Mesolithic Sites in Transbaikal and Mongolia. *The Paleolithic Cultures of Transbaikal and Mongolia: New Facts, Methods, and Hypotheses*, 88-92 (2005).
63 Lbova, L. Chronology and paleoecology of the Early Upper Paleolithic in the Transbaikal region (Siberia). *Eurasian Prehistory* **5** (2008).

64 Kuzmin, Y. V., Lbova, L. V., Jull, A. T. & Cruz, R. J. The Middle-to-Upper-Paleolithic transition in Transbaikal, Siberia: the Khotyk site chronology and archaeology. *Current Research in the Pleistocene* **23** (2006).

65 Tashak, V. in *Arkheologiya I Kulturnaya Antropologiya Dalnego Vostoka I Tsentralnoi Azii. Vladivostok* 25-33 (2002).

66 Antonova, Y. E. & Tashak, V. Stone Industry of Podzvonkaya South-East Complex: General Characterization. *The bulletin of Irkutsk State University.«Geoarchaeology, Ethnology, and Anthropology Series»*, 3-20 (2016).

67 Derevianko, A. *et al.* Early upper paleolithic stone tool technologies of northern Mongolia: the case of Tolbor-4 and Tolbor-15. *Archaeology, Ethnology and Anthropology of Eurasia* **41**, 21-37 (2013).

68 Zwyns, N. *Laminar technology and the onset of the Upper Paleolithic in the Altai, Siberia*. (Leiden University Press Leiden, 2012).

69 Zwyns, N. *et al.* The open-air site of Tolbor 16 (Northern Mongolia): Preliminary results and perspectives. *Quaternary International* **347**, 53-65 (2014).

70 Derevianko, A., Brantingham, P. J., Olsen, J. W. & Tseveendorj, D. in *The Early Upper Paleolithic Beyond Western Europe* 207-222 (University of California Press, 2004).

71 Li, F., Kuhn, S. L., Gao, X. & Chen, F.-y. Re-examination of the dates of large blade technology in China: A comparison of Shuidonggou Locality 1 and Locality 2. *Journal of Human Evolution* **64**, 161-168 (2013).

Table S1.1 Modern human specimens older than ~30,000 years cal. BP from which genome-wide data has been generated and their respective radiocarbon dates. Archaeological sites from which these specimens originate are plotted in Fig. 1. Radiocarbon dates calibrated with IntCal20[7] and OxCal 4.4.2[6].

Specimen	Radiocarbon date ID	Raw radiocarbon date BP	Date type and publication	Calibrated date with IntCal20[6] and OxCal 4.4.2, cal. BP 95.4%	Mean date, cal. BP, IntCal20 [6]and OxCal 4.4.2
Bacho Kiro CC7-335	ETH-86772	42,450±510	Direct-UF[3,4]	45,930-44,420	45,120
Bacho Kiro BB7-240	ETH-86770	41,850±480	Direct-UF[3,4]	45,550-43,940	44,690
Ust'Ishim	OxA-25516 & 30190	41,400±950	Direct-UF[15]	45,930-42,900	44,360
Bacho Kiro CC7-2289	ETH-86771	40,600±420	Direct-UF[3,4]	44,400-42,990	43,690
Bacho Kiro AA7-738	ETH-86769	39,750±380	Direct-UF[3,4]	43,930-42,580	43,110
Oase1	GrA-22810 and OxA-11711	34,950±900	Direct-UF[14]	41,860-37,950	40,020
Tianyuan	BA-03222	34,430±510	?[27]	40,850-38,070	39,570
Kostenki14	OxA-X-2395-15	33,250±500	HYP[28]	39,380-36,670	38,050
Bacho Kiro F6-597	ETH-86773, AIX-12025	31,660±140	Direct-UF[3,4]	36,320-35,600	36,000
Goyet Q116-1	GrA-46175	30,880±170	Direct-noUF[29]	35,630-34,720	35,210
Bacho Kiro BK-1653	ETH-86768, AIX-12024	30,570±120	Direct-UF[3,4]	35,290-34,610	34,950
Sunghir 2	OxA-X-2395-6	30,100±550	Direct-HYP[25]	35,790-33,430	34,610
Sunghir 3	OxA-X-2395-7	30,000±550	Direct-HYP[25]	35,640-33,270	34,520
Sunghir 4	OxA-X-2462-52	29,820±280	Direct-HYP[25]	34,850-33,720	34,320
Muierii2	OxA-16252	29,110±190	Direct-UF[30]	34,180-33,140	33,660
Sunghir 1	OxA-X-2464-12	28,890±430	Direct-HYP[25]	34,280-32,020	33,270
Cioclovina1	OxA-15527	28,510±170	Direct-UF[31]	33,300-32,010	32,660
Kostenki12	GrA-5552	28,500±140	layer date[32]	33,210-32,070	32,650
Paglicci133	UTC-1789 and UTC-1415	28,100±400 and 29,300±600	layer date[33]	33,370-31,230	32,260
Yana RHS	Beta-271412 and Beta-230442	27,940±115	layer date[26]	32,190-31,530	31,870
Vestonice16	Aix12030	27,220±110	Direct-UF[34]	31,530-31,080	31,250
Vestonice43	Aix12032	27,070±110	Direct-UF[34]	31,280-31,030	31,150
Vestonice13	Aix12027	27,040±100	Direct-UF[34]	31,240-31,030	31,140
KremsWA3	VERA-3941	26,870±220	layer date[35]	31,360-30,430	31,020
Vestonice14	Aix12028	26,760±100	Direct-UF[34]	31,150-30,860	31,010
Vestonice15	Aix12029	26,680±70	Direct-UF[34]	31,110-30,840	30,980
Pavlov1	Aix12026	25,490±90	Direct-UF[34]	30,050-29,320	29,800

Table S1.2 Archaeological sites with layers containing Initial Upper Palaeolithic (IUP) assemblage. These sites are plotted in Fig. 1, demonstrating distribution of IUP archaeological sites in Eurasia, and modified after Kuhn and Zwyns[18].

Number on the map in Fig. 1	Archaeological site with IUP	Country	Reference
19	Brno-Bohunice	Czech Republic	[36,37]
20	Stránská Skála III	Czech Republic	[36,38]
19	Bohunice-Kejbaly I, II	Czech Republic	[36]
21	Temnata	Bulgaria	[39]
1	Bacho Kiro Cave	Bulgaria	[3,4]
22	Kulychivka	Ukraine	[40,41]
23	Korolevo 1, 2	Ukraine	[42,43]
24	Shlyakh	Russia	[44]
25	Üçagizli Cave	Turkey	[19,45]
26	Kanal Cave	Turkey	[46]
27	Um el'Tlel	Syria	[47]
28	Jerf Ajlah	Syria	[48]
29	Yabrud II	Syria	[49]
30	Antelias	Lebanon	[50]
31	Abou Halka	Lebanon	[50]
32	Ksar Akil rockshelter	Lebanon	[51]
33	Emireh Cave	Israel	[52,53]
34	El Wad	Israel	[54]
35	Raqefet	Israel	[55]
36	Boker Tachtit	Israel	[56]
37	Denisova Cave	Russia	[57]
38	Kara-Bom	Russia	[58]
39	Ust-Karakol 1	Russia	[59]
40	Kara-Tenesh	Russia	[60]
41	Makarvo IV	Russia	[61]
42	Kamenka A-C	Russia	[62,63]
43	Khotyk	Russia	[63,64]
44	Podzvonkaya	Russia	[65,66]
45	Tolbor 4	Mongolia	[67,68]
46	Tolbor 16	Mongolia	[69]
47	Tsagan-Agui	Mongolia	[70]
48	Suindonggou 1	China	[71]
49,50	Suindonggou 2, 9	China	[71]

Supplementary Information 2

Ancient DNA processing, quality controls and contamination estimates

DNA extraction and library preparation

Data generation for the seven Bacho Kiro Cave specimens (specimen IDs*: F6-620, AA7-738, BB7-240, CC7-2289, CC7-335, F6-597* and *BK1653*) was based on DNA libraries prepared previously and detailed in Online Materials and Methods of *Hublin et al.*[1]. In short, five single-stranded DNA libraries[2] were prepared for each specimen on an automated liquid handling platform (Bravo NGS workstation B, Agilent Technologies)[3] by using ten µL of DNA extract as input, tagged with two unique index sequences[4,5] and amplified into plateau using AccuPrime Pfx DNA polymerase (Life Technologies)[6]. This amounted to a total of 35 libraries for Bacho Kiro Cave specimens (Tab. S2.1).

In order to generate additional data from *Oase1*, we extracted DNA from 15 mg of bone powder of the *Oase1* mandible[7,8]. Since the specimen was previously found to be highly contaminated with microbial and present-day human DNA, the bone powder was treated with 0.5% hypochlorite solution prior to DNA extraction[4]. Four single-stranded DNA libraries were prepared from the resulting extract in the same way as described above. Two additional libraries were prepared, each using 5 µL of the two DNA extracts generated previously[8] (E1406 and E1843) (Tab. S2.1).

All Bacho Kiro Cave and *Oase1* libraries were made omitting UDG treatment to maximize the recovery of endogenous DNA and to preserve deamination signals. Fifty µL of each of the amplified libraries were purified on an automated liquid handling platform using SPRI beads[3], and their concentration was determined on a NanoDrop 1000 Spectrophotometer (NanoDrop Technologies). To assess nuclear DNA preservation, the purified libraries were pooled together with libraries from other experiments and one-cycle PCR reaction with Herculase II Fusion DNA polymerase (Agilent Technologies)[7] and IS5 and IS6 primers[2,9] was used to remove heteroduplex formations. The pools of libraries were then sequenced directly on Illumina MiSeq or HiSeq 2500 platforms in a double index configuration (2x76 cycles)[5] and base calling was done using Bustard (Illumina).

Sequencing and alignment to the nuclear genome

For all sequencing runs we trimmed the adapters and merged overlapping forward and reverse reads into single sequences using *leeHom*[10] (version: https://bioinf.eva.mpg.de/leehom/). The Burrows-Wheeler Aligner (BWA, version: 0.5.10-evan.9-1-g44db244; https://github.com/mpieva/network-aware-bwa) with the parameters adjusted for ancient DNA ("-n 0.01 –o 2 –l 16500")[11] was used to align the data from all sequencing runs to the human reference genome (GRCh37/1000 Genomes release; ftp://ftp.1000genomes.ebi.ac.uk/vol1/ftp/technical/reference/phase2_reference_assembly_sequence/). Only reads that showed perfect matches to the expected index combinations were used for all downstream analyses. PCR duplicates were removed using *bam-rmdup* (version: 0.6.3; https://github.com/mpieva/biohazard-tools) and *SAMtools* (version: 1.3.1)[12] were used to filter for fragments that were at least 35 bp long and that had a mapping quality equal or greater than 25.

Mitochondrial DNA capture and sequencing

Mitochondrial DNA (mtDNA) captures of Bacho Kiro Cave libraries and their processing are detailed in *Hublin et al.*[1]. An aliquot of each newly generated *Oase1* library was also enriched for human mtDNA using a bead-based hybridization method[13]. Enriched libraries were pooled with libraries from other experiments and sequenced on an Illumina MiSeq platform in a double index configuration (2x76 cycles)[5]. Trimming of the adapters, merging of forward and reverse reads and the alignment parameters were the same as for the nuclear DNA data detailed above, with the difference of using the revised Cambridge Reference Sequence (NC_01290) for the alignment of the mtDNA data. The reads with perfect matches to the expected index combinations were retained for downstream analyses and PCR duplicates were removed using *bam-rmdup* (version: 0.6.3; https://github.com/mpieva/biohazard-tools). We used *SAMtools* (version: 1.3.1)[12] to merge libraries originating from the same extract, and filter for fragments of at least 35 bp with a mapping quality of 25 or greater.

In solution hybridization capture of nuclear DNA

We estimated the genomic coverage in each library that could be obtained by sequencing a library to exhaustion ("nuclear DNA content") by using the number of library molecules determined by quantitative PCR (qPCR) and the fraction of sequences of at least 35 base pairs (bp) that could be mapped to the human reference genome (Tab. S2.1)[9]. We selected the libraries with estimated genomic coverage of at least 1% after restricting the analyses to the

fragments showing cytosine (C) to thymine (T) substitutions at the first three and/or the last three positions of the alignment ends for further in solution hybridization captures to oligonucleotide probes[13].

Given the low nuclear DNA content in the Bacho Kiro Cave *F6-597* specimen (Tab. S2.1), the absence of C-to-T substitutions after restricting the analyses to sequences carrying a C-to-T substitution at the opposing end[14] ("conditional" substitutions, Tab. S2.2 and Extended Data Fig. 1) and high levels of present-day human DNA contamination as determined based on mitochondrial DNA analyses[1], we did not attempt in solution hybridization capture for this specimen.

We enriched the selected amplified libraries for ~3.7 million single nucleotide polymorphisms (SNPs) across the genome detailed in the Supplementary Data 2 of *Haak et al.*[15] (SNP Panel 1 or "390k" array), and Supplementary Data 1, 2 and 3 of *Fu et al.*[8] (SNP Panels 2, 3 and 4, or "840k", "1000k" and "Archaic admixture" arrays, respectively). For the identified male individuals (*F6-620, BB7-240* and *CC7-335;* see Supplementary Information 4), an aliquot of each library was additionally enriched for ~6.9 Mb of the Y chromosome[16]. All of the enriched libraries were sequenced on the Illumina HiSeq 2500 platforms in a double index configuration (2x76 cycles)[5] and base calling was done using Bustard (Illumina).

Processing of nuclear DNA capture data

In addition to the steps described in the "Sequencing and alignment to the nuclear genome" section above, BAM files of the libraries enriched for the specific subset of the nuclear genome were intersected with the BED files containing target SNP positions ("390k", "840k", "1000k", "Archaic admixture", a merged set of SNP Panels 1 and 2 or "1240k", and a merged set of SNP Panels 1, 2 and 3 or "2200k") and regions (Y chromosome) using *BEDtools*[17] (version: 2.24.0). In order to filter for endogenous ancient DNA or putatively deaminated fragments, we used elevated C-to-T substitutions relative to the reference genome at the first three and/or last three positions of the alignment ends[14]. We merged the libraries originating from the same specimen using *samtools merge*[12] to produce the final datasets for downstream analyses. Tables S2.3-S2.8 summarize the number of filter-passed fragments and SNPs covered per specimen for each library as well as for the merged data of all libraries stemming from the same specimen depending on the SNP Panel used. Extended Data Tab. 1 summarizes the number of filter-passed fragments and SNPs covered in the final merged dataset used for downstream analyses.

Ancient DNA substitution patterns

For each specimen we analysed substitution patterns along the fragments for all libraries separately (Tab. S2.2) and for the merged data of all libraries originating from the same specimen (Extended Data Fig. 1) by counting the number of substitutions relative to the human reference genome. As deamination of cytosine (C) to uracil (U) residues results in characteristic C-to-T substitutions in ancient DNA molecules[18], elevated C-to-T substitutions close to the alignment ends provide evidence for the presence of authentic ancient DNA in specimens[19,20]. The C-to-T substitution frequencies ranged between 23.11% and 55.78% on the 5'-ends, and between 15.13% and 43.02% on the 3'-ends of the enriched libraries (Extended Data Fig. 1). These frequencies increased substantially when filtering for sequences with a C-to-T at the opposing end ("conditional" substitutions)[14] for the Bacho Kiro Cave specimens *AA7-738* and *CC7-2289* and *Oase1,* indicating that both endogenous ancient DNA as well some present-day human DNA contamination are present[14]. For the other specimens these frequencies remained stable, indicating that the majority of the data stems from one population of sequences.

Random read sampling and consensus calling

We performed random read sampling using *bam-caller* (https://github.com/bodkan/bam-caller, version: 0.1) by picking a base with a base quality of at least 30 at each position in the "1240k" and "2200k" SNP Panels (Supplementary Information 2) that was covered by at least one fragment longer than 35 bp with a mapping quality equal or higher than 25 (L≥35bp, MQ≥25, BQ≥30). To mitigate the effect of deamination-derived substitutions on downstream analyses, we did not sample any Ts on the forward strands (in the orientation as sequenced) and any As on the reverse strands in the first three and/or last three positions from the alignment ends. Furthermore, we repeated each of the analyses using only transversion polymorphisms to make sure our inferences are robust to any aDNA damage.

Due to the haploid nature of the Y chromosome, we called genotypes across the ~6.9 Mb of the Y chromosome for the enriched libraries of male individuals by calling a consesus allele at each position by majority call requiring a minimum coverage of 3 for the specimens *F6-620* and *BB7-240* and of 2 for the specimen *CC7-335* using using *bam-caller* (https://github.com/bodkan/bam-caller, version: 0.1). Random allele calls of Bacho Kiro Cave individuals and *Oase1* for different SNP Panels and consensus calls for Y chromosome regions, both for all and putatively deaminated fragments are available in EIGENSTRAT format at http://cdna.eva.mpg.de/modern_human/BachoKiro/.

Contamination estimates

In addition of all analysed libraries needing to have a damage profile consistent with aDNA (Extended Data Fig. 1), we used four complementary approaches in estimating the proportion of present-day human DNA contamination in the generated data of Bacho Kiro Cave specimens and *Oase1*. The estimates of present-day human DNA contamination are summarized in the Table S2.10.

Mitochondrial DNA contamination estimates.

We analysed mitochondrial DNA (mtDNA) data from Bacho Kiro Cave specimens in a previous study[1] and estimated the proportion of present-day human DNA contamination to range between 0.2% to 2.9% among all fragments of specimens *F6-620, AA7-738, CC7-2289, CC7-335* and *BK1653,* and between 0% and 1.6% among putatively deaminated fragments, respectively. We estimated the proportion of present-day human DNA contamination among all fragments of the specimen *F6-597* to be 63.5% (95% confidence intervals (CI): 62.5-64.5%)[2] using *schmutzi*[21] (version: 1.5.5). Given the high contamination estimates[1] and low nuclear DNA content (<1% among putatively deaminated fragments (Tab. S2.1)), we excluded the libraries of the specimen *F6-597* from nuclear captures and downstream analyses.

We estimated proportion of present-day human DNA contamination in the newly generated *Oase1* libraries using six previously identified positions[8] where *Oase1* mtDNA genome differs from 99% of a world-wide panel of 311 present-day human mtDNAs[22]. We counted the number of recovered mtDNA fragments that cover these positions, while taking into account the strand orientation in cases where one of the diagnostic positions was a C or a G[14]. The proportion of present-day human DNA contamination among all fragments in the libraries prepared from two previously generated extracts[8] are 64.29% (95% CI: 58.36%-69.80%) and 71.96% (95% CI: 66.59%-76.77%), respectively, and 46.22% (95% CI: 40.50%-52.39%) in the libraries prepared from a new extract, indicating that the hypochlorite treatment did not substantially reduce the amount of present-day human DNA contamination. The proportion of present-day human DNA contamination among putatively deaminated fragments is 8.70% (95% CI: 2.42%-14.98%) and 9.38% (95% CI: 3.24%-15.52%) for the new libraries prepared from the two previously generated extracts[8] and 4.51% (95% CI: 0%-9.34%) for the libraries prepared from the new extract.

Contamination estimates based on the X chromosome polymorphisms in males.

We used ANGSD[23,24] (version: 0.929) to estimate contamination in male individuals where we have sufficient X coverage, i.e. at least 200 SNPs covered by at least two fragments[25]. Since males have only one copy of X chromosome, we do not expect polymorphisms in this part of their genome. For the *F6-620*, *BB7-240* and *CC7-335* contamination estimates inferred by ANGSD are 1.62% (standard error (SE): 0.12), 2.75% (SE: 0.37) and 3.41% (SE: 0.53) among all fragments, and 1.09% (SE: 0.40), 1.27% (SE: 1.03) and 2.13% (SE: 0.94) among deaminated fragments, respectively.

Contamination estimates based on the ancient DNA damage.

We used AuthentiCT[26] (version: 1.0.0), an approach that utilizes patterns of aDNA damage, to estimate the proportion of present-day human DNA contamination among nuclear sequences of the enriched libraries. Among the sequences overlapping "2200k" SNP Panel, the inferred proportion of present-day human DNA contamination ranges between 2.23% (standard error (SE): 0.54%, *F6-620*) and 42.36% (SE: 0.64%, *CC7-2289*) (Tab. S2.10).

Consistency of results from all fragments and deaminated fragments.

To test for evidence of contamination, we computed D-statistics using ADMIXTOOLS[27] (version: v5.1) as implemented in the R-package *admixr*[28] (version: 0.7.1) on SNPs from nuclear capture Panels 1, 2 and 3 ("2200k") covered by both all and putatively deaminated fragments[8,25] for specimens *F6-620*, *BB7-240*, *CC7-335* and *BK1653*. The number of overlapping informative sites between all and deaminated fragments for specimens *AA7-738* and *CC7-2289* is too low to confidently perform this test. We computed *D(BK specimen$_1$ all, BK specimen$_1$ deaminated; Test, Mbuti)* where *Test* is a present-day human population from Simons Genome Diversity Project (SGDP)[29] and three Mbuti individuals from SGDP are used as outgroup. We used a Weighted Block Jackknife[27,30] and a block size of 5 million base pairs (5 Mb) across all autosomes on the "2200k" SNP Panel to calculate these statistics.

Figures S2.1 ad S2.2 show there is no significant difference between using all fragments and restricting the analyses to deaminated fragments for *F6-620*, *BB7-240*, *CC7-335* and *BK1653* (all $|Z| < 3$). However, given the higher contamination estimates among all fragments of *BB7-240*, *CC7-335*, *CC7-2289* and *AA7-738* using AuthentiCT[26] (version: 1.0.0) (Tab. S2.10), we restricted all downstream analyses to deaminated fragments for these specimens, unless otherwise stated.

References SI2:

1 Hublin, J.-J. et al. Initial Upper Palaeolithic Homo sapiens from Bacho Kiro Cave, Bulgaria. *Nature* **581**, 299-302, doi:10.1038/s41586-020-2259-z (2020).

2 Gansauge, M. T. *et al.* Single-stranded DNA library preparation from highly degraded DNA using T4 DNA ligase. *Nucleic Acids Res.* **45**, e79, doi:10.1093/nar/gkx033 (2017).

3 Slon, V. *et al.* Neandertal and Denisovan DNA from Pleistocene sediments. *Science* **356**, 605-608, doi: 10.1126/science.aam9695 (2017).

4 Korlević, P. *et al.* Reducing microbial and human contamination in DNA extractions from ancient bones and teeth. *Biotechniques* **59**, 87-93, doi:10.2144/000114320 (2015).

5 Kircher, M., Sawyer, S. & Meyer, M. Double indexing overcomes inaccuracies in multiplex sequencing on the Illumina platform. *Nucleic Acids Res.* **40**, e3, doi:10.1093/nar/gkr771 (2012).

6 Dabney, J. & Meyer, M. Length and GC-biases during sequencing library amplification: a comparison of various polymerase-buffer systems with ancient and modern DNA sequencing libraries. *Biotechniques* **52**, 87-94, doi:10.2144/000113809 (2012).

7 Trinkaus, E. *et al.* An early modern human from the Peştera cu Oase, Romania. *Proc. Natl. Acad. Sci. U.S.A.* **100**, 11231-11236, doi: 10.1073/pnas.2035108100 (2003).

8 Fu, Q. *et al.* An early modern human from Romania with a recent Neanderthal ancestor. *Nature* **524**, 216-219, doi:10.1038/nature14558 (2015).

9 Glocke, I. & Meyer, M. Extending the spectrum of DNA sequences retrieved from ancient bones and teeth. *Genome Res.* **27**, 1230-1237, doi: 10.1101/gr.219675.116 (2017).

10 Renaud, G., Stenzel, U. & Kelso, J. leeHom: adaptor trimming and merging for Illumina sequencing reads. *Nucleic Acids Res.* **42**, e141, doi:10.1093/nar/gku699 (2014).

11 Meyer, M. *et al.* A high-coverage genome sequence from an archaic Denisovan individual. *Science* **338**, 222-226, doi:10.1126/science.1224344 (2012).

12 Li, H. *et al.* The Sequence Alignment/Map format and SAMtools. *Bioinformatics* **25**, 2078-2079, doi:10.1093/bioinformatics/btp352 (2009).

13 Fu, Q. *et al.* DNA analysis of an early modern human from Tianyuan Cave, China. *Proc. Natl. Acad. Sci. U.S.A.* **110**, 2223-2227, doi:10.1073/pnas.1221359110 (2013).

14 Meyer, M. *et al.* A mitochondrial genome sequence of a hominin from Sima de los Huesos. *Nature* **505**, 403-406, doi:10.1038/nature12788 (2014).

15 Haak, W. *et al.* Massive migration from the steppe was a source for Indo-European languages in Europe. *Nature* **522**, 207-211, doi:10.1038/nature14317 (2015).

16 Petr, M. *et al.* The evolutionary history of Neanderthal and Denisovan Y chromosomes. *Science* **369**, 1653-1656, doi: 10.1126/science.abb6460 (2020).

17 Quinlan, A. R. & Hall, I. M. BEDTools: a flexible suite of utilities for comparing genomic features. *Bioinformatics* **26**, 841-842, doi: 10.1093/bioinformatics/btq033 (2010).

18 Briggs, A. W. *et al.* Patterns of damage in genomic DNA sequences from a Neandertal. *Proc. Natl. Acad. Sci. U.S.A.* **104**, 14616-14621, doi:10.1073/pnas.0704665104 (2007).

19 Krause, J. *et al.* A complete mtDNA genome of an early modern human from Kostenki, Russia. *Curr. Biol.* **20**, 231-236, doi:10.1016/j.cub.2009.11.068 (2010).

20 Sawyer, S., Krause, J., Guschanski, K., Savolainen, V. & Paabo, S. Temporal patterns of nucleotide misincorporations and DNA fragmentation in ancient DNA. *PLoS One* **7**, e34131, doi:10.1371/journal.pone.0034131 (2012).

21 Renaud, G., Slon, V., Duggan, A. T. & Kelso, J. Schmutzi: estimation of contamination and endogenous mitochondrial consensus calling for ancient DNA. *Genome Biol.* **16**, 224, doi:10.1186/s13059-015-0776-0 (2015).

22 Green, R. E. *et al.* A complete Neandertal mitochondrial genome sequence determined by high-throughput sequencing. *Cell* **134**, 416-426, doi:10.1016/j.cell.2008.06.021 (2008).

23 Korneliussen, T. S., Albrechtsen, A. & Nielsen, R. ANGSD: analysis of next generation sequencing data. *BMC bioinformatics* **15**, 356 (2014).

24 Rasmussen, M. *et al.* An Aboriginal Australian genome reveals separate human dispersals into Asia. *Science* **334**, 94-98 (2011).

25 Fu, Q. *et al.* The genetic history of Ice Age Europe. *Nature* **534**, 200-205, doi:10.1038/nature17993 (2016).

26 Peyrégne, S. & Peter, B. M. AuthentiCT: a model of ancient DNA damage to estimate the proportion of present-day DNA contamination. *Genome Biol.* **21**, 246, doi: 10.1186/s13059-020-02123-y (2020).

27 Patterson, N. *et al.* Ancient admixture in human history. *Genetics* **192**, 1065-1093, doi:10.1534/genetics.112.145037 (2012).

28 Petr, M., Vernot, B. & Kelso, J. admixr—R package for reproducible analyses using ADMIXTOOLS. *Bioinformatics* **35**, 3194-3195 (2019).

29 Mallick, S. *et al.* The Simons Genome Diversity Project: 300 genomes from 142 diverse populations. *Nature* **538**, 201-206, doi:10.1038/nature18964 (2016).

30 Busing, F. M. T. A., Meijer, E. & Van Der Leeden, R. Delete-m jackknife for unequal m. *Statistics and Computing* **9**, 3-8, doi: 10.1023/A:1008800423698 (1999).

Table S2.1 The characteristics of Bacho Kiro Cave and *Oase1* ssDNA libraries and summary statistics of the shotgun data.

Specimen	Specimen ID	Amount of powder used for DNA extraction (mg)	Extract ID	Volume of extract used for library preparation (µL)	Library ID	Total number of DNA molecules in the library*	Number of spike-in molecules in the library*	Number of sequenced fragments	Number of fragments ≥35 bp	Number of mapped fragments ≥35bp, MQ≥25	Number of unique fragments ≥35bp, MQ≥25	% mapped fragments ≥35bp, MQ≥25	Average fragment length	Estimated coverage in the library (all fragments)	Number of deaminated fragments ≥35bp, MQ≥25	Average deaminated fragment length	Estimated coverage in the library (deaminated fragments)
Bacho Kiro F6-620	SP6931	29.3	E9293	10	A11197	3.18E+10	1.11E+06	2,403,103	1,438,335	19,650	19,571	**1.366**	58.50	**6.31**	4,929	56.20	**6.11**
				10	A12357	2.05E+10	1.42E+06	581,401	342,184	4,384	4,383	**1.281**	59.00	**3.72**	1,047	57.20	**3.52**
				10	A12550	1.48E+10	8.29E+05	2,927,791	1,728,732	23,601	23,529	**1.365**	59.20	**2.91**	5,702	57.20	**2.74**
				10	A12944	1.74E+10	9.93E+05	2,750,462	1,695,480	19,411	19,336	**1.145**	59.30	**3.01**	4,715	57.80	**2.88**
				10	A15716	2.86E+10	1.44E+06	1,348,729	846,882	9,854	9,806	**1.164**	59.90	**5.13**	2,310	58.20	**4.75**
Bacho Kiro AA7-738	SP7098	30.4	E9294	10	A11198	2.84E+09	1.07E+06	2,084,489	1,256,707	312	312	**0.025**	45.10	**0.01**	124	45.30	**0.01**
				10	A12358	4.58E+09	1.34E+06	535,634	321,994	100	100	**0.031**	46.70	**0.02**	32	45.80	**0.02**
				10	A12554	4.05E+09	7.37E+05	4,376,821	2,632,838	676	676	**0.026**	45.80	**0.01**	239	49.40	**0.02**
				10	A12945	5.88E+09	1.12E+06	1,446,743	913,218	170	170	**0.019**	45.90	**0.02**	48	45.10	**0.01**
				10	A15717	5.06E+09	9.95E+05	1,746,767	1,134,892	224	222	**0.020**	47.40	**0.02**	81	48.20	**0.02**
Bacho Kiro BB7-240	SP7099	32.1	E9295	10	A11199	1.35E+10	2.21E+05	2,927,566	1,596,869	7,227	7,197	**0.453**	50.40	**0.74**	2,417	49.40	**0.92**
				10	A12359	8.39E+09	2.09E+05	542,128	277,697	1,160	1,160	**0.418**	50.80	**0.40**	367	49.70	**0.47**
				10	A12555	7.90E+09	1.82E+05	3,986,361	2,046,644	9,148	9,112	**0.447**	50.10	**0.40**	2,958	45.50	**0.44**
				10	A12946	1.32E+10	2.80E+05	2,719,208	1,520,238	6,012	5,995	**0.395**	51.50	**0.66**	1,989	50.70	**0.82**
				10	A15718	1.72E+10	3.12E+05	1,405,586	814,990	3,171	3,158	**0.389**	52.00	**0.88**	1,012	51.20	**1.06**
Bacho Kiro CC7-2289	SP9100	34.3	E9296	10	A11200	5.60E+10	5.69E+05	2,549,574	1,524,941	41	41	**0.003**	47.60	**0.03**	10	45.70	**0.02**
				10	A12360	2.70E+10	9.17E+05	509,637	296,520	6	6	**0.002**	50.80	**0.01**	1	38.00	**0.00**
				10	A12556	2.12E+10	5.03E+05	3,539,956	2,049,743	76	75	**0.004**	47.10	**0.01**	20	49.30	**0.01**
				10	A12947	3.45E+10	7.84E+05	1,756,046	1,067,036	28	28	**0.003**	47.70	**0.02**	4	53.50	**0.01**
				10	A15719	3.56E+10	6.20E+05	1,289,201	818,443	19	19	**0.002**	43.10	**0.02**	5	42.20	**0.01**
Bacho Kiro CC7-335	SP9101	52.4	E9297	10	A11201	3.07E+09	9.20E+05	2,919,402	1,772,388	11,887	11,832	**0.671**	49.70	**0.27**	4,300	49.30	**0.37**
				10	A12361	4.17E+09	1.62E+06	587,919	346,613	2,058	2,058	**0.594**	48.70	**0.31**	756	48.00	**0.43**
				10	A12557	2.81E+09	7.00E+05	3,317,600	2,027,299	11,656	11,623	**0.575**	49.60	**0.21**	4,232	66.20	**0.39**
				10	A12948	4.45E+09	1.15E+06	1,450,595	916,440	4,403	4,384	**0.480**	49.70	**0.29**	1,568	49.40	**0.40**
				10	A15720	6.90E+09	1.31E+06	2,061,774	1,339,133	6,297	6,269	**0.470**	49.60	**0.45**	2,282	49.30	**0.63**
Bacho Kiro F6-597	SP9102	45.6	E9298	10	A11202	7.75E+10	7.46E+05	3,146,382	2,094,007	100	100	**0.005**	60.80	**0.13**	11	45.50	**0.00**
				10	A12362	4.76E+10	1.27E+06	540,795	346,748	16	16	**0.005**	61.80	**0.06**	-	54.50	**0.00**
				10	A12558	4.21E+10	6.55E+05	4,011,897	2,566,726	100	100	**0.004**	60.70	**0.05**	4	86.90	**0.00**
				10	A12949	4.89E+10	1.06E+06	1,691,740	1,128,437	52	52	**0.005**	53.70	**0.06**	1	43.00	**0.00**
				10	A15721	6.44E+10	1.04E+06	1,309,894	907,334	32	32	**0.004**	62.40	**0.10**	1	40.00	**0.00**
Bacho Kiro BK-1653	SP7103	67.9	E9299	10	A11203	2.44E+10	8.28E+05	2,530,593	1,381,741	11,825	11,783	**0.856**	55.70	**2.82**	1,880	55.00	**1.66**
				10	A12363	2.14E+10	1.47E+06	549,052	300,572	2,028	2,028	**0.675**	55.00	**1.97**	318	46.10	**0.95**
				10	A12562	1.63E+10	9.64E+05	3,625,907	2,020,940	14,612	14,567	**0.723**	55.50	**1.61**	2,266	55.10	**0.94**
				10	A12950	1.93E+10	1.01E+06	2,167,430	1,216,492	8,285	8,263	**0.681**	55.80	**1.83**	1,173	54.80	**0.95**
				10	A15722	3.06E+10	1.13E+06	1,735,623	1,007,674	6,486	6,456	**0.644**	56.10	**2.82**	929	56.10	**1.53**
Oase1	SP2538	24.8	E1406[+]	5	A12968	3.36E+10	8.85E+05	1,891,916	998,108	1,462	1,452	**0.146**	49.70	**0.54**	337	48.60	**0.10**
		10.3	E1843[+]	5	A12967	9.47E+10	8.38E+05	2,252,369	1,289,806	668	666	**0.052**	49.30	**0.66**	147	46.80	**0.10**
		15	E6735	10	A12384	2.11E+09	1.34E+06	488,744	236,662	350	350	**0.148**	48.90	**0.03**	90	50.00	**0.01**
				10	A12590	1.58E+09	8.57E+05	2,915,887	1,501,927	2,335	2,327	**0.155**	49.70	**0.03**	588	46.70	**0.01**
				10	A12955	2.10E+09	1.15E+06	2,174,525	1,111,248	1,411	1,406	**0.127**	50.00	**0.03**	334	49.00	**0.01**
				10	F9015	2.18E+09	1.41E+06	1,788,088	877,011	1,359	1,359	**0.155**	47.40	**0.03**	322	47.60	**0.01**

* As determined using quantitative PCR (qPCR), [+] DNA extracts made in the previous study (*Fu et al.*[8]); mg – milligram, µL – microlitre, bp – base pairs, MQ – mapping quality

Table S2.2 Frequencies of C-to-T substitutions at terminal positions of the sequence alignments for the libraries generated by shotgun sequencing. The C-to-T substitution frequencies are determined on the mapped fragments longer than 35 base pairs with mapping quality of at least 25 (MQ≥25) reported in the Table S2.1. 95% binomial confidence intervals (CI) are provided in brackets. C – cytosine, T – thymine.

Specimen	Library ID	All fragments		Fragments with C-to-T substitutions at the opposing end	
		5' C→T [95% CI]	3' C → T [95% CI]	5' C→T [95% CI]	3' C → T [95% CI]
Bacho Kiro F6-620	A11197	41.8 [40.3-43.3]	34 [32.5-35.4]	44.2 [38.8-49.7]	39.2 [34.0-44.1]
	A12357	42.0 [38.8-45.2]	29.7 [26.7-32.8]	50.0 [36.6-63.4]	29.8 [21.0-40.2]
	A12550	41.4 [40.0-42.7]	32.0 [30.7-33.4]	42.5 [37.2-47.4]	36.5 [31.8-41.0]
	A12944	41.2 [39.7-42.6]	33.0 [31.6-34.5]	42.7 [36.5-48.3]	32.3 [27.6-37.3]
	A15716	41.5 [39.4-43.6]	30.0 [28.0-32.0]	41.8 [33.4-50.7]	30.2 [23.2-36.9]
Bacho Kiro AA7-738	A11198	65.8 [53.3-74.3]	53.8 [41.6-63.3]	87.5 [52.9-97.8]	58.3 [25.4-74.6]
	A12358	76.9 [53.9-86.3]	37.5 [18.5-61.4]	66.7 [20.8-93.9]	66.7 [20.8-93.9]
	A12554	50.6 [43.0-58.2]	46.5 [37.8-54.0]	38.5 [17.7-64.5]	35.7 [11.7-54.6]
	A12945	45.2 [29.1-57.8]	35.7 [21.0-48.4]	66.7 [30.0-90.3]	57.1 [15.8-75.0]
	A15717	57.8 [43.3-71.0]	34.7 [21.2-46.6]	50.0 [9.5-90.5]	14.3 [2.6-51.3]
Bacho Kiro BB7-240	A11199	56.7 [54.3-59.0]	42.4 [39.9-44.8]	63.3 [54.3-70.2]	41.5 [35.1-48.2]
	A12359	50.0 [44.2-55.8]	41.3 [35.5-47.3]	46.2 [28.8-64.5]	40.0 [24.6-57.7]
	A12555	55.6 [53.5-57.7]	38.1 [35.9-40.2]	52.6 [45.0-59.1]	38.3 [32.3-44.0]
	A12946	53.7 [51.2-56.2]	38.9 [36.2-41.5]	49.7 [41.6-57.7]	38.2 [31.5-45.3]
	A15718	49.1 [45.5-52.4]	38.7 [34.9-42.3]	55.7 [42.7-65.4]	46.4 [35.0-55.9]
Bacho Kiro CC7-2289	A11200	43.8 [23.1-66.8]	33.3 [3.0-56.4]	100 [20.7-100.0]	100 [20.7-100.0]
	A12360	NA [N/A]	0.0 [0.0-65.8]	NA [N/A]	NA [NA]
	A12556	30.4 [15.6-50.9]	29.4 [13.3-53.1]	0.0 [0.0-79.3]	NA [NA]
	A12947	33.3 [6.3-54.7]	0.0 [0.0-39.0]	NA [N/A]	0.0 [0.0-79.3]
	A15719	75.0 [30.1-95.4]	0.0 [0.0-49.0]	NA [N/A]	0.0 [0.0-79.3]
Bacho Kiro CC7-335	A11201	58.7 [56.9-60.5]	45.1 [43.1-47.1]	56.5 [50.1-62.0]	42.9 [37.8-48.2]
	A12361	62.7 [58.1-66.7]	42.8 [38.1-47.6]	64.1 [45.9-75.1]	43.9 [30.2-55.0]
	A12557	56.3 [54.4-58.1]	45.6 [43.6-47.7]	51.4 [44.8-57.2]	44.8 [39.1-50.5]
	A12948	56.6 [53.5-59.5]	45.4 [42.0-48.6]	56.9 [46.6-64.9]	49.6 [41.0-58.2]
	A15720	58.8 [56.3-61.2]	43.9 [41.0-46.6]	58.7 [50.2-65.5]	44.8 [38.1-51.7]
Bacho Kiro F6-597	A11202	26.3 [8.5-43.3]	5.3 [0.0-16.8]	NA [N/A]	NA [NA]
	A12362	0.0 [0.0-56.2]	0.0 [0.0-65.8]	NA [N/A]	NA [NA]
	A12558	0.0 [0.0-20.4]	9.1 [0.8-21.8]	NA [N/A]	NA [NA]
	A12949	0.0 [0.0-27.8]	6.7 [1.2-29.8]	NA [N/A]	NA [NA]
	A15721	0.0 [0.0-35.4]	16.7 [3.0-56.4]	NA [N/A]	NA [NA]
Bacho Kiro BK-1653	A11203	26.8 [25.2-28.5]	18.9 [17.3-20.5]	30.1 [22.1-39.5]	22.1 [15.4-28.9]
	A12363	25.8 [22.1-30.0]	16.8 [13.4-20.9]	44.4 [20.3-61.4]	36.4 [19.7-57.0]
	A12562	24.8 [23.3-26.2]	18.4 [17.0-19.9]	29.1 [21.2-36.7]	25.0 [18.7-32.5]
	A12950	25.0 [23.1-27.0]	15.6 [13.8-17.4]	29.4 [19.9-41.1]	22.0 [14.7-31.5]
	A15722	27.1 [24.9-29.4]	13.7 [11.9-15.8]	48.1 [27.6-62.7]	14.3 [8.5-22.9]
Oase1	A12968*	38.5 [33.1-43.6]	37.6 [31.1-43.6]	50.0 [28.0-72.0]	38.1 [20.8-59.1]
	A12967*	39.1 [31.8-46.9]	30.4 [22.8-39.4]	80.0 [37.6-96.4]	40.0 [16.8-68.7]
	A12384	33.8 [24.3-44.6]	35.5 [23.3-46.3]	33.3 [0.0-56.2]	33.3 [0.0-56.2]
	A12590	36.7 [32.7-40.5]	32.7 [28.3-37.0]	37.2 [24.4-52.1]	42.1 [25.6-55.3]
	A12955	35.6 [30.5-41.0]	31.7 [26.3-37.7]	35.3 [13.3-53.1]	26.1 [9.7-41.9]
	F9015	34.2 [29.2-39.5]	36.9 [30.8-42.6]	29.2 [14.9-49.2]	41.2 [21.6-64.0]

***** New libraries prepared from two extracts used in a previous study (Fu et al.[8])

Table S2.3 Summary statistics of the Bacho Kiro and *Oase1* DNA libraries captured with the SNP Panel 1 or "390k"[15] array. The number of SNPs on target are determined using the unique fragments longer than 35 base pairs (L≥35 bp) with mapping quality of at least 25 (MQ≥25) that overlap the SNPs on the "390k" array[15].

		All fragments							Fragments with terminal C-to-T substitutions		
Specimen	**Library ID**	**Number of sequenced fragments**	**Number of fragments ≥35 bp**	**Number of mapped fragments ≥35bp, MQ≥25**	**Number of mapped fragments on target ≥35bp, MQ≥25**	**Number of unique fragments on target ≥35bp, MQ≥25**	**Number of SNPs on target**	**% of SNPs on target**	**Number of deaminated fragments on target ≥35bp, MQ≥25**	**Number of SNPs on target**	**% of SNPs on target**
Bacho Kiro F6-620	A11197	11,899,581	8,645,070	3,467,069	1,561,833	1,001,291	316,864	80.47	259,815	172,587	43.83
	A12357	10,869,174	8,052,475	2,598,741	1,317,844	880,398	300,283	76.25	213,441	149,237	37.90
	A12550	8,917,113	6,472,270	1,909,121	1,050,064	701,836	274,734	69.77	166,987	124,241	31.55
	A12944	9,586,753	7,103,310	2,090,003	1,024,769	677,230	272,094	69.10	159,465	120,418	30.58
	A15716	1,671,876	1,334,551	599,155	463,053	349,380	191,006	48.50	80,224	68,100	17.29
	merged	42,944,497	31,607,676	10,664,089	5,417,563	3,610,135	372,571	94.61	879,932	294,287	74.73
Bacho Kiro AA7-738	A11198	12,145,465	8,700,739	175,278	23,854	8,343	7,806	1.98	3,178	3,104	0.79
	A12358	1,410,251	1,047,605	38,811	12,811	7,112	6,793	1.73	1,895	1,885	0.48
	A12554	1,533,400	1,104,923	37,071	10,079	5,072	4,840	1.23	1,813	1,798	0.46
	A12945	1,635,213	1,227,385	31,282	10,294	5,381	5,128	1.30	2,000	1,980	0.50
	A15717	27,180,764	10,263,094	297,329	11,099	3,526	2,910	0.74	1,089	1,022	0.26
	merged	43,905,093	22,343,746	579,771	68,137	29,434	26,299	6.68	9,975	9,629	2.45
Bacho Kiro BB7-240	A11199	13,252,473	9,002,008	2,123,764	487,691	235,156	163,518	41.52	84,770	73,710	18.72
	A12359	12,593,847	8,262,403	1,227,745	374,230	198,565	143,427	36.42	69,051	61,084	15.51
	A12555	10,688,993	6,831,509	807,933	299,881	158,830	120,932	30.71	54,468	49,494	12.57
	A12946	10,720,721	7,377,939	946,511	329,501	182,060	132,737	33.71	60,886	54,551	13.85
	A15718	1,423,176	1,057,610	322,999	174,753	118,568	93,947	23.86	38,486	35,757	9.08
	merged	48,679,210	32,531,469	5,428,952	1,666,056	893,179	311,587	79.13	307,661	191,684	48.68
Bacho Kiro CC7-2289	A11200	11,083,652	7,875,798	26,040	7,442	2,427	2,375	0.60	583	586	0.15
	A12360	1,698,092	1,187,404	8,578	4,113	2,267	2,258	0.57	350	357	0.09
	A12556	1,440,718	1,007,689	5,788	2,839	1,521	1,504	0.38	339	337	0.09
	A12947	1,280,691	939,834	3,974	2,382	1,268	1,256	0.32	256	258	0.07
	A15719	1,496,778	1,115,292	7,269	3,034	1,614	1,405	0.36	300	284	0.07
	merged	16,999,931	12,126,017	51,649	19,810	9,097	8,659	2.20	1,828	1,816	0.46
Bacho Kiro CC7-335	A11201	11,973,014	8,804,658	2,337,293	418,725	165,324	126,717	32.18	63,194	56,815	14.43
	A12361	11,406,591	8,205,044	1,377,993	360,202	163,136	123,327	31.32	59,292	53,333	13.54
	A12557	10,742,241	7,714,075	1,012,327	325,196	147,895	113,536	28.83	55,405	50,031	12.71
	A12948	10,627,567	7,762,120	1,116,051	290,639	131,242	102,830	26.11	48,974	44,518	11.31
	A15720	1,584,771	1,275,920	412,202	163,168	99,826	81,481	20.69	36,322	33,796	8.58
	merged	46,334,184	33,761,817	6,255,866	1,557,930	707,423	290,832	73.85	263,187	174,782	44.38
Bacho Kiro BK-1653	A11203	11,703,301	8,659,849	2,859,809	1,100,323	599,073	273,924	69.56	96,817	83,025	21.08
	A12363	11,951,100	8,517,115	1,909,417	898,108	549,819	254,152	64.54	84,654	72,863	18.50
	A12562	10,428,783	7,311,600	1,643,754	669,793	398,421	218,118	55.39	60,080	54,159	13.75
	A12950	10,423,957	7,377,054	1,603,265	704,765	423,243	224,583	57.03	62,556	56,132	14.25
	A15722	24,068,105	10,618,989	5,828,548	953,264	539,986	272,135	69.11	77,161	69,213	17.58
	merged	68,575,246	42,484,607	13,844,793	4,326,253	2,510,542	393,788	93.41	381,268	215,802	54.8
Oase1	A12968*	9,450,683	6,293,578	316,504	225,313	91,716	76,988	19.55	19,613	18,981	4.82
	A12967*	8,702,207	5,908,403	147,181	106,039	41,967	39,035	9.91	7,468	7,456	1.89
	A12384	9,523,290	6,124,858	355,622	259,755	24,872	23,254	5.91	5,515	5,458	1.39
	A12590	10,954,958	7,076,935	380,208	272,863	22,833	21,538	5.47	5,651	5,584	1.42
	A12955	9,542,825	6,218,130	282,570	199,618	22,392	21,166	5.37	5,417	5,390	1.37
	F9015	10,928,126	6,664,522	364,795	256,619	19,621	18,620	4.73	4,892	4,845	1.23
	merged	59,102,089	38,286,426	1,846,880	1,320,207	223,401	155,508	39.49	48,556	44,591	11.32

***** New libraries prepared from two extracts used in a previous study (*Fu et al.*[8])

Table S2.4 Summary statistics of the Bacho Kiro and *Oase1* DNA libraries captured with the SNP Panel 2 or "840k"[8] array. The number of SNPs on target are determined using the unique fragments longer than 35 base pairs with mapping quality of at least 25 (MQ≥25) that overlap the SNPs on the "840k" array[8].

	All fragments								Fragments with terminal C-to-T substitutions		
Specimen	**Library ID**	**Number of sequenced fragments**	**Number of fragments ≥35 bp**	**Number of mapped fragments ≥35bp, MQ≥25**	**Number of mapped fragments on target ≥35bp, MQ≥25**	**Number of unique fragments on target ≥35bp, MQ≥25**	**Number of SNPs on target**	**% of SNPs on target**	**Number of deaminated fragments on target ≥35bp, MQ≥25**	**Number of SNPs on target**	**% of SNPs on target**
Bacho Kiro F6-620	A11197	22,926,356	17,251,602	6,317,820	4,319,293	1,741,983	616,855	73.21	453,942	315,619	37.46
	A12357	18,328,399	13,704,688	5,215,324	3,667,130	1,698,935	595,206	70.64	416,479	291,769	34.63
	A12550	9,342,745	6,882,903	2,425,491	1,693,850	971,643	458,798	54.45	232,921	185,707	22.04
	A12944	9,442,994	7,140,283	2,427,405	1,663,189	908,195	441,659	52.41	215,546	173,808	20.63
	A15716	8,821,338	7,040,301	2,635,727	1,826,406	1,029,637	480,163	56.98	241,148	192,930	22.90
	merged	68,861,832	52,019,777	19,021,767	13,169,868	6,350,393	757,051	89.84	1,560,036	558,143	66.24
Bacho Kiro AA7-738	A11198	23,445,403	17,152,839	310,849	186,370	15,639	14,804	1.76	5,889	5,835	0.69
	A12358	7,757,929	5,754,460	130,802	83,632	15,563	14,912	1.77	4,146	4,134	0.49
	A12554	11,338,006	8,280,216	126,265	74,600	11,717	11,193	1.33	4,257	4,235	0.50
	A12945	11,004,643	8,279,751	117,146	69,354	12,179	11,563	1.37	4,455	4,413	0.52
	A15717	9,125,030	7,040,076	105,180	65,037	8,940	8,561	1.02	3,182	3,162	0.38
	merged	62,671,011	46,507,342	790,242	478,993	64,038	58,037	6.89	21,929	21,376	2.54
Bacho Kiro BB7-240	A11199	23,835,075	16,599,615	3,378,384	2,167,599	412,089	298,929	35.48	148,602	131,835	15.65
	A12359	18,972,864	12,867,006	2,658,602	1,788,537	392,301	286,854	34.04	136,778	122,184	14.50
	A12555	9,876,045	6,388,464	1,089,368	687,569	248,874	198,827	23.60	85,335	79,414	9.42
	A12946	10,762,884	7,482,516	1,439,478	949,797	300,368	228,456	27.11	101,665	92,842	11.02
	A15718	8,597,668	6,361,984	1,249,878	818,538	296,802	228,514	27.12	98,833	90,938	10.79
	merged	72,044,536	49,699,585	9,815,710	6,412,040	1,650,434	610,752	72.48	571,213	362,810	43.06
Bacho Kiro CC7-2289	A11200	20,095,361	14,382,395	49,188	21,615	4,494	4,369	0.52	1,105	1,107	0.13
	A12360	9,231,418	6,549,521	31,000	16,370	4,685	4,673	0.55	707	718	0.09
	A12556	10,052,171	7,227,057	25,443	12,110	3,452	3,387	0.40	659	657	0.08
	A12947	8,705,372	6,410,889	20,132	9,369	3,090	3,074	0.36	643	654	0.08
	A15719	10,531,118	7,990,473	25,153	11,751	3,000	2,938	0.35	602	612	0.07
	merged	58,615,440	42,560,335	150,916	71,215	18,721	18,151	2.15	3,716	3,731	0.44
Bacho Kiro CC7-335	A11201	21,338,266	15,910,234	3,627,638	2,258,383	301,906	236,938	28.12	114,807	104,619	12.42
	A12361	17,989,048	13,218,581	2,762,393	1,794,352	317,663	242,641	28.80	116,021	105,046	12.47
	A12557	9,943,887	7,176,315	1,143,312	711,224	217,233	176,557	20.95	80,635	74,945	8.89
	A12948	10,700,557	7,881,140	1,482,421	951,441	218,273	177,072	21.01	81,473	75,681	8.98
	A15720	8,822,517	7,045,295	1,374,443	884,459	235,591	190,005	22.55	86,348	80,048	9.50
	merged	68,794,275	51,231,565	10,390,207	6,599,859	1,290,666	561,737	66.66	479,284	326,926	38.80
Bacho Kiro BK-1653	A11203	19,907,962	14,792,961	4,541,063	2,852,991	980,828	494,311	58.66	159,264	140,173	16.64
	A12363	18,577,919	13,793,835	3,967,259	2,598,268	1,083,564	498,360	59.14	168,722	145,511	17.27
	A12562	10,497,458	7,488,565	2,071,856	1,351,877	641,692	370,131	43.93	98,685	90,063	10.69
	A12950	10,134,905	7,228,788	2,022,122	1,333,879	573,808	347,593	41.25	86,127	79,755	9.47
	A15722	7,626,731	5,851,070	1,679,486	1,093,476	560,128	343,387	40.75	81,599	76,010	9.02
	merged	66,744,975	49,155,219	14,281,786	9,230,491	3,840,020	694,592	82.43	594,397	356,855	43.35
Oase1	A12968*	8,859,546	5,932,955	567,144	353,112	138,495	121,866	14.46	29,657	29,292	3.48
	A12967*	8,488,875	5,738,835	253,428	157,471	70,717	66,885	7.94	13,059	13,227	1.57
	A12384	8,056,658	5,150,984	593,089	393,101	45,129	42,925	5.09	10,051	10,074	1.20
	A12590	10,858,435	7,137,677	667,254	426,051	43,596	41,474	4.92	10,750	10,718	1.27
	A12955	9,605,636	6,282,106	387,272	236,849	37,587	36,004	4.27	9,086	9,113	1.08
	F9015	10,876,167	6,788,033	563,602	353,964	32,728	31,673	3.76	8,106	8,145	0.97
	merged	56,745,317	37,030,590	3,031,789	1,920,548	368,252	270,601	32.11	80,709	75,569	8.97

***** New libraries prepared from two extracts used in a previous study (*Fu et al.*[8])

Table S2.5 Summary statistics of the Bacho Kiro and *Oase1* DNA libraries captured with the SNP Panel 3 or "1000k"[8] array. The number of SNPs on target are determined using the unique fragments longer than 35 base pairs (L≥35 bp) with mapping quality of at least 25 (MQ≥25) that overlap the SNPs on the "1000k" array[8].

		All fragments							Fragments with terminal C-to-T substitutions		
Specimen	**Library ID**	**Number of sequenced fragments**	**Number of fragments ≥35 bp**	**Number of mapped fragments ≥35bp, MQ≥25**	**Number of mapped fragments on target ≥35bp, MQ≥25**	**Number of unique fragments on target ≥35bp, MQ≥25**	**Number of SNPs on target**	**% of SNPs on target**	**Number of deaminated fragments on target ≥35bp, MQ≥25**	**Number of SNPs on target**	**% of SNPs on target**
Bacho Kiro F6-620	A11197	21,991,234	16,842,418	6,151,477	4,155,525	1,474,347	608,886	61.02	369,294	279,759	28.04
	A12357	17,215,328	13,186,365	4,962,070	3,537,600	1,411,543	583,556	58.49	332,082	255,889	25.65
	A12550	11,263,593	8,296,609	2,744,780	1,884,129	914,395	464,625	46.57	211,720	177,776	17.82
	A12944	8,563,214	6,441,281	2,032,905	1,405,287	722,521	402,943	40.38	164,717	143,526	14.38
	A15716	10,575,449	8,523,083	3,338,770	2,401,967	790,645	447,152	44.81	177,656	156,368	15.67
	merged	69,608,818	53,289,756	19,230,002	13,384,508	5,313,451	808,722	81.05	1,255,469	537,525	53.87
Bacho Kiro AA7-738	A11198	23,090,198	17,199,659	253,576	138,541	12,213	11,956	1.20	4,476	4,549	0.46
	A12358	7,508,510	5,682,372	119,420	77,957	11,361	11,251	1.13	2,861	2,894	0.29
	A12554	9,771,730	7,268,861	131,135	75,322	7,169	7,141	0.72	2,508	2,584	0.26
	A12945	9,416,186	7,225,669	106,165	61,279	7,611	7,573	0.76	2,767	2,833	0.28
	A15717	11,764,615	4,719,341	67,686	45,702	3,006	3,069	0.31	955	999	0.10
	merged	61,551,239	42,095,902	677,982	398,801	41,360	39,660	3.97	13,567	13,677	1.37
Bacho Kiro BB7-240	A11199	25,195,252	17,475,054	3,123,776	1,971,708	327,492	258,903	25.95	113,777	106,242	10.65
	A12359	20,696,734	14,122,968	2,534,285	1,679,644	296,500	239,061	23.96	98,633	93,280	9.35
	A12555	10,138,039	6,494,073	878,841	536,288	181,137	157,496	15.78	59,747	58,737	5.89
	A12946	10,523,868	7,211,960	1,060,486	681,607	215,549	180,387	18.08	70,316	67,916	6.81
	A15718	8,836,672	6,540,204	1,393,464	952,349	188,610	163,965	16.43	60,393	59,249	5.94
	merged	75,390,565	51,844,259	8,990,852	5,821,596	1,209,288	565,852	56.71	402,866	294,403	29.51
Bacho Kiro CC7-2289	A11200	21,474,542	15,685,689	57,751	18,729	3,069	3,131	0.31	724	755	0.08
	A12360	7,803,992	5,694,060	31,163	14,834	2,034	2,123	0.21	270	285	0.03
	A12556	8,899,916	6,493,949	27,949	11,355	1,677	1,735	0.17	353	372	0.04
	A12947	8,181,325	6,124,722	22,437	8,110	1,487	1,561	0.16	273	293	0.03
	A15719	8,584,651	6,634,901	28,248	11,265	1,478	1,539	0.15	254	261	0.03
	merged	54,944,426	40,633,321	167,548	64,293	9,745	10,003	1.00	1,874	1,965	0.20
Bacho Kiro CC7-335	A11201	21,990,555	16,458,472	3,600,338	2,220,876	262,444	217,477	21.80	96,651	91,365	9.16
	A12361	20,500,220	15,249,848	3,227,366	2,105,982	267,013	217,295	21.78	94,622	89,027	8.92
	A12557	9,823,290	7,102,874	1,015,008	595,845	178,230	153,326	15.37	64,825	62,753	6.29
	A12948	11,125,768	8,140,989	1,347,104	845,655	176,385	151,287	15.16	64,004	61,709	6.18
	A15720	9,024,906	7,269,772	1,717,757	1,167,209	178,891	155,004	15.53	63,632	61,835	6.20
	merged	72,464,739	54,221,955	10,907,573	6,935,567	1,062,963	536,521	53.77	383,734	286,514	28.72
Bacho Kiro BK-1653	A11203	22,558,998	16,730,866	5,022,091	3,206,900	837,168	479,689	48.08	130,533	121,256	12.15
	A12363	19,237,335	14,309,074	4,072,250	2,730,583	817,869	457,572	45.86	122,614	113,883	11.41
	A12562	11,410,950	8,078,126	1,918,594	1,225,111	501,710	332,243	33.30	74,196	71,885	7.20
	A12950	9,658,498	6,839,385	1,730,548	1,146,618	444,284	305,733	30.64	64,164	62,821	6.30
	A15722	9,521,514	4,040,947	1,786,417	1,328,323	310,326	248,582	24.91	42,844	43,627	4.37
	merged	72,387,295	49,998,398	14,529,900	9,637,535	2,911,357	726,130	72.77	434,351	305,619	30.63
Oase1	A12968*	9,913,082	6,526,052	460,141	283,631	97,727	91,714	9.19	19,696	20,261	2.03
	A12967*	9,381,272	6,330,765	210,442	127,461	44,136	44,466	4.46	7,448	7,819	0.78
	A12384	9,326,741	6,042,399	461,129	293,613	38,011	37,284	3.74	7,837	8,053	0.81
	A12590	10,425,950	6,753,910	482,672	300,968	33,306	32,737	3.28	7,658	7,829	0.78
	A12955	10,204,276	6,685,185	358,928	211,600	31,440	31,056	3.11	7,020	7,175	0.72
	F9015	10,097,198	6,248,272	373,923	217,345	28,323	28,104	2.82	6,761	6,940	0.70
	merged	59,348,519	38,586,583	2,347,235	1,434,618	272,943	221,020	22.15	56,420	55,309	5.54

***** New libraries prepared from two extracts used in a previous study (*Fu et al.*[8])

Table S2.6 Summary statistics of the Bacho Kiro and *Oase1* DNA libraries captured with the SNP Panel 4 or "Archaic admixture"[8] array. The number of SNPs on target are determined using the unique fragments longer than 35 base pairs (L≥35 bp) with mapping quality of at least 25 (MQ≥25) that overlap the SNPs on the "Archaic admixture" array[8].

	All fragments								Fragments with terminal C-to-T substitutions		
Specimen	**Library ID**	**Number of sequenced fragments**	**Number of fragments ≥35 bp**	**Number of mapped fragments ≥35bp, MQ≥25**	**Number of mapped fragments on target ≥35bp, MQ≥25**	**Number of unique fragments on target ≥35bp, MQ≥25**	**Number of SNPs on target**	**% of SNPs on target**	**Number of deaminated fragments on target ≥35bp, MQ≥25**	**Number of SNPs on target**	**% of SNPs on target**
Bacho Kiro F6-620	A11197	31,930,399	23,542,084	6,780,310	4,055,151	1,886,935	953,809	54.52	484,643	421,808	24.11
	A12357	54,684,610	39,738,237	11,467,222	7,539,176	2,528,304	1,077,024	61.57	613,646	499,442	28.55
	A12550	9,906,107	7,226,662	2,157,336	1,415,846	883,285	597,714	34.17	210,651	213,726	12.22
	A12944	47,491,464	35,193,886	9,083,870	5,808,366	1,967,918	953,378	54.50	465,116	403,173	23.05
	A15716	9,770,314	7,684,551	2,374,589	1,639,090	995,819	657,661	37.59	230,700	233,098	13.32
	merged	153,782,894	113,385,420	31,863,327	20,457,629	8,262,261	1,405,078	80.32	2,004,756	927,570	53.02
Bacho Kiro AA7-738	A11198	41,109,419	30,072,270	421,964	163,706	22,805	21,351	1.22	7,658	8,277	0.47
	A12358	7,465,537	5,674,453	82,595	41,884	15,442	15,803	0.90	3,618	4,161	0.24
	A12554	9,618,811	7,113,815	98,615	46,775	13,118	12,786	0.73	4,311	4,807	0.27
	A12945	9,670,106	7,379,698	82,321	39,122	12,981	12,482	0.71	4,249	4,769	0.27
	A15717	6,610,421	5,163,955	56,111	24,879	8,616	8,319	0.48	2,674	2,969	0.17
	merged	74,474,294	55,404,191	741,606	316,366	72,962	67,495	3.86	22,510	24,423	1.40
Bacho Kiro BB7-240	A11199	41,842,444	27,505,936	3,002,098	1,565,980	456,423	399,472	22.83	162,041	166,099	9.49
	A12359	53,142,780	34,495,298	3,800,991	2,200,316	513,204	438,452	25.06	175,606	177,838	10.17
	A12555	9,076,243	5,626,312	599,482	327,430	180,668	184,926	10.57	61,690	69,813	3.99
	A12946	45,490,577	30,166,823	3,125,838	1,739,697	443,575	385,636	22.04	148,345	153,108	8.75
	A15718	9,772,037	6,950,850	849,105	525,769	258,325	251,177	14.36	85,290	94,051	5.38
	merged	159,324,081	104,745,219	11,377,514	6,359,192	1,852,195	947,950	54.19	632,972	500,142	28.59
Bacho Kiro CC7-2289	A11200	38,931,962	27,905,543	189,194	35,915	8,368	5,584	0.32	1,302	1,317	0.08
	A12360	11,622,682	8,339,022	54,265	15,711	6,541	5,653	0.32	791	879	0.05
	A12556	9,726,180	7,081,632	40,292	11,277	5,034	3,844	0.22	782	837	0.05
	A12947	8,434,644	6,293,372	32,732	7,484	4,042	3,055	0.17	598	648	0.04
	A15719	8,928,831	6,818,981	35,113	8,607	4,080	3,042	0.17	575	670	0.04
	merged	77,644,299	56,438,550	351,596	78,994	28,065	19,703	1.13	4,048	3,959	0.27
Bacho Kiro CC7-335	A11201	40,556,360	28,939,042	4,174,229	2,149,600	404,037	359,352	20.54	151,372	154,057	8.81
	A12361	53,641,009	38,346,940	4,946,301	2,861,939	488,498	415,698	23.76	176,473	176,345	10.08
	A12557	8,965,066	6,395,492	716,845	383,083	183,978	183,343	10.48	67,784	74,719	4.27
	A12948	44,912,691	32,003,257	3,821,315	2,174,713	352,918	315,426	18.03	129,552	132,902	7.60
	A15720	8,640,345	6,764,261	911,958	564,798	221,466	215,586	12.32	80,996	87,829	5.02
	merged	156,715,471	112,448,992	14,570,648	8,134,133	1,650,897	907,904	51.90	606,177	488,615	27.93
Bacho Kiro BK-1653	A11203	48,320,999	33,985,611	7,177,575	3,650,622	1,258,608	802,844	45.89	200,416	205,896	11.77
	A12363	61,016,010	43,460,571	8,599,758	5,124,135	1,668,317	911,485	52.10	255,301	252,830	14.45
	A12562	9,827,836	6,729,266	1,292,115	751,792	453,554	379,996	21.72	69,030	79,454	4.54
	A12950	34,594,832	23,503,008	4,963,426	3,109,725	864,009	615,238	35.17	127,311	136,555	7.81
	A15722	5,408,560	4,014,769	833,423	525,783	346,867	313,283	17.91	50,223	59,618	3.41
	merged	159,168,237	111,693,225	22,866,297	13,162,057	4,591,355	1,257,365	71.87	702,281	533,274	30.48
Oase1	A12968*	8,417,896	5,419,859	327,785	180,974	92,404	100,510	5.75	19,096	22,835	1.31
	A12967*	8,261,454	5,467,243	160,606	76,990	48,098	54,527	3.12	8,238	10,398	0.59
	A12384	7,386,323	4,672,927	306,814	176,572	46,342	48,541	2.77	9,523	10,662	0.61
	A12590	9,854,422	6,351,106	380,628	198,712	46,847	48,647	2.78	10,847	11,962	0.68
	A12955	9,203,696	6,067,413	266,099	127,307	37,659	39,768	2.27	8,544	9,632	0.55
	F9015	9,195,952	5,789,404	277,681	130,355	35,287	37,162	2.12	8,199	9,199	0.53
	merged	52,319,743	33,767,952	1,719,613	890,910	306,637	278,234	15.9	64,447	71,112	4.06

***** New libraries prepared from two extracts used in a previous study (*Fu et al.*[8])

Table S2.7 Summary statistics of the merged data of Bacho Kiro and *Oase1* DNA libraries captured with the SNP Panels 1 and 2 comprising ~1,2 million sites ("1240k"[8,15]). The number of SNPs on target are determined using the unique fragments longer than 35 base pairs (L≥35 bp) with mapping quality of at least 25 (MQ≥25) that overlap "1240k" SNPs of the "390k"[15] and "840k" arrays[8].

	All fragments								Fragments with terminal C-to-T substitutions		
Specimen	**Library ID**	**Number of sequenced fragments**	**Number of fragments ≥35 bp**	**Number of mapped fragments ≥35bp, MQ≥25**	**Number of mapped fragments on target ≥35bp, MQ≥25**	**Number of unique fragments on target ≥35bp, MQ≥25**	**Number of SNPs on target**	**% of SNPs on target**	**Number of deaminated fragments on target ≥35bp, MQ≥25**	**Number of SNPs on target**	**% of SNPs on target**
Bacho Kiro F6-620	A11197	34,825,937	25,896,672	9,784,889	7,005,396	2,734,893	792,855	64.30	494,881	371,839	30.16
	A12357	29,197,573	21,757,163	7,814,065	5,693,242	2,574,425	724,295	58.74	391,571	309,117	25.07
	A12550	18,259,858	13,355,173	4,334,612	3,164,364	1,672,203	738,448	59.89	399,697	313,922	25.46
	A12944	19,029,747	14,243,593	4,517,408	3,281,791	1,584,618	718,626	58.28	374,990	298,154	24.18
	A15716	10,493,214	8,374,852	3,234,882	2,303,292	1,378,233	676,799	54.89	321,233	264,651	21.46
	merged	111,806,329	83,627,453	29,685,856	21,448,085	9,944,372	1,129,285	91.59	1,982,372	855,977	69.42
Bacho Kiro AA7-738	A11198	35,590,868	25,853,578	486,127	308,044	23,880	18,975	1.54	7,467	7,483	0.61
	A12358	9,168,180	6,802,065	169,613	112,333	22,611	21,863	1.77	6,043	6,070	0.49
	A12554	12,871,406	9,385,139	163,336	100,989	16,774	16,148	1.31	6,070	6,088	0.49
	A12945	12,639,856	9,507,136	148,428	91,214	17,504	16,783	1.36	6,436	6,416	0.52
	A15717	36,305,794	17,303,170	402,509	305,738	12,444	11,569	0.94	4,268	4,218	0.34
	merged	106,576,104	68,851,088	1,370,013	918,318	93,213	84,856	6.88	30,284	31,219	2.53
Bacho Kiro BB7-240	A11199	37,087,548	25,601,623	5,502,148	3,730,345	644,850	379,762	30.80	180,486	164,379	13.33
	A12359	31,566,711	21,129,409	3,886,347	2,706,321	589,028	317,485	25.75	138,820	129,353	10.49
	A12555	20,565,038	13,219,973	1,897,301	1,271,913	407,180	322,662	26.17	139,666	130,265	10.56
	A12946	21,483,605	14,860,455	2,385,989	1,651,395	481,710	364,296	29.55	162,385	148,909	12.08
	A15718	10,020,844	7,419,594	1,572,877	1,067,462	414,636	325,394	26.39	137,117	128,007	10.38
	merged	120,723,746	82,231,054	15,244,662	10,427,436	2,537,404	924,367	74.97	758,474	557,717	45.23
Bacho Kiro CC7-2289	A11200	31,179,013	22,258,193	75,228	36,521	6,908	4,511	0.37	1,103	1,127	0.09
	A12360	10,929,510	7,736,925	39,578	22,160	6,954	7,031	0.57	1,052	1,088	0.09
	A12556	11,492,889	8,234,746	31,231	15,992	4,965	4,943	0.40	996	1,002	0.08
	A12947	9,986,063	7,350,723	24,106	11,915	4,363	4,381	0.36	900	920	0.07
	A15719	12,027,896	9,105,765	32,422	17,034	4,615	4,400	0.36	905	914	0.07
	merged	75,615,371	54,686,352	202,565	103,622	27,805	27,094	2.20	4,956	5,609	0.45
Bacho Kiro CC7-335	A11201	33,311,280	24,714,892	5,964,931	3,932,017	465,307	316,935	25.70	149,782	138,732	11.25
	A12361	29,395,639	21,423,625	4,140,386	2,791,855	479,330	288,770	23.42	129,872	121,116	9.82
	A12557	20,686,128	14,890,390	2,155,639	1,421,108	364,549	292,309	23.71	135,931	126,095	10.23
	A12948	21,328,124	15,643,260	2,598,472	1,748,502	348,854	281,960	22.87	130,234	121,219	9.83
	A15720	10,407,288	8,321,215	1,786,645	1,196,498	334,551	273,373	22.17	122,406	114,735	9.31
	merged	115,128,459	84,993,382	16,646,073	11,089,980	1,992,591	854,541	69.31	668,225	504,262	40.90
Bacho Kiro BK-1653	A11203	31,611,263	23,452,810	7,400,872	4,955,232	1,574,839	644,227	52.25	188,629	171,442	13.90
	A12363	30,529,019	22,310,950	5,876,676	4,032,969	1,629,916	585,937	47.52	159,277	146,519	11.88
	A12562	20,926,241	14,800,165	3,715,610	2,581,475	1,039,486	592,899	48.09	158,742	146,159	11.85
	A12950	20,558,862	14,605,842	3,625,387	2,533,013	996,740	576,910	46.79	148,692	137,858	11.18
	A15722	31,694,836	16,470,059	7,508,034	5,902,569	1,098,165	620,721	50.34	158,615	147,452	11.96
	merged	135,320,221	91,639,826	28,126,579	20,005,258	6,339,146	1,062,658	86.13	813,955	577,031	46.80
Oase1	A12968*	18,310,229	12,226,533	883,648	579,817	230,378	201,331	16.33	49,345	48,955	3.97
	A12967*	17,191,082	11,647,238	400,609	264,188	112,986	107,796	8.74	20,594	21,029	1.71
	A12384	17,579,948	11,275,842	948,711	654,060	69,694	66,541	5.40	15,525	15,625	1.27
	A12590	21,813,393	14,214,612	1,047,462	701,004	66,203	63,330	5.14	16,368	16,399	1.33
	A12955	19,148,461	12,500,236	669,842	437,921	59,770	57,511	4.66	14,455	14,596	1.18
	F9015	21,804,293	13,452,555	928,397	613,026	52,163	50,564	4.10	12,978	13,088	1.06
	merged	115,847,406	75,317,016	4,878,669	3,250,016	591,194	429,569	34.84	129,265	121,388	9.84

***** New libraries prepared from two extracts used in a previous study (*Fu et al.*[8])

Table S2.8 Summary statistics of the merged data of Bacho Kiro and *Oase1* DNA libraries captured with the SNP Panels 1, 2 and 3 comprising 2.2 million sites ("2200k"[8,15]). Results per library detailed in the table. The number of SNPs on target are determined using the unique fragments longer than 35 base pairs (L≥35 bp) with mapping quality of at least 25 (MQ≥25) and that overlap ~2.2 million SNPs of the "390k"[15], "840k"[8] and "1000k" arrays[8].

	All fragments								Fragments with terminal C-to-T substitutions		
Specimen	**Library ID**	**Number of sequenced fragments**	**Number of fragments ≥35 bp**	**Number of mapped fragments ≥35bp, MQ≥25**	**Number of mapped fragments on target ≥35bp, MQ≥25**	**Number of unique fragments on target ≥35bp, MQ≥25**	**Number of SNPs on target**	**% of SNPs on target**	**Number of deaminated fragments on target ≥35bp, MQ≥25**	**Number of SNPs on target**	**% of SNPs on target**
Bacho Kiro F6-620	A11197	56,817,171	42,739,090	15,936,366	11,244,167	4,115,646	1,504,437	70.15	1,058,735	764,952	35.67
	A12357	46,412,901	34,943,528	12,776,135	9,297,117	3,915,997	1,447,043	67.48	945,338	698,557	32.57
	A12550	29,523,451	21,651,782	7,079,392	5,086,346	2,557,164	1,184,154	55.22	605,245	494,054	23.04
	A12944	27,592,961	20,684,874	6,550,313	4,721,438	2,285,148	1,107,439	51.64	535,144	444,966	20.75
	A15716	21,068,663	16,897,935	6,573,652	4,739,589	2,148,695	1,110,491	51.78	494,820	424,879	19.81
	merged	181,415,147	136,917,209	48,915,858	35,088,657	15,022,650	1,867,749	87.09	3,639,282	1,362,667	64.54
Bacho Kiro AA7-738	A11198	58,681,066	43,053,237	739,703	450,345	34,952	33,992	1.59	13,082	13,288	0.62
	A12358	16,676,690	12,484,437	289,033	191,569	33,009	32,780	1.53	8,706	8,920	0.42
	A12554	22,643,136	16,654,000	294,471	178,049	23,439	23,170	1.08	8,400	8,657	0.40
	A12945	22,056,042	16,732,805	254,593	153,785	24,590	24,275	1.13	9,027	9,261	0.43
	A15717	48,070,409	22,022,511	470,195	354,291	15,203	14,665	0.68	5,160	5,256	0.25
	merged	168,127,343	110,946,990	2,047,995	1,328,039	131,193	123,265	5.75	44,375	44,610	2.08
Bacho Kiro BB7-240	A11199	62,282,800	43,076,677	8,625,924	5,748,173	943,806	710,330	33.12	336,713	309,131	14.42
	A12359	52,263,445	35,252,377	6,420,632	4,419,909	861,912	661,758	30.86	296,216	275,364	12.84
	A12555	30,703,077	19,714,046	2,776,142	1,822,904	578,138	478,374	22.31	196,214	189,300	8.83
	A12946	32,007,473	22,072,415	3,446,475	2,351,070	685,063	542,274	25.29	228,867	217,287	10.13
	A15718	18,857,516	13,959,798	2,966,341	2,035,310	593,947	488,639	22.79	194,726	188,221	8.78
	merged	196,114,311	134,075,313	24,235,514	16,377,366	3,662,866	1,451,175	67.67	1,252,736	840,421	39.19
Bacho Kiro CC7-2289	A11200	52,653,555	37,943,882	132,979	55,859	9,826	9,941	0.46	2,377	2,482	0.12
	A12360	18,733,502	13,430,985	70,741	37,338	8,930	9,341	0.44	1,322	1,405	0.07
	A12556	20,392,805	14,728,695	59,180	27,596	6,592	6,789	0.32	1,346	1,404	0.07
	A12947	18,167,388	13,475,445	46,543	20,229	5,832	6,057	0.28	1,171	1,236	0.06
	A15719	20,612,547	15,740,666	60,670	28,575	6,058	6,030	0.28	1,156	1,197	0.06
	merged	130,559,797	95,319,673	370,113	169,597	37,238	37,590	1.75	7,372	7,696	0.36
Bacho Kiro CC7-335	A11201	55,301,835	41,173,364	9,565,269	6,206,717	702,397	569,300	26.55	264,767	248,606	11.59
	A12361	49,895,859	36,673,473	7,367,752	4,939,653	722,934	573,966	26.76	261,318	244,569	11.40
	A12557	30,509,418	21,993,264	3,170,647	2,035,590	529,901	440,993	20.56	196,211	187,753	8.76
	A12948	32,453,892	23,784,249	3,945,576	2,616,487	512,068	428,364	19.97	189,611	181,578	8.47
	A15720	19,432,194	15,590,987	3,504,402	2,382,864	500,486	423,567	19.75	181,570	175,325	8.18
	merged	187,593,198	139,215,337	27,553,646	18,181,311	2,967,786	1,353,413	63.11	1,093,477	776,283	36.20
Bacho Kiro BK-1653	A11203	54,170,261	40,183,676	12,422,963	8,226,929	2,352,606	1,223,725	57.06	377,170	344,695	16.07
	A12363	49,766,354	36,620,024	9,948,926	6,813,993	2,402,877	1,191,416	55.56	369,224	335,185	15.63
	A12562	32,337,191	22,878,291	5,634,204	3,836,270	1,523,656	916,582	42.74	230,660	220,383	10.28
	A12950	30,217,360	21,445,227	5,355,935	3,707,402	1,425,078	876,042	40.85	210,684	202,809	9.46
	A15722	41,216,350	20,511,006	9,294,451	7,279,052	1,393,895	868,204	40.49	199,595	193,841	9.04
	merged	207,707,516	141,638,224	42,656,479	29,863,646	9,098,112	1,728,159	80.59	1,387,333	874,287	40.77
Oase1	A12968*	28,223,311	18,752,585	1,343,789	870,557	326,422	296,458	13.82	68,880	70,514	3.29
	A12967*	26,572,354	17,978,003	611,051	394,828	157,704	156,272	7.29	28,229	29,716	1.39
	A12384	26,906,689	17,318,241	1,409,840	954,614	104,016	102,077	4.76	22,677	23,361	1.09
	A12590	32,239,343	20,968,522	1,530,134	1,010,243	96,272	94,498	4.41	23,320	23,929	1.12
	A12955	29,352,737	19,185,421	1,028,770	655,370	88,281	87,220	4.07	20,853	21,525	1.00
	F9015	31,901,491	19,700,827	1,302,320	836,823	77,891	77,405	3.61	19,184	19,785	0.92
	merged	175,195,925	113,903,599	7,225,904	4,722,435	850,586	646,646	30.15	183,143	177,336	8.27

***** New libraries prepared from two extracts used in a previous study (*Fu et al.*[8])

Table S2.9 Summary statistics of the Bacho Kiro libraries enriched for ~6.9 Mb of the Y chromosome[16]. The coverage on target is determined using the unique fragments longer than 35 base pairs (L≥35 bp) with mapping quality of at least 25 (MQ≥25) and that overlap the target regions.

	All fragments							Fragments with terminal C-to-T substitutions	
Specimen	**Library ID**	**Number of sequenced fragments**	**Number of fragments ≥35 bp**	**Number of mapped fragments ≥35bp, MQ≥25**	**Number of mapped fragments on target ≥35bp, MQ≥25**	**Number of unique fragments on target ≥35bp, MQ≥25**	**Coverage on target**	**Number of deaminated fragments on target ≥35bp, MQ≥25**	**Coverage on target**
Bacho Kiro F6-620	A11197	6,649,928	5,127,264	2,500,217	2,036,336	308,614	2.75	78,144	0.68
	A12357	5,746,174	4,429,045	2,277,437	1,869,731	350,547	3.23	83,205	0.74
	A12550	6,429,418	5,015,419	2,569,376	2,090,273	361,743	3.34	84,186	0.75
	A12944	5,272,554	3,962,253	1,868,796	1,504,334	316,018	2.86	73,418	0.64
	A15716	7,000,727	5,682,409	2,790,390	2,254,962	328,009	3.02	75,048	0.67
	merged	31,098,801	24,216,390	12,006,216	9,755,636	**1,664,931**	**15.20**	**394,001**	**3.48**
Bacho Kiro BB7-240	A11199	6,602,187	4,757,307	1,896,804	1,577,430	57,527	0.44	19,984	0.15
	A12359	6,987,822	5,099,681	2,168,018	1,813,504	58,667	0.45	19,984	0.15
	A12555	8,244,030	5,797,923	2,447,936	2,042,714	63,411	0.49	21,114	0.16
	A12946	6,516,377	4,719,122	1,843,243	1,506,249	70,092	0.55	22,889	0.18
	A15718	6,816,864	5,315,156	1,923,820	1,585,029	65,126	0.52	21,059	0.16
	merged	35,167,280	25,689,189	10,279,821	8,524,926	**314,823**	**2.46**	**105,030**	**0.80**
Bacho Kiro CC7-335	A11201	5,892,475	4,509,883	1,889,636	1,558,502	35,318	0.26	13,064	0.10
	A12361	6,960,643	5,403,081	2,256,934	1,878,258	42,808	0.32	15,162	0.11
	A12557	10,484,235	7,808,450	3,181,164	2,638,950	46,134	0.34	16,888	0.12
	A12948	7,246,254	5,614,926	2,143,855	1,759,374	39,615	0.30	14,272	0.11
	A15720	7,224,312	5,900,108	2,279,432	1,882,344	39,383	0.30	13,894	0.10
	merged	37,807,919	29,236,448	11,751,021	9,717,428	**203,258**	**1.52**	**73,280**	**0.54**

564 **Table S2.10 Contamination estimates for Bacho Kiro Cave and *Oase 1* specimens.**

Specimen	Mitochondrial DNA contamination estimates		Sex-based contamination estimates for male individuals (ANGSD)[24] >200 SNPs covered		AuthentiCT[27] contamination estimates
	all fragments [95% CI]	deaminated fragments [95% CI]	all fragments [SE]	deaminated fragments [SE]	all fragments [SE]
Bacho Kiro F6-620	0.19 [0.08-0.44]	0.12 [0.02-0.65]	1.62 [0.12]	1.09 [0.40]	2.38 [0.54]
Bacho Kiro AA7-738	0.75 [0.21-2.70]	1.59 [0.28-8.46]	-	-	11.05 [0.36]
Bacho Kiro BB7-240	2.91 [2.21-3.83]	0.43 [0.15-1.26]	2.75 [0.37]	1.27 [1.03]	4.72 [0.42]
Bacho Kiro CC7-2289	1.00 [0-2.00]	0 [0-0.05]	-	-	42.36 [0.64]
Bacho Kiro CC7-335	0.42 [0.21-0.83]	0 [0-0.49]	3.41 [0.53]	2.13 [1.24]	4.46 [0.31]
Bacho Kiro BK-1653	1.63 [1.19-2.22]	1.14 [0.39-3.30]	-	-	3.53 [0.71]
Oase1 new extract	46.22 [40.50-52.39]	4.51 [0-9.34]	21.74 [4.56]	-	23.62 [0.44]
Oase1 old extracts	68.13 [62.48-73.29]	9.04 [2.83-15.25]			28.98 [0.48]

565 *SE – standard error

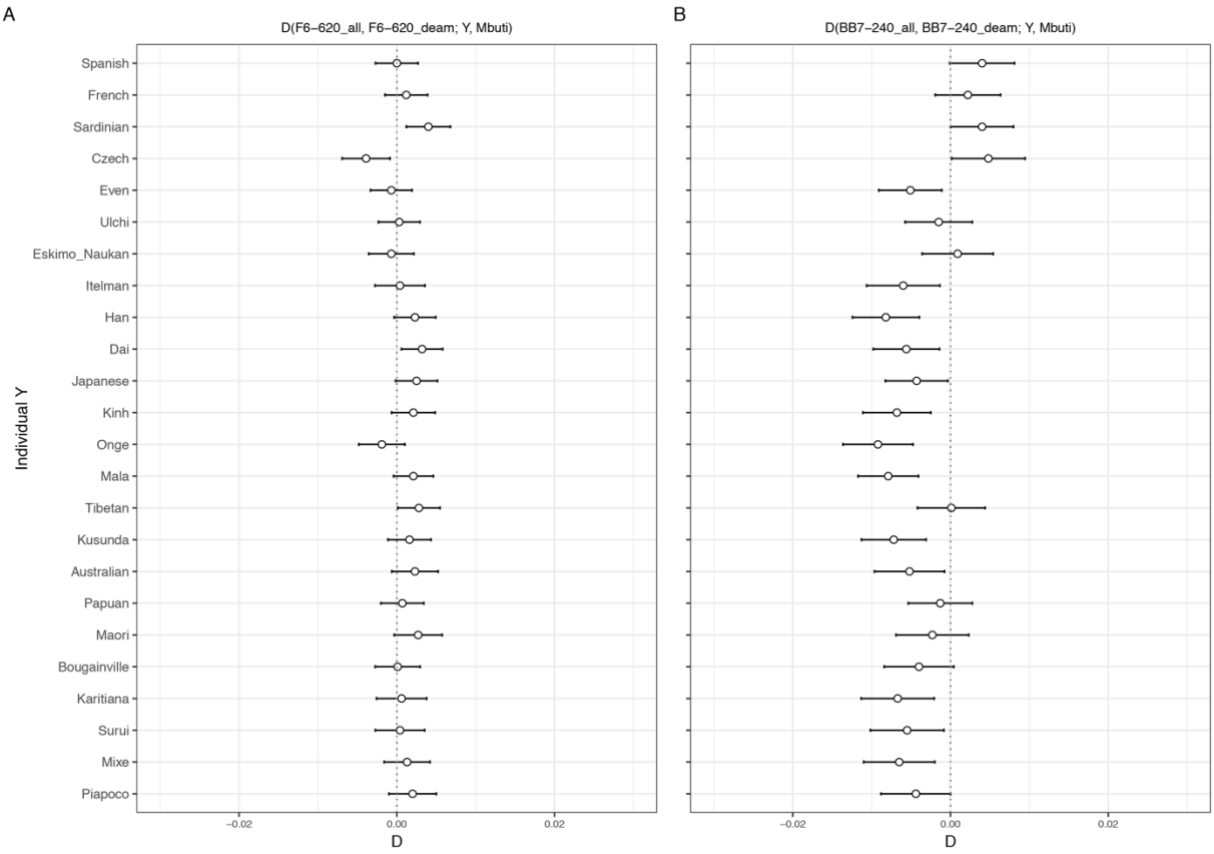

Figure S2.1 Statistics of the form *D(Bacho Kiro$_1$ all fragments, Bacho Kiro$_1$ deaminated fragments; Test, Mbuti)* comparing derived allele sharing between all fragments and deaminated fragments only from a given specimen with a present-day human population from SGDP[29]. A) Bacho Kiro *F6-620* and **B)** Bacho Kiro *BB7-240*. Points plotted on the *x*-axes correspond to the calculated *D*-values using ADMIXTOOLS[27] and as implemented in R-packge *admixr*[28]. Open circles indicate a non-significant Z-score, or |Z| < 3. Whiskers correspond to one standard error (SE) calculated using a Weighted Block Jackknife[27,30] and a block size of 5 Mb across all autosomes of "2200k" SNP Panel[8,15] covered by both all and deaminated DNA fragments of Bacho Kiro *F6-620* (panel A, n(SNPs) = 1,286,485) and Bacho Kiro *BB7-240* (panel B, n(SNPs) = 785,445). Three Mbuti individuals from SGDP[29] were used as outgroup.

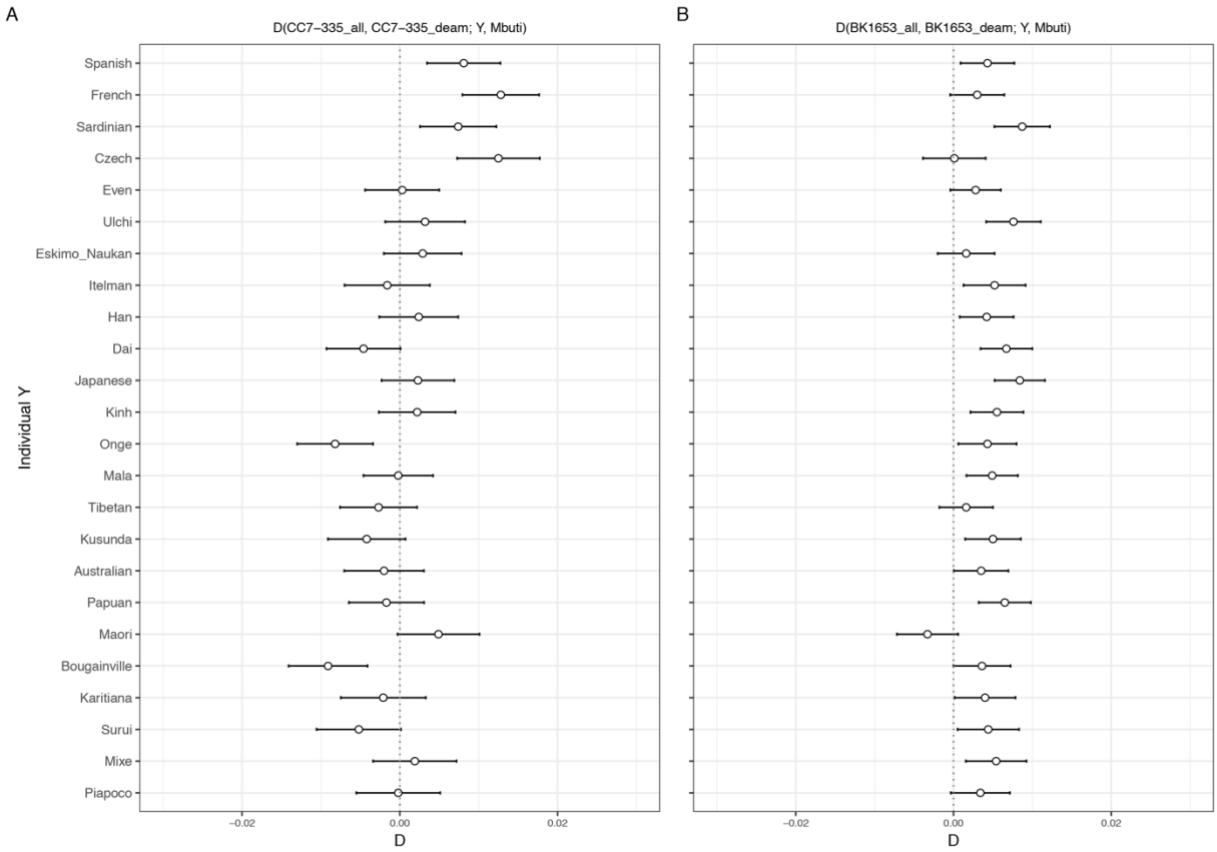

Figure S2.2 Statistics of the form *D(Bacho Kiro$_1$ all fragments, Bacho Kiro$_1$ deaminated fragments; Test, Mbuti)* comparing derived allele sharing between all fragments and deaminated fragments only from a given specimen with a present-day human population from SGDP[29]. A) Bacho Kiro *CC7-335* and **B)** Bacho Kiro *BK1653*. Points plotted on the x-axes correspond to the calculated *D*-values using ADMIXTOOLS[27] and as implemented in R-packge *admixr*[28]. Open circles indicate a non-significant Z-score, or |Z| < 3. Whiskers correspond to one standard error (SE) calculated using a Weighted Block Jackknife[27,30] and a block size of 5 Mb across all autosomes of "2200k"[8,15] SNP Panel covered by both all and deaminated DNA fragments of Bacho Kiro *CC7-335* (panel A, n(SNPs) = 720,319) and Bacho Kiro *BK1653* (panel B, n(SNPs) = 822,323). Three Mbuti individuals from SGDP[29] were used as outgroup.

Supplementary Information 3

Datasets for downstream analyses

We merged the data from the newly sequenced specimens detailed in the Supplementary Information 2 with datasets of previously published ancient and present-day humans, as well as the archaics. We used three different SNP panels ("1240k", "2240k" and "Archaic admixture") for all downstream analyses.

Analysis panels

"1240K" panel

This panel consists of combined 1,233,013 SNPs from the Panel 1 detailed in *Haak et al.* ("390k")[1] and the Panel 2 detailed in Fu *et al.* ("840k")[2]. These data include genotypes of 2,109 ancient and 2,974 present-day individuals compiled from published studies and available in the EIGENSTRAT format[3] through the https://reich.hms.harvard.edu/downloadable-genotypes-present-day-and-ancient-dna-data-compiled-published-papers/ (version 37.2, released February 22, 2019).

"2200K" panel

This panel consists of an extended panel of SNPs represented in the "1240k" together with the SNP Panel 3 detailed in *Fu et al.* ("1000k")[2] , for a total of 2,144,502 SNPs across the genome[2,4]. These data include published genetic data of ancient modern humans obtained through hybridization captures[2,4,5] and a range of present-day[6-8] and ancient modern humans[9-24], as well as the archaics[7,8,25-27], for which whole-genome shotgun data of varying coverage are available. For all low-coverage individuals we randomly sampled an allele at these ~2.2 million SNPs which passed the filters described in the Supplementary Information 2 (unique fragments of at least 35 bp with a mapping quality ≥25 and a base quality ≥20). For the high-coverage individuals we used their respective published genotypes intersecting ~2.2 million SNPs, with the exception of *Ust'Ishim*[23], the *Altai* Neandertal[7], the *Denisova 3* individual[8], *Loschbour*[19] and *Stuttgart*[19] for which we used the genotypes re-called with snpAD[28], and as described in detail in *Prüfer et al.*[25].

"Archaic admixture" panel

"Archaic admixture" panel consists of 1,749,385 (~1.7 million) SNPs informative about the Neandertal and Denisovan ancestry in a studied individual[2]. These data include 21 ancient modern humans directly enriched for these sites[2,4,5], as well as the genotypes of present-day[6-8] and ancient modern humans[9-24], as well as the archaics[7,8,25-27], for which whole-genome shotgun data are available and that were intersected with ~1.7 million SNPs of the "Archaic admixture" panel using *BEDTools*[29] (version: 2.24.0).

References for SI3:

1 Haak, W. *et al.* Massive migration from the steppe was a source for Indo-European languages in Europe. *Nature* **522**, 207-211, doi:10.1038/nature14317 (2015).

2 Fu, Q. *et al.* An early modern human from Romania with a recent Neanderthal ancestor. *Nature* **524**, 216-219, doi:10.1038/nature14558 (2015).

3 Patterson, N. *et al.* Ancient admixture in human history. *Genetics* **192**, 1065-1093, doi:10.1534/genetics.112.145037 (2012).

4 Fu, Q. *et al.* The genetic history of Ice Age Europe. *Nature* **534**, 200-205, doi:10.1038/nature17993 (2016).

5 Yang, M. A. *et al.* 40,000-Year-Old Individual from Asia Provides Insight into Early Population Structure in Eurasia. *Curr. Biol.* **27**, 3202-3208. e3209, doi: 10.1016/j.cub.2017.09.030 (2017).

6 Mallick, S. *et al.* The Simons Genome Diversity Project: 300 genomes from 142 diverse populations. *Nature* **538**, 201-206, doi:10.1038/nature18964 (2016).

7 Prüfer, K. *et al.* The complete genome sequence of a Neanderthal from the Altai Mountains. *Nature* **505**, 43-49, doi:10.1038/nature12886 (2014).

8 Meyer, M. *et al.* A high-coverage genome sequence from an archaic Denisovan individual. *Science* **338**, 222-226, doi:10.1126/science.1224344 (2012).

9 Seguin-Orlando, A. *et al.* Genomic structure in Europeans dating back at least 36,200 years. *Science* **346**, 1113-1118, doi:10.1126/science.aaa0114 (2014).

10 Raghavan, M. *et al.* Upper Palaeolithic Siberian genome reveals dual ancestry of Native Americans. *Nature* **505**, 87-91, doi:10.1038/nature12736 (2014).

11 Rasmussen, M. *et al.* Ancient human genome sequence of an extinct Palaeo-Eskimo. *Nature* **463**, 757-762, doi:10.1038/nature08835 (2010).

12 Rasmussen, M. *et al.* The genome of a Late Pleistocene human from a Clovis burial site in western Montana. *Nature* **506**, 225-229, doi:10.1038/nature13025 (2014).

13 Rasmussen, M. *et al.* The ancestry and affiliations of Kennewick Man. *Nature* **523**, 455-458, doi:10.1038/nature14625 (2015).
14 Sikora, M. *et al.* Ancient genomes show social and reproductive behavior of early Upper Paleolithic foragers. *Science* **358**, 659-662, doi: 10.1126/science.aao1807 (2017).
15 Sikora, M. *et al.* The population history of northeastern Siberia since the Pleistocene. *Nature* **570**, 182-188, doi: 10.1038/s41586-019-1279-z (2019).
16 Olalde, I. *et al.* Derived immune and ancestral pigmentation alleles in a 7,000-year-old Mesolithic European. *Nature* **507**, 225-228, doi:10.1038/nature12960 (2014).
17 Gallego Llorente, M. *et al.* Ancient Ethiopian genome reveals extensive Eurasian admixture throughout the African continent. *Science* **350**, 820-822, doi:10.1126/science.aad2879 (2015).
18 Keller, A. *et al.* New insights into the Tyrolean Iceman's origin and phenotype as inferred by whole-genome sequencing. *Nat. Commun.* **3**, 698, doi:10.1038/ncomms1701 (2012).
19 Lazaridis, I. *et al.* Ancient human genomes suggest three ancestral populations for present-day Europeans. *Nature* **513**, 409-413, doi:10.1038/nature13673 (2014).
20 Gamba, C. *et al.* Genome flux and stasis in a five millennium transect of European prehistory. *Nat. Commun.* **5**, 5257, doi:10.1038/ncomms6257 (2014).
21 Moreno-Mayar, J. V. *et al.* Terminal Pleistocene Alaskan genome reveals first founding population of Native Americans. *Nature* **553**, 203-207, doi: 10.1038/nature25173 (2018).
22 Moreno-Mayar, J. V. *et al.* Early human dispersals within the Americas. *Science* **362**, eaav2621, doi:10.1126/science.aav2621 (2018).
23 Fu, Q. *et al.* Genome sequence of a 45,000-year-old modern human from western Siberia. *Nature* **514**, 445-449, doi:10.1038/nature13810 (2014).
24 Jones, E. R. *et al.* Upper Palaeolithic genomes reveal deep roots of modern Eurasians. *Nat. Commun.* **6**, 8912, doi:10.1038/ncomms9912 (2015).
25 Prüfer, K. *et al.* A high-coverage Neandertal genome from Vindija Cave in Croatia. *Science* **358**, 655-658, doi: 10.1126/science.aao1887 (2017).
26 Hajdinjak, M. *et al.* Reconstructing the genetic history of late Neanderthals. *Nature* **555**, 652-656, doi:10.1038/nature26151 (2018).
27 Mafessoni, F. *et al.* A high-coverage Neandertal genome from Chagyrskaya Cave. *Proc. Natl. Acad. Sci. U.S.A.* **117**, 15132-15136, doi:10.1073/pnas.2004944117 (2020).

28 Prüfer, K. snpAD: An ancient DNA genotype caller. *Bioinformatics* **34**, 4165-4171, doi: 10.1093/bioinformatics/bty507 (2018).

29 Quinlan, A. R. & Hall, I. M. BEDTools: a flexible suite of utilities for comparing genomic features. *Bioinformatics* **26**, 841-842, doi: 10.1093/bioinformatics/btq033 (2010).

Supplementary Information 4

Relatedness, sex determination and Y chromosome analyses

Relatedness between different specimens

Given the fragmentary nature of human specimens recovered from Bacho Kiro Cave and our previous results demonstrating that the molar (specimen *F6-620*) and one of the fragments (specimen *AA7-738*) have an identical mtDNA sequence[1], we sought to determine the degree of relationship among IUP Bacho Kiro Cave specimens.

To assess whether specimens *F6-620* and *AA7-738* might come from the same individual, we used a similar approach as described in *Mittnik et al.*[2]. To obtain a baseline of what could be expected for specimens stemming from the same individual, we first calculated a pairwise mismatch rate between different libraries stemming from the same specimen using random allele calls of the autosomal data from the "2200k" SNP panel (Supplementary Information 3). The median value of the pairwise mismatch rate between different libraries originating from the same extract is 0.125 (interquartile range: 0.118-0.135) (Tab. S4.1 and Extended Data Fig. 2B). To obtain values of what is expected for unrelated individuals, we then calculated a pairwise mismatch rate among a range of ancient modern humans from previously published studies using random allele calls of "2200k" SNP panel (Supplementary Information 3). Median value of a pairwise mismatch rate between unrelated ancient individuals is 0.241 (interquartile range: 0.228-0.255) (Extended Data Fig. 2B).

When calculating a pairwise mismatch rate between Bacho Kiro Cave specimens, we find a pairwise mismatch rate of 0.125 between the specimens *F6-620* and *AA7-738*, which is identified as an outlier by a chi-square (χ^2) outlier test (p-value = 0.001). This value is indistinguishable of what is found between different libraries originating from the same specimen (chi-square (χ^2) outlier test > 0.05). A median value of a pairwise mismatch rate between other specimens from Bacho Kiro Cave is 0.231, with a first quartile at 0.225 and a third quartile at 0.251, which is not significantly different from what is found between pairs of unrelated ancient individuals from previously published studies (Extended Data Fig. 2B).

Furthermore, given the identical start and end coordinates of identified Neandertal segments across the genomes of *F6-620* and *AA7-738* (Supplementary Information 8, Extended Data Fig. 8A and Fig. S8.1), we conclude that the specimen *F6-620* found in the Layer J in the Main Sector of the Bacho Kiro Cave and the specimen *AA7-738* found in the Layer I of the Niche 1 belonged to the same individual.

Sex determination

We determined the sex of Bacho Kiro Cave specimens by counting the number of fragments aligning to the X chromosome and the autosomes[3,4]. Based on the expected ratios for female and male individuals, we concluded that the specimens *F6-620*, *AA7-738*, *BB7-240* and *CC7-335* belonged to male, whereas *CC7-2289* and *BK1653* belonged to female individuals (Extended Data Fig. 2A).

Y chromosome analyses

We enriched the amplified libraries of identified male individuals from Bacho Kiro Cave for ~6.9 Mb on the Y chromosome[5] and as detailed in Supplementary Information 2. Since we determined that specimens *F6-620* and *AA7-738* stem from the same individual, we enriched the amplified libraries of the specimen *F6-620* rather than *AA7-738* as they contain two orders of magnitude more nuclear DNA (Tab. S2.1, Supplementary Information 2) and have lower contamination estimates (Tab. S2.10, Supplementary Information 2).

After applying the filters detailed in Supplementary Information 2 and restricting our analyses to fragments of at least 35 bp with a mapping quality of at least 25 that overlap ~6.9 Mb of the Y chromosome, we obtained 15.2-fold coverage at these positions for Bacho Kiro Cave specimen *F6-620*, 2.5-fold for *BB7-240* and 1.5-fold for *CC7-335*, respectively (Tab. S2.9). We called an allele at each position by majority call requiring a minimum coverage of 3 for the specimens *F6-620* and *BB7-240* and of 2 for the specimen *CC7-335* using *bam-caller* (https://github.com/bodkan/bam-caller, version: 0.1). Furthermore, we used an aDNA-specific genotype caller *snpAD*[6] (version: 0.3.4) for generating genotype calls for the Bacho Kiro *F6-620* given the high coverage of the enriched Y chromosome regions for this individual.

Y chromosome haplogroup assignment

We extracted genotypes at SNP positions included in the Y-haplogroup tree from the International Society of Genetic Genealogy (ISOGG, http://www.isogg.org, version: 13.38) to determine the Y chromosome haplogroup of male individuals. Haplogroup calling was performed using *yHaplo*[7] (version: 1.0.18) using default parameters with the exception of setting the parameter *ancStopThresh* to 1e6 in order to achieve a full Y-haplogroup tree search.

All three male individuals had Y chromosome haplogroups that fell basal to the supercluster of haplogroups CT and F that are typically found outside of Sub-Saharan Africa today[8]. The specimen with the highest coverage, *F6-620*, was assigned to Y haplogroup F-M89. Bacho Kiro *F6-620* carries 22 out of 25 defining mutations of C and FT described by

Karafet et al.[8], with no fragments covering three additional defining mutations (M213, P142, and P187). Next to these 22 mutations, *F6-620* carries three additional mutations that have been identified to define haplogroup F: M235, P316, and L132.1 (ISOGG, version 13.38). Specimens *BB7-240* and *CC7-335* were both identified as having Y haplogroup C1 with the defining SNP F3393. However, due to their lower coverage and only three and two additional mutations defining haplogroup C, respectively, it was not possible to further assess the exact location of these lineages within haplogroup C.

Both haplogroups F and C1 are rare in present-day individuals. While lineages of haplogroup C are found commonly in males from East Asia and Oceania, haplogroup F and C1 and were only found in a few males from mainland Southeast Asia and Japan[9,10]. Therefore, it had been hypothesized that these haplogroups emerged in Asia after the human migration out of Africa. However, since the coalescent time for the dispersal of all non-African haplogroups, including C and F, has been estimated to 47-52 kya (95% CI: 36-62 kya)[11] and thus overlaps with the estimated age of the Bacho Kiro Cave specimens, it is more plausible to assume that these Y chromosome haplogroups emerged closely after the migration out of Africa and spread through Eurasia before being later replaced in all parts of Eurasia but East Asia and Oceania.

References SI4:

1 Hublin, J.-J. et al. Initial Upper Palaeolithic Homo sapiens from Bacho Kiro Cave, Bulgaria. *Nature* **581**, 299-302, doi:10.1038/s41586-020-2259-z (2020).

2 Mittnik, A. *et al.* Kinship-based social inequality in Bronze Age Europe. *Science* **366**, 731-734, doi: 10.1126/science.aax6219 (2019).

3 Meyer, M. *et al.* Nuclear DNA sequences from the Middle Pleistocene Sima de los Huesos hominins. *Nature* **531**, 504-507, doi:10.1038/nature17405 (2016).

4 Fu, Q. *et al.* The genetic history of Ice Age Europe. *Nature* **534**, 200-205, doi:10.1038/nature17993 (2016).

5 Petr, M. *et al.* The evolutionary history of Neanderthal and Denisovan Y chromosomes. *Science* **369**, 1653-1656, doi: 10.1126/science.abb6460 (2020).

6 Prüfer, K. snpAD: An ancient DNA genotype caller. *Bioinformatics* **34**, 4165-4171, doi: 10.1093/bioinformatics/bty507 (2018).

7 Poznik, G. D. Identifying Y-chromosome haplogroups in arbitrarily large samples of sequenced or genotyped men. *bioRxiv*, 088716 (2016).

8 Karafet, T. M. *et al.* New binary polymorphisms reshape and increase resolution of the human Y chromosomal haplogroup tree. *Genome Res.* **18**, 830-838, doi: 10.1101/gr.7172008 (2008).
9 Poznik, G. D. *et al.* Punctuated bursts in human male demography inferred from 1,244 worldwide Y-chromosome sequences. *Nat. Genet.* **48**, 593-599, doi: 10.1038/ng.3559 (2016).
10 Kutanan, W. *et al.* Contrasting paternal and maternal genetic histories of Thai and Lao populations. *Mol. Biol. Evol.* **36**, 1490-1506, doi: 10.1093/molbev/msz083 (2019).
11 Karmin, M. *et al.* A recent bottleneck of Y chromosome diversity coincides with a global change in culture. *Genome Res.* **25**, 459-466, doi: 10.1101/gr.186684.114 (2015).

Table S4.1 The pairwise mismatch rate between different libraries of Bacho Kiro Cave specimens originating from the same extract.

Specimen	Library1	Library2	nSNPs	Number of mismatches	Mismatch	Specimen	Library1	Library2	nSNPs	Number of mismatches	Mismatch
BK_F6_620	A11197	A12357	1,149,331	140,259	0.12	BK_CC7_2289	A11200	A12360	82	9	0.11
	A11197	A12550	972,999	118,929	0.12		A11200	A12556	56	12	0.21
	A11197	A12944	919,264	112,759	0.12		A11200	A12947	46	9	0.20
	A11197	A15716	907,171	111,301	0.12		A11200	A15719	57	15	0.26
	A12357	A12550	951,472	115,727	0.12		A12360	A12556	44	10	0.23
	A12357	A12944	900,051	109,650	0.12		A12360	A12947	65	17	0.26
	A12357	A15716	888,549	108,622	0.12		A12360	A15719	59	13	0.22
	A12550	A12944	785,946	95,928	0.12		A12556	A12947	40	5	0.13
	A12550	A15716	766,463	93,566	0.12		A12556	A15719	38	6	0.16
	A12944	A15716	728,129	89,263	0.12		A12947	A15719	33	5	0.15
BK_AA7_738	A11198	A12358	798	118	0.15	BK_CC7_335	A11201	A12361	184,218	24,549	0.13
	A11198	A12554	645	82	0.13		A11201	A12557	148,295	19,700	0.13
	A11198	A12945	650	71	0.11		A11201	A12948	143,923	19,136	0.13
	A11198	A15717	413	45	0.11		A11201	A15720	140,618	19,035	0.14
	A12358	A12554	605	75	0.12		A12361	A12557	153,709	20,794	0.14
	A12358	A12945	636	80	0.13		A12361	A12948	149,491	20,276	0.14
	A12358	A15717	408	56	0.14		A12361	A15720	146,432	20,073	0.14
	A12554	A12945	508	54	0.11		A12557	A12948	122,988	16,362	0.13
	A12554	A15717	321	42	0.13		A12557	A15720	119,343	16,020	0.13
	A12945	A15717	313	39	0.12		A12948	A15720	116,575	15,815	0.14
BK_BB7_240	A11199	A12359	270,665	36,026	0.13	BK_1653	A11203	A12363	825,158	94,016	0.11
	A11199	A12555	205,160	27,372	0.13		A11203	A12562	661,181	75,081	0.11
	A11199	A12946	232,601	31,271	0.13		A11203	A12950	635,860	72,355	0.11
	A11199	F9162	207,892	28,194	0.14		A11203	A15722	623,297	72,535	0.12
	A12359	A12555	194,282	25,974	0.13		A12363	A12562	659,532	75,433	0.11
	A12359	A12946	220,265	29,906	0.14		A12363	A12950	633,979	72,743	0.11
	A12359	A15718	198,899	27,313	0.14		A12363	A15722	617,845	71,759	0.12
	A12555	A12946	171,637	23,117	0.13		A12562	A12950	522,808	59,664	0.11
	A12555	A15718	153,784	21,068	0.14		A12562	A15722	509,476	59,031	0.12
	A12946	A15718	174,514	23,938	0.14		A12950	A15722	493,663	57,293	0.12

Supplementary Information 5

Population relationships

Principal Component Analysis (PCA)

As a first assessment of the genetic affinities of the studied individuals, we carried out Principal Component Analysis (PCA) using *smartpca* from the EIGENSOFT package[1,2]. We used 2,970 present-day humans genotyped on 597,573 SNPs of the Affymetrix Human Origins array[3] (https://reich.hms.harvard.edu/downloadable-genotypes-present-day-and-ancient-dna-data-compiled-published-papers, version V37.2, released February 2019) to estimate the eigenvectors. We then projected 22 ancient individuals older than 30,000 years before present (BP)[4-8] with more than 30,000 of the informative SNPs covered onto the plane defined by these eigenvectors using the 'lsqproject' option in *smartpca*[1] (Extended Data Fig. 2C). We further restricted constructing principle components to a set of 1,444 present-day Eurasians and Native Americans, and repeated the projection of 22 ancient individuals onto the plane defined by these eigenvectors (Extended Data Fig. 2D).

In the first PCA plot relating present-day African and non-African populations, IUP Bacho Kiro Cave individuals fall closer to present-day non-Africans than to Africans (Extended Data Fig. 2C). In the second PCA plot focused on present-day non-African populations, IUP Bacho Kiro Cave individuals fall close to the origin, similar to the ~45,000-year-old individual from Siberia (*Ust'Ishim*)[4] and the ~40,000-year-old individual from Romania (*Oase1*)[5] (Extended Data Fig. 2D). In contrast, Aurignacian individual from Bacho Kiro Cave, *BK1653*, forms a cluster with later Upper Palaeolithic (UP) individuals from Western Eurasia which is shifted away from the centre and towards present-day Western Eurasians in both PCA plots (Extended Data Fig. 2C and D).

Outgroup f3-statistics

We computed the statistics of the form *f3(X, Y; Mbuti)*, which measures the amount of shared genetic drift between populations X and Y since their separation from an outgroup[3]. We calculated *f3(IUP BK, Y; Mbuti)* for the three IUP Bacho Kiro Cave individuals (Fig. 2A, Tab. S5.1, Fig. S5.1) and *f3(BK1653, Y; Mbuti)* (Tab. S5.5 and Extended Data Fig. 3B) as implemented in the R package *admixr*[9] (version: 0.7.1) and using 263 present-day individuals from the Simons Genome Diversity Project (SGDP)[10]. Three Mbuti individuals from the same panel were used as outgroup. Fig. 2A and Tab. S5.1 were calculated using a pool of the three

IUP Bacho Kiro individuals (*F6-620, BB7-240 and CC7-335*, nsnps = 1,813,821), whereas panels in the Fig. S5.1 and Tab. S5.2-S5.4. show the results for each individual separately.

We find that IUP Bacho Kiro individuals share more genetic drift with present-day populations from East Asia, Central Asia and the Americas (Fig. 2A, Fig. S5.1, Tab. S5.1-S5.4), similar to *Ust'Ishim*[4] (Fig. S5.2A) and *Oase1*[5] (Fig. S5.2B). In contrast, *BK1653* shares more genetic drift with present-day West Eurasians (Extended Data Fig. 3B, Tab. S5.5), similar to other UP individuals from Europe from ~38,000 years BP onwards[6,11] (Extended Data Fig. 3C).

We performed the genetic clustering of ancient modern humans using outgroup f_3-*statistics*[6], restricting this analysis to ancient individuals with at least 30,000 SNPs on the "2200k" Panel. We find that IUP Bacho Kiro individuals share more drift with each other than with other ancient humans (Extended Data Fig. 3A), whereas *BK1653* shares most drift with later UP individuals in Europe, specifically ~35,000-year-old *GoyetQ116-1* from Belgium and the members of the 'Vêstonice' genetic cluster[6] (Extended Data Fig. 3A).

Relationship of Bacho Kiro individuals to present-day populations

In order to investigate the relationship of Bacho Kiro Cave individuals to present-day humans in more detail, we used genotype calls of 263 present-day humans from the Simons Genome Diversity Project (SGDP)[10] overlapping "2200k" SNPs, and as described in the Supplementary Information 3. We used *D-statistics*[3] (version: v5.1) as implemented in the R package *admixr*[9] (version: 0.7.1) to infer the relationships among individuals, computing standard errors using a Weighted Block Jackknife[3,12] across all autosomes with equally sized blocks of 5 million base pairs (5 Mb). Guided by the results of the PCA and outgroup f_3*-statistics*, we first computed *D (African, non-African; Bacho Kiro Cave individual, Chimpanzee)* using genomes of present-day Mbuti, Yoruba, San and Dinka, as well as genomes of present-day non-Africans from SGDP[10], and the genome of a chimpanzee (*panTro2*) as outgroup. We find that all Bacho Kiro Cave individuals are significantly closer to present-day non-Africans than to present-day Africans ($|Z| > 41.49$, Fig. S5.3-S5.6).

We further explored whether Bacho Kiro Cave individuals are particularly close to a certain present-day population outside of Africa by calculating *D (non-African*$_1$*, non-African*$_2$*; Bacho Kiro Cave individual, Chimpanzee)* and *D (non-African*$_1$*, non-African*$_2$*; Bacho Kiro Cave individual, Mbuti).* We find that IUP Bacho Kiro Cave individuals share significantly more alleles with present-day East Asians, Southeast Asians and Native Americans than with present-day Europeans (Fig. S5.7 and S5.8). However, present-day Europeans derive part of

their ancestry from a population that diverged from other non-Africans before they diverged from each other ('a Basal Eurasian' population)[13-15] and similar results are obtained when substituting IUP Bacho Kiro Cave individuals in these statistics with *Oase1*[5] or *Ust'Ishim*[4] (Fig. S5.9 and S5.10), both of whom are known not to have contributed their ancestry to later populations.

Thus, we replaced present-day Europeans in these statistics with Upper Palaeolithic[6,7,11] and Mesolithic[13] individuals that lack Basal Eurasian ancestry. Whereas in those instances, and with the additional data from *Oase 1*, both *Oase 1* and *Ust'Ishim* share equally many alleles with Europeans before the introduction of agriculture as with present-day East Asians and Native Americans[5], ($|Z| < 3$, Extended Data Fig. 4B and C), IUP Bacho Kiro Cave individuals continue to share significantly more alleles with present-day East Asians and Native Americans, and some Central Asians and Siberians from SGDP than with pre-agricultural Europeans such as the ~38,000-year-old *Kostenki 14* ($3.08 \leq |Z| \leq 5.32$, Extended Data Fig. 4A). These results remain stable after restricting the analyses to transversion polymorphisms which are not susceptible to errors due to aDNA modifications ($2.22 \leq Z \leq 3.92$, Fig. S5.13).

Given the slightly higher Neandertal ancestry in present-day East Asians than in West Eurasians[16,17] and the higher Neandertal ancestry in IUP Bacho Kiro individuals (see Supplementary Information 7 and 8), we substituted Mbuti as outgroup in *D(pre-agricultural European, non-African$_2$; IUP Bacho Kiro, Outgroup)* with the high coverage genome of *Vindija 33.19* Neandertal[17] to account for a possible attraction to East Asians due to the higher Neandertal ancestry. We find, however, that the results of these statistics remain significant regardless of the outgroup ($3.05 \leq Z \leq 5.90$, Fig. S5.14).

In contrast to the IUP Bacho Kiro Cave individuals, *BK1653* that lived ~11,000 years later[18,19] shares significantly more alleles with present-day Europeans than with any other superpopulation in SGDP[10] (Fig. S5.11 and S5.12), as it was previously found for other Upper Palaeolithic individuals from Western Eurasia starting with the ~38,000-year-old *Kostenki14* from Russia[6,11].

Relationship of Bacho Kiro Cave individuals other ancient humans

We computed *D(ancient$_1$, ancient$_2$; IUP Bacho Kiro, Mbuti)* and *D(ancient$_1$, IUP Bacho Kiro; ancient$_2$, Mbuti)* for a range of ancient modern humans using "1240k" and/or "2200k" SNP Panels, depending on the set of sites for which the data of previously published individuals are available (see Supplementary Information 3 for dataset details). By computing *D(IUP Bacho Kiro$_1$, IUP Bacho Kiro$_2$; X, Mbuti)* we find that the *IUP Bacho Kiro F6-620, BB7-240* and

CC7-335 form a clade to exclusion of other ancient individuals (all |Z| <3, Tab. S5.8-S5.10). Since we were able to recover only 7,696 SNPs on the "2200k" Panel for the IUP *Bacho Kiro CC7-2289* (Extended Data Tab. 1, Supplementary Information 2, Tab. S2.8), we used *D(IUP Bacho Kiro$_1$, X; Bacho Kiro CC7-2289, Mbuti)* to explore broad population affiliations of this individual. We find, to the limits of our resolution, that she on average shares significantly more alleles with other IUP Bacho Kiro Cave individuals than with other ancient modern humans (Tab. S5.7). Furthermore, we find *D(IUP Bacho Kiro$_1$, IUP Bacho Kiro$_2$; IUP Bacho Kiro$_3$, Mbuti)*~ 0 for all combinations of IUP Bacho Kiro Cave individuals (Tab. S5.6).

Interestingly, when comparing IUP Bacho Kiro Cave individuals to other early Upper Palaeolithic humans from Eurasia, we find that they share significantly more alleles with the ~40,000-year-old *Tianyuan* individual from China[20] than with the ~38,000-year-old *Kostenki14* from west Russia ($3.17 \leq |Z| \leq 4.21$, Fig. 2B and C, Tab. S5.12-S5.14). Furthermore, IUP *Bacho Kiro F6-620* shares significantly more alleles with ancient Native Americans such as the ~13,000-year-old *Anzick*[21], ~11,000-year-old *Upward Sun River* and *Spirit Cave* individuals[22,23], the ~9,000-year-old *Kennewick*[24], and even with the ~4,000-year-old *Saqqaq*[25] than with *Kostenki14* ($3.70 \leq |Z| \leq 4.72$, Fig. 2C, Tab. S5.15). From other West Eurasian Upper Palaeolithic humans, IUP Bacho Kiro Cave individuals share significantly more derived alleles with *Oase1* ($3.56 \leq |Z| \leq 4.26$, Fig. 2C, Tab. S5.12-S5.14) and the ~35,000-year-old *Goyet Q116-1* from Belgium ($3.24 \leq |Z| \leq 4.25$, Fig. 2C, Tab. S5.12-S5.14) than with *Kostenki14*. We note, however, that the higher proportion of Neandertal ancestry (see Supplementary Information 7 and 8) could be driving the excess of alleles shared by the IUP Bacho Kiro Cave individuals and the *Oase1*. Alternatively, the IUP Bacho Kiro Cave individuals and *Oase1* could belong to related but not identical populations, given that they differ in their overall relationship to later populations.

We find that *Bacho Kiro BK1653* shares significantly more alleles with later West Eurasians than with the IUP Bacho Kiro Cave individuals by *D(Test, IUP Bacho Kiro; BK1653, Mbuti)* >> 0 ($3.01 \leq |Z| \leq 17.39$) where *Test* individual is any of the later West Eurasians starting with *Kostenki14*. Specifically, *Bacho Kiro BK1653* is closest to the *GoyetQ116-1* and to the members of the 'Vêstonice' genetic cluster, i.e. individuals that lived between ~34,000 and ~26,000 years ago and were associated with the Gravettian period. Moreover, *D(GoyetQ116-1, Vestonice16; BK1653, Mbuti), D(BK1653, GoyetQ116-1; Vestonice16, Mbuti)* and *D(BK1653, Vestonice16; GoyetQ116-1, Mbuti)* are all ~0 (all |Z| < 3, Tab. S5.11 and Tab. S5.15), indicating that *BK1653* shares equally many alleles with these individuals.

References SI5:

1 Patterson, N., Price, A. L. & Reich, D. Population structure and eigenanalysis. *PLoS Genet* **2**, e190, doi:10.1371/journal.pgen.0020190 (2006).

2 Price, A. L. *et al.* Principal components analysis corrects for stratification in genome-wide association studies. *Nat. Genet.* **38**, 904-909, doi: 10.1038/ng1847 (2006).

3 Patterson, N. *et al.* Ancient admixture in human history. *Genetics* **192**, 1065-1093, doi:10.1534/genetics.112.145037 (2012).

4 Fu, Q. *et al.* Genome sequence of a 45,000-year-old modern human from western Siberia. *Nature* **514**, 445-449, doi:10.1038/nature13810 (2014).

5 Fu, Q. *et al.* An early modern human from Romania with a recent Neanderthal ancestor. *Nature* **524**, 216-219, doi:10.1038/nature14558 (2015).

6 Fu, Q. *et al.* The genetic history of Ice Age Europe. *Nature* **534**, 200-205, doi:10.1038/nature17993 (2016).

7 Sikora, M. *et al.* Ancient genomes show social and reproductive behavior of early Upper Paleolithic foragers. *Science* **358**, 659-662, doi: 10.1126/science.aao1807 (2017).

8 Sikora, M. *et al.* The population history of northeastern Siberia since the Pleistocene. *Nature* **570**, 182-188, doi: 10.1038/s41586-019-1279-z (2019).

9 Petr, M., Vernot, B. & Kelso, J. admixr—R package for reproducible analyses using ADMIXTOOLS. *Bioinformatics* **35**, 3194-3195 (2019).

10 Mallick, S. *et al.* The Simons Genome Diversity Project: 300 genomes from 142 diverse populations. *Nature* **538**, 201-206, doi:10.1038/nature18964 (2016).

11 Seguin-Orlando, A. *et al.* Genomic structure in Europeans dating back at least 36,200 years. *Science* **346**, 1113-1118, doi:10.1126/science.aaa0114 (2014).

12 Busing, F. M. T. A., Meijer, E. & Van Der Leeden, R. Delete-m jackknife for unequal m. *Statistics and Computing* **9**, 3-8, doi:Doi 10.1023/A:1008800423698 (1999).

13 Lazaridis, I. *et al.* Ancient human genomes suggest three ancestral populations for present-day Europeans. *Nature* **513**, 409-413, doi:10.1038/nature13673 (2014).

14 Lazaridis, I. *et al.* Genomic insights into the origin of farming in the ancient Near East. *Nature* **536**, 419-424, doi: 10.1038/nature19310 (2016).

15 Lazaridis, I. *et al.* Paleolithic DNA from the Caucasus reveals core of West Eurasian ancestry. *bioRxiv*, 423079 (2018).

16 Wall, J. D. *et al.* Higher levels of neanderthal ancestry in East Asians than in Europeans. *Genetics* **194**, 199-209, doi:10.1534/genetics.112.148213 (2013).

17 Prüfer, K. *et al.* A high-coverage Neandertal genome from Vindija Cave in Croatia. *Science* **358**, 655-658, doi: 10.1126/science.aao1887 (2017).
18 Hublin, J.-J. et al. Initial Upper Palaeolithic Homo sapiens from Bacho Kiro Cave, Bulgaria. *Nature* **581**, 299-302, doi:10.1038/s41586-020-2259-z (2020).
19 Fewlass, H. et al. A 14 C chronology for the Middle to Upper Palaeolithic transition at Bacho Kiro Cave, Bulgaria. *Nat. Ecol. Evol.* **4**, 794-801, doi: 10.1038/s41559-020-1136-3 (2020).
20 Yang, M. A. *et al.* 40,000-Year-Old Individual from Asia Provides Insight into Early Population Structure in Eurasia. *Curr. Biol.* **27**, 3202-3208. e3209, doi: 10.1016/j.cub.2017.09.030 (2017).
21 Rasmussen, M. *et al.* The genome of a Late Pleistocene human from a Clovis burial site in western Montana. *Nature* **506**, 225-229, doi:10.1038/nature13025 (2014).
22 Moreno-Mayar, J. V. *et al.* Terminal Pleistocene Alaskan genome reveals first founding population of Native Americans. *Nature* **553**, 203-207, doi: 10.1038/nature25173 (2018).
23 Moreno-Mayar, J. V. *et al.* Early human dispersals within the Americas. *Science* **362**, eaav2621, doi:10.1126/science.aav2621 (2018).
24 Rasmussen, M. *et al.* The ancestry and affiliations of Kennewick Man. *Nature* **523**, 455-458, doi:10.1038/nature14625 (2015).
25 Rasmussen, M. *et al.* Ancient human genome sequence of an extinct Palaeo-Eskimo. *Nature* **463**, 757-762, doi:10.1038/nature08835 (2010).

Table S5.1 Shared genetic drift between IUP Bacho Kiro Cave individuals and present-day humans as measured by *f3(IUP Bacho Kiro Cave individuals, present-day humans; Mbuti)*. Present-day modern human genomes from SGDP[10] were used. *f3* values reported were calculated using ADMIXTOOLS[3] as implemented in *admixr*[9] and were used for plotting Fig. 2A in the main text. Standard errors (SE) were computed using a Weighted Block Jackknife[3,12] across all autosomes of the "2200k" Panel using a block size of 5Mb. Number of SNPs overlapping among individuals reported in the column "nsnps".

A	B	C	f3	SE	Zscore	nsnps
IUP_BKs	She	Mbuti	0.2250	0.0034	65.94	1,241,880
IUP_BKs	Japanese	Mbuti	0.2250	0.0034	67.04	1,268,517
IUP_BKs	Ami	Mbuti	0.2240	0.0034	65.56	1,238,449
IUP_BKs	Han	Mbuti	0.2240	0.0034	65.87	1,244,308
IUP_BKs	Yi	Mbuti	0.2239	0.0034	65.67	1,245,099
IUP_BKs	Kinh	Mbuti	0.2236	0.0034	65.50	1,244,971
IUP_BKs	Lahu	Mbuti	0.2236	0.0034	66.48	1,241,407
IUP_BKs	Oroqen	Mbuti	0.2234	0.0034	65.97	1,242,864
IUP_BKs	Tujia	Mbuti	0.2234	0.0034	65.85	1,243,408
IUP_BKs	Karitiana	Mbuti	0.2234	0.0034	64.92	1,217,789
IUP_BKs	Dai	Mbuti	0.2234	0.0034	66.20	1,269,344
IUP_BKs	Sherpa	Mbuti	0.2233	0.0034	66.54	1,240,952
IUP_BKs	Tibetan	Mbuti	0.2231	0.0034	65.28	1,245,035
IUP_BKs	Dusun	Mbuti	0.2231	0.0034	65.90	1,239,008
IUP_BKs	Eskimo_Naukan	Mbuti	0.2230	0.0033	67.17	1,235,556
IUP_BKs	Miao	Mbuti	0.2230	0.0033	67.07	1,242,930
IUP_BKs	Igorot	Mbuti	0.2229	0.0034	64.82	1,235,592
IUP_BKs	Naxi	Mbuti	0.2229	0.0034	65.83	1,271,797
IUP_BKs	Korean	Mbuti	0.2228	0.0033	66.56	1,244,759
IUP_BKs	Yakut	Mbuti	0.2227	0.0035	63.87	1,245,519
IUP_BKs	Ulchi	Mbuti	0.2226	0.0033	67.12	1,242,300
IUP_BKs	Onge	Mbuti	0.2226	0.0033	66.85	1,228,377
IUP_BKs	Eskimo_Chaplin	Mbuti	0.2224	0.0034	65.25	1,196,996
IUP_BKs	Atayal	Mbuti	0.2222	0.0035	62.77	1,195,780
IUP_BKs	Eskimo_Sireniki	Mbuti	0.2222	0.0033	67.10	1,239,857
IUP_BKs	Burmese	Mbuti	0.2221	0.0033	66.75	1,249,617
IUP_BKs	Xibo	Mbuti	0.2220	0.0034	65.80	1,245,927
IUP_BKs	Thai	Mbuti	0.2219	0.0034	65.58	1,247,431
IUP_BKs	Hezhen	Mbuti	0.2219	0.0034	66.21	1,243,812
IUP_BKs	Tu	Mbuti	0.2218	0.0034	65.29	1,248,856
IUP_BKs	Even	Mbuti	0.2218	0.0034	65.33	1,272,478
IUP_BKs	Chipewyan	Mbuti	0.2217	0.0035	64.16	1,232,134
IUP_BKs	Surui	Mbuti	0.2216	0.0034	64.99	1,218,304
IUP_BKs	Daur	Mbuti	0.2216	0.0035	63.76	1,201,096
IUP_BKs	Cambodian	Mbuti	0.2215	0.0033	66.15	1,246,554
IUP_BKs	Khonda_Dora	Mbuti	0.2212	0.0034	64.56	1,199,909
IUP_BKs	Mayan	Mbuti	0.2210	0.0033	66.06	1,234,796
IUP_BKs	Piapoco	Mbuti	0.2208	0.0033	65.93	1,229,698
IUP_BKs	Itelman	Mbuti	0.2206	0.0035	63.60	1,198,070
IUP_BKs	Kurumba	Mbuti	0.2206	0.0034	65.20	1,199,474
IUP_BKs	Botocudo	Mbuti	0.2205	0.0034	64.56	1,111,320
IUP_BKs	Zapotec	Mbuti	0.2204	0.0033	66.20	1,237,121
IUP_BKs	Chane	Mbuti	0.2203	0.0034	65.07	1,196,463
IUP_BKs	Mixe	Mbuti	0.2202	0.0034	65.69	1,230,707
IUP_BKs	Kharia	Mbuti	0.2196	0.0034	64.47	1,200,711
IUP_BKs	Kusunda	Mbuti	0.2195	0.0033	66.63	1,239,127
IUP_BKs	Nahua	Mbuti	0.2193	0.0034	64.38	1,198,257
IUP_BKs	Quechua	Mbuti	0.2192	0.0033	66.56	1,255,945
IUP_BKs	Bougainville	Mbuti	0.2186	0.0034	64.98	1,232,440
IUP_BKs	Altaian	Mbuti	0.2185	0.0034	64.03	1,202,284
IUP_BKs	Kyrgyz	Mbuti	0.2184	0.0033	66.50	1,256,462
IUP_BKs	Hawaiian	Mbuti	0.2184	0.0035	63.13	1,199,752
IUP_BKs	Pima	Mbuti	0.2183	0.0034	64.41	1,229,699
IUP_BKs	Cree	Mbuti	0.2180	0.0033	66.79	1,251,803
IUP_BKs	Aleut	Mbuti	0.2171	0.0033	66.50	1,252,508
IUP_BKs	Papuan	Mbuti	0.2171	0.0034	64.18	1,300,909
IUP_BKs	Australian	Mbuti	0.2171	0.0034	64.01	1,246,350
IUP_BKs	Yadava	Mbuti	0.2170	0.0033	66.41	1,253,859
IUP_BKs	Mala	Mbuti	0.2168	0.0032	67.45	1,287,674
IUP_BKs	Chukchi	Mbuti	0.2161	0.0033	64.78	1,209,162
IUP_BKs	Tubalar	Mbuti	0.2161	0.0033	65.38	1,254,292
IUP_BKs	Mansi	Mbuti	0.2159	0.0033	65.33	1,256,117
IUP_BKs	Madiga	Mbuti	0.2157	0.0033	65.57	1,255,390
IUP_BKs	Relli	Mbuti	0.2154	0.0033	65.81	1,254,885
IUP_BKs	Irula	Mbuti	0.2153	0.0033	65.73	1,252,206
IUP_BKs	Mixtec	Mbuti	0.2152	0.0033	65.60	1,245,981
IUP_BKs	Kapu	Mbuti	0.2149	0.0033	64.35	1,256,970
IUP_BKs	Hazara	Mbuti	0.2149	0.0033	64.46	1,257,243
IUP_BKs	Uygur	Mbuti	0.2148	0.0032	66.33	1,261,144
IUP_BKs	Bengali	Mbuti	0.2144	0.0032	66.70	1,257,345
IUP_BKs	Punjabi	Mbuti	0.2137	0.0032	66.90	1,312,715
IUP_BKs	Tlingit	Mbuti	0.2133	0.0033	65.45	1,257,431
IUP_BKs	Brahmin	Mbuti	0.2125	0.0032	66.53	1,258,918
IUP_BKs	Saami	Mbuti	0.2116	0.0033	64.01	1,256,098
IUP_BKs	Sindhi	Mbuti	0.2115	0.0033	63.35	1,258,843
IUP_BKs	Pathan	Mbuti	0.2111	0.0032	65.29	1,260,590
IUP_BKs	Burusho	Mbuti	0.2110	0.0032	65.13	1,260,397
IUP_BKs	Kashmiri_Pandit	Mbuti	0.2107	0.0033	63.59	1,206,177
IUP_BKs	Finnish	Mbuti	0.2098	0.0032	66.10	1,292,610
IUP_BKs	Kalash	Mbuti	0.2095	0.0032	66.18	1,251,539
IUP_BKs	Icelandic	Mbuti	0.2095	0.0033	64.09	1,261,703
IUP_BKs	Maori	Mbuti	0.2093	0.0033	63.16	1,210,165
IUP_BKs	Czech	Mbuti	0.2093	0.0033	62.58	1,208,755
IUP_BKs	Tajik	Mbuti	0.2090	0.0032	64.67	1,258,992
IUP_BKs	Estonian	Mbuti	0.2090	0.0033	62.46	1,261,200
IUP_BKs	Bergamo	Mbuti	0.2088	0.0034	61.38	1,209,000
IUP_BKs	Russian	Mbuti	0.2087	0.0033	63.74	1,261,648
IUP_BKs	French	Mbuti	0.2080	0.0032	64.80	1,260,502
IUP_BKs	Orcadian	Mbuti	0.2080	0.0032	64.53	1,261,779
IUP_BKs	English	Mbuti	0.2077	0.0032	65.63	1,261,866
IUP_BKs	Albanian	Mbuti	0.2077	0.0033	63.88	1,208,168
IUP_BKs	Hungarian	Mbuti	0.2071	0.0033	62.86	1,262,301
IUP_BKs	Brahui	Mbuti	0.2070	0.0032	65.51	1,259,647
IUP_BKs	Greek	Mbuti	0.2070	0.0032	65.51	1,260,821
IUP_BKs	Adygei	Mbuti	0.2067	0.0032	64.85	1,261,156
IUP_BKs	North_Ossetian	Mbuti	0.2067	0.0032	64.72	1,261,983
IUP_BKs	Abkhasian	Mbuti	0.2067	0.0033	63.21	1,260,283
IUP_BKs	Polish	Mbuti	0.2065	0.0034	60.33	1,208,763
IUP_BKs	Sardinian	Mbuti	0.2063	0.0032	64.20	1,260,434
IUP_BKs	Armenian	Mbuti	0.2061	0.0033	63.30	1,233,323
IUP_BKs	Bulgarian	Mbuti	0.2059	0.0031	65.72	1,262,386
IUP_BKs	Basque	Mbuti	0.2059	0.0033	63.02	1,260,211
IUP_BKs	Balochi	Mbuti	0.2059	0.0034	60.92	1,202,820
IUP_BKs	Iranian	Mbuti	0.2056	0.0032	65.12	1,261,197
IUP_BKs	Turkish	Mbuti	0.2056	0.0033	63.00	1,261,498
IUP_BKs	Georgian	Mbuti	0.2055	0.0032	64.64	1,261,255
IUP_BKs	Chechen	Mbuti	0.2055	0.0033	62.35	1,208,291
IUP_BKs	Lezgin	Mbuti	0.2053	0.0032	64.31	1,261,140
IUP_BKs	Spanish	Mbuti	0.2052	0.0032	64.17	1,261,884
IUP_BKs	Crete	Mbuti	0.2050	0.0033	61.54	1,208,721
IUP_BKs	Tuscan	Mbuti	0.2049	0.0033	62.63	1,263,034
IUP_BKs	Iraqi_Jew	Mbuti	0.2024	0.0032	63.54	1,260,134
IUP_BKs	Makrani	Mbuti	0.2024	0.0032	63.98	1,259,368
IUP_BKs	Druze	Mbuti	0.2010	0.0031	64.31	1,260,987
IUP_BKs	Samaritan	Mbuti	0.1996	0.0032	62.18	1,202,831
IUP_BKs	Yemenite_Jew	Mbuti	0.1965	0.0031	62.83	1,260,131
IUP_BKs	Jordanian	Mbuti	0.1964	0.0031	63.22	1,296,397
IUP_BKs	BedouinB	Mbuti	0.1962	0.0031	63.58	1,255,127
IUP_BKs	Palestinian	Mbuti	0.1945	0.0031	62.31	1,299,657
IUP_BKs	Saharawi	Mbuti	0.1771	0.0030	59.31	1,270,496
IUP_BKs	Mozabite	Mbuti	0.1735	0.0030	57.64	1,271,305
IUP_BKs	Somali	Mbuti	0.1362	0.0030	45.71	1,204,964
IUP_BKs	Masai	Mbuti	0.1130	0.0026	44.20	1,270,410
IUP_BKs	Dinka	Mbuti	0.0918	0.0024	37.82	1,267,654
IUP_BKs	Mandenka	Mbuti	0.0879	0.0024	36.94	1,286,047
IUP_BKs	Gambian	Mbuti	0.0877	0.0023	37.87	1,285,227
IUP_BKs	Luo	Mbuti	0.0862	0.0023	37.45	1,279,191
IUP_BKs	BantuKenya	Mbuti	0.0853	0.0023	36.33	1,280,312
IUP_BKs	Esan	Mbuti	0.0838	0.0023	36.18	1,287,115
IUP_BKs	Luhya	Mbuti	0.0838	0.0024	35.56	1,279,996
IUP_BKs	Yoruba	Mbuti	0.0830	0.0023	36.78	1,288,387
IUP_BKs	Igbo	Mbuti	0.0819	0.0023	35.22	1,286,896
IUP_BKs	Mende	Mbuti	0.0818	0.0023	35.61	1,285,776
IUP_BKs	Lemande	Mbuti	0.0806	0.0023	35.42	1,283,720
IUP_BKs	Kongo	Mbuti	0.0794	0.0024	33.53	1,213,147
IUP_BKs	BantuHerero	Mbuti	0.0781	0.0023	34.47	1,280,684
IUP_BKs	BantuTswana	Mbuti	0.0730	0.0021	34.23	1,279,719
IUP_BKs	Biaka	Mbuti	0.0517	0.0019	27.08	1,259,090
IUP_BKs	Ju_hoan_North	Mbuti	0.0479	0.0018	25.88	1,284,494
IUP_BKs	Khomani_San	Mbuti	0.0451	0.0019	23.85	1,243,210

Table S5.2 Shared genetic drift between *Bacho Kiro F6-620* and present-day humans as measured by *f3(F6-620, present-day humans; Mbuti)*. Present-day modern human genomes from SGDP[10] were used. *f3* values reported were calculated using ADMIXTOOLS[3] as implemented in *admixr*[9] and were used for plotting Fig. S5.1A. Standard errors (SE) were computed using a Weighted Block Jackknife[3,12] across all autosomes using a block size of 5Mb. Number of SNPs overlapping among individuals reported in the column "nsnps".

A	B	C	f3	SE	Zscore	nsnps
F6_620	Japanese	Mbuti	0.2248	0.0036	62.81	1,228,053
F6_620	She	Mbuti	0.2247	0.0037	60.76	1,197,191
F6_620	Yi	Mbuti	0.2235	0.0037	61.06	1,201,115
F6_620	Karitiana	Mbuti	0.2235	0.0037	60.50	1,168,378
F6_620	Han	Mbuti	0.2234	0.0036	61.33	1,200,062
F6_620	Kinh	Mbuti	0.2232	0.0037	60.88	1,200,593
F6_620	Tujia	Mbuti	0.2231	0.0036	61.52	1,198,922
F6_620	Dai	Mbuti	0.2230	0.0036	62.01	1,228,660
F6_620	Sherpa	Mbuti	0.2230	0.0036	62.22	1,196,177
F6_620	Tibetan	Mbuti	0.2230	0.0037	60.80	1,200,705
F6_620	Dusun	Mbuti	0.2229	0.0036	61.42	1,193,697
F6_620	Eskimo_Naukan	Mbuti	0.2228	0.0035	63.08	1,189,590
F6_620	Ami	Mbuti	0.2227	0.0037	60.34	1,193,155
F6_620	Oroqen	Mbuti	0.2226	0.0036	61.15	1,198,307
F6_620	Igorot	Mbuti	0.2225	0.0037	60.10	1,189,720
F6_620	Korean	Mbuti	0.2225	0.0036	61.95	1,200,345
F6_620	Miao	Mbuti	0.2224	0.0036	62.23	1,198,347
F6_620	Lahu	Mbuti	0.2223	0.0036	61.85	1,196,775
F6_620	Yakut	Mbuti	0.2223	0.0037	59.45	1,201,060
F6_620	Naxi	Mbuti	0.2223	0.0036	61.57	1,231,524
F6_620	Eskimo_Sireniki	Mbuti	0.2223	0.0036	62.56	1,194,560
F6_620	Onge	Mbuti	0.2222	0.0036	62.48	1,181,660
F6_620	Eskimo_Chaplin	Mbuti	0.2220	0.0036	60.94	1,144,393
F6_620	Ulchi	Mbuti	0.2219	0.0036	62.47	1,197,616
F6_620	Xibo	Mbuti	0.2216	0.0036	62.24	1,201,887
F6_620	Atayal	Mbuti	0.2215	0.0038	57.77	1,143,068
F6_620	Chipewyan	Mbuti	0.2214	0.0037	59.67	1,185,370
F6_620	Burmese	Mbuti	0.2213	0.0035	62.62	1,206,044
F6_620	Hezhen	Mbuti	0.2210	0.0036	61.73	1,199,172
F6_620	Tu	Mbuti	0.2210	0.0036	60.62	1,205,016
F6_620	Thai	Mbuti	0.2210	0.0036	61.08	1,203,523
F6_620	Surui	Mbuti	0.2210	0.0037	60.21	1,169,153
F6_620	Piapoco	Mbuti	0.2207	0.0036	61.11	1,182,349
F6_620	Mayan	Mbuti	0.2206	0.0036	61.28	1,188,183
F6_620	Kurumba	Mbuti	0.2204	0.0037	59.85	1,147,705
F6_620	Daur	Mbuti	0.2204	0.0037	59.41	1,149,476
F6_620	Even	Mbuti	0.2204	0.0036	60.82	1,232,019
F6_620	Khonda_Dora	Mbuti	0.2202	0.0037	59.21	1,148,262
F6_620	Chane	Mbuti	0.2201	0.0037	59.86	1,143,287
F6_620	Mixe	Mbuti	0.2201	0.0036	61.25	1,183,413
F6_620	Zapotec	Mbuti	0.2199	0.0036	61.87	1,190,997
F6_620	Cambodian	Mbuti	0.2197	0.0036	61.51	1,202,894
F6_620	Nahua	Mbuti	0.2196	0.0037	59.82	1,145,281
F6_620	Botocudo	Mbuti	0.2195	0.0037	59.77	1,059,982
F6_620	Itelman	Mbuti	0.2190	0.0037	58.78	1,145,492
F6_620	Quechua	Mbuti	0.2190	0.0035	61.89	1,212,610
F6_620	Kharia	Mbuti	0.2186	0.0037	59.77	1,149,294
F6_620	Bougainville	Mbuti	0.2182	0.0037	58.88	1,185,863
F6_620	Pima	Mbuti	0.2180	0.0036	60.17	1,182,167
F6_620	Altaian	Mbuti	0.2180	0.0036	59.91	1,150,627
F6_620	Kusunda	Mbuti	0.2179	0.0035	61.77	1,194,069
F6_620	Kyrgyz	Mbuti	0.2175	0.0035	62.37	1,213,289
F6_620	Hawaiian	Mbuti	0.2173	0.0038	57.76	1,147,586
F6_620	Cree	Mbuti	0.2170	0.0035	62.53	1,207,557
F6_620	Papuan	Mbuti	0.2168	0.0037	59.37	1,263,180
F6_620	Australian	Mbuti	0.2166	0.0037	59.23	1,202,072
F6_620	Aleut	Mbuti	0.2165	0.0035	62.43	1,208,644
F6_620	Yadava	Mbuti	0.2160	0.0035	61.76	1,210,425
F6_620	Mala	Mbuti	0.2159	0.0034	62.85	1,248,835
F6_620	Mansi	Mbuti	0.2156	0.0035	61.28	1,212,531
F6_620	Chukchi	Mbuti	0.2149	0.0036	59.85	1,157,925
F6_620	Relli	Mbuti	0.2148	0.0035	61.23	1,211,822
F6_620	Tubalar	Mbuti	0.2147	0.0035	61.12	1,210,720
F6_620	Mixtec	Mbuti	0.2145	0.0035	61.48	1,200,846
F6_620	Madiga	Mbuti	0.2143	0.0035	61.41	1,212,463
F6_620	Uygur	Mbuti	0.2142	0.0034	62.96	1,218,184
F6_620	Irula	Mbuti	0.2142	0.0035	60.68	1,208,825
F6_620	Kapu	Mbuti	0.2137	0.0036	59.67	1,213,956
F6_620	Hazara	Mbuti	0.2136	0.0035	60.24	1,213,978
F6_620	Bengali	Mbuti	0.2131	0.0034	62.41	1,214,446

A	B	C	f3	SE	Zscore	nsnps
F6_620	Punjabi	Mbuti	0.2124	0.0034	63.00	1,276,307
F6_620	Tlingit	Mbuti	0.2123	0.0034	61.88	1,213,542
F6_620	Brahmin	Mbuti	0.2116	0.0034	62.37	1,215,848
F6_620	Saami	Mbuti	0.2105	0.0035	59.79	1,211,942
F6_620	Sindhi	Mbuti	0.2101	0.0035	59.53	1,215,486
F6_620	Pathan	Mbuti	0.2100	0.0035	60.78	1,217,387
F6_620	Kashmiri_Pandit	Mbuti	0.2096	0.0036	58.36	1,154,404
F6_620	Burusho	Mbuti	0.2094	0.0034	60.84	1,217,354
F6_620	Finnish	Mbuti	0.2090	0.0033	62.39	1,252,667
F6_620	Kalash	Mbuti	0.2087	0.0034	62.15	1,206,735
F6_620	Maori	Mbuti	0.2084	0.0036	57.58	1,158,963
F6_620	Icelandic	Mbuti	0.2080	0.0035	60.26	1,217,708
F6_620	Bergamo	Mbuti	0.2080	0.0036	57.50	1,156,648
F6_620	Tajik	Mbuti	0.2078	0.0034	60.40	1,214,934
F6_620	Estonian	Mbuti	0.2076	0.0035	58.77	1,217,041
F6_620	Czech	Mbuti	0.2074	0.0036	58.01	1,156,831
F6_620	Russian	Mbuti	0.2071	0.0035	59.55	1,217,844
F6_620	English	Mbuti	0.2069	0.0034	61.27	1,217,798
F6_620	French	Mbuti	0.2068	0.0034	61.17	1,216,429
F6_620	Albanian	Mbuti	0.2066	0.0035	59.19	1,155,708
F6_620	Orcadian	Mbuti	0.2063	0.0034	60.55	1,217,886
F6_620	Brahui	Mbuti	0.2061	0.0033	62.06	1,215,558
F6_620	Abkhasian	Mbuti	0.2060	0.0035	59.31	1,215,995
F6_620	Hungarian	Mbuti	0.2060	0.0035	59.17	1,218,236
F6_620	North_Ossetian	Mbuti	0.2054	0.0034	60.41	1,217,940
F6_620	Greek	Mbuti	0.2054	0.0033	61.71	1,216,650
F6_620	Adygei	Mbuti	0.2053	0.0034	60.15	1,217,032
F6_620	Iranian	Mbuti	0.2052	0.0033	61.46	1,217,134
F6_620	Armenian	Mbuti	0.2051	0.0035	58.82	1,185,190
F6_620	Polish	Mbuti	0.2050	0.0037	55.48	1,156,609
F6_620	Georgian	Mbuti	0.2049	0.0034	60.83	1,216,976
F6_620	Sardinian	Mbuti	0.2048	0.0034	59.42	1,215,977
F6_620	Balochi	Mbuti	0.2046	0.0036	57.22	1,149,984
F6_620	Bulgarian	Mbuti	0.2044	0.0033	62.42	1,218,484
F6_620	Lezgin	Mbuti	0.2043	0.0034	60.45	1,216,833
F6_620	Crete	Mbuti	0.2042	0.0035	57.78	1,156,472
F6_620	Turkish	Mbuti	0.2042	0.0034	59.39	1,217,458
F6_620	Chechen	Mbuti	0.2041	0.0035	58.25	1,156,214
F6_620	Basque	Mbuti	0.2040	0.0035	58.52	1,215,909
F6_620	Spanish	Mbuti	0.2037	0.0034	60.01	1,217,634
F6_620	Tuscan	Mbuti	0.2032	0.0035	58.17	1,218,914
F6_620	Iraqi_Jew	Mbuti	0.2015	0.0034	58.86	1,215,640
F6_620	Makrani	Mbuti	0.2012	0.0033	60.20	1,214,842
F6_620	Druze	Mbuti	0.2002	0.0033	60.12	1,216,365
F6_620	Samaritan	Mbuti	0.1978	0.0035	57.32	1,149,203
F6_620	Yemenite_Jew	Mbuti	0.1956	0.0033	59.10	1,215,229
F6_620	Jordanian	Mbuti	0.1955	0.0033	59.80	1,255,736
F6_620	BedouinB	Mbuti	0.1945	0.0033	59.45	1,209,568
F6_620	Palestinian	Mbuti	0.1931	0.0033	58.64	1,259,275
F6_620	Saharawi	Mbuti	0.1761	0.0032	55.63	1,224,879
F6_620	Mozabite	Mbuti	0.1718	0.0032	54.29	1,225,170
F6_620	Somali	Mbuti	0.1357	0.0031	43.32	1,147,736
F6_620	Masai	Mbuti	0.1128	0.0026	42.69	1,219,956
F6_620	Dinka	Mbuti	0.0917	0.0025	36.39	1,214,506
F6_620	Mandenka	Mbuti	0.0878	0.0025	35.51	1,232,569
F6_620	Gambian	Mbuti	0.0876	0.0024	36.70	1,231,938
F6_620	Luo	Mbuti	0.0858	0.0024	36.50	1,226,077
F6_620	BantuKenya	Mbuti	0.0850	0.0024	35.02	1,227,124
F6_620	Esan	Mbuti	0.0839	0.0024	35.13	1,233,222
F6_620	Luhya	Mbuti	0.0831	0.0024	34.36	1,226,634
F6_620	Yoruba	Mbuti	0.0825	0.0023	35.38	1,234,861
F6_620	Mende	Mbuti	0.0814	0.0024	34.17	1,232,278
F6_620	Igbo	Mbuti	0.0814	0.0024	33.87	1,233,141
F6_620	Lemande	Mbuti	0.0800	0.0023	34.17	1,230,077
F6_620	Kongo	Mbuti	0.0793	0.0025	31.84	1,152,001
F6_620	BantuHerero	Mbuti	0.0775	0.0023	33.05	1,226,363
F6_620	BantuTswana	Mbuti	0.0730	0.0022	32.97	1,225,213
F6_620	Biaka	Mbuti	0.0512	0.0020	25.97	1,202,579
F6_620	Ju_hoan_North	Mbuti	0.0480	0.0019	24.88	1,229,370
F6_620	Khomani_San	Mbuti	0.0449	0.0020	22.79	1,184,667

Table S5.3 Shared genetic drift between *Bacho Kiro BB7-240* and present-day humans as measured by *f3(BB7-240, present-day humans; Mbuti)*. Present-day modern human genomes from SGDP[10] were used. *f3* values reported were calculated using ADMIXTOOLS[3] as implemented in *admixr*[9] and were used for plotting Fig. S5.1B. Standard errors (SE) were computed using a Weighted Block Jackknife[3,12] across all autosomes using a block size of 5Mb. Number of SNPs overlapping among individuals reported in the column "nsnps".

A	B	C	f3	SE	Zscore	nsnps
BB7_240	She	Mbuti	0.2286	0.0035	64.70	532,598
BB7_240	Ami	Mbuti	0.2280	0.0037	62.47	530,941
BB7_240	Lahu	Mbuti	0.2272	0.0036	62.33	532,013
BB7_240	Kinh	Mbuti	0.2265	0.0036	62.69	533,949
BB7_240	Yi	Mbuti	0.2265	0.0036	62.95	534,375
BB7_240	Japanese	Mbuti	0.2262	0.0035	64.07	546,821
BB7_240	Miao	Mbuti	0.2262	0.0036	63.43	533,135
BB7_240	Cambodian	Mbuti	0.2260	0.0035	64.29	534,583
BB7_240	Igorot	Mbuti	0.2259	0.0037	61.53	529,140
BB7_240	Han	Mbuti	0.2258	0.0036	62.94	533,885
BB7_240	Tujia	Mbuti	0.2257	0.0037	61.65	533,432
BB7_240	Naxi	Mbuti	0.2255	0.0036	62.84	548,346
BB7_240	Dai	Mbuti	0.2255	0.0036	62.12	546,838
BB7_240	Atayal	Mbuti	0.2254	0.0038	59.55	507,848
BB7_240	Even	Mbuti	0.2252	0.0036	63.44	548,278
BB7_240	Sherpa	Mbuti	0.2252	0.0036	62.53	531,777
BB7_240	Xibo	Mbuti	0.2251	0.0037	61.68	534,906
BB7_240	Oroqen	Mbuti	0.2251	0.0035	63.50	532,877
BB7_240	Yakut	Mbuti	0.2248	0.0037	61.13	534,349
BB7_240	Ulchi	Mbuti	0.2246	0.0036	62.76	532,736
BB7_240	Thai	Mbuti	0.2244	0.0036	62.33	535,488
BB7_240	Korean	Mbuti	0.2243	0.0035	63.42	534,120
BB7_240	Hezhen	Mbuti	0.2242	0.0036	62.60	533,450
BB7_240	Karitiana	Mbuti	0.2239	0.0037	60.60	519,356
BB7_240	Kusunda	Mbuti	0.2239	0.0035	64.14	530,584
BB7_240	Dusun	Mbuti	0.2238	0.0036	62.06	531,211
BB7_240	Eskimo_Chaplin	Mbuti	0.2238	0.0037	60.50	508,117
BB7_240	Surui	Mbuti	0.2238	0.0037	60.74	519,448
BB7_240	Tibetan	Mbuti	0.2238	0.0036	61.72	534,575
BB7_240	Tu	Mbuti	0.2236	0.0035	63.27	535,878
BB7_240	Daur	Mbuti	0.2236	0.0037	60.30	510,506
BB7_240	Burmese	Mbuti	0.2236	0.0035	64.01	536,295
BB7_240	Mayan	Mbuti	0.2236	0.0035	63.40	528,227
BB7_240	Chipewyan	Mbuti	0.2236	0.0036	62.13	526,818
BB7_240	Khonda_Dora	Mbuti	0.2236	0.0037	60.71	510,255
BB7_240	Eskimo_Sireniki	Mbuti	0.2235	0.0036	62.76	531,205
BB7_240	Onge	Mbuti	0.2233	0.0037	60.74	525,377
BB7_240	Kharia	Mbuti	0.2232	0.0037	60.38	510,489
BB7_240	Piapoco	Mbuti	0.2230	0.0036	62.35	525,552
BB7_240	Botocudo	Mbuti	0.2229	0.0037	60.19	481,609
BB7_240	Zapotec	Mbuti	0.2228	0.0035	62.88	529,419
BB7_240	Eskimo_Naukan	Mbuti	0.2228	0.0036	62.62	528,993
BB7_240	Itelman	Mbuti	0.2225	0.0037	59.88	508,865
BB7_240	Hawaiian	Mbuti	0.2218	0.0036	61.44	509,840
BB7_240	Chane	Mbuti	0.2216	0.0038	59.10	507,933
BB7_240	Mixe	Mbuti	0.2214	0.0036	61.76	525,871
BB7_240	Quechua	Mbuti	0.2214	0.0035	62.43	539,236
BB7_240	Altaian	Mbuti	0.2213	0.0037	59.32	511,563
BB7_240	Kurumba	Mbuti	0.2212	0.0036	61.24	509,836
BB7_240	Kyrgyz	Mbuti	0.2210	0.0035	63.18	539,507
BB7_240	Australian	Mbuti	0.2209	0.0037	59.53	534,341
BB7_240	Nahua	Mbuti	0.2208	0.0036	61.25	508,891
BB7_240	Pima	Mbuti	0.2208	0.0036	61.29	525,609
BB7_240	Cree	Mbuti	0.2206	0.0035	62.68	537,258
BB7_240	Tubalar	Mbuti	0.2205	0.0035	62.52	538,596
BB7_240	Mala	Mbuti	0.2194	0.0034	64.69	555,568
BB7_240	Kapu	Mbuti	0.2192	0.0035	62.36	539,529
BB7_240	Papuan	Mbuti	0.2190	0.0037	59.85	562,780
BB7_240	Mansi	Mbuti	0.2189	0.0035	61.96	539,466
BB7_240	Madiga	Mbuti	0.2188	0.0035	62.68	539,210
BB7_240	Aleut	Mbuti	0.2188	0.0035	62.03	537,617
BB7_240	Hazara	Mbuti	0.2186	0.0035	62.77	539,936
BB7_240	Bougainville	Mbuti	0.2186	0.0036	61.20	527,796
BB7_240	Irula	Mbuti	0.2185	0.0034	63.45	537,545
BB7_240	Yadava	Mbuti	0.2185	0.0034	63.64	538,491
BB7_240	Chukchi	Mbuti	0.2184	0.0035	61.68	514,377
BB7_240	Mixtec	Mbuti	0.2175	0.0035	62.58	534,136
BB7_240	Relli	Mbuti	0.2172	0.0034	63.44	538,987
BB7_240	Bengali	Mbuti	0.2171	0.0034	63.32	540,042
BB7_240	Uygur	Mbuti	0.2167	0.0035	61.07	542,257

A	B	C	f3	SE	Zscore	nsnps
BB7_240	Tlingit	Mbuti	0.2167	0.0035	62.57	540,128
BB7_240	Punjabi	Mbuti	0.2164	0.0034	63.89	568,585
BB7_240	Pathan	Mbuti	0.2151	0.0034	62.67	541,520
BB7_240	Brahmin	Mbuti	0.2150	0.0034	63.13	540,905
BB7_240	Burusho	Mbuti	0.2147	0.0034	62.59	541,528
BB7_240	Sindhi	Mbuti	0.2143	0.0035	61.50	540,375
BB7_240	Saami	Mbuti	0.2141	0.0035	60.60	539,338
BB7_240	Czech	Mbuti	0.2141	0.0036	59.81	513,798
BB7_240	Icelandic	Mbuti	0.2132	0.0035	60.75	541,774
BB7_240	Kashmiri_Pandit	Mbuti	0.2127	0.0035	60.30	512,650
BB7_240	Russian	Mbuti	0.2124	0.0034	62.23	541,749
BB7_240	Tajik	Mbuti	0.2122	0.0035	61.28	540,555
BB7_240	Kalash	Mbuti	0.2121	0.0034	61.88	536,812
BB7_240	Finnish	Mbuti	0.2112	0.0034	62.80	558,414
BB7_240	Orcadian	Mbuti	0.2112	0.0035	60.95	542,056
BB7_240	Maori	Mbuti	0.2111	0.0034	62.83	515,289
BB7_240	French	Mbuti	0.2110	0.0034	62.27	541,241
BB7_240	Bergamo	Mbuti	0.2109	0.0036	59.23	513,789
BB7_240	Estonian	Mbuti	0.2108	0.0035	59.94	541,818
BB7_240	Greek	Mbuti	0.2107	0.0034	62.23	541,395
BB7_240	Albanian	Mbuti	0.2100	0.0035	60.47	513,904
BB7_240	North_Ossetian	Mbuti	0.2095	0.0033	62.79	541,984
BB7_240	English	Mbuti	0.2095	0.0034	62.46	541,896
BB7_240	Polish	Mbuti	0.2094	0.0035	59.38	514,290
BB7_240	Basque	Mbuti	0.2093	0.0034	61.10	541,124
BB7_240	Adygei	Mbuti	0.2091	0.0033	63.40	541,777
BB7_240	Brahui	Mbuti	0.2091	0.0034	62.08	540,608
BB7_240	Hungarian	Mbuti	0.2090	0.0034	61.16	542,362
BB7_240	Sardinian	Mbuti	0.2086	0.0033	62.55	540,702
BB7_240	Balochi	Mbuti	0.2086	0.0036	57.35	510,826
BB7_240	Tuscan	Mbuti	0.2085	0.0034	60.75	542,235
BB7_240	Bulgarian	Mbuti	0.2082	0.0034	60.36	542,292
BB7_240	Turkish	Mbuti	0.2079	0.0034	60.97	541,696
BB7_240	Spanish	Mbuti	0.2079	0.0034	61.08	541,883
BB7_240	Abkhasian	Mbuti	0.2075	0.0034	60.32	541,142
BB7_240	Lezgin	Mbuti	0.2074	0.0034	61.72	541,771
BB7_240	Chechen	Mbuti	0.2073	0.0035	59.06	513,663
BB7_240	Crete	Mbuti	0.2066	0.0036	58.05	513,898
BB7_240	Georgian	Mbuti	0.2064	0.0034	61.50	541,603
BB7_240	Armenian	Mbuti	0.2063	0.0034	60.61	526,973
BB7_240	Iranian	Mbuti	0.2047	0.0034	60.78	541,863
BB7_240	Makrani	Mbuti	0.2046	0.0034	61.05	540,505
BB7_240	Iraqi_Jew	Mbuti	0.2031	0.0033	62.44	541,085
BB7_240	Druze	Mbuti	0.2013	0.0033	60.95	541,580
BB7_240	Samaritan	Mbuti	0.2012	0.0035	57.90	510,297
BB7_240	BedouinB	Mbuti	0.1999	0.0033	60.60	537,914
BB7_240	Yemenite_Jew	Mbuti	0.1980	0.0034	58.47	540,581
BB7_240	Palestinian	Mbuti	0.1979	0.0033	59.95	560,334
BB7_240	Jordanian	Mbuti	0.1979	0.0033	59.69	558,898
BB7_240	Saharawi	Mbuti	0.1793	0.0032	56.54	544,487
BB7_240	Mozabite	Mbuti	0.1766	0.0032	55.40	544,187
BB7_240	Somali	Mbuti	0.1358	0.0031	43.87	509,538
BB7_240	Masai	Mbuti	0.1127	0.0026	42.72	541,153
BB7_240	Dinka	Mbuti	0.0917	0.0025	36.50	537,784
BB7_240	Mandenka	Mbuti	0.0878	0.0025	35.18	545,374
BB7_240	Gambian	Mbuti	0.0871	0.0024	36.08	544,833
BB7_240	Luo	Mbuti	0.0867	0.0025	34.61	542,610
BB7_240	BantuKenya	Mbuti	0.0854	0.0025	34.85	542,758
BB7_240	Luhya	Mbuti	0.0842	0.0024	34.88	542,410
BB7_240	Yoruba	Mbuti	0.0839	0.0024	35.30	546,023
BB7_240	Esan	Mbuti	0.0832	0.0024	34.42	545,266
BB7_240	Igbo	Mbuti	0.0821	0.0025	33.42	544,689
BB7_240	Mende	Mbuti	0.0818	0.0024	33.54	544,878
BB7_240	Lemande	Mbuti	0.0809	0.0024	33.07	543,905
BB7_240	Kongo	Mbuti	0.0804	0.0025	32.18	509,798
BB7_240	BantuHerero	Mbuti	0.0781	0.0024	33.03	542,214
BB7_240	BantuTswana	Mbuti	0.0725	0.0022	32.28	542,733
BB7_240	Biaka	Mbuti	0.0522	0.0020	26.08	532,391
BB7_240	Ju_hoan_North	Mbuti	0.0470	0.0019	24.62	546,805
BB7_240	Khomani_San	Mbuti	0.0443	0.0019	22.77	526,124

Table S5.4 Shared genetic drift between *Bacho Kiro CC7-335* and present-day humans as measured by *f3(CC7-335, present-day humans; Mbuti)*. Present-day modern human genomes from SGDP[10] were used. *f3* values reported were calculated using ADMIXTOOLS[3] as implemented in *admixr*[9] and were used for plotting Fig. S5.1C. Standard errors (SE) were computed using a Weighted Block Jackknife[3,12] across all autosomes using a block size of 5Mb. Number of SNPs overlapping among individuals reported in the column "nsnps".

A	B	C	f3	SE	Zscore	nsnps
CC7_335	Lahu	Mbuti	0.2250	0.0037	60.37	486,320
CC7_335	Oroqen	Mbuti	0.2248	0.0038	59.38	487,060
CC7_335	Ulchi	Mbuti	0.2242	0.0037	61.25	486,763
CC7_335	Han	Mbuti	0.2241	0.0038	59.09	487,752
CC7_335	Daur	Mbuti	0.2241	0.0039	57.08	466,483
CC7_335	Yi	Mbuti	0.2241	0.0038	58.86	487,903
CC7_335	Eskimo_Naukan	Mbuti	0.2239	0.0037	60.82	483,473
CC7_335	Japanese	Mbuti	0.2239	0.0037	60.07	499,886
CC7_335	Itelman	Mbuti	0.2239	0.0039	57.51	464,834
CC7_335	Surui	Mbuti	0.2238	0.0038	58.80	474,876
CC7_335	Even	Mbuti	0.2238	0.0038	59.09	501,167
CC7_335	Ami	Mbuti	0.2237	0.0037	60.26	485,326
CC7_335	Dusun	Mbuti	0.2234	0.0038	59.55	485,207
CC7_335	Khonda_Dora	Mbuti	0.2234	0.0038	58.78	466,143
CC7_335	Eskimo_Chaplin	Mbuti	0.2233	0.0038	58.02	464,589
CC7_335	Hezhen	Mbuti	0.2233	0.0038	58.93	487,762
CC7_335	Dai	Mbuti	0.2233	0.0037	60.28	499,888
CC7_335	Korean	Mbuti	0.2232	0.0037	59.94	488,017
CC7_335	Burmese	Mbuti	0.2232	0.0037	60.17	490,199
CC7_335	Karitiana	Mbuti	0.2231	0.0039	57.47	474,521
CC7_335	Igorot	Mbuti	0.2231	0.0038	58.39	483,610
CC7_335	Kinh	Mbuti	0.2230	0.0038	59.38	488,238
CC7_335	Sherpa	Mbuti	0.2229	0.0037	60.56	486,096
CC7_335	Cambodian	Mbuti	0.2229	0.0037	59.48	488,908
CC7_335	Onge	Mbuti	0.2229	0.0036	61.47	480,136
CC7_335	Chipewyan	Mbuti	0.2228	0.0038	58.93	481,723
CC7_335	Naxi	Mbuti	0.2228	0.0037	59.92	501,277
CC7_335	Thai	Mbuti	0.2228	0.0037	60.36	489,285
CC7_335	Tujia	Mbuti	0.2227	0.0038	59.31	487,384
CC7_335	Miao	Mbuti	0.2226	0.0037	60.19	487,206
CC7_335	Yakut	Mbuti	0.2225	0.0038	58.87	488,441
CC7_335	Tibetan	Mbuti	0.2223	0.0037	60.17	488,222
CC7_335	Tu	Mbuti	0.2221	0.0038	58.85	489,983
CC7_335	She	Mbuti	0.2221	0.0037	59.30	487,033
CC7_335	Kusunda	Mbuti	0.2220	0.0036	61.33	485,064
CC7_335	Botocudo	Mbuti	0.2217	0.0039	57.47	440,853
CC7_335	Mayan	Mbuti	0.2215	0.0037	59.90	483,026
CC7_335	Kurumba	Mbuti	0.2214	0.0037	59.91	465,616
CC7_335	Atayal	Mbuti	0.2213	0.0038	57.88	464,424
CC7_335	Eskimo_Sireniki	Mbuti	0.2212	0.0036	61.99	485,676
CC7_335	Zapotec	Mbuti	0.2210	0.0037	60.29	483,828
CC7_335	Xibo	Mbuti	0.2210	0.0038	58.77	488,834
CC7_335	Chane	Mbuti	0.2208	0.0037	60.19	464,254
CC7_335	Cree	Mbuti	0.2207	0.0036	62.05	490,741
CC7_335	Kyrgyz	Mbuti	0.2207	0.0037	59.69	493,250
CC7_335	Mixe	Mbuti	0.2204	0.0038	58.49	480,981
CC7_335	Yadava	Mbuti	0.2201	0.0036	60.73	491,886
CC7_335	Hawaiian	Mbuti	0.2201	0.0040	54.83	465,927
CC7_335	Piapoco	Mbuti	0.2198	0.0036	60.62	480,561
CC7_335	Quechua	Mbuti	0.2195	0.0036	60.66	492,928
CC7_335	Kharia	Mbuti	0.2194	0.0037	59.73	466,848
CC7_335	Madiga	Mbuti	0.2194	0.0037	60.09	492,548
CC7_335	Aleut	Mbuti	0.2193	0.0037	60.04	491,282
CC7_335	Pima	Mbuti	0.2191	0.0038	58.23	480,344
CC7_335	Bougainville	Mbuti	0.2191	0.0036	60.08	481,995
CC7_335	Nahua	Mbuti	0.2187	0.0038	57.52	465,105
CC7_335	Chukchi	Mbuti	0.2187	0.0036	60.12	470,182
CC7_335	Tubalar	Mbuti	0.2180	0.0036	60.01	492,383
CC7_335	Irula	Mbuti	0.2179	0.0035	61.81	491,403
CC7_335	Altaian	Mbuti	0.2178	0.0038	57.02	467,186
CC7_335	Mala	Mbuti	0.2177	0.0035	62.04	507,743
CC7_335	Papuan	Mbuti	0.2176	0.0037	59.10	514,723
CC7_335	Hazara	Mbuti	0.2171	0.0037	59.10	493,262
CC7_335	Punjabi	Mbuti	0.2171	0.0035	61.22	519,396
CC7_335	Kapu	Mbuti	0.2170	0.0036	60.06	493,356
CC7_335	Mansi	Mbuti	0.2167	0.0035	61.38	492,953
CC7_335	Relli	Mbuti	0.2165	0.0035	61.74	492,801
CC7_335	Mixtec	Mbuti	0.2164	0.0037	58.81	487,871
CC7_335	Bengali	Mbuti	0.2163	0.0035	61.12	493,518
CC7_335	Uygur	Mbuti	0.2156	0.0035	61.47	495,209

A	B	C	f3	SE	Zscore	nsnps
CC7_335	Tlingit	Mbuti	0.2154	0.0036	59.30	493,493
CC7_335	Australian	Mbuti	0.2152	0.0037	57.45	488,597
CC7_335	Sindhi	Mbuti	0.2145	0.0036	59.95	493,942
CC7_335	Burusho	Mbuti	0.2141	0.0036	60.27	494,720
CC7_335	Saami	Mbuti	0.2139	0.0036	58.88	492,664
CC7_335	Brahmin	Mbuti	0.2135	0.0035	60.66	494,553
CC7_335	Estonian	Mbuti	0.2131	0.0036	59.32	494,602
CC7_335	Kashmiri_Pandit	Mbuti	0.2129	0.0037	58.25	468,262
CC7_335	Russian	Mbuti	0.2124	0.0036	58.26	495,113
CC7_335	Czech	Mbuti	0.2124	0.0037	57.21	469,531
CC7_335	Pathan	Mbuti	0.2124	0.0035	60.25	494,836
CC7_335	Finnish	Mbuti	0.2123	0.0035	60.59	509,846
CC7_335	Icelandic	Mbuti	0.2122	0.0035	59.80	494,918
CC7_335	Maori	Mbuti	0.2117	0.0036	58.12	470,475
CC7_335	Polish	Mbuti	0.2112	0.0037	56.84	469,527
CC7_335	Orcadian	Mbuti	0.2110	0.0035	60.69	494,892
CC7_335	Tajik	Mbuti	0.2109	0.0035	60.04	494,050
CC7_335	Basque	Mbuti	0.2107	0.0035	59.80	493,880
CC7_335	Kalash	Mbuti	0.2104	0.0035	60.01	490,352
CC7_335	French	Mbuti	0.2103	0.0036	57.89	494,422
CC7_335	Albanian	Mbuti	0.2102	0.0036	58.66	469,393
CC7_335	Balochi	Mbuti	0.2102	0.0038	54.93	466,571
CC7_335	English	Mbuti	0.2100	0.0035	60.15	494,908
CC7_335	Bulgarian	Mbuti	0.2100	0.0036	59.15	495,201
CC7_335	Bergamo	Mbuti	0.2099	0.0038	54.73	469,393
CC7_335	Hungarian	Mbuti	0.2098	0.0037	57.31	495,273
CC7_335	Chechen	Mbuti	0.2097	0.0037	57.25	469,420
CC7_335	Adygei	Mbuti	0.2096	0.0035	59.34	494,760
CC7_335	Greek	Mbuti	0.2094	0.0036	58.78	494,448
CC7_335	Armenian	Mbuti	0.2094	0.0036	58.53	481,404
CC7_335	Turkish	Mbuti	0.2094	0.0036	58.23	494,654
CC7_335	Sardinian	Mbuti	0.2093	0.0035	60.16	494,116
CC7_335	North_Ossetian	Mbuti	0.2091	0.0035	59.35	495,272
CC7_335	Abkhasian	Mbuti	0.2091	0.0036	58.31	494,457
CC7_335	Tuscan	Mbuti	0.2087	0.0035	58.91	495,405
CC7_335	Brahui	Mbuti	0.2087	0.0035	59.17	494,007
CC7_335	Spanish	Mbuti	0.2086	0.0035	59.09	494,911
CC7_335	Lezgin	Mbuti	0.2082	0.0035	59.41	494,705
CC7_335	Iranian	Mbuti	0.2077	0.0034	60.58	494,963
CC7_335	Georgian	Mbuti	0.2071	0.0035	58.97	494,680
CC7_335	Crete	Mbuti	0.2067	0.0037	55.52	469,483
CC7_335	Iraqi_Jew	Mbuti	0.2057	0.0034	60.23	493,625
CC7_335	Makrani	Mbuti	0.2054	0.0036	56.84	493,589
CC7_335	Samaritan	Mbuti	0.2044	0.0036	57.12	466,236
CC7_335	Druze	Mbuti	0.2031	0.0034	59.06	494,414
CC7_335	BedouinB	Mbuti	0.1997	0.0034	58.65	491,331
CC7_335	Yemenite_Jew	Mbuti	0.1994	0.0035	57.73	494,009
CC7_335	Jordanian	Mbuti	0.1977	0.0034	57.95	510,776
CC7_335	Palestinian	Mbuti	0.1970	0.0034	57.63	511,746
CC7_335	Saharawi	Mbuti	0.1795	0.0032	56.60	497,555
CC7_335	Mozabite	Mbuti	0.1772	0.0033	54.01	497,130
CC7_335	Somali	Mbuti	0.1381	0.0032	42.53	465,274
CC7_335	Masai	Mbuti	0.1139	0.0028	41.01	494,670
CC7_335	Dinka	Mbuti	0.0920	0.0026	35.62	491,883
CC7_335	Gambian	Mbuti	0.0880	0.0025	35.23	498,645
CC7_335	Mandenka	Mbuti	0.0873	0.0025	34.68	499,105
CC7_335	Luo	Mbuti	0.0865	0.0025	34.21	496,230
CC7_335	BantuKenya	Mbuti	0.0861	0.0026	33.57	496,815
CC7_335	Luhya	Mbuti	0.0859	0.0026	33.03	496,498
CC7_335	Esan	Mbuti	0.0842	0.0025	33.07	499,118
CC7_335	Yoruba	Mbuti	0.0836	0.0025	34.06	499,368
CC7_335	Mende	Mbuti	0.0833	0.0025	33.98	498,637
CC7_335	Igbo	Mbuti	0.0828	0.0025	33.31	498,676
CC7_335	Lemande	Mbuti	0.0818	0.0025	33.17	497,854
CC7_335	BantuHerero	Mbuti	0.0790	0.0025	32.15	496,294
CC7_335	Kongo	Mbuti	0.0781	0.0026	29.96	466,479
CC7_335	BantuTswana	Mbuti	0.0728	0.0024	30.98	496,443
CC7_335	Biaka	Mbuti	0.0521	0.0021	24.88	487,451
CC7_335	Ju_hoan_North	Mbuti	0.0478	0.0020	23.36	500,326
CC7_335	Khomani_San	Mbuti	0.0455	0.0021	21.71	481,422

Table S5.5 Shared genetic drift between *Bacho Kiro BK1653* and present-day humans as measured by *f3(BK1653, present-day humans; Mbuti)*. Present-day modern human genomes from SGDP[10] were used. *f3* values reported were calculated using ADMIXTOOLS[3] as implemented in *admixr*[9] and were used for plotting Extended Data Fig. 3B. Standard errors (SE) were computed using a Weighted Block Jackknife[3,12] across all autosomes using a block size of 5Mb. Number of SNPs overlapping among individuals reported in the column "nsnps".

A	B	C	f3	stderr	Zscore	nsnps
BK1653	Icelandic	Mbuti	0.2412	0.0035	68.12	567,146
BK1653	Czech	Mbuti	0.2403	0.0036	66.79	538,697
BK1653	Estonian	Mbuti	0.2393	0.0036	65.99	566,739
BK1653	Finnish	Mbuti	0.2389	0.0034	70.63	583,875
BK1653	English	Mbuti	0.2386	0.0036	67.21	567,076
BK1653	Orcadian	Mbuti	0.2381	0.0035	67.77	567,147
BK1653	French	Mbuti	0.2381	0.0035	67.21	566,370
BK1653	Basque	Mbuti	0.2378	0.0035	67.82	566,063
BK1653	Sardinian	Mbuti	0.2378	0.0035	68.44	565,999
BK1653	Saami	Mbuti	0.2375	0.0036	65.92	565,404
BK1653	Hungarian	Mbuti	0.2373	0.0036	66.05	567,453
BK1653	Bergamo	Mbuti	0.2372	0.0036	65.37	538,614
BK1653	Spanish	Mbuti	0.2372	0.0036	66.37	567,155
BK1653	Russian	Mbuti	0.2350	0.0035	68.10	567,223
BK1653	Bulgarian	Mbuti	0.2349	0.0035	67.96	568,141
BK1653	Greek	Mbuti	0.2349	0.0034	68.13	566,767
BK1653	Crete	Mbuti	0.2345	0.0038	62.05	538,818
BK1653	Polish	Mbuti	0.2344	0.0037	64.15	539,127
BK1653	Tuscan	Mbuti	0.2332	0.0036	65.01	567,863
BK1653	Albanian	Mbuti	0.2329	0.0036	64.67	538,698
BK1653	Adygei	Mbuti	0.2322	0.0035	66.21	567,075
BK1653	Chukchi	Mbuti	0.2319	0.0036	64.70	540,554
BK1653	Abkhasian	Mbuti	0.2306	0.0035	65.28	567,007
BK1653	Georgian	Mbuti	0.2303	0.0034	67.08	566,996
BK1653	North_Ossetian	Mbuti	0.2301	0.0035	65.31	568,126
BK1653	Tajik	Mbuti	0.2299	0.0035	65.45	566,732
BK1653	Mansi	Mbuti	0.2299	0.0035	65.76	566,474
BK1653	Cree	Mbuti	0.2297	0.0035	65.18	564,306
BK1653	Chechen	Mbuti	0.2296	0.0036	63.23	539,041
BK1653	Lezgin	Mbuti	0.2294	0.0035	66.37	567,006
BK1653	Tlingit	Mbuti	0.2289	0.0035	65.97	566,773
BK1653	Pathan	Mbuti	0.2281	0.0035	65.70	568,261
BK1653	Aleut	Mbuti	0.2277	0.0035	65.13	564,802
BK1653	Turkish	Mbuti	0.2276	0.0034	66.27	567,643
BK1653	Armenian	Mbuti	0.2274	0.0037	61.95	552,929
BK1653	Chipewyan	Mbuti	0.2271	0.0036	63.00	554,621
BK1653	Chane	Mbuti	0.2261	0.0038	59.84	534,539
BK1653	Iranian	Mbuti	0.2261	0.0035	64.82	567,592
BK1653	Druze	Mbuti	0.2261	0.0033	67.56	567,073
BK1653	Mayan	Mbuti	0.2261	0.0035	63.76	555,908
BK1653	Kashmiri_Pandit	Mbuti	0.2261	0.0036	63.28	538,491
BK1653	Surui	Mbuti	0.2260	0.0037	61.07	546,837
BK1653	Iraqi_Jew	Mbuti	0.2259	0.0035	64.52	566,698
BK1653	Burusho	Mbuti	0.2255	0.0035	64.29	568,480
BK1653	Tubalar	Mbuti	0.2253	0.0035	64.61	566,190
BK1653	Quechua	Mbuti	0.2252	0.0036	62.57	567,153
BK1653	Pima	Mbuti	0.2250	0.0035	63.52	552,950
BK1653	Kalash	Mbuti	0.2250	0.0035	65.17	563,325
BK1653	Piapoco	Mbuti	0.2249	0.0037	61.35	553,043
BK1653	Zapotec	Mbuti	0.2249	0.0036	63.05	557,066
BK1653	Nahua	Mbuti	0.2247	0.0037	60.68	535,895
BK1653	Karitiana	Mbuti	0.2247	0.0037	61.41	546,931
BK1653	Kyrgyz	Mbuti	0.2246	0.0034	66.06	567,611
BK1653	Eskimo_Naukan	Mbuti	0.2246	0.0035	64.56	556,829
BK1653	Samaritan	Mbuti	0.2245	0.0038	59.79	535,337
BK1653	Maori	Mbuti	0.2243	0.0037	60.96	541,257
BK1653	Eskimo_Chaplin	Mbuti	0.2242	0.0038	59.11	535,586
BK1653	Hazara	Mbuti	0.2242	0.0035	64.62	567,606
BK1653	Brahmin	Mbuti	0.2241	0.0034	66.08	567,961
BK1653	Sindhi	Mbuti	0.2240	0.0035	64.19	567,568
BK1653	Itelman	Mbuti	0.2240	0.0036	62.20	535,848
BK1653	Mixtec	Mbuti	0.2239	0.0035	63.89	561,248
BK1653	Altaian	Mbuti	0.2237	0.0036	62.72	538,383
BK1653	Punjabi	Mbuti	0.2237	0.0033	66.79	596,704
BK1653	Balochi	Mbuti	0.2234	0.0037	60.66	536,702
BK1653	Mixe	Mbuti	0.2234	0.0036	61.52	553,752
BK1653	Uygur	Mbuti	0.2229	0.0035	64.40	569,437
BK1653	Brahui	Mbuti	0.2229	0.0034	65.15	567,046
BK1653	Eskimo_Sireniki	Mbuti	0.2227	0.0035	64.24	559,266
BK1653	Yadava	Mbuti	0.2225	0.0034	65.31	565,596

A	B	C	f3	stderr	Zscore	nsnps
BK1653	Yemenite_Jew	Mbuti	0.2222	0.0035	63.75	566,408
BK1653	Kapu	Mbuti	0.2218	0.0034	65.09	567,249
BK1653	BedouinB	Mbuti	0.2216	0.0034	65.25	563,344
BK1653	Madiga	Mbuti	0.2214	0.0034	64.24	566,852
BK1653	Bengali	Mbuti	0.2212	0.0034	64.26	567,824
BK1653	Mala	Mbuti	0.2212	0.0033	66.52	583,946
BK1653	Makrani	Mbuti	0.2210	0.0035	63.56	566,729
BK1653	Yakut	Mbuti	0.2205	0.0035	62.91	562,835
BK1653	Even	Mbuti	0.2204	0.0035	63.00	577,274
BK1653	Relli	Mbuti	0.2203	0.0034	65.03	567,044
BK1653	Kurumba	Mbuti	0.2203	0.0036	61.59	537,067
BK1653	Palestinian	Mbuti	0.2201	0.0034	64.00	586,450
BK1653	Khonda_Dora	Mbuti	0.2193	0.0036	61.75	537,853
BK1653	She	Mbuti	0.2191	0.0035	62.32	561,439
BK1653	Irula	Mbuti	0.2191	0.0034	64.95	565,501
BK1653	Jordanian	Mbuti	0.2190	0.0034	64.63	585,458
BK1653	Oroqen	Mbuti	0.2190	0.0034	63.81	561,439
BK1653	Ulchi	Mbuti	0.2187	0.0035	62.86	560,932
BK1653	Miao	Mbuti	0.2186	0.0035	62.98	561,446
BK1653	Kinh	Mbuti	0.2182	0.0036	61.20	562,644
BK1653	Kharia	Mbuti	0.2180	0.0035	61.74	538,015
BK1653	Han	Mbuti	0.2180	0.0035	63.00	562,450
BK1653	Tibetan	Mbuti	0.2177	0.0035	62.20	563,061
BK1653	Dai	Mbuti	0.2176	0.0035	62.46	575,587
BK1653	Burmese	Mbuti	0.2175	0.0034	63.71	565,166
BK1653	Thai	Mbuti	0.2175	0.0035	62.45	563,920
BK1653	Naxi	Mbuti	0.2173	0.0035	62.25	577,546
BK1653	Ami	Mbuti	0.2173	0.0036	60.05	559,436
BK1653	Korean	Mbuti	0.2171	0.0035	62.51	562,443
BK1653	Onge	Mbuti	0.2171	0.0036	61.10	553,779
BK1653	Hezhen	Mbuti	0.2169	0.0034	63.15	561,938
BK1653	Daur	Mbuti	0.2169	0.0036	59.64	538,188
BK1653	Tujia	Mbuti	0.2168	0.0035	61.37	561,915
BK1653	Kusunda	Mbuti	0.2167	0.0035	62.73	559,039
BK1653	Xibo	Mbuti	0.2167	0.0035	61.54	563,581
BK1653	Yi	Mbuti	0.2164	0.0035	62.54	563,195
BK1653	Lahu	Mbuti	0.2164	0.0035	61.94	560,869
BK1653	Tu	Mbuti	0.2162	0.0034	62.75	564,421
BK1653	Botocudo	Mbuti	0.2162	0.0036	59.51	507,705
BK1653	Sherpa	Mbuti	0.2159	0.0035	62.54	560,765
BK1653	Atayal	Mbuti	0.2158	0.0037	58.47	535,879
BK1653	Australian	Mbuti	0.2157	0.0036	59.81	563,162
BK1653	Igorot	Mbuti	0.2156	0.0036	60.07	557,799
BK1653	Japanese	Mbuti	0.2156	0.0034	62.73	576,154
BK1653	Cambodian	Mbuti	0.2156	0.0035	61.50	564,057
BK1653	Dusun	Mbuti	0.2155	0.0035	60.82	559,626
BK1653	Hawaiian	Mbuti	0.2145	0.0037	58.54	537,517
BK1653	Bougainville	Mbuti	0.2137	0.0035	60.42	555,929
BK1653	Papuan	Mbuti	0.2129	0.0035	60.26	592,384
BK1653	Saharawi	Mbuti	0.1985	0.0034	59.19	570,351
BK1653	Mozabite	Mbuti	0.1963	0.0034	58.02	570,096
BK1653	Somali	Mbuti	0.1474	0.0033	45.19	535,618
BK1653	Masai	Mbuti	0.1192	0.0028	42.61	569,367
BK1653	Dinka	Mbuti	0.0924	0.0026	35.02	566,732
BK1653	Mandenka	Mbuti	0.0894	0.0026	34.93	574,270
BK1653	Gambian	Mbuti	0.0879	0.0024	36.30	573,546
BK1653	Luo	Mbuti	0.0864	0.0026	33.67	571,520
BK1653	Luhya	Mbuti	0.0853	0.0024	34.86	571,591
BK1653	BantuKenya	Mbuti	0.0852	0.0025	34.73	571,422
BK1653	Esan	Mbuti	0.0831	0.0025	33.28	574,167
BK1653	Yoruba	Mbuti	0.0830	0.0024	34.06	574,776
BK1653	Mende	Mbuti	0.0827	0.0025	33.54	573,964
BK1653	Igbo	Mbuti	0.0824	0.0024	33.88	574,063
BK1653	Lemande	Mbuti	0.0815	0.0025	32.49	572,791
BK1653	Kongo	Mbuti	0.0812	0.0026	31.51	537,560
BK1653	BantuHerero	Mbuti	0.0794	0.0024	33.15	571,057
BK1653	BantuTswana	Mbuti	0.0723	0.0023	31.26	571,965
BK1653	Biaka	Mbuti	0.0520	0.0019	26.74	561,347
BK1653	Ju_hoan_North	Mbuti	0.0465	0.0020	23.53	576,762
BK1653	Khomani_San	Mbuti	0.0462	0.0021	22.27	554,629

Table S5.6 *D(IUP Bacho Kiro1, IUP Bacho Kiro2; IUP Bacho Kiro3, Mbuti)*. Derived allele sharing among IUP Bacho Kiro Cave specimens. These statistics were calculated using ADMIXTOOLS[3] as implemented in *admixr*[9]. Standard errors (SE) were computed using a Weighted Block Jackknife[3,12] across all autosomes of the "2200k" Panel and using a block size of 5Mb. Three Mbuti individuals from SGDP[10] were used as outgroup. Number of SNPs overlapping among individuals reported in the column "#SNPs".

WW	X	Y	Z	D	SE	Z-score	ABBA	BABA	#SNPs
BachoKiro_F6_620	BachoKiro_CC7_2289	BachoKiro_BB7_240	Mbuti	-0.0844	0.0429	-1.966	196	232	4,280
BachoKiro_F6_620	BachoKiro_CC7_335	BachoKiro_BB7_240	Mbuti	-0.026	0.0103	-2.523	17,437	18,370	383,549
BachoKiro_CC7_2289	BachoKiro_CC7_335	BachoKiro_BB7_240	Mbuti	0.0949	0.0564	1.681	139	115	2,592
BachoKiro_F6_620	BachoKiro_BB7_240	BachoKiro_CC7_335	Mbuti	-0.0062	0.0107	-0.578	18,144	18,370	383,549
BachoKiro_F6_620	BachoKiro_CC7_2289	BachoKiro_CC7_335	Mbuti	-0.0511	0.0454	-1.126	173	191	3,824
BachoKiro_BB7_240	BachoKiro_CC7_2289	BachoKiro_CC7_335	Mbuti	-0.0278	0.0597	-0.466	115	122	2,592
BachoKiro_BB7_240	BachoKiro_CC7_2289	BachoKiro_F6_620	Mbuti	-0.0227	0.0426	-0.534	196	205	4,280
BachoKiro_BB7_240	BachoKiro_CC7_335	BachoKiro_F6_620	Mbuti	-0.0199	0.0102	-1.953	17,437	18,144	383,549
BachoKiro_CC7_2289	BachoKiro_CC7_335	BachoKiro_F6_620	Mbuti	-0.0067	0.0480	-0.139	170	173	3,824

Table S5.7 *D(IUP Bacho Kiro$_1$, X; IUP Bacho Kiro CC7-2289, Mbuti)*. Derived allele sharing between Bacho Kiro *CC7-2289* and the remaining three IUP Bacho Kiro Cave individuals. These statistics were calculated using ADMIXTOOLS[3] as implemented in *admixr*[9]. Standard errors (SE) were computed using a Weighted Block Jackknife[3,12] across all autosomes of the "2200k" Panel and using a block size of 5Mb. Number of SNPs overlapping among individuals reported in the column "#SNPs". Significant statistics (*Z-score*) or $Z \geq 3$ highlighted in yellow.

W	X	Y	Z	D	SE	Z-score	ABBA	BABA	#SNPs
BachoKiro_F6_620	UstIshim	BachoKiro_CC7_2289	Mbuti	0.1209	0.030523	3.96	380	298	6,630
BachoKiro_F6_620	Tianyuan	BachoKiro_CC7_2289	Mbuti	0.1367	0.034261	3.99	366	278	6,440
BachoKiro_F6_620	Kostenki14	BachoKiro_CC7_2289	Mbuti	0.156	0.035395	4.41	383	280	6,495
BachoKiro_F6_620	SunghirIII	BachoKiro_CC7_2289	Mbuti	0.1535	0.030878	4.97	396	291	6,629
BachoKiro_F6_620	GoyetQ116-1	BachoKiro_CC7_2289	Mbuti	0.0711	0.039682	1.79	270	234	4,733
BachoKiro_F6_620	Vestonice16	BachoKiro_CC7_2289	Mbuti	0.0747	0.038493	1.94	291	251	5,210
BachoKiro_F6_620	Yana_old	BachoKiro_CC7_2289	Mbuti	0.1185	0.030971	3.83	412	325	6,898
BachoKiro_F6_620	Malta1	BachoKiro_CC7_2289	Mbuti	0.117	0.036479	3.21	292	231	4,993
BachoKiro_F6_620	ElMiron	BachoKiro_CC7_2289	Mbuti	0.0878	0.041912	2.10	259	217	4,723
BachoKiro_F6_620	Villabruna	BachoKiro_CC7_2289	Mbuti	0.1224	0.035597	3.44	357	279	6,015
BachoKiro_F6_620	Bichon	BachoKiro_CC7_2289	Mbuti	0.1322	0.031973	4.13	411	315	6,887
BachoKiro_F6_620	Satsurblia	BachoKiro_CC7_2289	Mbuti	0.1156	0.038892	2.97	279	221	4,643
BachoKiro_F6_620	Kotias	BachoKiro_CC7_2289	Mbuti	0.1575	0.031806	4.95	410	299	6,895
BachoKiro_F6_620	Karelia	BachoKiro_CC7_2289	Mbuti	0.128	0.033567	3.81	340	263	6,030
BachoKiro_F6_620	Loschbour	BachoKiro_CC7_2289	Mbuti	0.1465	0.029846	4.91	388	289	6,630
BachoKiro_F6_620	LaBrana1	BachoKiro_CC7_2289	Mbuti	0.1142	0.033225	3.44	391	311	6,678
BachoKiro_F6_620	LBK	BachoKiro_CC7_2289	Mbuti	0.1174	0.030731	3.82	388	307	6,630
BachoKiro_F6_620	Saqqaq	BachoKiro_CC7_2289	Mbuti	0.136	0.033334	4.08	390	297	6,747
BachoKiro_BB7_240	UstIshim	BachoKiro_CC7_2289	Mbuti	0.1417	0.036482	3.88	247	186	4,150
BachoKiro_BB7_240	Tianyuan	BachoKiro_CC7_2289	Mbuti	0.1415	0.042673	3.32	239	180	4,150
BachoKiro_BB7_240	Kostenki14	BachoKiro_CC7_2289	Mbuti	0.1882	0.040817	4.61	259	177	4,030
BachoKiro_BB7_240	SunghirIII	BachoKiro_CC7_2289	Mbuti	0.1947	0.037684	5.17	248	167	4,149
BachoKiro_BB7_240	GoyetQ116-1	BachoKiro_CC7_2289	Mbuti	0.1395	0.045057	3.10	204	154	3,216
BachoKiro_BB7_240	Vestonice16	BachoKiro_CC7_2289	Mbuti	0.1246	0.04492	2.77	202	158	3,525
BachoKiro_BB7_240	Yana_old	BachoKiro_CC7_2289	Mbuti	0.1551	0.040902	3.79	259	189	4,307
BachoKiro_BB7_240	Malta1	BachoKiro_CC7_2289	Mbuti	0.1421	0.044923	3.16	185	139	3,131
BachoKiro_BB7_240	ElMiron	BachoKiro_CC7_2289	Mbuti	0.1232	0.046449	2.65	187	146	3,263
BachoKiro_BB7_240	Villabruna	BachoKiro_CC7_2289	Mbuti	0.1503	0.041844	3.59	246	182	3,986
BachoKiro_BB7_240	Bichon	BachoKiro_CC7_2289	Mbuti	0.1454	0.041171	3.53	255	190	4,301
BachoKiro_BB7_240	Satsurblia	BachoKiro_CC7_2289	Mbuti	0.1731	0.045897	3.77	185	130	2,919
BachoKiro_BB7_240	Kotias	BachoKiro_CC7_2289	Mbuti	0.1605	0.040556	3.96	266	192	4,306
BachoKiro_BB7_240	Karelia	BachoKiro_CC7_2289	Mbuti	0.1283	0.042825	3.00	236	182	3,808
BachoKiro_BB7_240	Loschbour	BachoKiro_CC7_2289	Mbuti	0.1829	0.037259	4.91	257	178	4,151
BachoKiro_BB7_240	LaBrana1	BachoKiro_CC7_2289	Mbuti	0.1511	0.040459	3.74	257	190	4,194
BachoKiro_BB7_240	LBK	BachoKiro_CC7_2289	Mbuti	0.1455	0.036741	3.96	259	193	4,150
BachoKiro_BB7_240	Saqqaq	BachoKiro_CC7_2289	Mbuti	0.167	0.040003	4.17	252	180	4,246
BachoKiro_CC7_335	UstIshim	BachoKiro_CC7_2289	Mbuti	0.1158	0.040286	2.87	200	158	3,711
BachoKiro_CC7_335	Tianyuan	BachoKiro_CC7_2289	Mbuti	0.1594	0.044517	3.58	209	151	3,719
BachoKiro_CC7_335	Kostenki14	BachoKiro_CC7_2289	Mbuti	0.1778	0.048147	3.69	207	145	3,616
BachoKiro_CC7_335	SunghirIII	BachoKiro_CC7_2289	Mbuti	0.1618	0.039198	4.13	215	155	3,710
BachoKiro_CC7_335	GoyetQ116-1	BachoKiro_CC7_2289	Mbuti	0.108	0.048589	2.22	172	138	2,832
BachoKiro_CC7_335	Vestonice16	BachoKiro_CC7_2289	Mbuti	0.0802	0.045406	1.77	186	158	3,135
BachoKiro_CC7_335	Yana_old	BachoKiro_CC7_2289	Mbuti	0.1377	0.042943	3.21	215	163	3,855
BachoKiro_CC7_335	Malta1	BachoKiro_CC7_2289	Mbuti	0.1068	0.051949	2.06	145	117	2,805
BachoKiro_CC7_335	ElMiron	BachoKiro_CC7_2289	Mbuti	0.137	0.050974	2.69	178	135	2,902
BachoKiro_CC7_335	Villabruna	BachoKiro_CC7_2289	Mbuti	0.155	0.045352	3.42	211	154	3,527
BachoKiro_CC7_335	Bichon	BachoKiro_CC7_2289	Mbuti	0.1405	0.040644	3.46	220	166	3,852
BachoKiro_CC7_335	Kotias	BachoKiro_CC7_2289	Mbuti	0.1738	0.040859	4.25	223	157	3,851
BachoKiro_CC7_335	Karelia	BachoKiro_CC7_2289	Mbuti	0.1354	0.043918	3.08	186	142	3,372
BachoKiro_CC7_335	Loschbour	BachoKiro_CC7_2289	Mbuti	0.1399	0.040158	3.48	203	153	3,710
BachoKiro_CC7_335	LaBrana1	BachoKiro_CC7_2289	Mbuti	0.1099	0.043837	2.51	206	165	3,760
BachoKiro_CC7_335	LBK	BachoKiro_CC7_2289	Mbuti	0.1086	0.04105	2.65	210	169	3,711
BachoKiro_CC7_335	Saqqaq	BachoKiro_CC7_2289	Mbuti	0.1384	0.041355	3.35	208	158	3,805

Table S5.8 Z-scores of the statistics *D(Bacho Kiro F6-620, X; Y Mbuti)*. Standard errors (SE) were computed using a Weighted Block Jackknife[3,12] across all autosomes of the "2200k" Panel and using a block size of 5Mb. Blue: Z-score ≤ -3; Yellow: Z-score ≥ 3.

X/Y	BachoKiro_BB7_240	BachoKiro_CC7_335	UstIshim	Oase1	Tianyuan	Kostenki14	GoyetQ116-1	BachoKiro_BK_1653	SunghirIII	Yana_old	Vestonice16	Malta1	ElMiron	Villabruna	Bichon	Clovis	Satsurblia	Kolyma_River	Kotias	Karelia	Loschbour	LaBrana1	Hungarian.KO1	Motala12	LBK	Saqqaq
BachoKiro_BB7_240	NA	-0.58	-0.73	0.84	1.66	-1.99	-2.67	-1.85	-2.04	-0.21	-2.11	-0.40	-2.16	-2.57	-2.89	-1.25	-1.53	-0.46	-1.69	-0.72	-2.17	-1.91	-1.79	-2.14	-0.76	-0.41
BachoKiro_CC7_335	-2.52	NA	-1.01	-0.28	0.93	-2.30	-2.36	0.15	-1.34	-0.06	-2.52	-0.74	-0.84	-2.87	-2.36	-0.79	-1.79	-1.52	-1.11	-0.71	-2.41	-2.10	-1.48	-2.01	-1.82	-0.26
UstIshim	8.67	9.63	NA	5.94	0.63	-4.02	-3.14	-1.23	-3.10	-1.10	-3.74	-2.36	-2.41	-3.21	-3.91	-0.95	-3.37	-1.72	-2.00	-0.80	-3.84	-3.34	-1.48	-3.61	-2.17	0.20
Oase1	4.64	6.66	2.73	NA	2.50	0.94	1.09	2.00	1.55	2.71	1.20	2.23	0.55	0.15	0.54	2.92	0.14	1.38	2.06	1.67	0.85	0.69	0.89	1.24	1.19	2.27
Tianyuan	6.79	8.30	-1.59	3.47	NA	-3.27	-4.20	-1.68	-3.53	-5.69	-3.05	-3.56	-2.78	-3.81	-4.47	-8.05	-2.62	-8.74	-2.95	-4.19	-4.48	-4.21	-3.41	-4.01	-1.54	-8.87
Kostenki14	8.98	11.46	-1.84	5.58	1.01	NA	-11.57	-12.26	-17.98	-10.17	-15.93	-9.26	-12.87	-14.31	-14.56	-2.94	-9.35	-2.52	-9.13	-10.37	-15.42	-14.95	-12.56	-13.88	-10.10	-0.83
GoyetQ116-1_old	5.77	7.66	-3.04	3.33	-2.20	-14.94	NA	-15.82	-13.80	-10.15	-15.46	-10.66	-22.26	-15.01	-16.22	-4.26	-8.41	-4.66	-9.17	-11.33	-18.84	-20.03	-14.21	-15.43	-12.57	-2.89
BachoKiro_BK_1653	8.50	11.46	-0.18	5.52	0.98	-13.16	-13.34	NA	-12.38	-7.61	-17.39	-7.00	-14.48	-15.82	-15.72	-1.84	-7.28	-2.06	-7.82	-10.02	-15.60	-16.72	-13.01	-13.83	-12.34	-0.55
SunghirIII	9.14	11.47	-1.80	5.71	-0.29	-19.14	-11.76	-12.37	NA	-7.59	-21.64	-9.47	-13.79	-15.43	-16.54	-2.59	-9.05	-2.72	-9.74	-11.55	-16.70	-16.67	-14.72	-14.17	-11.44	-1.60
Yana_old	9.48	11.55	-1.49	5.66	-3.74	-12.54	-9.67	-9.21	-9.22	NA	-11.94	-11.18	-9.53	-10.52	-12.06	-7.10	-7.86	-6.04	-8.24	-11.14	-12.16	-11.87	-11.06	-10.41	-9.18	-5.66
Vestonice16	7.73	9.56	-2.08	4.64	0.33	-17.21	-12.22	-17.39	-21.84	-10.69	NA	-11.04	-16.90	-19.03	-18.32	-3.94	-9.09	-3.21	-9.08	-12.44	-20.30	-18.25	-18.60	-16.40	-12.94	-1.78
Malta1	9.25	10.19	-1.91	4.77	-1.51	-11.61	-9.59	-8.32	-10.18	-10.34	-11.68	NA	-9.98	-12.10	-14.21	-13.35	-11.45	-11.56	-11.26	-21.53	-14.56	-13.11	-13.88	-19.81	-9.84	-8.75
ElMiron	7.80	9.32	-1.64	3.51	-0.07	-15.49	-19.76	-14.87	-13.87	-8.63	-17.41	-9.16	NA	-26.67	-28.54	-5.34	-8.98	-3.94	-11.08	-14.38	-30.94	-34.40	-23.10	-22.09	-14.99	-2.40
Villabruna	8.39	10.27	-1.48	4.15	-0.12	-14.52	-12.24	-15.03	-14.62	-8.34	-18.22	-10.37	-24.63	NA	-41.40	-4.54	-12.63	-4.39	-14.00	-19.97	-44.93	-37.85	-38.04	-32.43	-19.41	-2.73
Bichon	8.66	11.09	-1.66	5.85	-0.05	-14.56	-12.80	-13.67	-14.83	-8.72	-16.98	-12.02	-26.40	-39.83	NA	-4.79	-13.44	-5.29	-13.51	-20.57	-45.57	-38.74	-36.29	-32.40	-18.59	-4.06
Clovis	8.41	10.38	-1.83	5.17	-6.15	-6.03	-4.20	-3.68	-4.80	-7.42	-5.82	-13.73	-6.77	-7.01	-8.41	NA	-8.67	-22.65	-7.58	-15.26	-10.01	-9.52	-8.89	-12.10	-6.57	-21.38
Satsurblia	12.59	12.99	1.51	7.82	4.27	-5.96	-2.54	-3.16	-4.96	-1.98	-4.75	-6.91	-4.90	-9.01	-11.55	-2.20	NA	-2.12	-27.74	-10.59	-11.13	-9.08	-10.59	-11.71	-15.05	-0.09
Kolyma_River	8.91	9.96	-2.61	4.19	-7.13	-5.46	-4.96	-3.99	-5.00	-6.84	-5.23	-12.44	-5.48	-7.35	-9.04	-23.97	-8.23	NA	-7.67	-14.57	-8.52	-7.96	-8.82	-11.27	-6.45	-25.92
Kotias	11.61	14.34	1.59	8.24	3.25	-7.06	-3.93	-4.66	-6.41	-3.38	-6.00	-7.20	-7.19	-10.66	-12.07	-2.38	-28.28	-2.57	NA	-11.96	-12.56	-11.23	-11.48	-13.63	-15.85	-2.05
Karelia	9.56	11.64	-0.06	5.67	-0.96	-12.29	-9.50	-10.18	-11.74	-9.43	-12.72	-20.23	-14.47	-21.12	-23.90	-13.93	-15.77	-13.04	-15.25	NA	-24.22	-22.41	-25.03	-29.50	-16.22	-9.70
Loschbour	9.40	11.06	-1.50	6.23	-0.06	-14.38	-14.74	-14.08	-14.81	-8.91	-17.50	-11.81	-27.59	-41.83	-44.77	-6.03	-13.24	-4.81	-13.72	-21.12	NA	-39.30	-37.19	-33.99	-19.70	-3.90
LaBrana1	9.65	11.46	-1.17	5.92	0.22	-13.79	-16.06	-14.75	-14.65	-8.77	-15.92	-10.76	-30.41	-35.90	-39.47	-5.90	-11.58	-4.60	-13.38	-19.28	-41.59	NA	-32.81	-29.36	-17.90	-4.19
Hungarian.KO1	9.54	11.18	0.01	5.02	0.88	-13.19	-11.35	-12.29	-13.81	-8.62	-16.21	-12.37	-20.83	-37.69	-38.10	-6.02	-13.88	-5.83	-14.46	-22.87	-39.56	-36.23	NA	-32.48	-21.44	-4.69
Motala12	10.64	12.21	-1.10	6.01	0.54	-12.52	-11.80	-12.05	-11.88	-7.30	-14.55	-16.84	-19.15	-31.00	-32.02	-8.54	-14.52	-7.32	-16.18	-27.37	-34.22	-29.47	-30.83	NA	-19.78	-5.13
LBK	12.58	13.58	1.32	8.16	4.40	-8.05	-6.49	-8.89	-8.34	-3.97	-9.42	-5.88	-10.58	-15.81	-16.79	-1.23	-15.68	-1.14	-16.46	-12.06	-17.91	-15.58	-17.59	-17.53	NA	-1.04
Saqqaq	8.26	10.27	-1.55	4.56	-7.68	-4.62	-3.84	-3.37	-4.52	-7.08	-4.49	-10.84	-4.67	-6.16	-8.18	-23.90	-7.22	-27.06	-8.12	-12.61	-8.44	-8.50	-8.51	-9.44	-7.28	NA

Table S5.9 Z-scores of the statistics *D(Bacho Kiro BB7-240, X; Y Mbuti)*. Standard errors (SE) were computed using a Weighted Block Jackknife[3,12] across all autosomes of the "2200k" Panel and using a block size of 5Mb. Blue: Z-score ≤ -3; Yellow: Z-score ≥ 3.

X/Y	BachoKiro_F6_620	BachoKiro_CC7_335	UstIshim	Oase1	Tianyuan	Kostenki14	GoyetQ116-1	BachoKiro_BK1653	SunghirIII	Yana_old	Vestonice16	Malta1	ElMiron	Villabruna	Bichon	Clovis	Satsurblia	Kolyma_River	Kotias	Karelia	Loschbour	LaBrana1	Hungarian.KO1	Motala12	LBK	Saqqaq
BachoKiro_F6_620	NA	0.58	0.73	0.84	1.66	1.99	2.67	1.85	2.04	0.21	2.11	0.40	2.16	2.57	2.89	1.25	1.53	0.46	1.69	0.72	2.17	1.91	1.79	2.14	0.76	0.41
BachoKiro_CC7_335	-1.95	NA	0.09	0.97	0.73	-0.01	0.94	2.01	0.91	0.53	0.09	-0.15	0.07	-0.53	0.45	0.49	-0.24	-0.40	0.72	0.59	0.68	-0.26	0.52	0.40	-0.33	0.94
UstIshim	9.42	10.87	NA	6.62	1.23	-1.86	0.22	0.72	-1.41	-1.07	-1.57	-1.59	-0.42	-0.66	-1.07	-0.33	-2.00	-1.87	-0.55	-0.11	-1.82	-1.47	-0.20	-1.66	-1.82	0.06
Oase1	5.28	6.62	2.70	NA	2.53	1.86	3.25	1.86	2.23	2.95	3.36	2.12	2.63	1.34	2.41	2.77	1.87	1.13	2.38	1.16	2.90	2.31	1.64	1.50	1.57	2.20
Tianyuan	8.56	9.95	-1.23	3.88	NA	-1.04	-0.50	0.97	-1.43	-4.86	-0.08	-2.88	-0.59	-1.02	-1.26	-6.10	-0.55	-7.98	-0.84	-2.89	-2.11	-1.39	-1.39	-1.60	-0.86	-7.70
Kostenki14	11.45	11.97	-1.29	6.15	2.28	NA	-8.32	-9.78	-15.47	-9.24	-12.17	-8.36	-9.82	-10.67	-11.03	-2.12	-6.93	-2.74	-7.83	-9.79	-12.45	-11.55	-11.25	-10.75	-9.49	-0.67
GoyetQ116-1_old	9.13	9.00	-2.66	4.07	-1.17	-12.41	NA	-13.19	-11.68	-9.02	-11.08	-9.15	-19.80	-11.83	-13.01	-2.88	-6.06	-3.90	-7.04	-9.72	-16.28	-16.39	-11.60	-12.65	-10.94	-2.46
BachoKiro_BK1653	10.69	12.45	0.60	6.31	3.07	-11.26	-9.89	NA	-11.36	-7.10	-13.61	-6.45	-11.93	-12.41	-11.58	-0.61	-5.04	-1.09	-6.56	-9.19	-13.26	-12.79	-10.12	-10.88	-10.93	0.34
SunghirIII	11.59	13.38	-1.44	6.22	1.26	-16.11	-8.15	-10.04	NA	-7.76	-17.90	-8.63	-11.85	-12.15	-13.94	-2.07	-7.68	-3.17	-9.19	-10.72	-15.05	-13.99	-13.34	-13.02	-11.91	-1.47
Yana_old	10.23	12.44	-0.73	6.91	-2.12	-9.54	-5.96	-6.63	-7.42	NA	-8.27	-10.75	-6.69	-7.00	-8.11	-5.45	-5.92	-5.98	-6.78	-9.87	-10.00	-9.56	-9.15	-8.56	-8.64	-5.05
Vestonice16	10.79	10.70	-2.08	6.16	1.64	-13.75	-9.04	-14.52	-18.20	-9.81	NA	-8.99	-14.51	-15.38	-14.99	-2.42	-7.16	-2.99	-7.72	-12.17	-17.54	-14.67	-15.03	-14.16	-11.72	-1.56
Malta1	10.01	10.92	-1.65	5.35	-0.71	-9.29	-6.37	-6.40	-8.72	-10.46	-8.59	NA	-7.44	-9.19	-11.20	-11.87	-10.17	-10.33	-10.35	-20.15	-12.46	-11.52	-12.16	-16.55	-9.80	-8.71
ElMiron	10.16	10.28	-1.30	4.91	1.00	-11.75	-16.22	-12.32	-12.59	-8.26	-13.39	-7.51	NA	-22.51	-24.94	-4.00	-6.59	-3.40	-8.69	-12.95	-29.63	-29.23	-20.19	-20.08	-13.62	-1.98
Villabruna	11.14	11.70	-0.93	4.77	1.10	-11.65	-8.59	-12.20	-12.78	-7.62	-14.14	-9.37	-21.80	NA	-35.78	-3.37	-10.80	-3.99	-12.27	-18.47	-42.27	-32.07	-33.40	-29.12	-18.12	-2.27
Bichon	12.24	12.18	-1.38	6.51	0.86	-11.36	-9.73	-11.19	-13.62	-8.72	-13.61	-11.80	-23.91	-36.56	NA	-4.39	-11.99	-5.64	-12.54	-19.34	-41.86	-35.65	-32.01	-30.86	-18.26	-3.82
Clovis	9.51	11.50	-1.21	5.76	-3.80	-3.67	-0.49	-1.04	-2.94	-6.71	-2.78	-12.69	-4.11	-3.95	-4.87	NA	-6.63	-21.88	-5.82	-14.33	-7.44	-6.29	-6.71	-9.88	-5.84	-20.01
Satsurblia	13.75	13.66	1.52	7.93	5.31	-3.62	0.76	-1.21	-3.23	-2.23	-2.25	-5.74	-2.39	-5.89	-7.55	-1.32	NA	-2.02	-24.16	-8.84	-8.20	-6.88	-8.26	-8.75	-13.33	0.68
Kolyma_River	9.70	11.18	-1.97	4.98	-5.34	-3.48	-1.34	-1.51	-3.34	-6.29	-2.65	-10.93	-2.96	-4.49	-5.59	-21.98	-6.63	NA	-6.52	-13.13	-6.27	-5.55	-6.99	-8.73	-6.02	-24.59
Kotias	13.18	15.11	2.28	8.10	4.60	-5.15	-0.89	-3.00	-5.02	-3.45	-3.42	-6.86	-4.96	-7.85	-8.74	-1.53	-25.62	-2.94	NA	-10.59	-10.26	-9.12	-10.17	-11.93	-14.69	-1.75
Karelia	10.24	11.86	0.36	6.06	0.37	-9.24	-5.94	-7.84	-9.88	-8.78	-9.78	-17.91	-11.59	-16.80	-18.26	-12.39	-13.54	-11.97	-13.69	NA	-21.59	-18.62	-21.29	-26.48	-14.95	-9.31
Loschbour	11.56	12.82	-1.15	7.15	1.28	-11.34	-11.36	-11.42	-13.61	-8.69	-13.97	-10.92	-25.18	-38.85	-39.63	-5.41	-11.53	-5.03	-12.81	-20.43	NA	-36.56	-34.40	-33.30	-19.25	-3.81
LaBrana1	11.96	12.54	-0.69	6.61	1.86	-10.48	-11.77	-11.08	-13.08	-8.50	-12.06	-9.90	-25.83	-31.08	-34.94	-4.49	-10.20	-4.41	-12.08	-17.63	-38.33	NA	-29.65	-26.68	-17.19	-3.43
Hungarian.KO1	11.52	11.86	0.34	5.47	1.63	-11.06	-7.56	-9.41	-11.83	-8.30	-12.34	-11.02	-18.44	-32.09	-32.04	-5.21	-11.91	-5.79	-13.77	-21.21	-36.71	-30.64	NA	-30.18	-20.75	-4.28
Motala12	12.43	13.29	-0.18	6.35	2.15	-9.17	-7.72	-8.87	-10.02	-7.08	-11.11	-14.40	-16.80	-27.45	-26.44	-6.83	-12.25	-6.58	-14.03	-24.65	-32.07	-25.08	-28.45	NA	-18.09	-4.40
LBK	13.14	14.70	1.68	8.49	5.33	-5.56	-3.00	-6.35	-6.82	-4.19	-6.31	-5.13	-8.06	-12.51	-12.65	-0.68	-13.57	-1.54	-14.39	-10.59	-15.19	-13.54	-15.66	-15.34	NA	-1.27
Saqqaq	8.85	11.16	-1.19	4.98	-5.71	-2.49	-0.44	-1.13	-2.77	-6.44	-1.78	-8.81	-2.59	-3.12	-4.73	-20.03	-5.12	-24.82	-6.50	-11.49	-5.69	-5.34	-5.94	-7.40	-7.08	NA

Table S5.10 Z-scores of the statistics *D(Bacho Kiro CC7-335, X; Y Mbuti)*. Standard errors (SE) were computed using a Weighted Block Jackknife[3,12] across all autosomes of the "2200k" Panel and using a block size of 5Mb. Blue: Z-score ≤ -3; Yellow: Z-score ≥ 3.

X/Y	BachoKiro_F6_620	BachoKiro_BB7_240	UstIshim	Oase1	Tianyuan	Kostenki14	GoyetQ116-1	BachoKiro_BK1653	SunghirIII	Yana_old2	Vestonice16	Malta1	ElMiron	Villabruna	Bichon	Clovis	Satsurblia	Kolyma_River	Kotias	Karelia	Loschbour	LaBrana1	Hungarian.KO1	Motala12	LBK	Saqqaq
BachoKiro_F6_620	NA	2.52	1.01	0.28	0.93	2.30	2.36	0.15	1.34	0.06	2.52	0.74	0.84	2.87	2.36	0.79	1.79	1.52	1.11	0.71	2.41	2.10	1.48	2.01	1.82	0.26
BachoKiro_BB7_240	1.95	NA	-0.09	-0.97	-0.73	0.01	-0.94	-2.01	-0.91	-0.53	-0.09	0.15	-0.07	0.53	-0.45	-0.49	0.24	0.40	-0.72	-0.59	-0.68	0.26	-0.52	-0.40	0.33	-0.94
UstIshim	11.04	11.00	NA	5.93	1.35	-2.20	-0.70	-1.60	-2.34	-1.10	-1.52	-0.67	-1.26	-0.40	-2.13	-0.69	-1.25	-0.87	-0.89	-0.46	-2.06	-1.25	-0.78	-1.91	-0.89	0.12
Oase1	6.88	5.55	3.34	NA	2.43	1.38	2.06	1.00	1.74	2.16	1.71	2.02	1.37	1.53	1.49	2.78	1.76	2.08	2.44	0.83	2.54	3.11	1.27	1.77	2.14	2.33
Tianyuan	9.32	9.40	-0.50	3.52	NA	-1.49	-1.83	-1.30	-2.64	-5.44	-0.65	-1.78	-0.98	-0.53	-1.94	-7.18	-0.59	-7.52	-1.41	-3.23	-2.10	-1.82	-2.24	-2.05	-0.14	-8.08
Kostenki14	13.68	12.01	-1.00	4.86	1.79	NA	-8.97	-11.46	-16.30	-9.84	-12.43	-7.68	-9.96	-10.85	-11.95	-1.98	-6.39	-1.52	-7.41	-9.96	-12.05	-11.24	-11.18	-11.00	-8.60	-1.18
GoyetQ116-1	10.51	7.96	-2.59	2.43	-2.07	-12.24	NA	-15.02	-12.29	-10.02	-12.29	-8.70	-20.44	-12.01	-14.15	-3.38	-6.33	-4.07	-8.63	-11.30	-17.05	-16.81	-12.49	-13.57	-11.38	-2.75
BachoKiro_BK1653	11.31	10.34	0.74	5.57	2.65	-10.45	-10.12	NA	-10.94	-7.30	-13.76	-5.34	-11.43	-11.98	-11.70	-0.83	-4.14	-0.36	-6.24	-8.73	-12.38	-12.21	-10.47	-10.68	-9.74	-0.45
SunghirIII	13.39	12.46	-0.82	5.07	0.61	-15.78	-8.56	-12.18	NA	-7.43	-18.09	-7.48	-11.00	-11.84	-13.99	-1.79	-6.18	-1.97	-7.95	-10.54	-13.46	-13.09	-12.54	-11.28	-9.89	-1.28
Yana_old2	11.81	11.58	-0.20	5.19	-2.40	-10.07	-6.31	-8.30	-8.00	NA	-8.79	-9.65	-7.27	-6.64	-8.77	-6.23	-4.98	-5.21	-6.41	-9.76	-9.25	-8.45	-9.00	-8.53	-7.10	-5.75
Vestonice16	12.42	10.46	-1.80	4.01	0.97	-14.48	-9.55	-16.46	-20.06	-10.74	NA	-9.22	-14.67	-16.24	-15.37	-2.80	-6.51	-2.40	-8.65	-11.91	-17.12	-14.28	-15.15	-15.28	-11.36	-2.14
Malta1	11.46	10.86	-0.97	4.21	-0.48	-9.30	-6.84	-8.13	-9.46	-10.72	-9.23	NA	-7.62	-8.89	-11.10	-12.67	-9.10	-10.41	-10.72	-20.10	-11.78	-10.32	-11.76	-16.01	-8.78	-9.09
ElMiron	10.60	10.47	-1.56	3.16	0.32	-12.58	-17.40	-14.52	-13.38	-9.30	-15.13	-7.99	NA	-22.49	-26.66	-5.12	-6.73	-4.04	-10.33	-14.14	-27.51	-29.21	-19.58	-20.91	-13.32	-2.95
Villabruna	13.20	11.92	-0.29	4.20	1.50	-12.14	-9.03	-13.65	-13.26	-7.98	-15.08	-8.62	-20.36	NA	-37.03	-3.32	-9.68	-3.59	-11.78	-19.07	-39.86	-32.15	-34.90	-28.54	-17.54	-2.12
Bichon	13.76	11.74	-0.89	5.12	0.79	-12.74	-10.40	-13.48	-14.45	-9.03	-14.06	-10.67	-23.35	-36.62	NA	-4.54	-10.88	-4.60	-12.40	-19.20	-40.98	-35.69	-32.07	-28.77	-17.05	-4.21
Clovis	11.54	10.63	-0.60	5.26	-4.59	-3.52	-1.38	-3.19	-3.37	-7.09	-2.85	-11.92	-4.48	-3.86	-5.34	NA	-6.19	-21.79	-6.14	-15.12	-6.68	-6.42	-7.05	-10.31	-4.95	-20.41
Satsurblia	15.43	14.99	2.45	6.85	4.19	-4.04	-0.64	-3.01	-4.10	-1.98	-2.38	-4.90	-2.69	-6.26	-8.25	-2.06	NA	-1.47	-24.76	-9.39	-8.66	-7.47	-9.00	-8.89	-12.81	-0.37
Kolyma_River	12.09	11.65	-1.33	4.13	-6.06	-3.36	-2.32	-3.86	-4.05	-6.81	-2.65	-10.90	-3.93	-4.27	-6.11	-23.51	-6.36	NA	-6.87	-13.74	-5.94	-5.30	-7.27	-8.48	-4.78	-24.48
Kotias	15.03	14.67	3.19	7.91	4.61	-4.32	-1.83	-4.32	-5.09	-2.87	-3.62	-5.98	-4.80	-7.21	-8.84	-1.53	-22.46	-1.59	NA	-10.40	-9.29	-8.53	-9.62	-10.55	-13.98	-1.91
Karelia	13.00	11.48	1.19	5.26	0.14	-9.50	-6.98	-9.63	-10.38	-9.45	-9.79	-18.31	-11.60	-17.20	-19.05	-12.86	-11.76	-11.51	-13.46	NA	-19.73	-18.66	-21.54	-26.14	-13.99	-9.51
Loschbour	14.00	12.63	-0.57	5.71	1.11	-12.16	-12.26	-14.50	-14.05	-9.15	-14.73	-10.38	-24.95	-39.05	-42.52	-5.86	-11.14	-4.21	-12.89	-20.74	NA	-37.32	-35.09	-31.18	-18.45	-3.94
LaBrana1	13.66	12.45	-0.17	6.27	1.32	-11.39	-13.22	-13.64	-13.90	-8.95	-12.63	-9.19	-27.08	-33.15	-36.21	-5.51	-10.13	-3.84	-12.11	-19.23	-38.03	NA	-30.22	-27.96	-17.17	-4.26
Hungarian.KO1	12.87	11.63	0.67	4.43	1.42	-10.73	-8.22	-11.63	-12.39	-8.05	-12.48	-9.68	-17.65	-31.76	-31.32	-4.97	-10.74	-4.70	-12.85	-21.12	-33.89	-28.81	NA	-27.21	-18.28	-4.03
Motala12	14.56	13.14	0.45	5.35	2.08	-10.24	-8.58	-11.26	-10.68	-7.65	-11.72	-13.24	-16.45	-26.65	-27.73	-7.53	-10.81	-5.86	-13.88	-25.70	-30.31	-26.02	-27.39	NA	-17.29	-4.29
LBK	15.66	15.65	2.74	7.69	5.46	-5.73	-4.07	-8.41	-7.17	-3.82	-6.48	-4.06	-8.11	-11.99	-12.74	-0.79	-12.39	-0.07	-14.93	-11.52	-14.02	-12.59	-14.95	-14.10	NA	-0.89
Saqqaq	11.08	10.45	-0.18	4.72	-6.10	-2.71	-1.04	-3.55	-3.11	-7.17	-1.68	-9.12	-2.88	-2.66	-5.36	-20.90	-4.61	-24.84	-6.90	-11.56	-5.29	-5.61	-6.02	-6.87	-5.37	NA

Table S5.11 Z-scores of the statistics *D(Bacho Kiro BK1653, X; Y Mbuti)*. Standard errors (SE) were computed using a Weighted Block Jackknife[3,12] across all autosomes of the "2200k" Panel and using a block size of 5Mb. Blue: Z-score ≤ -3; Yellow: Z-score ≥ 3.

X/Y	BachoKiro_F6_620	BachoKiro_BB7_240	BachoKiro_CC7_335	UstIshim	Oase1	Tianyuan	Kostenki14	GoyetQ116-1	SunghirIII	Yana_old	Vestonice16	Malta1	ElMiron	Villabruna	Bichon	Clovis	Satsurblia	Kolyma_River	Kotias	Karelia	Loschbour	LaBrana1	Hungarian.KO1	Motala12	LBK	Saqqaq
BachoKiro_F6_620	NA	-8.50	-11.46	0.18	-5.52	0.98	13.16	13.34	12.38	7.61	17.39	7.00	14.48	15.82	15.72	1.84	7.28	2.06	7.82	10.02	15.60	16.72	13.01	13.83	12.34	0.55
BachoKiro_BB7_240	-10.69	NA	-12.45	-0.60	-6.31	-3.07	11.26	9.89	11.36	7.10	13.61	6.45	11.93	12.41	11.58	0.61	5.04	1.09	6.56	9.19	13.26	12.79	10.12	10.88	10.93	-0.34
BachoKiro_CC7_335	-11.31	-10.34	NA	-0.74	-5.57	-2.65	10.45	10.12	10.94	7.30	13.76	5.34	11.43	11.98	11.70	0.83	4.14	0.36	6.24	8.73	12.38	12.21	10.47	10.68	9.74	0.45
UstIshim	-0.91	0.11	-2.24	NA	0.07	-1.05	9.13	9.93	9.58	6.37	13.33	5.26	12.42	12.77	11.52	0.51	3.80	-0.22	5.73	9.84	12.46	13.21	12.00	10.53	9.32	0.51
Oase1	-3.33	-4.24	-4.18	2.28	NA	0.43	11.87	11.80	11.53	8.32	15.02	7.46	12.62	11.89	13.70	2.30	5.08	2.26	7.80	9.42	14.52	12.98	10.09	11.06	10.24	2.29
Tianyuan	-2.63	-1.94	-4.13	-1.33	-2.03	NA	10.70	9.74	9.04	2.58	14.92	4.11	11.78	12.36	10.88	-6.10	4.61	-7.26	5.12	6.54	11.69	12.26	10.37	9.97	10.10	-8.29
Kostenki14	0.56	0.80	-1.37	-2.20	-0.25	-0.10	NA	2.27	-5.26	-2.02	1.98	-1.88	2.41	2.58	1.59	-1.22	-2.09	-1.10	-1.37	0.25	0.96	2.06	0.54	1.45	2.08	-0.64
GoyetQ116-1	-1.99	-3.41	-4.20	-4.10	-2.38	-4.18	-1.08	NA	-1.18	-2.36	2.73	-2.84	-8.14	0.66	-1.19	-2.05	-1.81	-3.29	-1.95	-0.88	-2.87	-3.68	-1.11	-1.24	0.62	-3.39
SunghirIII	-0.15	0.40	-1.13	-2.28	-0.69	-2.19	-5.24	2.01	NA	0.38	-3.03	-1.81	1.28	1.35	-0.84	-1.09	-2.33	-1.64	-2.19	-0.92	-1.18	-0.21	-1.52	0.21	0.38	-1.71
Yana_old	-1.81	0.52	-1.48	-1.51	-0.29	-5.30	2.11	4.79	4.32	NA	6.89	-4.28	6.23	6.15	5.27	-5.51	-0.25	-5.09	-0.04	-0.04	4.32	5.19	3.22	3.44	4.23	-5.94
Vestonice16	0.30	-0.61	-2.30	-2.37	-0.52	-1.23	-3.66	1.48	-8.08	-2.59	NA	-3.15	-1.99	-2.79	-2.63	-1.53	-2.07	-1.65	-1.99	-2.03	-3.90	-1.38	-3.98	-2.24	-0.15	-1.43
Malta1	-1.10	0.03	-2.89	-2.77	-1.47	-3.49	2.34	4.06	2.71	-3.85	6.19	NA	4.39	3.68	1.70	-12.94	-3.96	-10.48	-4.45	-11.12	1.41	2.68	-0.83	-5.23	1.67	-9.30
ElMiron	-1.22	-0.69	-2.76	-1.58	-1.41	-2.15	-0.73	-7.10	-1.68	-1.00	0.03	-1.47	NA	-11.41	-14.37	-3.87	-2.32	-2.71	-4.26	-4.91	-16.04	-16.89	-10.69	-8.67	-3.03	-3.14
Villabruna	0.16	-0.43	-2.43	-1.64	-2.53	-1.62	0.01	2.43	-0.94	-0.67	0.49	-2.64	-9.86	NA	-26.05	-3.11	-6.08	-3.24	-6.57	-9.70	-28.64	-20.91	-24.32	-19.05	-6.95	-2.92
Bichon	1.07	0.20	-1.79	-2.12	-0.65	-1.92	0.16	1.02	-2.02	-0.34	1.18	-4.11	-12.08	-24.52	NA	-3.80	-7.50	-4.57	-6.75	-10.22	-29.10	-21.73	-23.06	-18.35	-6.88	-4.19
Clovis	-1.83	-0.45	-2.66	-2.13	-1.81	-7.90	8.71	11.23	9.17	1.20	13.06	-6.36	8.86	9.61	8.39	NA	-1.06	-21.49	0.63	-4.69	7.71	8.39	4.96	2.02	6.02	-21.17
Satsurblia	3.90	3.71	1.22	1.42	1.64	2.97	7.52	11.17	7.91	6.36	12.55	1.47	10.26	6.36	5.18	-1.08	NA	-0.42	-19.17	-0.11	4.68	7.04	2.37	2.83	-1.92	0.16
Kolyma_River	-2.02	-0.42	-3.41	-3.11	-2.67	-9.62	8.65	10.13	8.35	1.45	13.85	-4.50	9.82	9.80	7.72	-21.97	-1.18	NA	-0.37	-3.86	8.10	9.15	5.01	3.16	6.20	-26.61
Kotias	2.63	3.17	1.52	1.84	1.83	1.73	7.73	9.72	6.89	5.14	12.63	-0.02	8.03	6.04	4.46	-0.90	-21.17	-1.49	NA	-0.98	3.98	4.78	1.75	0.50	-3.75	-1.63
Karelia	0.02	0.85	-1.05	-0.14	-0.20	-2.69	2.92	4.71	2.00	-1.18	6.01	-12.70	1.42	-4.46	-5.88	-12.19	-8.28	-12.01	-7.75	NA	-6.97	-5.15	-9.66	-14.46	-3.42	-10.20
Loschbour	0.69	0.84	-1.48	-2.10	-0.18	-1.93	-0.52	-0.92	-2.47	-1.27	0.20	-4.46	-14.15	-26.37	-29.39	-5.21	-7.47	-4.03	-7.58	-12.21	NA	-25.94	-25.40	-21.39	-8.01	-4.42
LaBrana1	0.89	0.79	-1.34	-1.51	0.17	-1.19	0.26	-1.35	-1.65	-0.79	2.43	-3.84	-13.94	-18.70	-22.82	-4.25	-5.25	-3.89	-6.57	-10.11	-24.34	NA	-19.30	-15.47	-5.44	-4.43
Hungarian.KO1	0.86	0.82	-1.07	-0.22	-0.68	-1.32	0.77	2.89	-0.85	-0.14	1.86	-4.58	-7.00	-21.07	-21.15	-4.66	-6.94	-5.17	-7.48	-12.67	-23.77	-18.44	NA	-19.19	-8.98	-4.62
Motala12	1.35	1.37	-0.63	-1.37	-0.50	-1.22	2.49	3.40	1.30	0.12	4.07	-8.62	-4.34	-15.10	-15.61	-7.40	-7.41	-6.59	-8.28	-16.95	-17.94	-12.82	-17.86	NA	-7.60	-6.02
LBK	2.47	3.85	1.19	1.23	1.81	2.42	6.54	8.93	5.26	4.78	10.27	1.95	5.26	1.13	0.16	-0.06	-8.59	0.24	-8.55	-1.16	-0.61	1.86	-3.86	-2.79	NA	-1.11
Saqqaq	-2.89	-1.56	-3.25	-1.85	-1.75	-9.78	9.27	10.59	8.83	0.90	14.56	-2.43	10.78	10.98	8.62	-20.57	0.19	-25.59	0.01	-1.60	8.33	8.81	5.53	4.39	5.02	NA

Table S5.12 Z-scores of the statistics *D(X,Y; Bacho Kiro F6-620, Mbuti)*. Standard errors (SE) were computed using a Weighted Block Jackknife[3,12] across all autosomes of the "2200k" Panel and using a block size of 5Mb. Blue: Z-score ≤ -3; Yellow: Z-score ≥ 3.

X/Y	BachoKiro_BB7_240	BachoKiro_CC7_335	UstIshim	Oase1	Tianyuan	Kostenki14	GoyetQ116-1	BachoKiro_BK_1653	SunghirIII	Yana_old	Vestonice16	Malta1	ElMiron	Villabruna	Bichon	Clovis	Satsurblia	Kolyma_River	Kotias	Karelia	Loschbour	LaBrana1	Hungarian.KO1	Motala12	LBK	Saqqaq
BachoKiro_BB7_240	NA	-1.95	9.42	5.28	8.56	11.45	9.13	10.69	11.59	9.71	10.79	10.01	10.16	11.14	12.24	9.51	13.75	9.70	13.18	10.24	11.56	11.96	11.52	12.43	13.14	8.85
BachoKiro_CC7_335	1.95	NA	11.04	6.88	9.32	13.68	10.51	11.31	13.39	12.14	12.42	11.46	10.60	13.20	13.76	11.54	15.43	12.09	15.03	13.00	14.00	13.66	12.87	14.56	15.66	11.08
UstIshim	-9.42	-11.04	NA	-2.92	-2.26	1.94	-0.16	0.91	1.09	-0.50	1.57	0.19	0.55	1.61	2.06	-1.09	4.73	-1.11	3.47	0.68	1.99	1.83	1.41	2.20	3.37	-1.81
Oase1	-5.28	-6.88	2.92	NA	0.94	4.26	2.20	3.33	3.88	2.38	3.37	2.39	3.01	3.74	4.97	2.31	7.11	2.78	5.67	3.60	5.30	4.92	3.87	4.47	6.47	2.28
Tianyuan	-8.56	-9.32	2.26	-0.94	NA	4.21	1.85	2.63	3.33	1.58	3.29	2.06	2.74	3.68	4.45	1.34	6.99	1.54	6.13	3.32	4.21	4.32	4.17	4.34	5.93	0.61
Kostenki14	-11.45	-13.68	-1.94	-4.26	-4.21	NA	-3.24	-0.56	-0.87	-2.72	-0.83	-2.07	-2.00	-0.84	0.19	-3.26	2.93	-3.07	2.21	-1.44	0.26	-0.07	-0.32	0.24	1.91	-3.96
GoyetQ116-1	-9.13	-10.51	0.16	-2.20	-1.85	3.24	NA	1.99	2.08	0.15	2.63	0.80	1.59	2.40	3.03	-0.07	5.74	-0.43	5.20	1.41	3.06	2.94	2.36	2.77	5.04	-1.03
BachoKiro_BK_1653	-10.69	-11.31	-0.91	-3.33	-2.63	0.56	-1.99	NA	-0.15	-1.71	0.30	-1.10	-1.22	0.16	1.07	-1.83	3.90	-2.02	2.63	0.02	0.69	0.89	0.86	1.35	2.47	-2.89
SunghirIII	-11.59	-13.39	-1.09	-3.88	-3.33	0.87	-2.08	0.15	NA	-1.78	0.32	-1.06	-0.41	0.46	1.16	-2.36	4.14	-2.43	2.76	-0.59	1.06	0.89	0.65	1.38	2.61	-3.12
Yana_old	-9.71	-12.14	0.50	-2.38	-1.58	2.72	-0.15	1.71	1.78	NA	2.00	0.62	1.33	2.45	2.96	-0.59	5.44	-0.63	4.39	1.35	2.84	2.66	2.60	3.06	4.23	-1.38
Vestonice16	-10.79	-12.42	-1.57	-3.37	-3.29	0.83	-2.63	-0.30	-0.32	-2.00	NA	-1.07	-0.95	-0.14	0.73	-2.19	4.04	-2.32	2.66	-0.74	0.60	0.78	0.98	0.84	2.60	-2.97
Malta1	-10.01	-11.46	-0.19	-2.39	-2.06	2.07	-0.80	1.10	1.06	-0.62	1.07	NA	1.07	1.40	2.05	-1.37	4.50	-1.27	3.98	0.56	1.99	2.07	1.67	2.22	3.75	-2.52
ElMiron	-10.16	-10.60	-0.55	-3.01	-2.74	2.00	-1.59	1.22	0.41	-1.33	0.95	-1.07	NA	1.05	2.07	-1.55	4.15	-1.44	3.94	0.36	1.51	2.03	2.02	1.94	4.13	-2.29
Villabruna	-11.14	-13.20	-1.61	-3.74	-3.68	0.84	-2.40	-0.16	-0.46	-2.45	0.14	-1.40	-1.05	NA	0.82	-2.61	3.61	-2.94	2.91	-1.14	0.49	0.85	0.28	1.10	2.66	-3.34
Bichon	-12.24	-13.76	-2.06	-4.97	-4.45	-0.19	-3.03	-1.07	-1.16	-2.96	-0.73	-2.05	-2.07	-0.82	NA	-3.68	2.84	-3.77	1.89	-1.87	-0.17	-0.48	-0.58	0.15	1.56	-4.29
Clovis	-9.51	-11.54	1.09	-2.31	-1.34	3.26	0.07	1.83	2.36	0.59	2.19	1.37	1.55	2.61	3.68	NA	6.39	-0.05	5.45	2.19	3.68	3.53	3.16	3.78	5.41	-1.12
Satsurblia	-13.75	-15.43	-4.73	-7.11	-6.99	-2.93	-5.74	-3.90	-4.14	-5.44	-4.04	-4.50	-4.15	-3.61	-2.84	-6.39	NA	-6.56	-1.53	-5.20	-3.21	-3.11	-3.39	-3.09	-1.76	-7.32
Kolyma_River	-9.70	-12.09	1.11	-2.78	-1.54	3.07	0.43	2.02	2.43	0.63	2.32	1.27	1.44	2.94	3.77	0.05	6.56	NA	5.21	2.08	3.61	3.47	3.26	3.86	5.29	-1.18
Kotias	-13.18	-15.03	-3.47	-5.67	-6.13	-2.21	-5.20	-2.63	-2.76	-4.39	-2.66	-3.98	-3.94	-2.91	-1.89	-5.45	1.53	-5.21	NA	-4.00	-1.85	-2.32	-2.67	-1.96	-0.35	-6.12
Karelia	-10.24	-13.00	-0.68	-3.60	-3.32	1.44	-1.41	-0.02	0.59	-1.35	0.74	-0.56	-0.36	1.14	1.87	-2.19	5.20	-2.08	4.00	NA	1.72	1.70	1.51	1.93	3.46	-2.99
Loschbour	-11.56	-14.00	-1.99	-5.30	-4.21	-0.26	-3.06	-0.69	-1.06	-2.84	-0.60	-1.99	-1.51	-0.49	0.17	-3.68	3.21	-3.61	1.85	-1.72	NA	-0.17	-0.61	0.31	1.70	-4.46
LaBrana1	-11.96	-13.66	-1.83	-4.92	-4.32	0.07	-2.94	-0.89	-0.89	-2.66	-0.78	-2.07	-2.03	-0.85	0.48	-3.53	3.11	-3.47	2.32	-1.70	0.17	NA	-0.34	0.47	1.92	-4.27
Hungarian.KO1	-11.52	-12.87	-1.41	-3.87	-4.17	0.32	-2.36	-0.86	-0.65	-2.60	-0.98	-1.67	-2.02	-0.28	0.58	-3.16	3.39	-3.26	2.67	-1.51	0.61	0.34	NA	0.58	2.19	-4.01
Motala12	-12.43	-14.56	-2.20	-4.47	-4.34	-0.24	-2.77	-1.35	-1.38	-3.06	-0.84	-2.22	-1.94	-1.10	-0.15	-3.78	3.09	-3.86	1.96	-1.93	-0.31	-0.47	-0.58	NA	1.86	-4.47
LBK	-13.14	-15.66	-3.37	-6.47	-5.93	-1.91	-5.04	-2.47	-2.61	-4.23	-2.60	-3.75	-4.13	-2.66	-1.56	-5.41	1.76	-5.29	0.35	-3.46	-1.70	-1.92	-2.19	-1.86	NA	-6.14
Saqqaq	-8.85	-11.08	1.81	-2.28	-0.61	3.96	1.03	2.89	3.12	1.38	2.97	2.52	2.29	3.34	4.29	1.12	7.32	1.18	6.12	2.99	4.46	4.27	4.01	4.47	6.14	NA

Table S5.13 Z-scores of the statistics *D(X,Y; Bacho Kiro BB7-240, Mbuti)*. Standard errors (SE) were computed using a Weighted Block Jackknife[3,12] across all autosomes of the "2200k" Panel and using a block size of 5Mb. Blue: Z-score ≤ -3; Yellow: Z-score ≥ 3.

X/Y	BachoKiro_F6_620	BachoKiro_CC7_335	UstIshim	Oase1	Tianyuan	Kostenki14	GoyetQ116-1	BachoKiro_BK_1653	SunghirIII	Yana_old	Vestonice16	Malta1	ElMiron	Villabruna	Bichon	Clovis	Satsurblia	Kolyma_River	Kotias	Karelia	Loschbour	LaBrana1	Hungarian.KO1	Motala12	LBK	Saqqaq
BachoKiro_F6_620	NA	-2.52	8.67	4.64	6.79	8.98	5.77	8.50	9.14	9.48	7.73	9.25	7.80	8.39	8.66	8.41	12.59	8.91	11.61	9.56	9.40	9.65	9.54	10.64	12.58	8.26
BachoKiro_CC7_335	2.52	NA	11.00	5.55	9.40	12.01	7.96	10.34	12.46	11.58	10.46	10.86	10.47	11.92	11.74	10.63	14.99	11.65	14.67	11.48	12.63	12.45	11.63	13.14	15.65	10.45
UstIshim	-8.67	-11.00	NA	-3.91	-2.38	0.59	-2.97	-0.11	-0.02	0.37	-0.51	-0.15	-0.94	-0.28	-0.34	-0.86	3.53	-0.22	2.76	0.45	0.55	0.74	0.53	1.37	3.36	-1.21
Oase1	-4.64	-5.55	3.91	NA	1.52	3.95	1.01	4.24	3.88	3.84	2.65	3.12	2.47	3.25	4.11	2.84	5.73	3.66	5.71	4.70	4.32	4.33	3.75	4.95	6.69	2.84
Tianyuan	-6.79	-9.40	2.38	-1.52	NA	3.35	-0.68	1.94	2.84	2.85	1.66	2.09	1.54	2.05	2.16	1.87	6.03	2.48	5.34	3.12	3.20	3.30	2.99	3.62	6.16	1.55
Kostenki14	-8.98	-12.01	-0.59	-3.95	-3.35	NA	-4.25	-0.80	-0.81	-0.26	-1.80	-0.90	-1.85	-1.60	-1.01	-1.66	3.23	-0.91	2.40	-0.19	0.02	0.23	-0.33	0.50	3.07	-1.94
GoyetQ116-1	-5.77	-7.96	2.97	-1.01	0.68	4.25	NA	3.41	3.46	3.61	2.46	2.71	2.91	2.98	2.98	2.48	7.15	2.65	5.97	3.73	4.04	4.39	4.03	4.33	7.62	1.98
BachoKiro_BK_1653	-8.50	-10.34	0.11	-4.24	-1.94	0.80	-3.41	NA	0.40	0.52	-0.61	0.03	-0.69	-0.43	0.20	-0.45	3.71	-0.42	3.17	0.85	0.84	0.79	0.82	1.37	3.85	-1.56
SunghirIII	-9.14	-12.46	0.02	-3.88	-2.84	0.81	-3.46	-0.40	NA	0.41	-0.53	-0.51	-0.84	-0.44	-0.38	-1.00	4.38	-0.22	3.10	0.47	0.73	0.87	1.11	1.84	4.15	-1.50
Yana_old	-9.48	-11.58	-0.37	-3.84	-2.85	0.26	-3.61	-0.52	-0.41	NA	-1.20	-0.64	-1.85	-0.95	-0.78	-1.33	3.66	-0.65	2.70	0.10	0.22	0.52	0.24	0.96	3.52	-1.75
Vestonice16	-7.73	-10.46	0.51	-2.65	-1.66	1.80	-2.46	0.61	0.53	1.20	NA	0.09	0.16	0.23	0.85	-0.46	4.58	0.33	3.69	1.55	1.46	1.82	1.91	2.12	4.60	-0.36
Malta1	-9.25	-10.86	0.15	-3.12	-2.09	0.90	-2.71	-0.03	0.51	0.64	-0.09	NA	-0.37	-0.01	-0.39	-0.84	4.11	-0.17	3.25	0.76	0.86	1.41	0.97	1.46	4.26	-0.69
ElMiron	-7.80	-10.47	0.94	-2.47	-1.54	1.85	-2.91	0.69	0.84	1.85	-0.16	0.37	NA	0.02	0.67	0.07	4.17	0.57	3.67	1.57	1.78	1.86	1.37	2.20	5.07	-0.65
Villabruna	-8.39	-11.92	0.28	-3.25	-2.05	1.60	-2.98	0.43	0.44	0.95	-0.23	0.01	-0.02	NA	0.21	-0.63	4.64	-0.35	3.61	0.91	1.14	1.73	1.51	1.87	4.79	-1.01
Bichon	-8.66	-11.74	0.34	-4.11	-2.16	1.01	-2.98	-0.20	0.38	0.78	-0.85	0.39	-0.67	-0.21	NA	-0.56	4.50	0.13	3.70	1.00	1.23	1.64	1.11	2.19	4.71	-0.94
Clovis	-8.41	-10.63	0.86	-2.84	-1.87	1.66	-2.48	0.45	1.00	1.33	0.46	0.84	-0.07	0.63	0.56	NA	5.59	0.84	4.21	1.78	1.69	1.97	1.82	2.59	5.17	-0.35
Satsurblia	-12.59	-14.99	-3.53	-5.73	-6.03	-3.23	-7.15	-3.71	-4.38	-3.66	-4.58	-4.11	-4.17	-4.64	-4.50	-5.59	NA	-4.73	-1.24	-3.87	-3.90	-3.27	-3.62	-3.60	-0.46	-6.03
Kolyma_River	-8.91	-11.65	0.22	-3.66	-2.48	0.91	-2.65	0.42	0.22	0.65	-0.33	0.17	-0.57	0.35	-0.13	-0.84	4.73	NA	3.41	0.86	0.90	1.11	1.04	1.79	4.27	-1.36
Kotias	-11.61	-14.67	-2.76	-5.71	-5.34	-2.40	-5.97	-3.17	-3.10	-2.70	-3.69	-3.25	-3.67	-3.61	-3.70	-4.21	1.24	-3.41	NA	-2.99	-2.64	-2.66	-2.98	-1.89	0.71	-4.59
Karelia	-9.56	-11.48	-0.45	-4.70	-3.12	0.19	-3.73	-0.85	-0.47	-0.10	-1.55	-0.76	-1.57	-0.91	-1.00	-1.78	3.87	-0.86	2.99	NA	0.19	0.67	0.08	0.91	3.42	-1.98
Loschbour	-9.40	-12.63	-0.55	-4.32	-3.20	-0.02	-4.04	-0.84	-0.73	-0.22	-1.46	-0.86	-1.78	-1.14	-1.23	-1.69	3.90	-0.90	2.64	-0.19	NA	0.39	-0.22	0.98	3.76	-2.13
LaBrana1	-9.65	-12.45	-0.74	-4.33	-3.30	-0.23	-4.39	-0.79	-0.87	-0.52	-1.82	-1.41	-1.86	-1.73	-1.64	-1.97	3.27	-1.11	2.66	-0.67	-0.39	NA	-0.29	0.56	3.35	-2.29
Hungarian.KO1	-9.54	-11.63	-0.53	-3.75	-2.99	0.33	-4.03	-0.82	-1.11	-0.24	-1.91	-0.97	-1.37	-1.51	-1.11	-1.82	3.62	-1.04	2.98	-0.08	0.22	0.29	NA	1.22	4.01	-1.95
Motala12	-10.64	-13.14	-1.37	-4.95	-3.62	-0.50	-4.33	-1.37	-1.84	-0.96	-2.12	-1.46	-2.20	-1.87	-2.19	-2.59	3.60	-1.79	1.89	-0.91	-0.98	-0.56	-1.22	NA	2.79	-3.23
LBK	-12.58	-15.65	-3.36	-6.69	-6.16	-3.07	-7.62	-3.85	-4.15	-3.52	-4.60	-4.26	-5.07	-4.79	-4.71	-5.17	0.46	-4.27	-0.71	-3.42	-3.76	-3.35	-4.01	-2.79	NA	-5.62
Saqqaq	-8.26	-10.45	1.21	-2.84	-1.55	1.94	-1.98	1.56	1.50	1.75	0.36	0.69	0.65	1.01	0.94	0.35	6.03	1.36	4.59	1.98	2.13	2.29	1.95	3.23	5.62	NA

Table S5.14 Z-scores of the statistics *D(X,Y; Bacho Kiro CC7-335, Mbuti)*. Standard errors (SE) were computed using a Weighted Block Jackknife[3,12] across all autosomes of the "2200k" Panel and using a block size of 5Mb. Blue: Z-score ≤ -3; Yellow: Z-score ≥ 3.

X/Y	BachoKiro_F6_620	BachoKiro_BB7_240	UstIshim	Oase1	Tianyuan	Kostenki14	GoyetQ116-1	BachoKiro_BK_1653	SunghirIII	Yana_old	Vestonice16	Malta1	ElMiron	Villabruna	Bichon	Clovis	Satsurblia	Kolyma_River	Kotias	Karelia	Loschbour	LaBrana1	Hungarian.KO1	Motala12	LBK	Saqqaq
BachoKiro_F6_620	NA	-0.58	9.63	6.66	8.30	11.46	7.66	11.46	11.47	11.55	9.56	10.19	9.32	10.27	11.09	10.38	12.99	9.96	14.34	11.64	11.06	11.46	11.18	12.21	13.58	10.27
BachoKiro_BB7_240	0.58	NA	10.87	6.62	9.95	11.97	9.00	12.45	13.38	12.44	10.70	10.92	10.28	11.70	12.18	11.50	13.66	11.18	15.11	11.86	12.82	12.54	11.86	13.29	14.70	11.16
UstIshim	-9.63	-10.87	NA	-2.36	-1.71	1.05	-1.94	2.24	1.35	0.80	-0.23	-0.31	-0.36	0.08	1.03	0.01	3.50	-0.55	3.99	1.55	1.27	0.95	1.31	2.08	3.42	-0.28
Oase1	-6.66	-6.62	2.36	NA	1.11	3.56	0.43	4.18	3.22	3.06	2.04	2.33	1.72	2.52	3.31	2.50	4.77	2.04	5.39	4.03	2.97	2.94	3.03	3.29	5.31	2.36
Tianyuan	-8.30	-9.95	1.71	-1.11	NA	3.17	-0.17	4.13	3.14	2.98	1.57	1.28	1.40	2.10	2.79	1.90	4.81	1.43	6.14	3.35	3.24	3.24	3.70	4.13	5.80	1.86
Kostenki14	-11.46	-11.97	-1.05	-3.56	-3.17	NA	-3.32	1.37	0.32	-0.38	-1.74	-1.60	-1.81	-1.27	-0.43	-1.39	2.45	-1.79	3.10	0.05	0.09	-0.22	0.23	0.68	2.58	-1.65
GoyetQ116-1	-7.66	-9.00	1.94	-0.43	0.17	3.32	NA	4.20	3.31	3.28	1.97	1.33	2.48	2.24	3.37	1.89	5.50	1.55	6.77	3.26	3.69	3.51	3.58	4.11	6.24	1.58
BachoKiro_BK_1653	-11.46	-12.45	-2.24	-4.18	-4.13	-1.37	-4.20	NA	-1.13	-1.48	-2.30	-2.89	-2.76	-2.43	-1.79	-2.66	1.22	-3.41	1.52	-1.05	-1.48	-1.34	-1.07	-0.63	1.19	-3.25
SunghirIII	-11.47	-13.38	-1.35	-3.22	-3.14	-0.32	-3.31	1.13	NA	-0.60	-1.45	-1.75	-1.53	-1.32	-0.48	-1.45	1.96	-2.06	2.98	0.21	-0.19	-0.61	0.64	0.81	2.37	-1.92
Yana_old	-11.55	-12.44	-0.80	-3.06	-2.98	0.38	-3.28	1.48	0.60	NA	-1.28	-1.23	-1.33	-1.07	0.18	-0.91	3.09	-1.55	3.54	0.79	0.44	0.15	0.89	1.20	2.98	-1.33
Vestonice16	-9.56	-10.70	0.23	-2.04	-1.57	1.74	-1.97	2.30	1.45	1.28	NA	-0.47	-0.49	0.37	1.42	-0.18	3.90	-0.33	4.64	1.43	1.36	1.30	2.40	2.45	4.07	0.36
Malta1	-10.19	-10.92	0.31	-2.33	-1.28	1.60	-1.33	2.89	1.75	1.23	0.47	NA	0.26	0.43	1.30	0.54	4.32	-0.23	4.75	1.82	1.64	1.61	2.40	2.66	4.34	-0.12
ElMiron	-9.32	-10.28	0.36	-1.72	-1.40	1.81	-2.48	2.76	1.53	1.33	0.49	-0.26	NA	0.78	1.41	0.29	3.90	-0.06	5.30	1.63	1.63	1.22	1.42	3.02	4.28	-0.13
Villabruna	-10.27	-11.70	-0.08	-2.52	-2.10	1.27	-2.24	2.43	1.32	1.07	-0.37	-0.43	-0.78	NA	1.01	-0.62	3.68	-0.81	4.46	1.07	1.15	1.15	1.58	2.44	4.18	-0.59
Bichon	-11.09	-12.18	-1.03	-3.31	-2.79	0.43	-3.37	1.79	0.48	-0.18	-1.42	-1.30	-1.41	-1.01	NA	-1.16	2.78	-1.82	3.84	0.55	0.33	0.18	0.57	1.17	2.95	-1.49
Clovis	-10.38	-11.50	-0.01	-2.50	-1.90	1.39	-1.89	2.66	1.45	0.91	0.18	-0.54	-0.29	0.62	1.16	NA	4.04	-0.80	4.61	1.66	1.42	1.27	2.18	2.32	4.06	-0.16
Satsurblia	-12.99	-13.66	-3.50	-4.77	-4.81	-2.45	-5.50	-1.22	-1.96	-3.09	-3.90	-4.32	-3.90	-3.68	-2.78	-4.04	NA	-5.11	0.64	-2.32	-2.52	-2.48	-1.71	-1.77	-0.27	-4.36
Kolyma_River	-9.96	-11.18	0.55	-2.04	-1.43	1.79	-1.55	3.41	2.06	1.55	0.33	0.23	0.06	0.81	1.82	0.80	5.11	NA	5.25	2.14	2.09	1.86	2.56	2.79	4.65	0.31
Kotias	-14.34	-15.11	-3.99	-5.39	-6.14	-3.10	-6.77	-1.52	-2.98	-3.54	-4.64	-4.75	-5.30	-4.46	-3.84	-4.61	-0.64	-5.25	NA	-3.37	-3.54	-3.70	-3.12	-2.76	-0.85	-5.09
Karelia	-11.64	-11.86	-1.55	-4.03	-3.35	-0.05	-3.26	1.05	-0.21	-0.79	-1.43	-1.82	-1.63	-1.07	-0.55	-1.66	2.32	-2.14	3.37	NA	-0.32	-0.11	0.31	1.04	2.35	-2.49
Loschbour	-11.06	-12.82	-1.27	-2.97	-3.24	-0.09	-3.69	1.48	0.19	-0.44	-1.36	-1.64	-1.63	-1.15	-0.33	-1.42	2.52	-2.09	3.54	0.32	NA	-0.38	0.54	1.10	2.72	-1.79
LaBrana1	-11.46	-12.54	-0.95	-2.94	-3.24	0.22	-3.51	1.34	0.61	-0.15	-1.30	-1.61	-1.22	-1.15	-0.18	-1.27	2.48	-1.86	3.70	0.11	0.38	NA	0.83	1.03	3.02	-1.62
Hungarian.KO1	-11.18	-11.86	-1.31	-3.03	-3.70	-0.23	-3.58	1.07	-0.64	-0.89	-2.40	-2.40	-1.42	-1.58	-0.57	-2.18	1.71	-2.56	3.12	-0.31	-0.54	-0.83	NA	0.10	1.91	-2.09
Motala12	-12.21	-13.29	-2.08	-3.29	-4.13	-0.68	-4.11	0.63	-0.81	-1.20	-2.45	-2.66	-3.02	-2.44	-1.17	-2.32	1.77	-2.79	2.76	-1.04	-1.10	-1.03	-0.10	NA	1.98	-2.76
LBK	-13.58	-14.70	-3.42	-5.31	-5.80	-2.58	-6.24	-1.19	-2.37	-2.98	-4.07	-4.34	-4.28	-4.18	-2.95	-4.06	0.27	-4.65	0.85	-2.35	-2.72	-3.02	-1.91	-1.98	NA	-4.56
Saqqaq	-10.27	-11.16	0.28	-2.36	-1.86	1.65	-1.58	3.25	1.92	1.33	-0.36	0.12	0.13	0.59	1.49	0.16	4.36	-0.31	5.09	2.49	1.79	1.62	2.09	2.76	4.56	NA

Table S5.15 Z-scores of the statistics *D(X,Y; Bacho Kiro BK1653, Mbuti)*. Standard errors (SE) were computed using a Weighted Block Jackknife[3,12] across all autosomes of the "2200k" Panel and using a block size of 5Mb. Blue: Z-score ≤ -3; Yellow: Z-score ≥ 3.

X/Y	BachoKiro_F6_620	BachoKiro_BB7_240	BachoKiro_CC7_335	UstIshim	Oase1	Tianyuan	Kostenki14	GoyetQ116-1	SunghirIII	Yana_old	Vestonice16	Malta1	ElMiron	Villabruna	Bichon	Clovis	Satsurblia	Kolyma_River	Kotias	Karelia	Loschbour	LaBrana1	Hungarian.KO1	Motala12	LBK	Saqqaq
BachoKiro_F6_620	NA	-2.36	0.15	-1.23	2.00	-1.68	-12.26	-15.82	-12.37	-9.21	-17.39	-8.32	-14.87	-15.03	-13.67	-3.68	-3.16	-3.99	-4.66	-10.18	-14.08	-14.75	-12.29	-12.05	-8.89	-3.37
BachoKiro_BB7_240	2.36	NA	2.01	0.72	1.86	0.97	-9.78	-13.19	-10.04	-6.63	-14.52	-6.40	-12.32	-12.20	-11.19	-1.04	-1.21	-1.51	-3.00	-7.84	-11.42	-11.08	-9.41	-8.87	-6.35	-1.13
BachoKiro_CC7_335	-0.15	-2.01	NA	-1.60	1.00	-1.30	-11.46	-15.02	-12.18	-8.30	-16.46	-8.13	-14.52	-13.65	-13.48	-3.19	-3.01	-3.86	-4.32	-9.63	-14.50	-13.64	-11.63	-11.26	-8.41	-3.55
UstIshim	1.23	-0.72	1.60	NA	2.38	-0.30	-12.03	-14.52	-12.01	-8.44	-17.32	-7.65	-14.17	-14.84	-14.06	-2.62	-2.29	-2.93	-3.66	-9.86	-14.46	-14.66	-12.01	-11.75	-8.21	-2.32
Oase1	-2.00	-1.86	-1.00	-2.38	NA	-2.40	-11.87	-14.89	-12.26	-9.24	-15.86	-8.87	-14.31	-14.42	-13.94	-4.14	-3.55	-5.00	-5.72	-9.84	-14.63	-13.28	-11.07	-10.95	-8.97	-3.90
Tianyuan	1.68	-0.97	1.30	0.30	2.40	NA	-10.79	-15.38	-12.06	-8.61	-16.34	-8.04	-14.66	-14.41	-13.55	-1.96	-1.62	-2.49	-2.87	-8.97	-13.24	-13.56	-11.80	-11.71	-7.41	-1.83
Kostenki14	12.26	9.78	11.46	12.03	11.87	10.79	NA	-3.47	-0.10	4.06	-5.57	4.23	-3.14	-2.65	-1.41	10.15	9.58	9.92	8.90	2.83	-1.49	-1.74	0.23	0.99	4.66	9.88
GoyetQ116-1	15.82	13.19	15.02	14.52	14.89	15.38	3.47	NA	3.22	7.69	-1.21	7.17	0.98	1.84	2.24	13.86	13.03	14.17	12.16	5.43	2.03	2.38	4.17	4.41	8.62	14.48
SunghirIII	12.37	10.04	12.18	12.01	12.26	12.06	0.10	-3.22	NA	4.07	-5.27	4.40	-2.89	-2.26	-1.21	10.46	9.96	9.79	8.79	2.83	-1.39	-1.50	0.59	1.10	4.82	10.72
Yana_old	9.21	6.63	8.30	8.44	9.24	8.61	-4.06	-7.69	-4.07	NA	-9.66	0.45	-7.25	-7.21	-5.46	6.90	6.75	6.66	5.16	-1.20	-5.73	-5.96	-3.26	-3.47	0.93	7.00
Vestonice16	17.39	14.52	16.46	17.32	15.86	16.34	5.57	1.21	5.27	9.66	NA	9.41	2.03	3.24	3.86	15.60	15.27	16.07	14.91	8.21	3.94	3.91	5.83	6.63	10.60	16.19
Malta1	8.32	6.40	8.13	7.65	8.87	8.04	-4.23	-7.17	-4.40	-0.45	-9.41	NA	-5.94	-6.28	-5.85	6.63	5.29	5.92	4.15	-1.59	-6.05	-6.43	-3.93	-3.66	0.32	6.69
ElMiron	14.87	12.32	14.52	14.17	14.31	14.66	3.14	-0.98	2.89	7.25	-2.03	5.94	NA	1.55	2.22	14.08	12.91	13.07	11.96	6.14	1.92	2.21	3.87	4.10	8.45	13.95
Villabruna	15.03	12.20	13.65	14.84	14.42	14.41	2.65	-1.84	2.26	7.21	-3.24	6.28	-1.55	NA	1.04	13.31	13.01	13.07	12.41	5.36	0.81	0.91	3.41	3.55	8.27	14.23
Bichon	13.67	11.19	13.48	14.06	13.94	13.55	1.41	-2.24	1.21	5.46	-3.86	5.85	-2.22	-1.04	NA	12.70	12.66	12.27	11.27	4.48	-0.20	-0.25	2.10	2.80	6.90	13.14
Clovis	3.68	1.04	3.19	2.62	4.14	1.96	-10.15	-13.86	-10.46	-6.90	-15.60	-6.63	-14.08	-13.31	-12.70	NA	-0.07	-0.40	-1.53	-8.13	-13.03	-12.93	-10.30	-10.21	-6.29	0.30
Satsurblia	3.16	1.21	3.01	2.29	3.55	1.62	-9.58	-13.03	-9.96	-6.75	-15.27	-5.29	-12.91	-13.01	-12.66	0.07	NA	-0.78	-2.05	-8.08	-12.37	-12.81	-9.44	-9.89	-6.79	0.03
Kolyma_River	3.99	1.51	3.86	2.93	5.00	2.49	-9.92	-14.17	-9.79	-6.66	-16.07	-5.92	-13.07	-13.07	-12.27	0.40	0.78	NA	-1.10	-7.67	-12.47	-13.05	-9.86	-9.93	-5.97	0.50
Kotias	4.66	3.00	4.32	3.66	5.72	2.87	-8.90	-12.16	-8.79	-5.16	-14.91	-4.15	-11.96	-12.41	-11.27	1.53	2.05	1.10	NA	-6.85	-11.36	-11.73	-9.02	-8.78	-4.76	1.54
Karelia	10.18	7.84	9.63	9.86	9.84	8.97	-2.83	-5.43	-2.83	1.20	-8.21	1.59	-6.14	-5.36	-4.48	8.13	8.08	7.67	6.85	NA	-4.89	-5.15	-3.02	-2.13	2.17	8.29
Loschbour	14.08	11.42	14.50	14.46	14.63	13.24	1.49	-2.03	1.39	5.73	-3.94	6.05	-1.92	-0.81	0.20	13.03	12.37	12.47	11.36	4.89	NA	-0.20	2.32	3.07	7.49	12.87
LaBrana1	14.75	11.08	13.64	14.66	13.28	13.56	1.74	-2.38	1.50	5.96	-3.91	6.43	-2.21	-0.91	0.25	12.93	12.81	13.05	11.73	5.15	0.20	NA	2.59	3.06	7.54	13.26
Hungarian.KO1	12.29	9.41	11.63	12.01	11.07	11.80	-0.23	-4.17	-0.59	3.26	-5.83	3.93	-3.87	-3.41	-2.10	10.30	9.44	9.86	9.02	3.02	-2.32	-2.59	NA	0.75	4.82	10.58
Motala12	12.05	8.87	11.26	11.75	10.95	11.71	-0.99	-4.41	-1.10	3.47	-6.63	3.66	-4.10	-3.55	-2.80	10.21	9.89	9.93	8.78	2.13	-3.07	-3.06	-0.75	NA	4.66	10.35
LBK	8.89	6.35	8.41	8.21	8.97	7.41	-4.66	-8.62	-4.82	-0.93	-10.60	-0.32	-8.45	-8.27	-6.90	6.29	6.79	5.97	4.76	-2.17	-7.49	-7.54	-4.82	-4.66	NA	5.95
Saqqaq	3.37	1.13	3.55	2.32	3.90	1.83	-9.88	-14.48	-10.72	-7.00	-16.19	-6.69	-13.95	-14.23	-13.14	-0.30	-0.03	-0.50	-1.54	-8.29	-12.87	-13.26	-10.58	-10.35	-5.95	NA

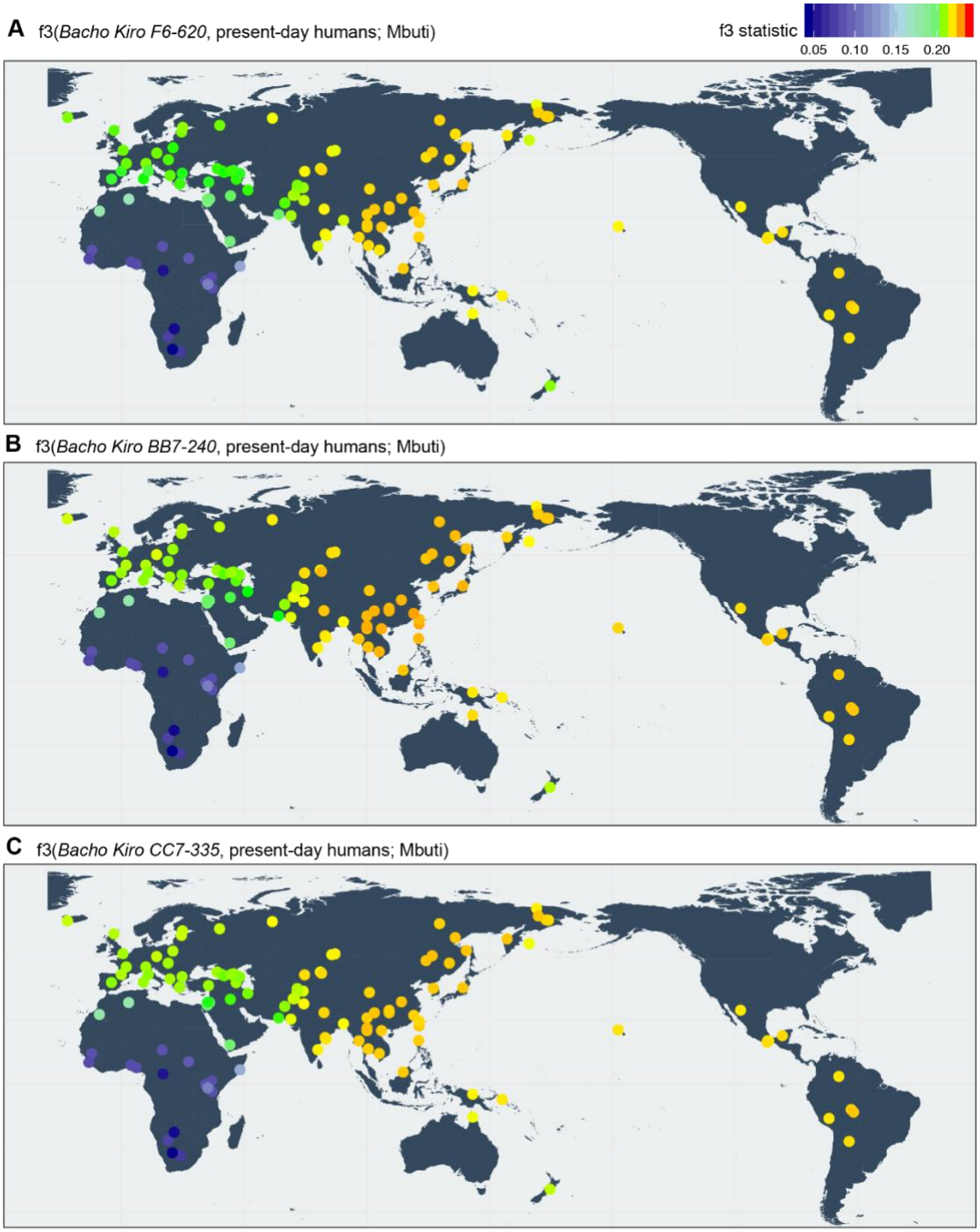

Figure S5.1 Heatmap of the shared genetic drift between the IUP Bacho Kiro Cave individuals and present-day human populations calculated as *f3(IUP Bacho Kiro individual, present-day humans; Mbuti)*. A) *Bacho Kiro F6-620*, **B)** *Bacho Kiro BB7-240*, **C)** *Bacho Kiro CC7-335*. Present-day modern human genomes from SGDP[10] were used for calculating these statistics. Plotted *f3* values were calculated using ADMIXTOOLS[3] as implemented in *admixr*[9], and which are reported in detail in Tables S5.2-S5.4 along with the number of SNPs used for these calculations. A higher *f3*-value is indicated with warmer colour and corresponds to the higher shared genetic drift between an IUP Bacho Kiro Cave individual

and a given present-day human population. Standard errors (SE) were computed using a Weighted Block Jackknife[3,12] across all autosomes of the "2200k" Panel and using a block size of 5Mb. Three Mbuti individuals from SGDP[10] were used as outgroup. Coordinates for present-day humans were obtained from *Mallick et al.*[10]. The heatmap scale is kept consistent with the Fig. 2A, Extended Data Fig. 3B and C, and Fig. S5.2.

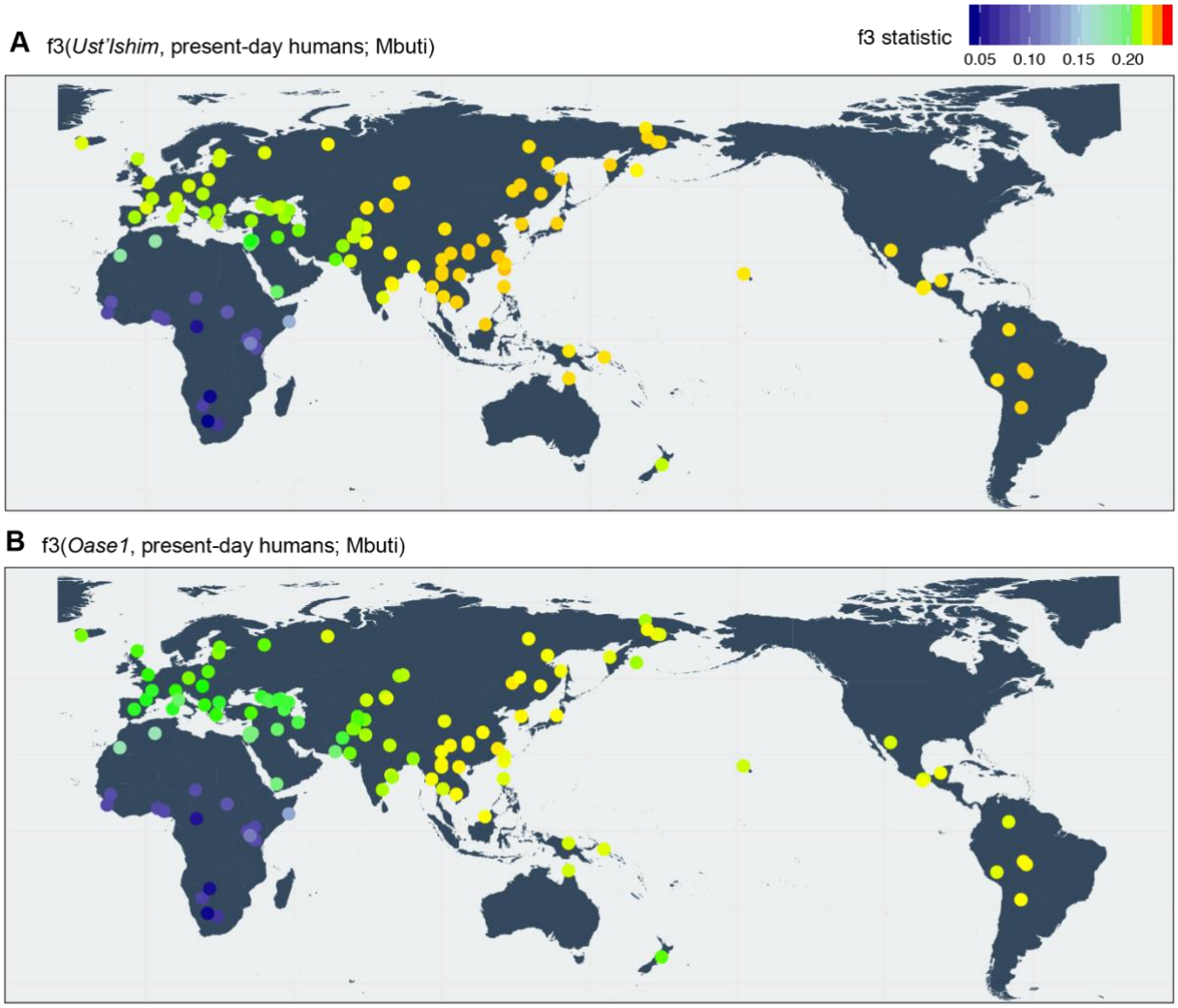

Figure S5.2 Heatmap of the shared genetic drift between the *Ust'Ishim* or *Oase1* and present-day human populations calculated as *f3(Ust'Ishim/Oase1, present-day humans; Mbuti)*. Present-day modern human genomes from SGDP[10] were used for calculating these statistics. Plotted *f3* values were calculated using ADMIXTOOLS[3] as implemented in *admixr*[9]. A higher *f3*-value is indicated with warmer colour and corresponds to higher shared genetic drift between **A)** *Ust'Ishim* or **B)** *Oase1* and a given present-day human population. Standard errors (SE) were computed using a Weighted Block Jackknife[3,12] across all autosomes of the "2200k" Panel (nsnps (*Ust'Ishim*) = 1,951,462; nsnps (*Oase 1*) = 402,526), and using a block size of 5Mb. Three Mbuti individuals from SGDP[10] were used as outgroup. Coordinates for present-day humans were obtained from *Mallick et al.*[10]. The heatmap scale is kept consistent with the Fig. 2A, Extended Data Fig. 3B and C, and Fig. S5.1.

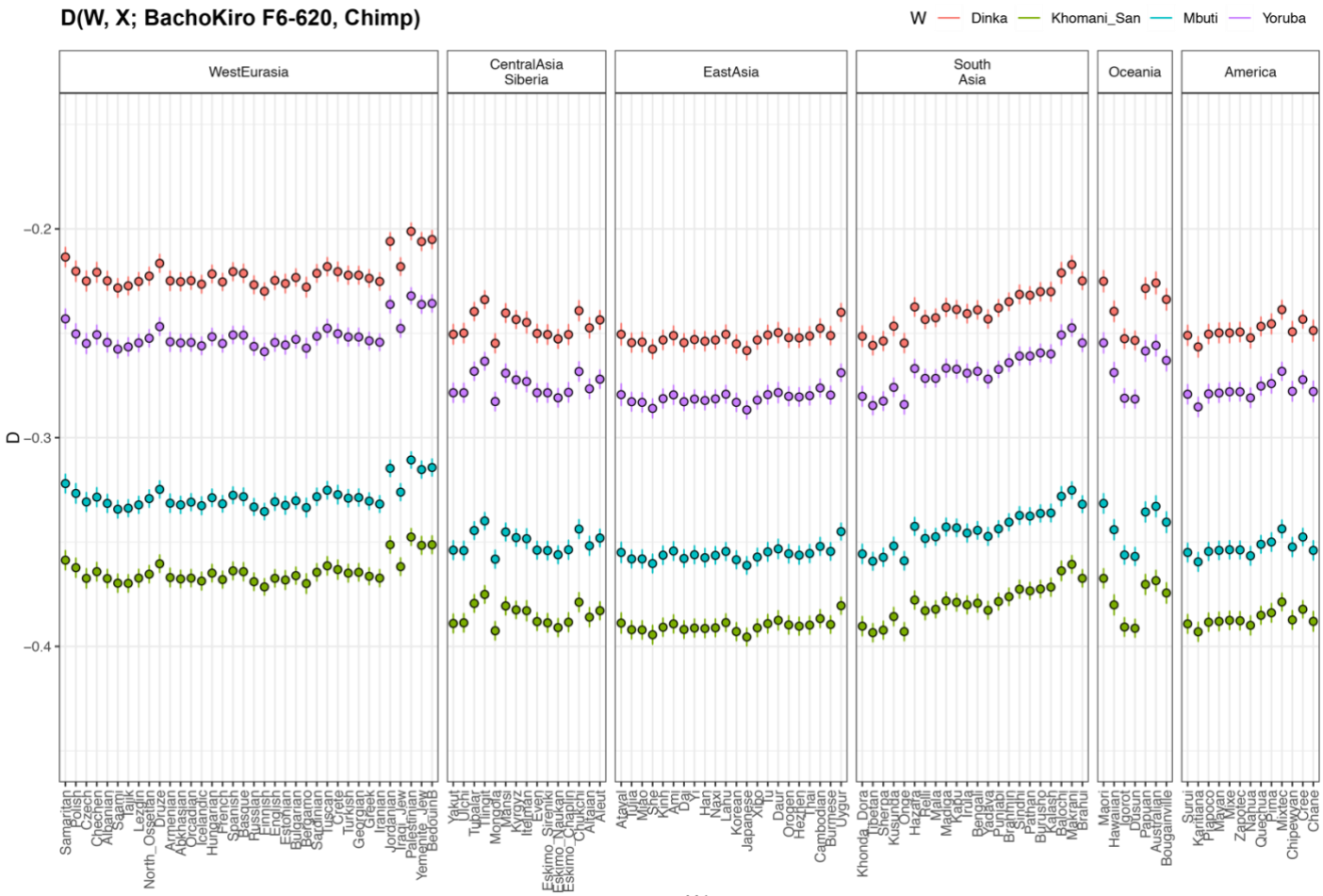

Figure S5.3 D-statistics of the form *D(W, X; Bacho Kiro F6-620, Chimpanzee)* where *W* is a present-day African population and *X* is a present-day non-African population from SGDP[10]. *Bacho Kiro F6-620* is significantly closer to present-day non-Africans than present-day Africans. *D* values plotted on the *y*-axis were calculated using ADMIXTOOLS[3] as implemented in *admixr*[9]. Filled-in circles indicate a significant Z-score or $|Z| \geq 3$, and open circles indicate a non-significant Z-score or $|Z| < 3$. Whiskers on each side of the plotted *D* values correspond to one standard error calculated using a Weighted Block Jackknife[3,12] across all autosomes on the "2200k" Panel (nsnps (*Bacho Kiro F6-620*) = 1,779,883) and a block size of 5 Mb.

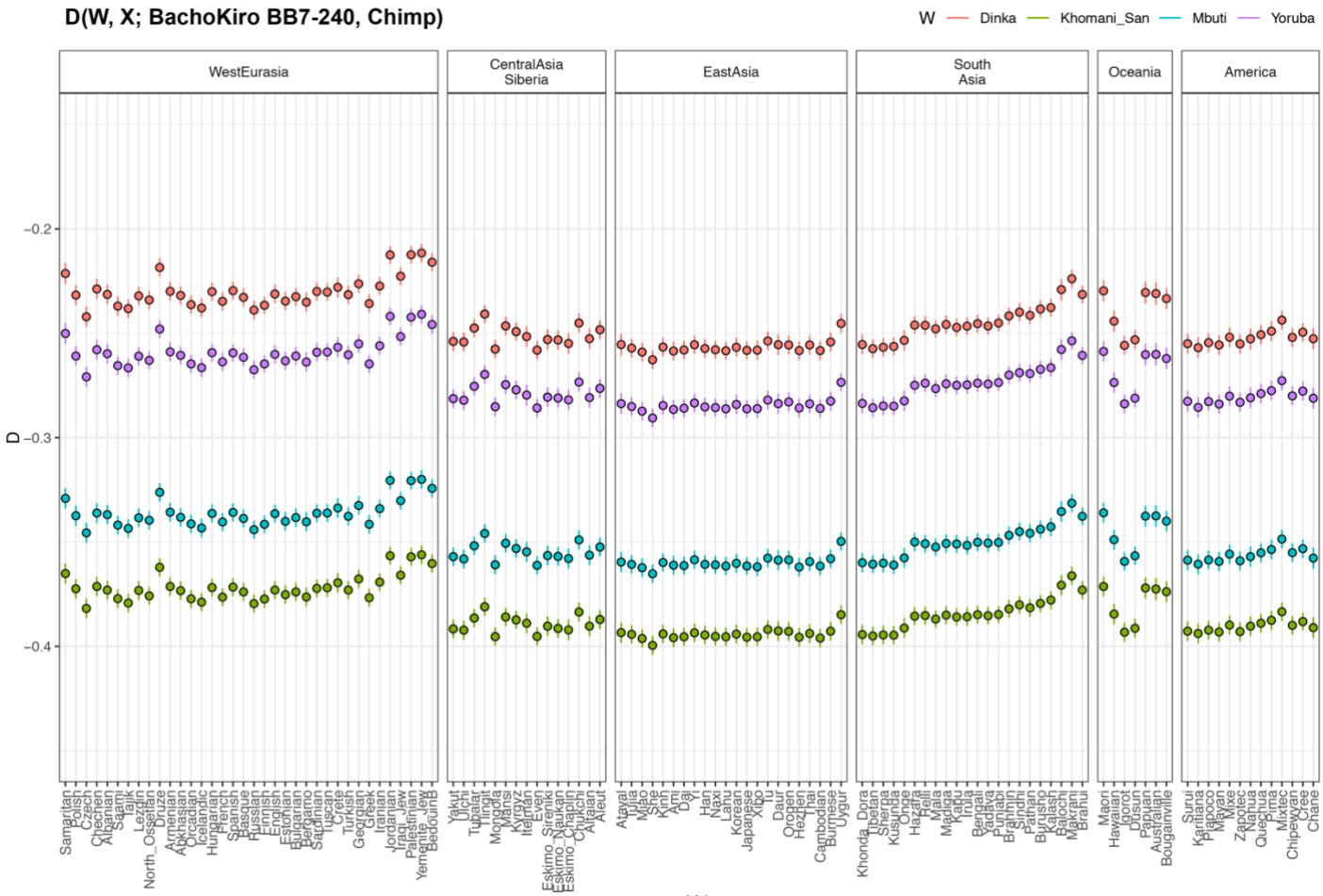

Figure S5.4 D-statistics of the form *D(W, X; Bacho Kiro BB7-240, Chimpanzee)* where *W* is a present-day African population and *X* is a present-day non-African population from SGDP[10]. *Bacho Kiro BB7-240* is significantly closer to present-day non-Africans than present-day Africans. *D* values plotted on the *y*-axis were calculated using ADMIXTOOLS[3] as implemented in *admixr*[9]. Filled-in circles indicate a significant Z-score or $|Z| \geq 3$, and open circles indicate a non-significant Z-score or $|Z| < 3$. Whiskers on each side of the plotted *D* values correspond to one standard error calculated using a Weighted Block Jackknife[3,12] across all autosomes on the "2200k" Panel (nsnps (*Bacho Kiro BB7-240*) = 787,706) and a block size of 5 Mb.

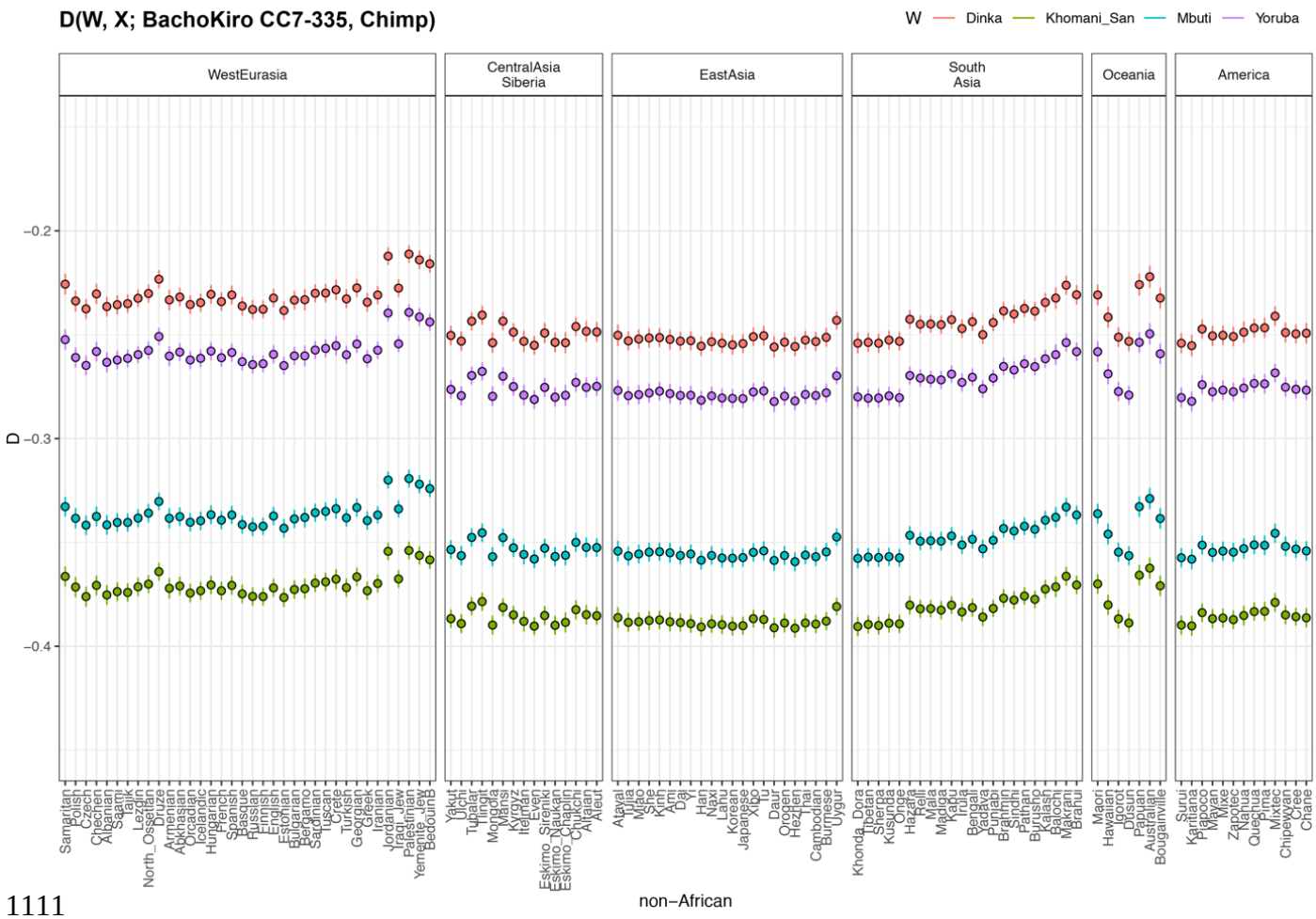

Figure S5.5 D-statistics of the form *D(W, X; Bacho Kiro CC7-335, Chimpanzee)* where *W* is a present-day African population and *X* is a present-day non-African population from SGDP[10]. *Bacho Kiro CC7-335* is significantly closer to present-day non-Africans than present-day Africans. *D* values denoted as circles and plotted on the *y*-axis were calculated using ADMIXTOOLS[3] as implemented in *admixr*[9]. Filled-in circles indicate a significant Z-score or $|Z| \geq 3$, and open circles indicate a non-significant Z-score or $|Z| < 3$. Whiskers on each side of the plotted *D* values correspond to one standard error calculated using a Weighted Block Jackknife[3,12] across all autosomes on the "2200k" Panel (nsnps (*Bacho Kiro CC7-335*) = 723,129) and a block size of 5 Mb.

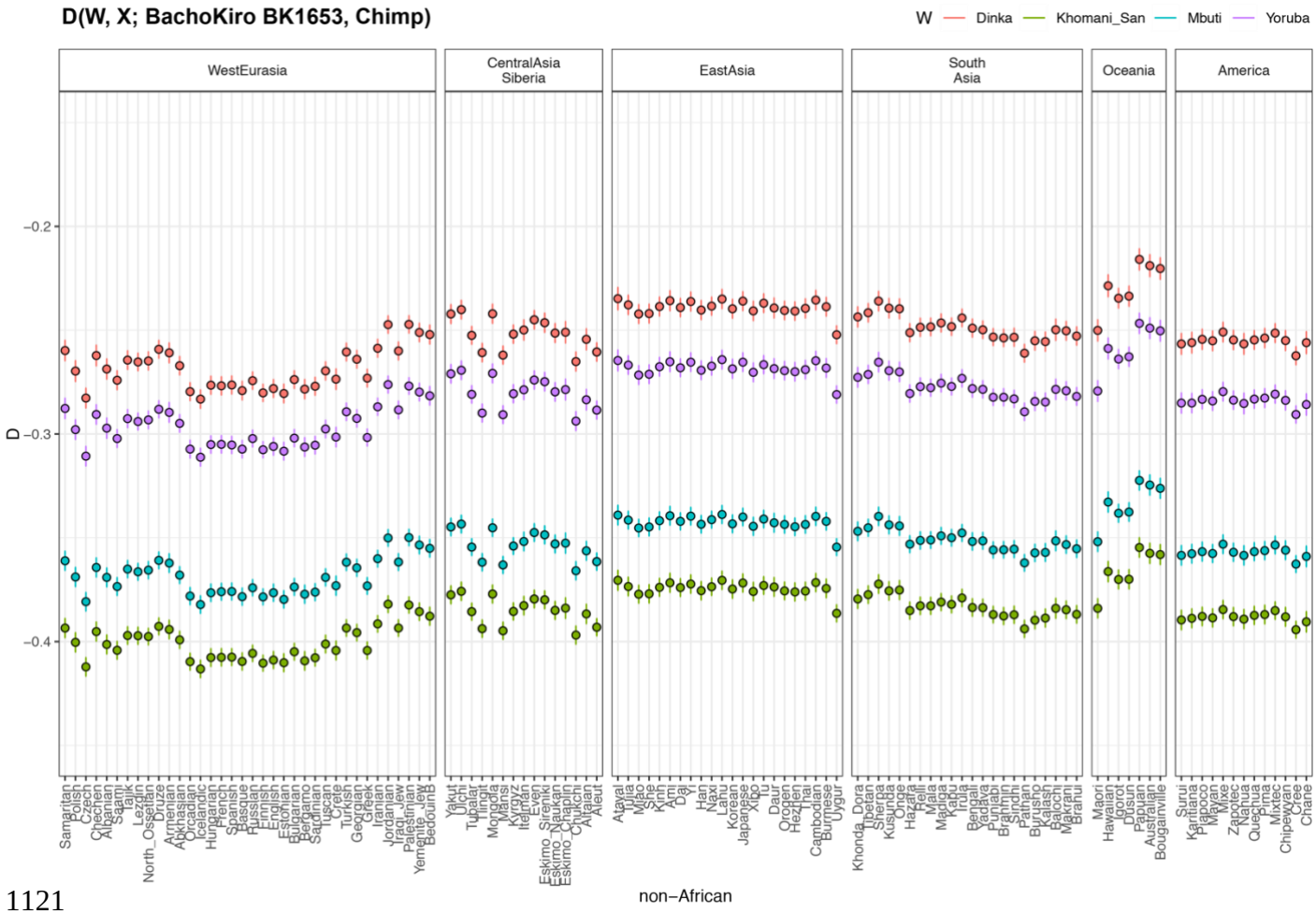

Figure S5.6 D-statistics of the form *D(W, X; Bacho Kiro BK1653, Chimpanzee)* where *W* is a present-day African population and *X* is a present-day non-African population from SGDP[10]. *Bacho Kiro BK1653* is significantly closer to present-day non-Africans than present-day Africans. *D* values denoted as circles and plotted on the *y*-axis were calculated using ADMIXTOOLS[3] as implemented in *admixr*[9]. Filled-in circles indicate a significant Z-score or $|Z| \geq 3$, and open circles indicate a non-significant Z-score or $|Z| < 3$. Whiskers on each side of the plotted *D* values correspond to one standard error calculated using a Weighted Block Jackknife[3,12] across all autosomes on the "2200k" Panel (nsnps (*Bacho Kiro BK1653*) = 825,379) and a block size of 5 Mb.

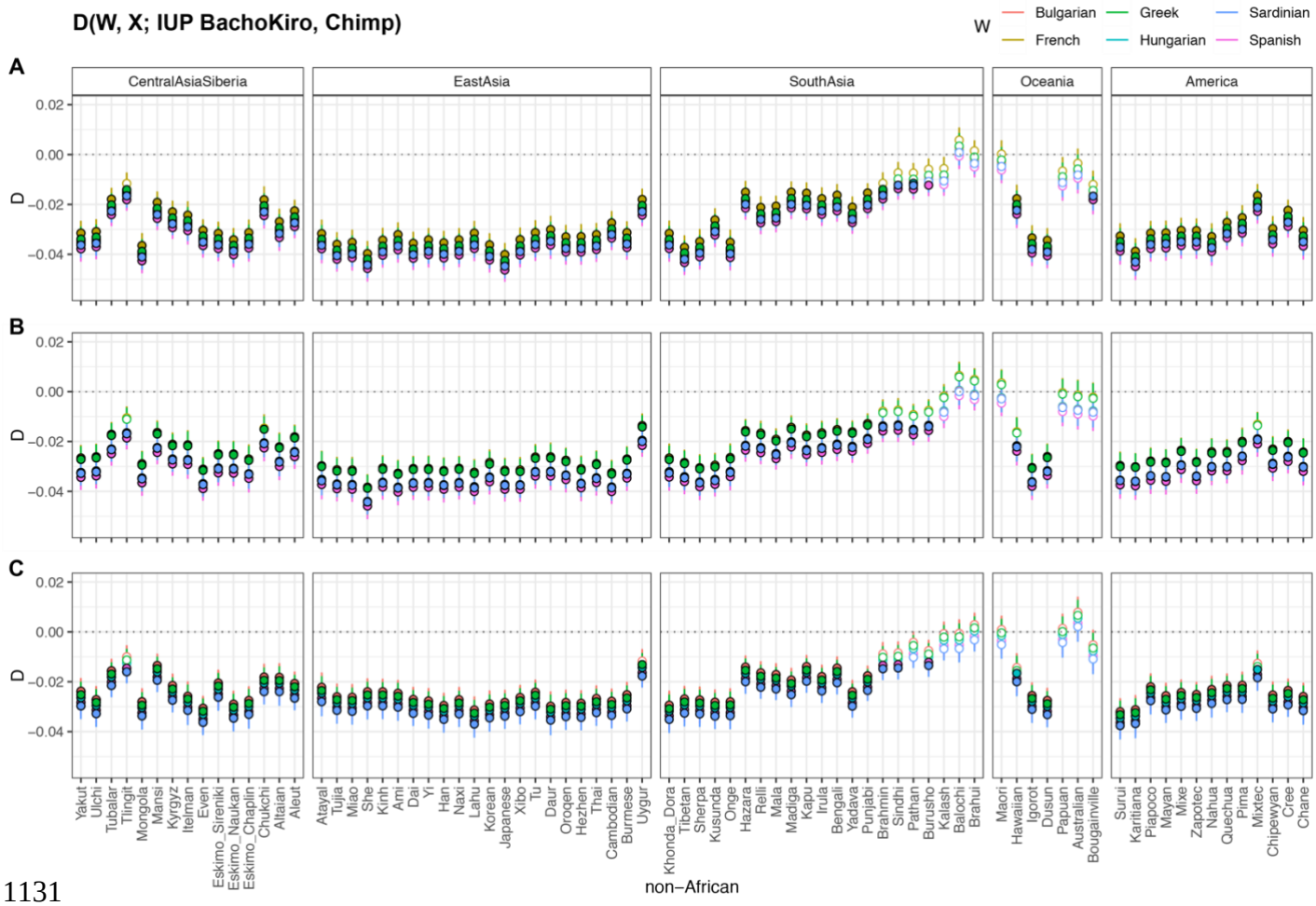

Figure S5.7 D-statistics of the form *D(W, X; IUP Bacho Kiro individual, Chimpanzee)* where *W* is one of the six present-day West Eurasian populations and *X* is a present-day non-African population from Central Asia and Siberia, East Asia, South Asia, Oceania or Americas. A) *Bacho Kiro F6-620* (nsnps = 1,779,883), **B)** *Bacho Kiro BB7-240* (nsnps = 787,706) and **C)** *Bacho Kiro CC7-335* (nsnps = 723,129). *D* values denoted as circles and plotted on the *y*-axes were calculated using ADMIXTOOLS[3] as implemented in *admixr*[9]. Present-day human genomes from SGDP[10] were used in these statistics, and a genome of *panTro2* as an outgroup. Filled-in circles indicate a significant Z-score or $|Z| \geq 3$, and open circles indicate a non-significant Z-score or $|Z| < 3$. Whiskers on each side of the plotted *D* values correspond to one standard error calculated using a Weighted Block Jackknife[3,12] across all autosomes on the "2200k" Panel and a block size of 5 Mb.

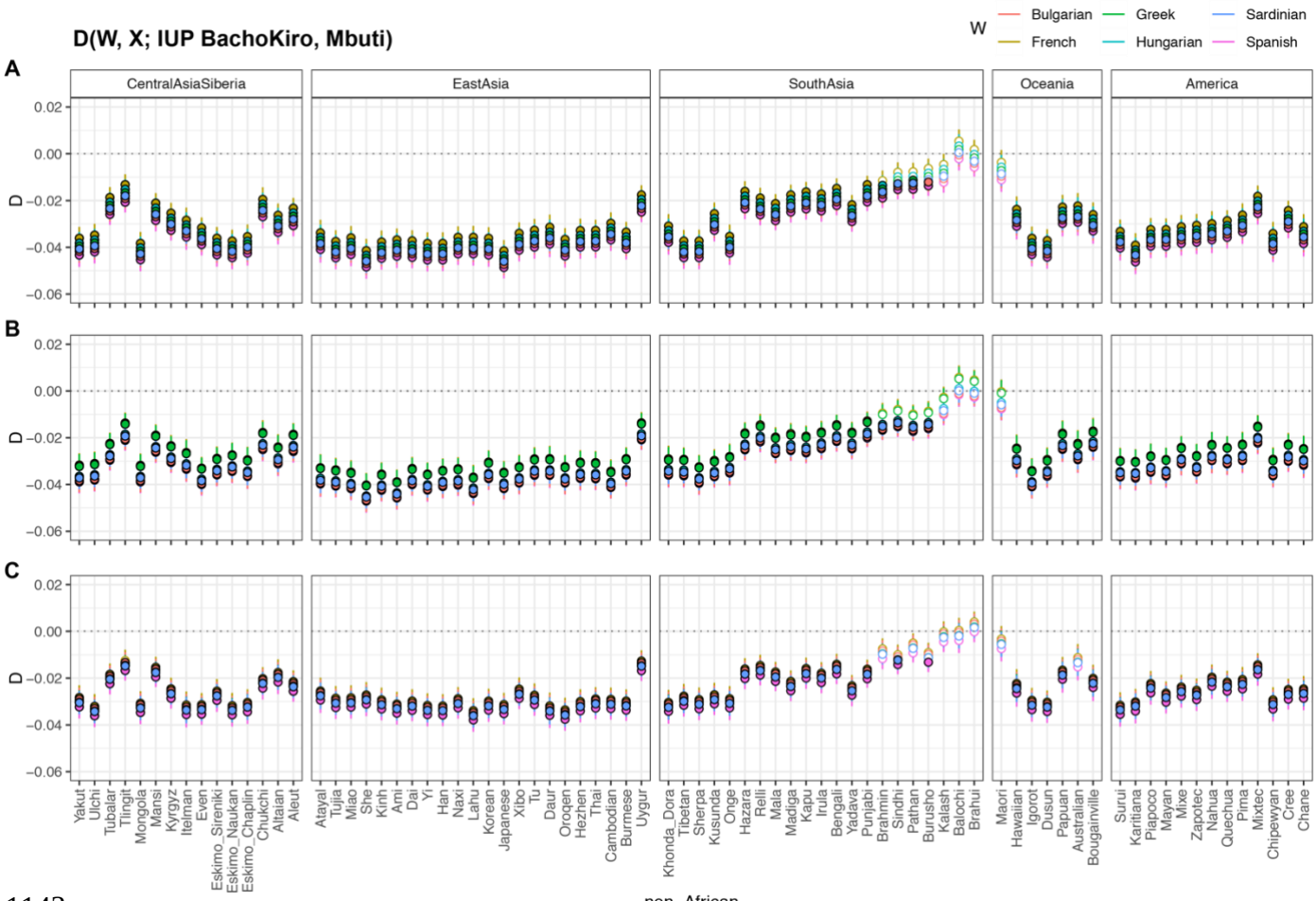

Figure S5.8 D-statistics of the form *D(W, X; Bacho Kiro BK1653, Mbuti)* where *W* is one of the six present-day West Eurasian populations and *X* is a present-day non-African population from Central Asia and Siberia, East Asia, South Asia, Oceania or Americas. **A)** *Bacho Kiro F6-620* (nsnps = 1,779,883), **B)** *Bacho Kiro BB7-240* (nsnps = 787,706) and **C)** *Bacho Kiro CC7-335* (nsnps = 723,129). *D* values denoted as circles and plotted on the *y*-axes were calculated using ADMIXTOOLS[3] as implemented in *admixr*[9]. Present-day human genomes from SGDP[10] were used in these statistics, and three Mbuti individuals from the same panel were used as outgroup. Filled-in circles indicate a significant Z-score or $|Z| \geq 3$, and open circles indicate a non-significant Z-score or $|Z| < 3$. Whiskers on each side of the plotted *D* values correspond to one standard error calculated using a Weighted Block Jackknife[3,12] across all autosomes on the "2200k" Panel and a block size of 5 Mb.

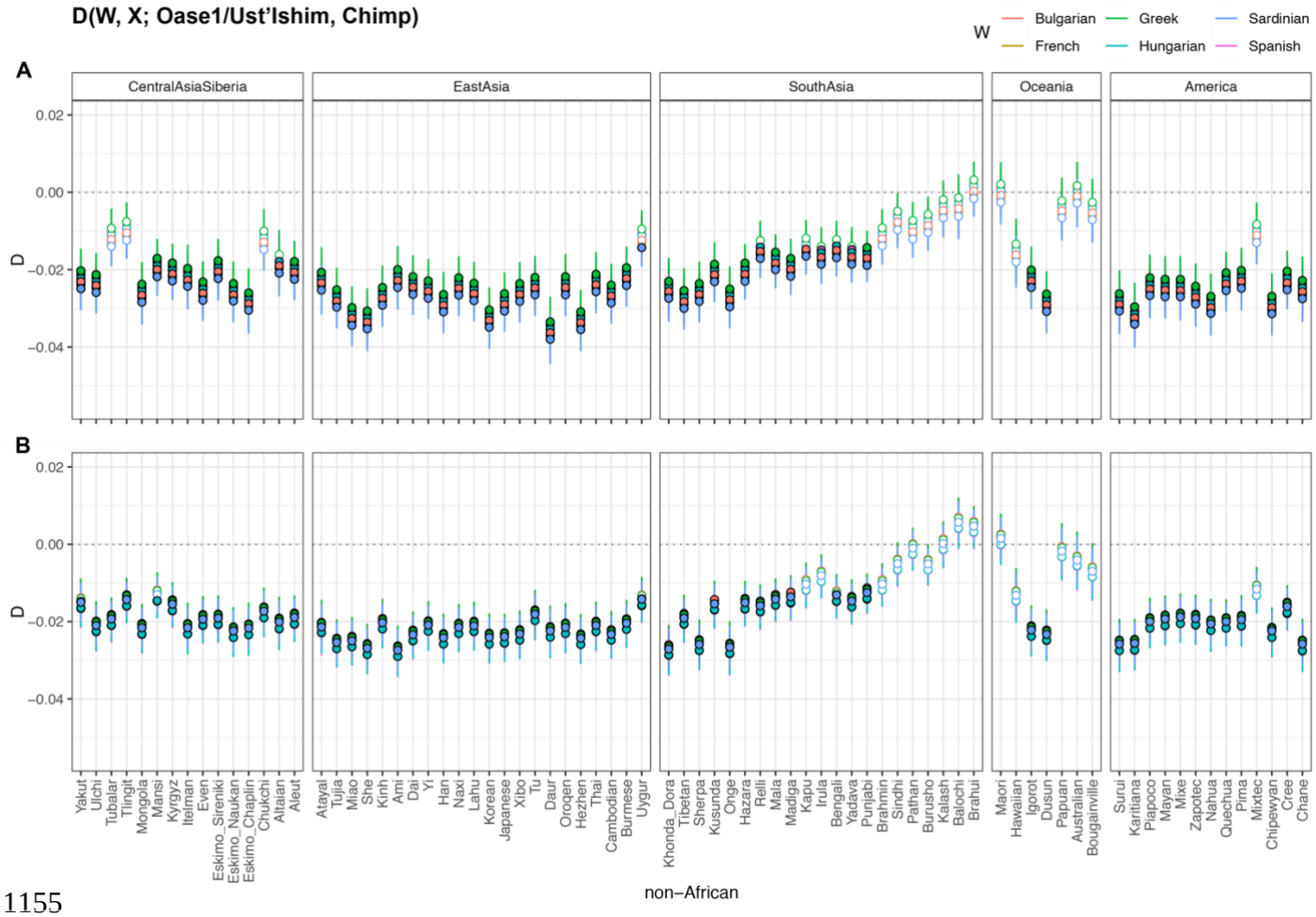

Figure S5.9 D-statistics of the form *D(W, X; Ust'Ishim/Oase1, Chimpanzee)* where *W* is one of the six present-day West Eurasian populations and *X* is a present-day non-African population from Central Asia and Siberia, East Asia, South Asia, Oceania or Americas. A) *Oase1* (nsnps = 402,526) and **B)** *Ust'Ishim* (nsnps = 1,951,462). *D* values denoted as circles and plotted on the *y*-axes were calculated using ADMIXTOOLS[3] as implemented in *admixr*[9]. Present-day human genomes from SGDP[10] were used in these statistics, and a genome of *panTro2* as an outgroup. Filled-in circles indicate a significant Z-score or $|Z| \geq 3$, and open circles indicate a non-significant Z-score or $|Z| < 3$. Whiskers on each side of the plotted *D* values correspond to one standard error calculated using a Weighted Block Jackknife[3,12] across all autosomes on the "2200k" Panel and a block size of 5 Mb.

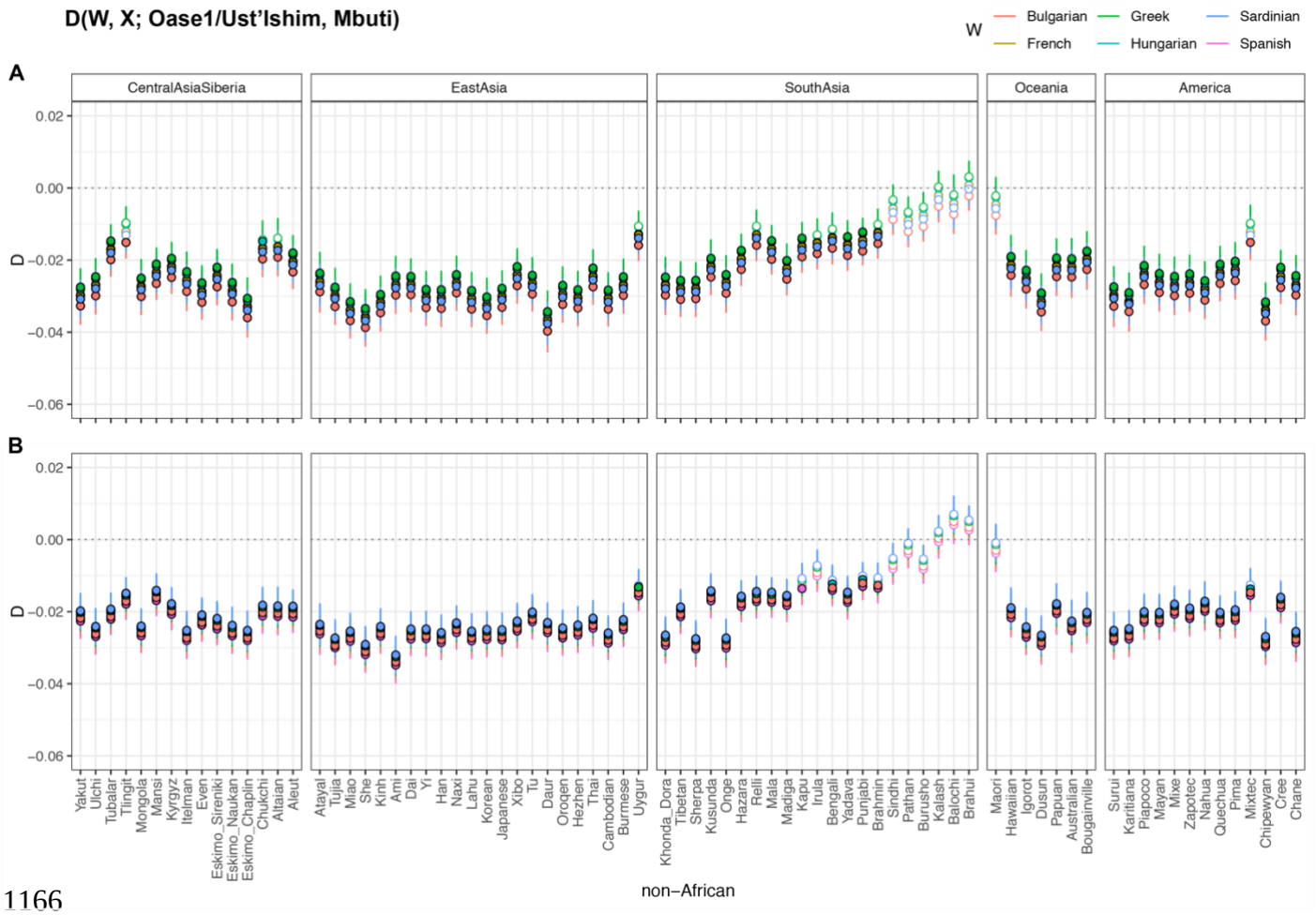

Figure S5.10 D-statistics of the form *D(W, X; Ust'Ishim/Oase1, Mbuti)* where *W* is one of the six present-day West Eurasian populations and *X* is a present-day non-African population from Central Asia and Siberia, East Asia, South Asia, Oceania or Americas. **A)** *Oase1* (nsnps = 402,526) and **B)** *Ust'Ishim* (nsnps = 1,951,462). *D* values denoted as circles and plotted on the *y*-axes were calculated using ADMIXTOOLS[3] as implemented in *admixr*[9]. Present-day human genomes from SGDP[10] were used in these statistics, and three Mbuti individuals from the same panel were used as outgroup. Filled-in circles indicate a significant Z-score or $|Z| \geq 3$, and open circles indicate a non-significant Z-score or $|Z| < 3$. Whiskers on each side of the plotted *D* values correspond to one standard error calculated using a Weighted Block Jackknife[3,12] across all autosomes on the "2200k" Panel and a block size of 5 Mb.

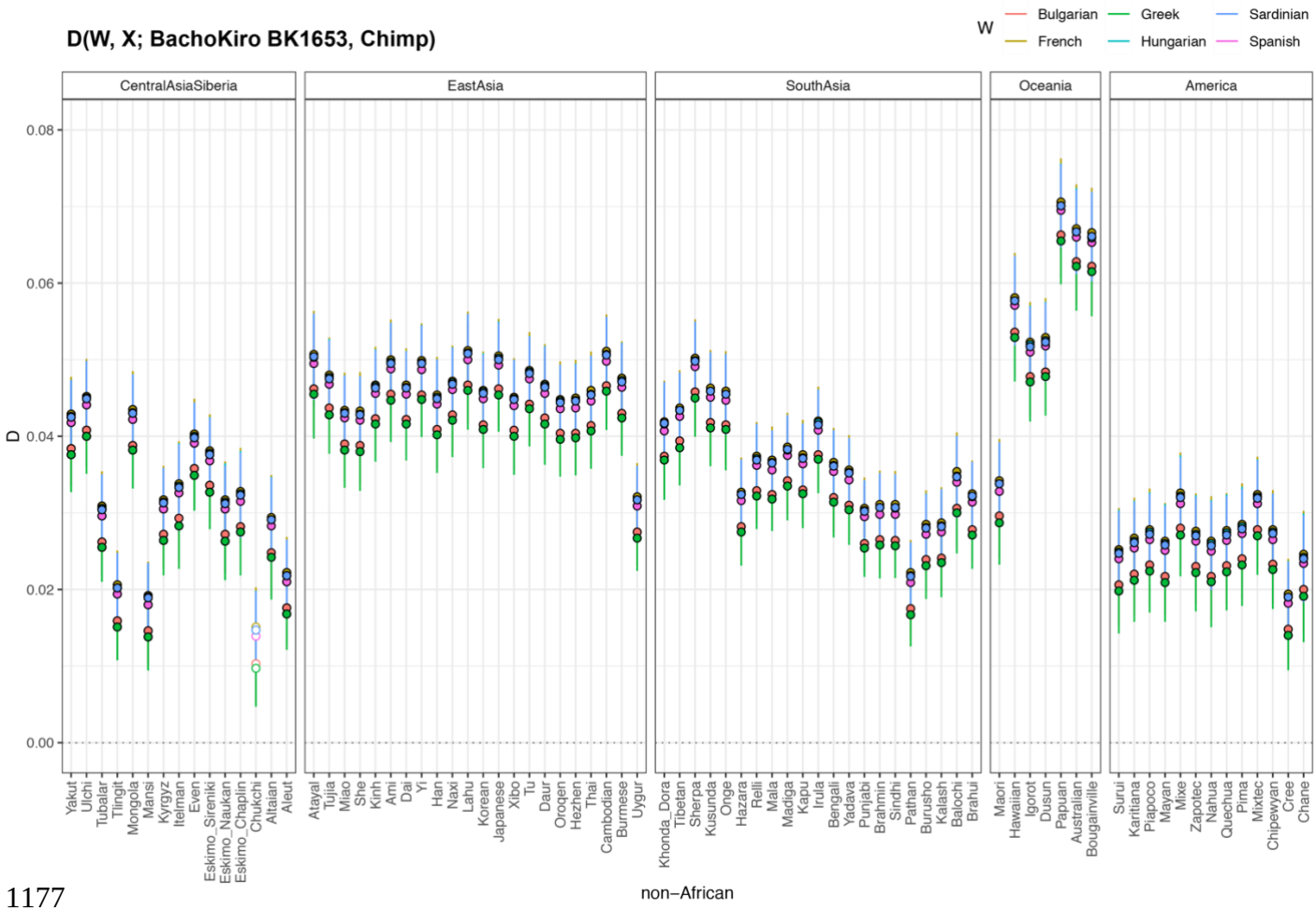

Figure S5.11 D-statistics of the form *D(W, X; Bacho Kiro BK1653, Chimpanzee)* where *W* is one of the six present-day West Eurasian populations and *X* is a present-day non-African population from Central Asia and Siberia, East Asia, South Asia, Oceania or Americas. *D* values denoted as circles and plotted on the *y*-axis were calculated using ADMIXTOOLS[3] as implemented in *admixr*[9]. Present-day human genomes from SGDP[10] were used in these statistics, and a genome of *panTro2* as an outgroup. *Bacho Kiro BK1653* (nsnps = 825,379) is significantly closer to present-day West Eurasians than to any other superpopulation from SGDP. Filled-in circles indicate a significant Z-score or $|Z| \geq 3$, and open circles indicate a non-significant Z-score or $|Z| < 3$. Whiskers on each side of the plotted *D* values correspond to one standard error calculated using a Weighted Block Jackknife[3,12] across all autosomes on the "2200k" Panel and a block size of 5 Mb.

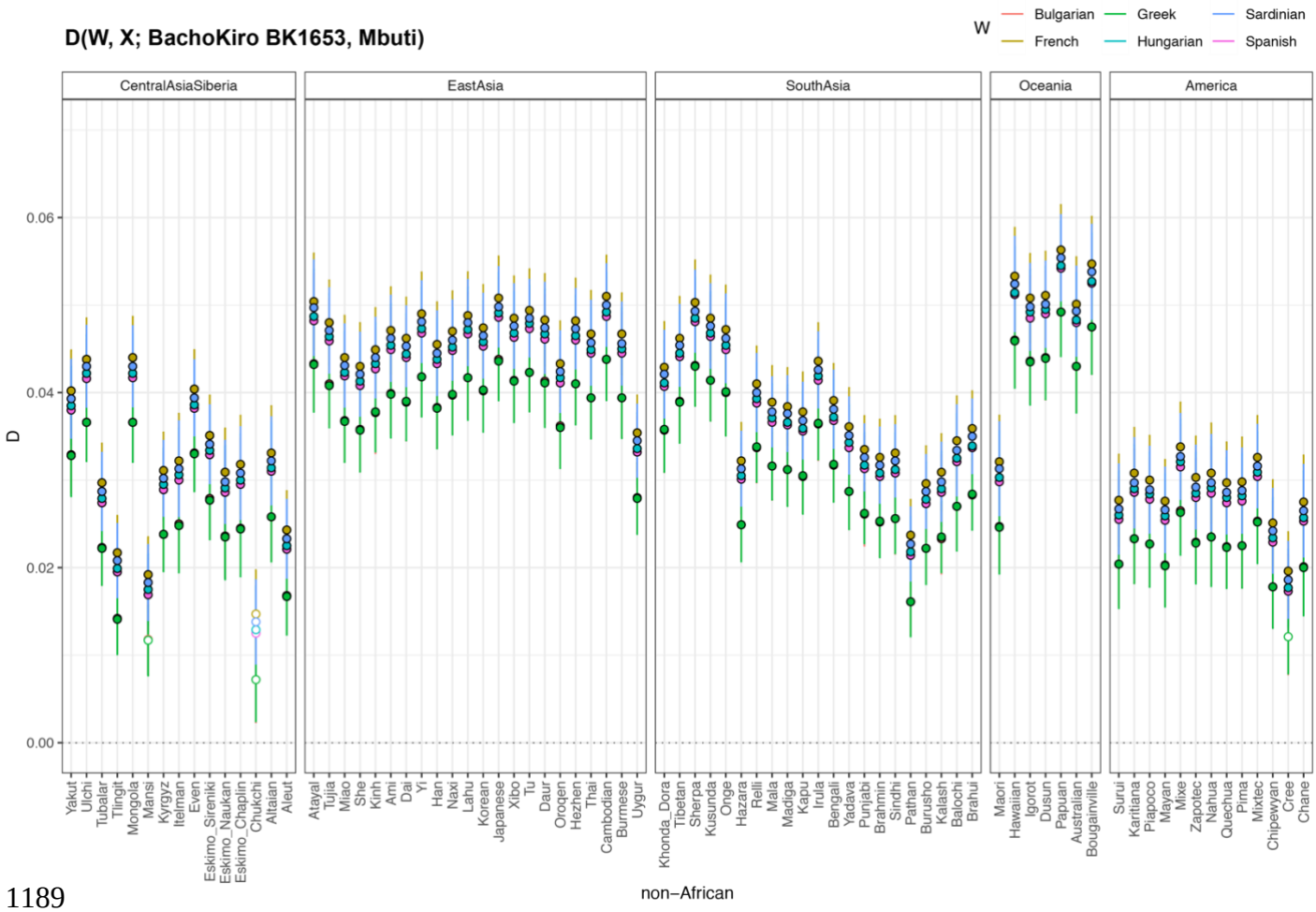

Figure S5.12 D-statistics of the form *D(W, X; Bacho Kiro BK1653, Mbuti)* where *W* is one of the six present-day West Eurasian populations and *X* is a present-day non-African population from Central Asia and Siberia, East Asia, South Asia, Oceania or Americas. *D* values denoted as circles and plotted on the *y*-axis were calculated using ADMIXTOOLS[3] as implemented in *admixr*[9]. Present-day human genomes from SGDP[10] were used in these statistics, and three Mbuti individuals from the same panel were used as outgroup. *Bacho Kiro BK1653* (nsnps = 825,379) is significantly closer to present-day West Eurasians than to any other superpopulation from SGDP. Filled-in circles indicate a significant Z-score or $|Z| \geq 3$, and open circles indicate a non-significant Z-score or $|Z| < 3$. Whiskers on each side of the plotted *D* values correspond to one standard error calculated using a Weighted Block Jackknife[3,12] across all autosomes on the "2200k" Panel and a block size of 5 Mb.

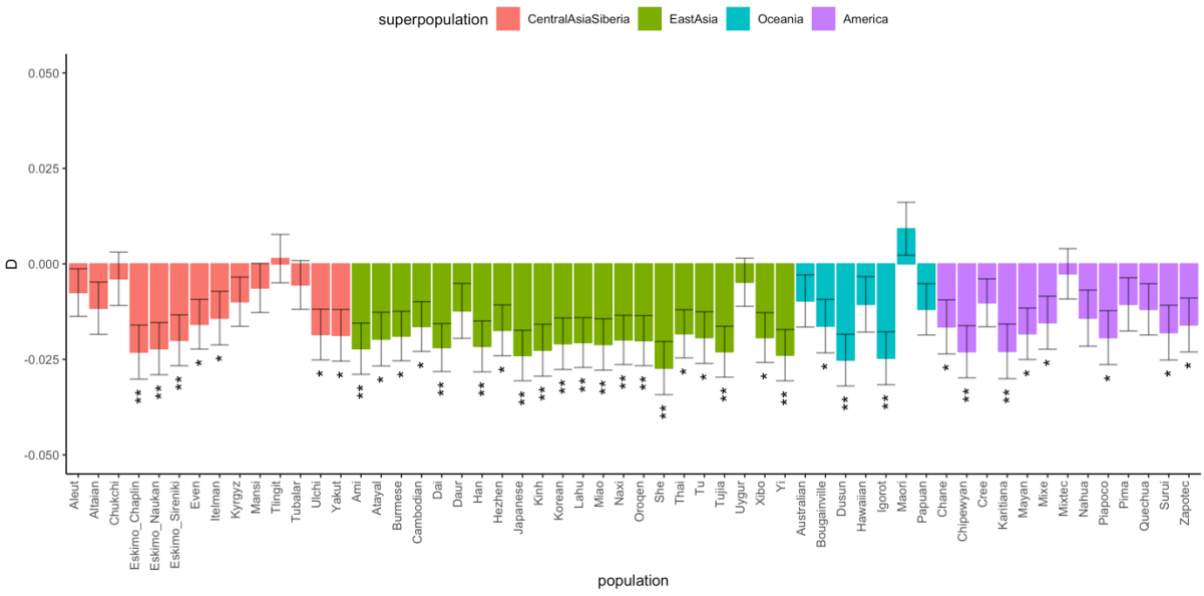

Figure S5.13 *D(Kostenki14, X; IUP BachoKiro, Mbuti)* restricted to transversion polymorphisms where *X* is a present-day non-African population from Central Asia and Siberia, East Asia, South Asia, Oceania or Americas. *D* values denoted as bars plotted on the *y*-axis were calculated using ADMIXTOOLS[3] as implemented in *admixr*[9]. Positive *D*-value indicates higher proportion of alleles shared between IUP Bacho Kiro Cave individuals and *Kostenki 14*, whereas a negative *D*-value indicates higher proportion of alleles shared between IUP Bacho Kiro Cave individuals and a given present-day human population indicated on *x*-axis. Present-day human genomes from SGDP[10] were used in these statistics, and three Mbuti individuals from the same panel were used as outgroup. Two stars (**) indicate a significant Z-score or $|Z| \geq 3$, and one star (*) indicates $|Z| \geq 2$. Standard errors (SE) plotted around the centre of *D*-values were calculated using a Weighted Block Jackknife[3,12] across all autosomes on the "2200k" Panel (nsnps (IUP Bacho Kiro individuals) = 945,785) and a block size of 5 Mb.

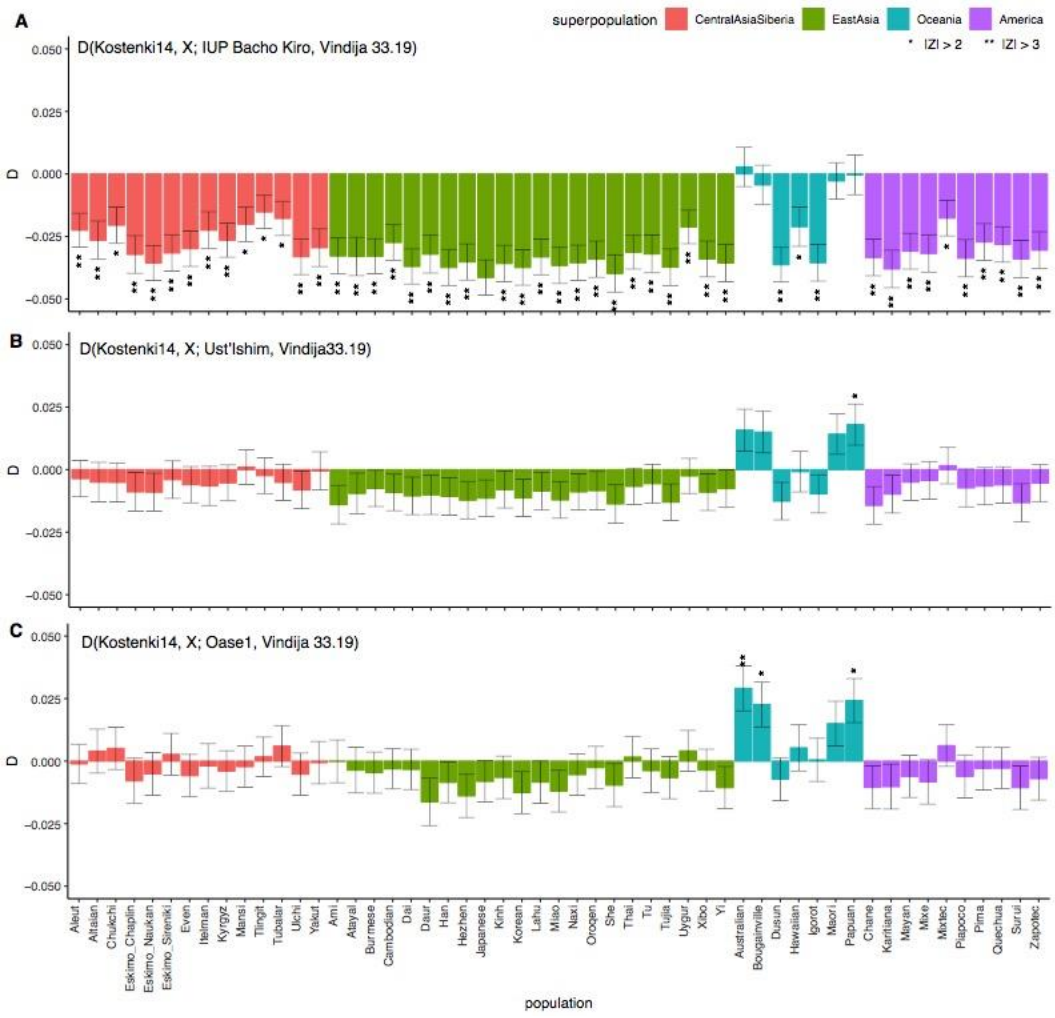

Figure S5.14 ***D(Kostenki14, X; IUP BachoKiro/Ust'Ishim/Oase1, Vindija 33.19)*** **where *X* is a present-day non-African population from Central Asia and Siberia, East Asia, South Asia, Oceania or Americas. A)** IUP Bacho Kiro Cave individuals, **B)** *Ust'Ishim* and **C)** *Oase 1*. *D* values denoted as bars plotted on the *y*-axis were calculated using ADMIXTOOLS[3] as implemented in *admixr*[9]. Positive *D*-value indicates higher proportion of alleles shared between IUP Bacho Kiro Cave individuals (panel A), *Ust'Ishim* (panel B) or *Oase 1* (panel C) and *Kostenki 14*, whereas a negative *D*-value indicates higher proportion of alleles shared between former individuals and a given present-day human population indicated on *x*-axes. Present-day human genomes from SGDP[10] were used in these statistics, and *Vindija 33.19* Neandertal[17] was used as outgroup. Two stars (**) indicate a significant Z-score or $|Z| \geq 3$, and one star (*) indicates $|Z| \geq 2$. Standard errors (SE) plotted around *D*-values were calculated using a Weighted Block Jackknife[3,12] across all autosomes on the "2200k" Panel (nsnps (IUP Bacho Kiro individuals) = 1,813,821; nsnps (*Ust'Ishim*) = 1,951,462; nsnps (*Oase 1*) = 402,526) and a block size of 5 Mb.

Supplementary Information 6

Admixture Graph Modelling

We used program *qpGraph* (Admixture Graph) from ADMIXTOOLS[1] (version: v5.1) to test models of the relationship among Initial Upper Palaeolithic Bacho KiroCave individuals, ~34,000-year-old *Bacho Kiro BK1653* and other ancient modern humans from Eurasia older than 30,000 years BP. Admixture Graph examines whether a proposed model or a graph fits the data by determining whether the estimated values of all possible f_2-, f_3-, and f_4-statistics among all pairs, triples, and quadruples of individuals or populations match the observed values, and evaluates the significance of the difference between them using a Weighted Block Jackknife[1,2]. We run *qpGraph* on the "2200k" SNP Panel, using a Weighted Block Jackknife across all autosomes with a block size of 5 Mb and the following parameters:

outpop: NULL, blgsize: 0.005, lsqmode: YES, diag: .0001, hires: YES, lambdascale: 1, useallsnps: NO, bigiter: 6, forcezmode: YES

We begin with a simple model (Fig. S6.1) that relates three high coverage Mbuti individuals from SGDP[3], the ~45,000-year-old *Ust'Ishim* from Siberia[4], the ~40,000-year-old *Tianyuan*[5] from China, the ~38,000-year-old *Kostenki14*[6,7] and the ~34,000-year-old *SunghirIII*[8], both from Russia. We use the capture data of *Kostenki14*[7] for most of our *qpGraph* analyses due to the higher coverage of SNPs in the "2200k" Panel. In each of the Admixture Graphs shown in this supplementary note labels on solid branches correspond to the estimated drift in f_2-units of squared frequency difference and labels on the dotted edges give admixture proportions.

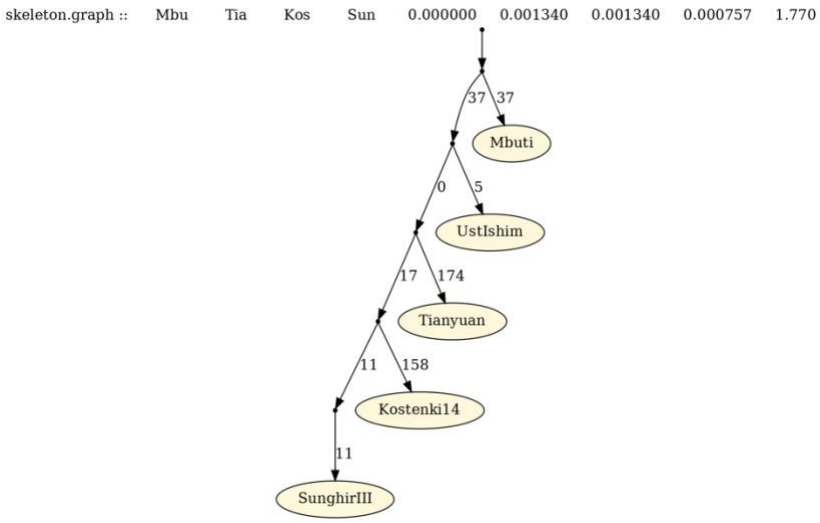

Figure S6.1 Base (skeleton) graph. This model uses 886,336 SNPs covered in all individuals.

We proceed by attempting to fit the ~45,000-year-old Initial Upper Palaeolithic (IUP) Bacho Kiro individual with highest coverage (*Bacho Kiro F6-620*) to this base graph. We add IUP *Bacho Kiro F6-620* to all possible nodes of the graph in Fig. S6.1, either as a simple branch without mixture, or as a mixture between branches. Altogether, we identify two models that fit the data (maximum |Z-score| < 3) and show these in Fig. S6.2. In both graphs the 40,000-year-old *Tianyuan* is modelled as a mixture with a lineage related to *Bacho Kiro F6-620*.

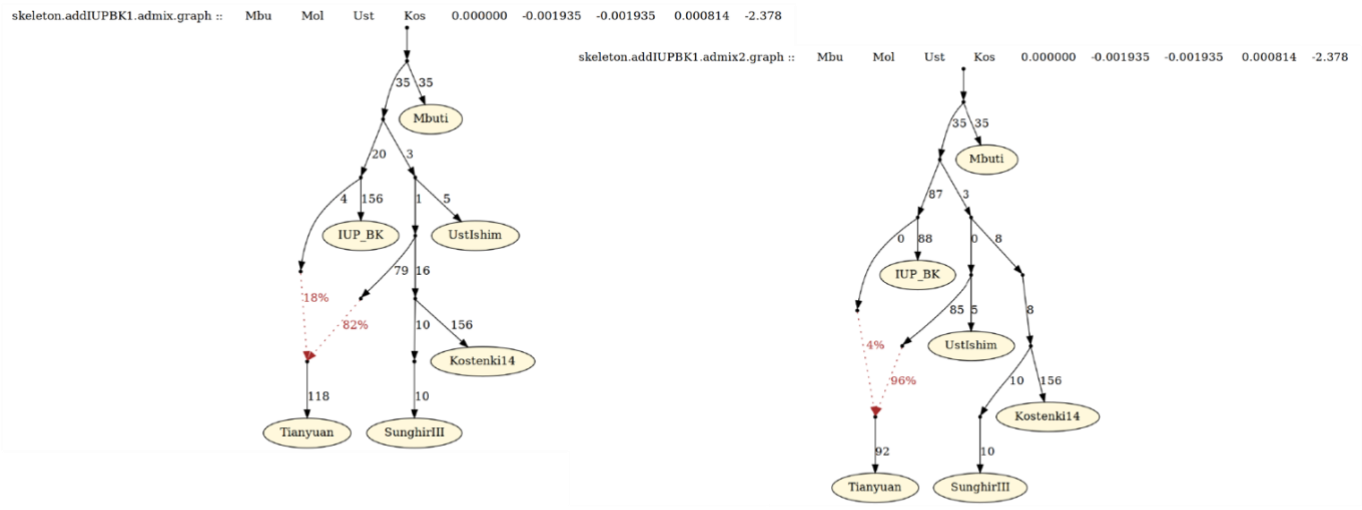

Figure S6.2 Adding *Bacho Kiro F6-620* to the base graph. These models use 879,787 SNPs in all individuals.

Given the higher Neandertal ancestry in *Bacho Kiro F6-620* than in other ancient modern humans included in these models (see Supplementary Information 7 and 8), we account for this and for the archaic ancestry in other ancient modern humans by adding the high coverage genomes of *Vindija 33.19* Neandertal[9] and *Denisova 3*[10] to the graphs in Fig. S6.2.

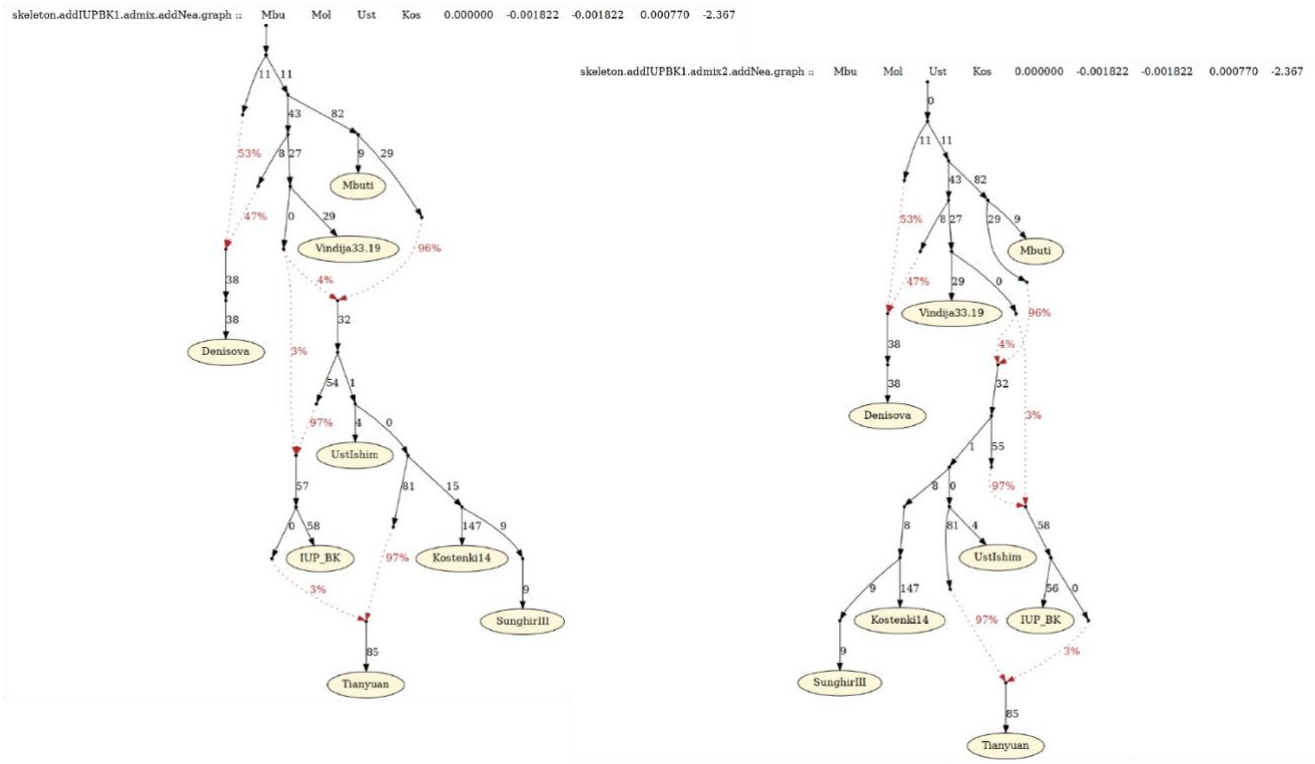

Figure S6.3 Adding *Vindija 33.19* Neandertal and *Denisova 3*. These models use 832,495 SNPs in all individuals.

We further proceed to fit the ~35,000-year-old *GoyetQ116-1* from Belgium[7], the younger ~34,000-year-old *Bacho Kiro BK1653* and the ~30,000-year-old *Vestonice16* from Czech Republic[7] to the graphs in Fig. S6.3, starting with the oldest individual and moving forward in time.

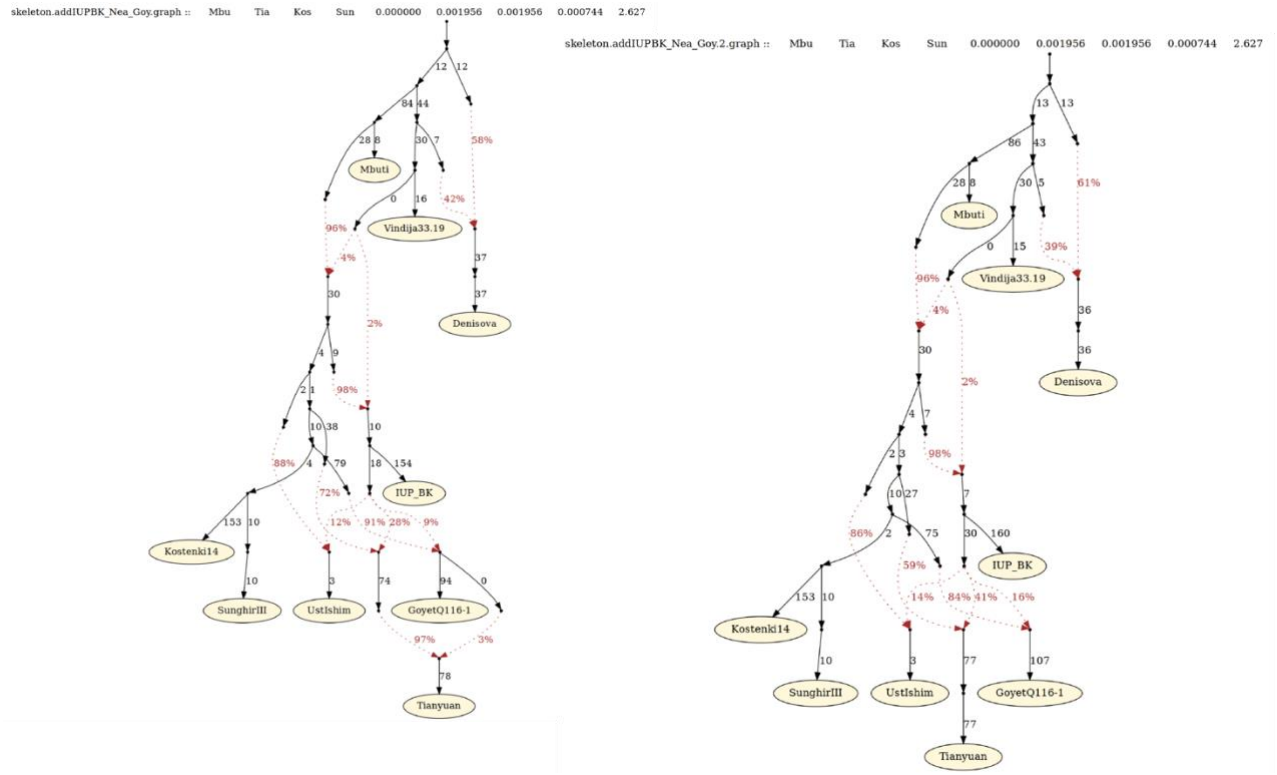

Figure S6.4 Adding the ~35,000-year-old *Goyet Q116-1* from Belgium. These models use 520,102 SNPs in all individuals.

Interestingly, after adding the ~35,000-year-old *Goyet Q116-1* to all the possible nodes shown in the Fig. S6.3 either as a simple branch without mixture or as a mixture between branches, the ~45,000-year-old *Ust'Ishim*, the ~40,000-year-old *Tianyuan* and *Goyet Q116-1* all fit the models best as being admixed with a lineage related to the *Bacho Kiro F6-620*, with *Tianyuan* having the largest contribution from this lineage (between 28% and 41%, depending on the model). Furthermore, having part of the ancestry of *GoyetQ116-1* deriving from a lineage related to IUP Bacho Kiro eliminates the need for an additional admixture edge between *GoyetQ116-1* and *Tianyuan* (Fig. S6.4). We note, however, that both models with and without this additional admixture edge fit the data with no outliers (maximum |Z-score| < 3) (Fig. S6.4). We also tested whether the connections observed between *Ust'Ishim* or *GoyetQ116-1* and *Bacho Kiro F6-620* could be explained by the underlying models requiring an additional admixture edge from Neandertals to these individuals. However, these models are rejected (|Z-score| > 3) in favour of the models presented in Fig. S6.4.

We next add the ~34,000-year-old *Bacho Kiro 1653* to the models in Fig. S6.4 either as a simple branch without mixture or as a mixture between branches. We infer for this individual to be best modelled as admixed between a lineage related to *GoyetQ116-1* and a lineage related to *Kostenki14/SunghirIII*, with one outlier remaining (*f4(Mbuti, Tianyuan; Kostenki14, Sunghir)*, Z-score = 3.01). In the models highlighted in the Fig. S6.5, an additional admixture

edge stemming from a deep Eurasian branch that splits before the separation of *IUP Bacho Kiro*, *Ust'Ishim* and other Eurasians is required to explain the data. These models fit the data best to the limits of our resolution, albeit with a single outlier (Z-score = 3.01). To investigate this outlier further, we compute the statistics *D(Mbuti, Tianyuan; Kostenki14, SunghirIII)* and obtain a Z-score of 1.56 (all SNPs). Given the number of statistics we are computing to test the fit of these models to the data, we do not view a single outlier at |Z|>3 as a strong rejection of the models highlighted in Fig. S6.5.

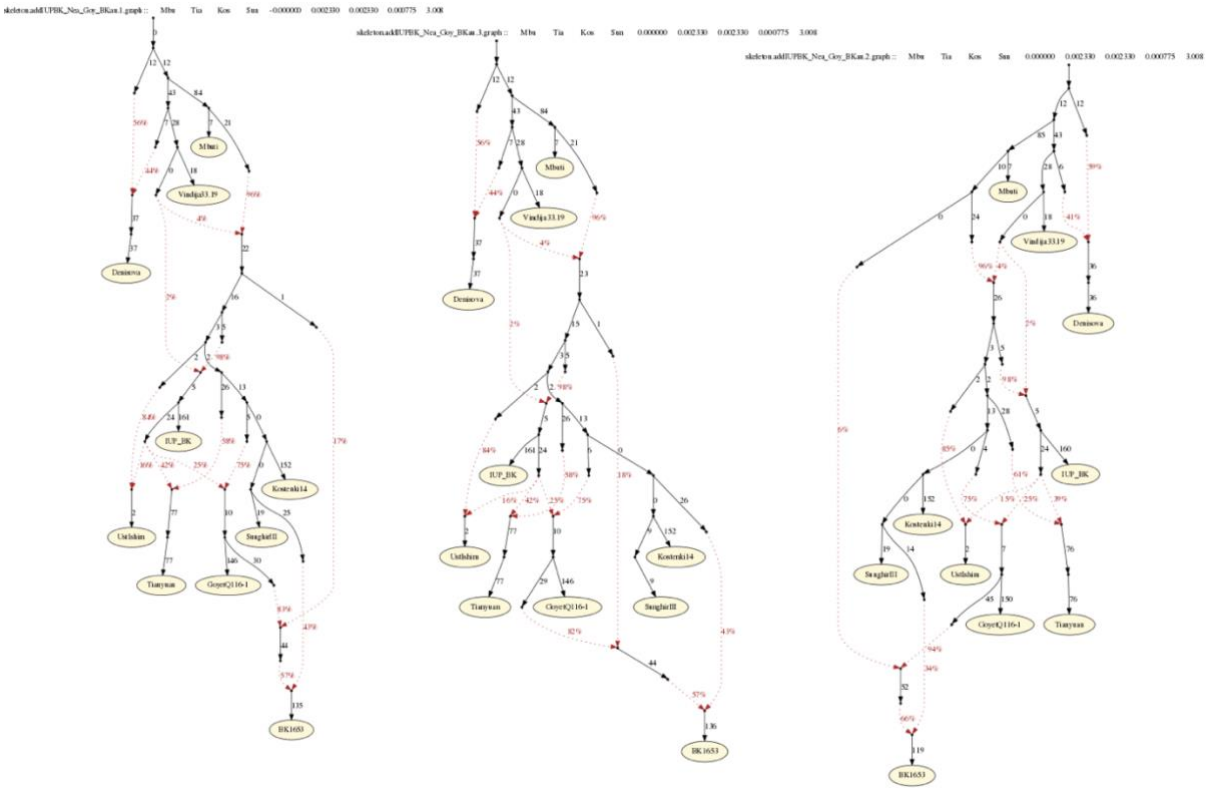

Figure S6.5 Adding 34,000-year-old *Bacho Kiro BK1653*. These models use 326,550 SNPs in all individuals.

We added the ~30,000-year-old *Vestonice16* to all possible branches of the models outlined in the Fig. S6.5, removing in each case the deep branching lineage contributing to *Bacho Kiro BK1653*. Two models fit the data best (Fig. S6.6 and Fig. S6.7), albeit each with one outlier and still requiring a deep branching lineage, with either *Vestonice16* being admixed between lineages related to *Bacho Kiro BK1653* and a lineage related to *Kostenki14/SunghirIII* or *Bacho Kiro BK1653* being admixed between the lineages related to *GoyetQ116-1* and *Vestonice16*. In each case we are left with a single outlier to the data, *f4(Tianyuan, SunghirIII; GoyetQ116-1, BachoKiro BK1653)* (Z-score = 3.22) and *f4(Mbuti, Vestonice16; Kostenki14, Vestonice16)* (Z-score = 3.67).

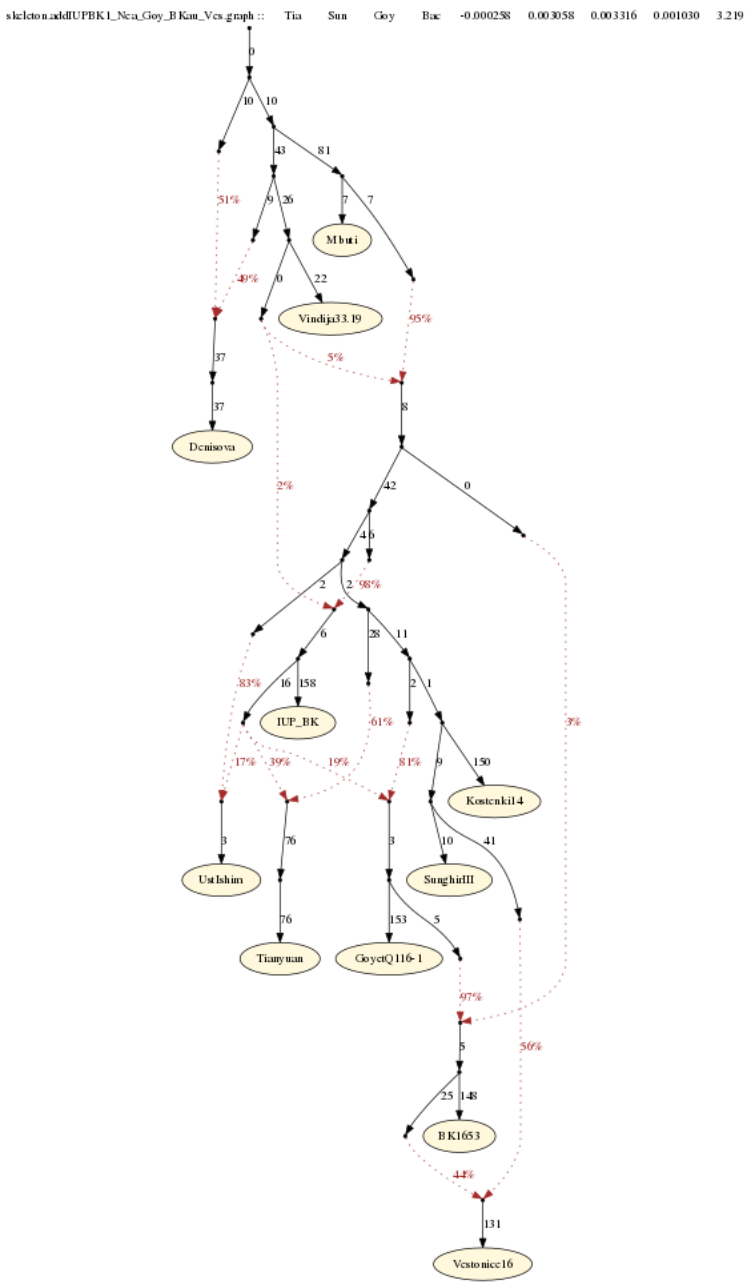

Figure S6.6 Adding *Vestonice16*, with *Vestonice16* being admixed. This model uses 281,732 SNPs in all individuals.

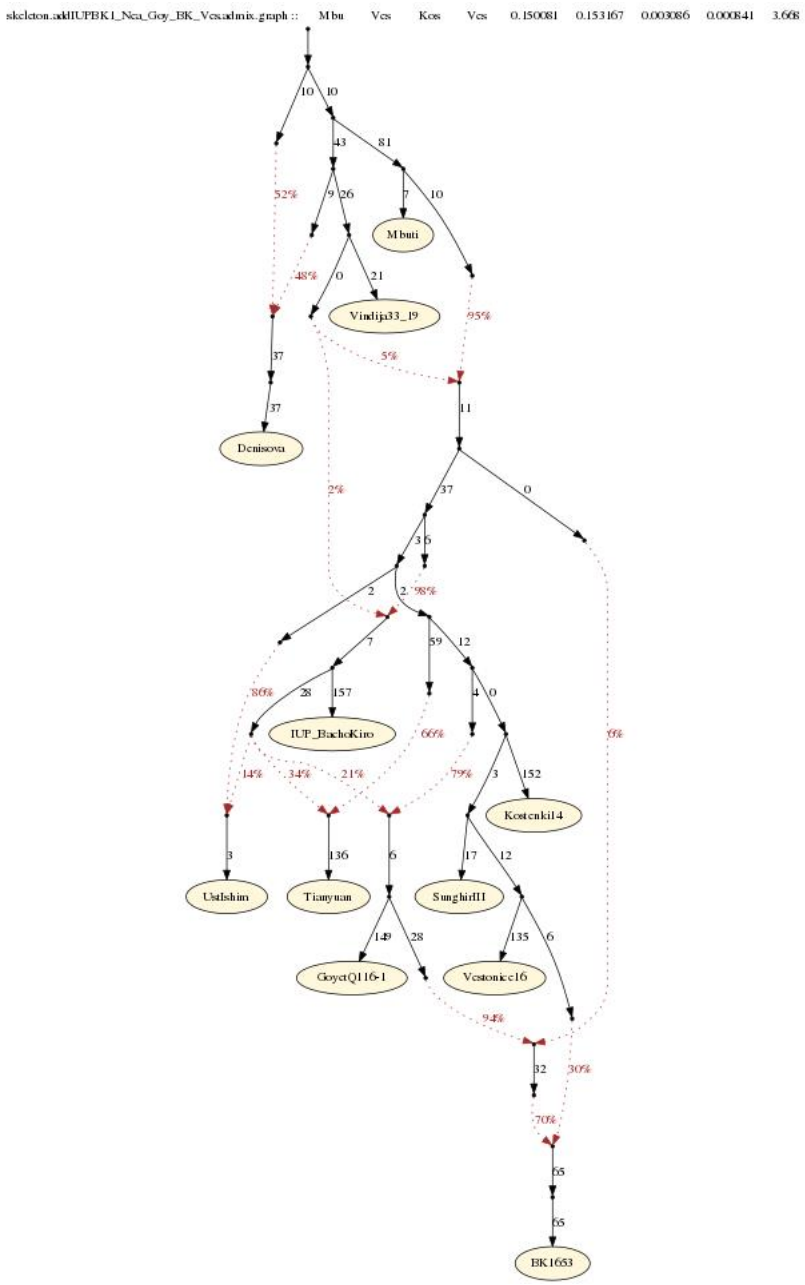

Figure S6.7 Adding *Vestonice16*, with *BachoKiro BK1653* being admixed. This model uses 281,732 SNPs in all individuals.

We additionally explored the relationship of *Bacho Kiro BK1653* to other Upper Palaeolithic West Eurasian ancient modern humans by reducing the graph to a smaller number of individuals (Fig S6.8). We confirm the placement of *Bacho Kiro BK1653* as being closest to a lineage related to *GoyetQ116-1*, further contributing her ancestry to *Vestonice16*, or alternatively being an admixed individual herself between the lineages related to *GoyetQ116-1* and *Kostenki14/SunghirIII* or *Vestonice16* and *GoyetQ116-1*. All of these models fit with the data with no outliers, albeit with invoking a very small contribution of a lineage that splits off from *IUP Bacho Kiro, Ust'Ishim* and other Eurasians before they split from each other.

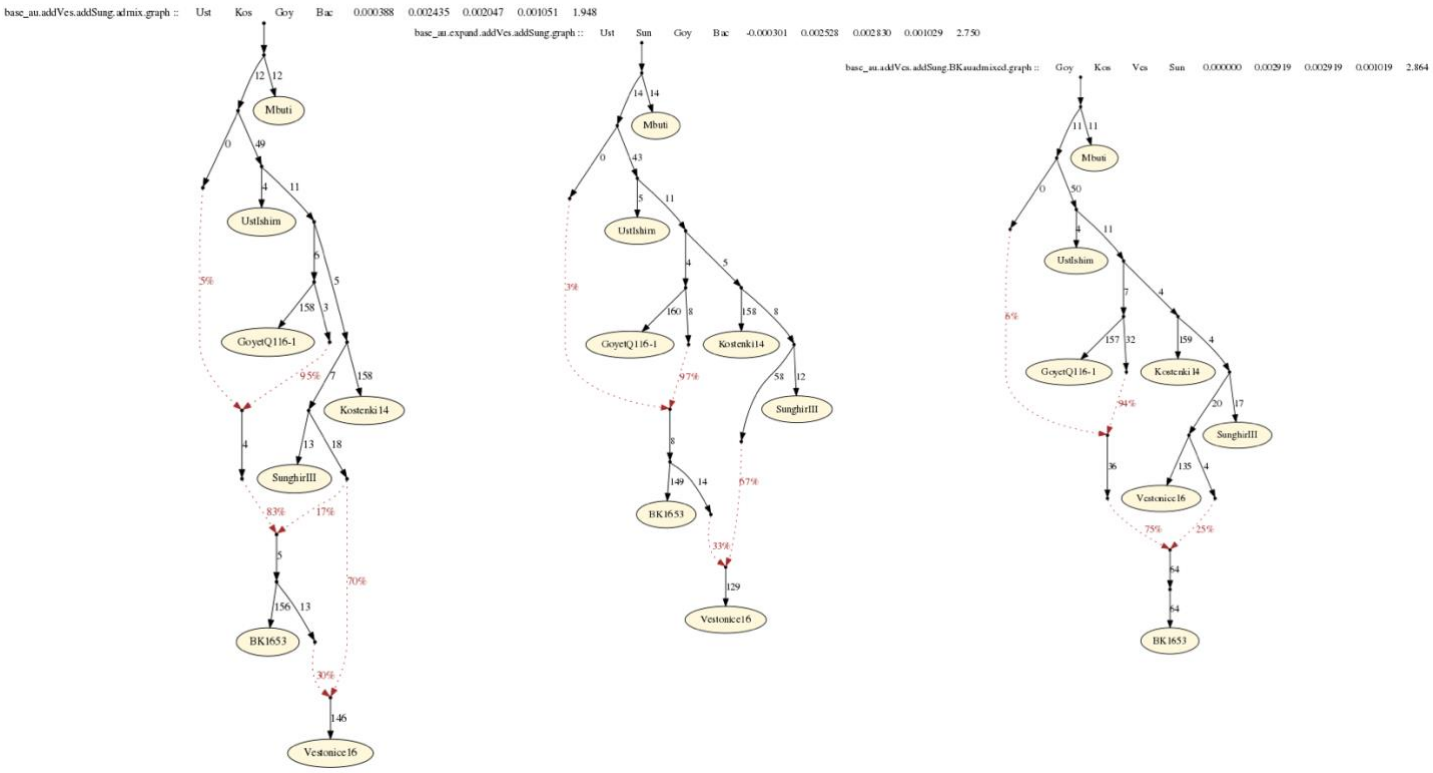

Figure S6.8 Admixture Graphs relating smaller number of ancient West Eurasians older than 30,000 years BP. These models use 327,698 SNPs in all individuals.

References SI6:

1 Patterson, N. *et al.* Ancient admixture in human history. *Genetics* **192**, 1065-1093, doi:10.1534/genetics.112.145037 (2012).

2 Busing, F. M. T. A., Meijer, E. & Van Der Leeden, R. Delete-m jackknife for unequal m. *Statistics and Computing* **9**, 3-8, doi:Doi 10.1023/A:1008800423698 (1999).

3 Mallick, S. *et al.* The Simons Genome Diversity Project: 300 genomes from 142 diverse populations. *Nature* **538**, 201-206, doi:10.1038/nature18964 (2016).

4 Fu, Q. *et al.* Genome sequence of a 45,000-year-old modern human from western Siberia. *Nature* **514**, 445-449, doi:10.1038/nature13810 (2014).

5 Yang, M. A. *et al.* 40,000-Year-Old Individual from Asia Provides Insight into Early Population Structure in Eurasia. *Curr. Biol.* **27**, 3202-3208.e9, doi: 10.1016/j.cub.2017.09.030 (2017).

6 Seguin-Orlando, A. *et al.* Genomic structure in Europeans dating back at least 36,200 years. *Science* **346**, 1113-1118, doi:10.1126/science.aaa0114 (2014).

7 Fu, Q. *et al.* The genetic history of Ice Age Europe. *Nature* **534**, 200-205, doi:10.1038/nature17993 (2016).

8 Sikora, M. *et al.* Ancient genomes show social and reproductive behavior of early Upper Paleolithic foragers. *Science* **358**, 659-662, doi: 10.1126/science.aao1807 (2017).

9 Prüfer, K. *et al.* A high-coverage Neandertal genome from Vindija Cave in Croatia. *Science* **358**, 655-658, doi: 10.1126/science.aao1887 (2017).

10 Meyer, M. *et al.* A high-coverage genome sequence from an archaic Denisovan individual. *Science* **338**, 222-226, doi:10.1126/science.1224344 (2012).

Supplementary Information 7

Neandertal ancestry in Bacho Kiro individuals

Estimates of Neandertal ancestry proportions

We calculated the proportion of Neandertal ancestry in Bacho Kiro individuals and other ancient and present-day modern humans by computing a direct *f_4-ratio* that takes advantage of the two high-coverage Neandertal genomes[1], the ~130,000-year-old *Denisova 5* (*'Altai')* Neandertal from Siberia[2] and the ~45,000-year-old *Vindija 33.19* Neandertal from Croatia[3]. We also re-calculated the proportion of Neandertal ancestry in *Oase1* after merging previously published data[4] with new data from additional libraries prepared for this study (see Supplementary Information 2). We used ADMIXTOOLS[5] as implemented in the R package *admixr*[6], with a Weighted Block Jackknife[5,7] and a block size of 5 million base pairs (5Mb) to calculate alpha (α) on the "2200k" SNP Panel as:

$$\alpha = \frac{f4(Altai\ Neandertal, Chimpanzee; X, Mbuti)}{f4(Altai\ Neandertal, Chimpanzee; Vindija\ 33.19\ Neandertal, Mbuti)}$$

We find that Bacho Kiro individuals *F6-620*, *BB7-240* and *CC7-335* have 3.82% (95% confidence interval (CI): 3.28-4.37%), 3.01% (95% CI: 2.43-3.58%) and 3.43% (95% CI: 2.84-4.02%) Neandertal ancestry, respectively, which is more than the average of 1.95% (95% CI: 1.52-2.38%) found in other Upper Palaeolithic modern humans older than 30,000 years BP, with the exception of *Oase1*[4] (6.39% (95% CI: 5.65-7.13%)) (Extended Data Figure 6A). In contrast, Bacho Kiro *BK1653* has 1.91% (95% CI: 1.44-2.37%) Neandertal ancestry, similar to other ancient and present-day modern humans (Extended Data Figure 6A).

To test formally if IUP Bacho Kiro individuals share significantly more derived alleles with archaics than other ancient and present-day humans, we computed *D(IUP Bacho Kiro, Test; Neandertal, Outgroup)*. We used the genomes of Dinka, Yoruba and Mbuti individuals from the Simons Genome Diversity Panel (SGDP)[8] as outgroups. Since these statistics are expected to be skewed significantly positive for the Upper Palaeolithic individuals such as the ~45,000-year-old *Ust'Ishim* (Fig. S7.4) and the ~38,000-year-old *Kostenki14* (Fig. S7.6) due to gene-flow with Africans[1] or when a *Test* individual post-dates the introduction of "Basal Eurasian" ancestry[9,10], we compute the same statistics using the genome of a chimpanzee (*panTro2*) as an outgroup and restricting analyses to transversion polymorphisms to mitigate the effect of ancient DNA damage (Fig. S7.8-S7.14).

We find that IUP Bacho Kiro Cave individuals share significantly more derived alleles with the three high coverage Neandertals[2,3,11] than most other Upper Palaeolithic ancient humans (Fig. S7.1-S7.3 and Fig. S7.8-S7.10) with an exception of *Oase1*[4] (Z-score < -3.01). They also share significantly more alleles with Neandertals than present-day non-Africans (Fig. S7.8-S7.10), similar to *Oase1* (Fig. S7.12) and unlike *Ust'Ishim* (Fig. S7.11), *Kostenki14* (Fig. S7.13) or Bacho Kiro *BK1653* (Fig. S7.14). When present-day Papuans, Australians and Bougainville individuals are used as a *Test* population, the statistics *D(IUP Bacho Kiro, Test; Neandertal, Outgroup)* are not significantly different from 0 (Fig. S7.8-S7.10), likely due to the additional gene flow from Denisovans, a sister group of Neandertals, into these populations[12-15].

Introgressing Neandertal(s)

We tested if IUP Bacho Kiro Cave individuals share more derived alleles with one of the already sequenced Neandertal genomes by calculating *D(Archaic$_1$, Archaic$_2$; IUP Bacho Kiro, Outgroup)*. We first investigated whether there is a significant difference in derived allele sharing with the genomes of the ~50,000-year-old *Denisova 3* individual and any of the high coverage Neandertals (~130,000-year-old *Altai*[2] Neandertal, ~80,000-year-old *Chagyrskaya 8*[11] and ~45,000-year-old *Vindija 33.19*[3]) or if there are differences in allele sharing when comparing between the high coverage Neandertals. For the high-coverage genomes of the archaics we used their *snpAD*[3,16] genotype calls that overlap positions on the "2200k" SNP Panel. We used the genomes of *panTro2*, and Dinka, Yoruba and Mbuti individuals from the Simons Genome Diversity Panel (SGDP)[8] as outgroups.

We find that Bacho Kiro individuals share significantly more derived alleles with Neandertals than with the Denisovan individual (Z-score < -26.27, Fig. S7.15 and S7.16). Furthermore, the three IUP Bacho Kiro individuals and *BK1653* share significantly more derived alleles with *Chagyrskaya 8* and *Vindija 33.19* than they do with the *Altai* Neandertal (-5.08 < Z-score < -2.77, Fig. S7.15, and -5.03 < Z-score < -3.01, Fig. S7.16), similar to what has been previously observed for other ancient and present-day humans[3,11,17].

Investigating overlapping sites with late Neandertals and *Mezmaiskaya1*

Given that IUP Bacho Kiro Cave individuals overlap in time with late Neandertals, we co-analysed the low-coverage late Neandertal genomes of *Les Cottés Z4-1514, Goyet Q56-1, Mezmaiskaya 2* and *Spy 94a*[17] with the genome of a >70,000-year-old *Mezmaiskaya 1* Neandertal[3] and the high-coverage archaic genomes. For the late Neandertals and *Mezmaiskaya 1*, we randomly sampled an allele from fragments longer than 35 base pairs that had a mapping quality of at least 25 and that overlapped positions on the "2200k" SNP Panel. The analyses involving low-coverage Neandertals were further restricted to the fragments that showed C-to-T substitutions with respect to the human reference genome in the first and/or last three positions to diminish the impact of present-day human DNA contamination[18] that was previously inferred for these samples[3,17]. To make these analyses comparable with those of high-coverage archaics and minimize the differences in the statistics that involve genomes of substantially different qualities, we followed the same filtering as above for the high coverage *Altai* and *Vindija 33.19* Neandertals and randomly sampled an allele from fragments longer than 35 base pairs that had a mapping quality of at least 25 and that overlapped positions on the "2200k" SNP Panel, thereby effectively lowering the qualities of the high coverage genomes to similar levels as the low-coverage Neandertals.

However, the number of informative sites in low-coverage Neandertals that overlap "2200k" SNP Panel is low (Tab. S7.1). This is best demonstrated calculating *D(Altai Neandertal, Vindija33.19; Modern Human Test, Outgroup)* where down-sampling high-coverage Neandertal genomes to the coverage of late Neandertals and *Mezmaiskaya1* causes otherwise significantly positive statistics (Fig. S7.15 and Fig. S7.16) to become not significantly different from 0 (Fig. S7.17). Thus, we do not have enough power to detect any potential differences among late Neandertal populations that contributed additional Neandertal ancestry to IUP Bacho Kiro individuals when compared to other ancient modern humans, even if such differences may exist.

References SI7:

1 Petr, M., Pääbo, S., Kelso, J. & Vernot, B. Limits of long-term selection against Neandertal introgression. *Proc. Natl. Acad. Sci. U.S.A.* **116**, 1639-1644 (2019).

2 Prüfer, K. *et al.* The complete genome sequence of a Neanderthal from the Altai Mountains. *Nature* **505**, 43-49, doi:10.1038/nature12886 (2014).

3 Prüfer, K. *et al.* A high-coverage Neandertal genome from Vindija Cave in Croatia. *Science* **358**, 655-658, doi: 10.1126/science.aao1887 (2017).

4 Fu, Q. *et al.* An early modern human from Romania with a recent Neanderthal ancestor. *Nature* **524**, 216-219, doi:10.1038/nature14558 (2015).
5 Patterson, N. *et al.* Ancient admixture in human history. *Genetics* **192**, 1065-1093, doi:10.1534/genetics.112.145037 (2012).
6 Petr, M., Vernot, B. & Kelso, J. admixr—R package for reproducible analyses using ADMIXTOOLS. *Bioinformatics* **35**, 3194-3195 (2019).
7 Busing, F. M. T. A., Meijer, E. & Van Der Leeden, R. Delete-m jackknife for unequal m. *Statistics and Computing* **9**, 3-8, doi:Doi 10.1023/A:1008800423698 (1999).
8 Mallick, S. *et al.* The Simons Genome Diversity Project: 300 genomes from 142 diverse populations. *Nature* **538**, 201-206, doi:10.1038/nature18964 (2016).
9 Lazaridis, I. *et al.* Ancient human genomes suggest three ancestral populations for present-day Europeans. *Nature* **513**, 409-413, doi:10.1038/nature13673 (2014).
10 Lazaridis, I. *et al.* Genomic insights into the origin of farming in the ancient Near East. *Nature* **536**, 419-424 (2016).
11 Mafessoni, F. *et al.* A high-coverage Neandertal genome from Chagyrskaya Cave. *Proc. Natl. Acad. Sci. U.S.A.* **117**, 15132-15136, doi:10.1073/pnas.2004944117 (2020).
12 Reich, D. *et al.* Genetic history of an archaic hominin group from Denisova Cave in Siberia. *Nature* **468**, 1053-1060, doi:10.1038/nature09710 (2010).
13 Meyer, M. *et al.* A high-coverage genome sequence from an archaic Denisovan individual. *Science* **338**, 222-226, doi:10.1126/science.1224344 (2012).
14 Vernot, B. *et al.* Excavating Neandertal and Denisovan DNA from the genomes of Melanesian individuals. *Science* **352**, 235-239, doi:10.1126/science.aad9416 (2016).
15 Sankararaman, S., Mallick, S., Patterson, N. & Reich, D. The Combined Landscape of Denisovan and Neanderthal Ancestry in Present-Day Humans. *Curr. Biol.* **26**, 1241-1247, doi:10.1016/j.cub.2016.03.037 (2016).
16 Prüfer, K. snpAD: An ancient DNA genotype caller. *Bioinformatics* **34**, 4165-4171 (2018).
17 Hajdinjak, M. *et al.* Reconstructing the genetic history of late Neanderthals. *Nature* **555**, 652-656, doi:10.1038/nature26151 (2018).
18 Meyer, M. *et al.* A mitochondrial genome sequence of a hominin from Sima de los Huesos. *Nature* **505**, 403-406, doi:10.1038/nature12788 (2014).
19 Fu, Q. *et al.* The genetic history of Ice Age Europe. *Nature* **534**, 200-205, doi:10.1038/nature17993 (2016).

Table S7.1 Number of informative sites in late Neandertals and *Mezmaiskaya1* overlapping "2200k" SNP Panel after filtering for fragments ≥35 bp and MQ≥25 that showed C-to-T substitutions in the first three and/or the last three positions relative to the reference genome.

Individual	# of SNPs	# of transversion SNPs
Les Cottes Z4-1514	1,074,561	587,467
Spy 94a	330,889	182,085
Goyet Q56-1	446,309	238,416
Mezmaiskaya 2	760,142	402,957
Mezmaiskaya 1	546,819	306,969

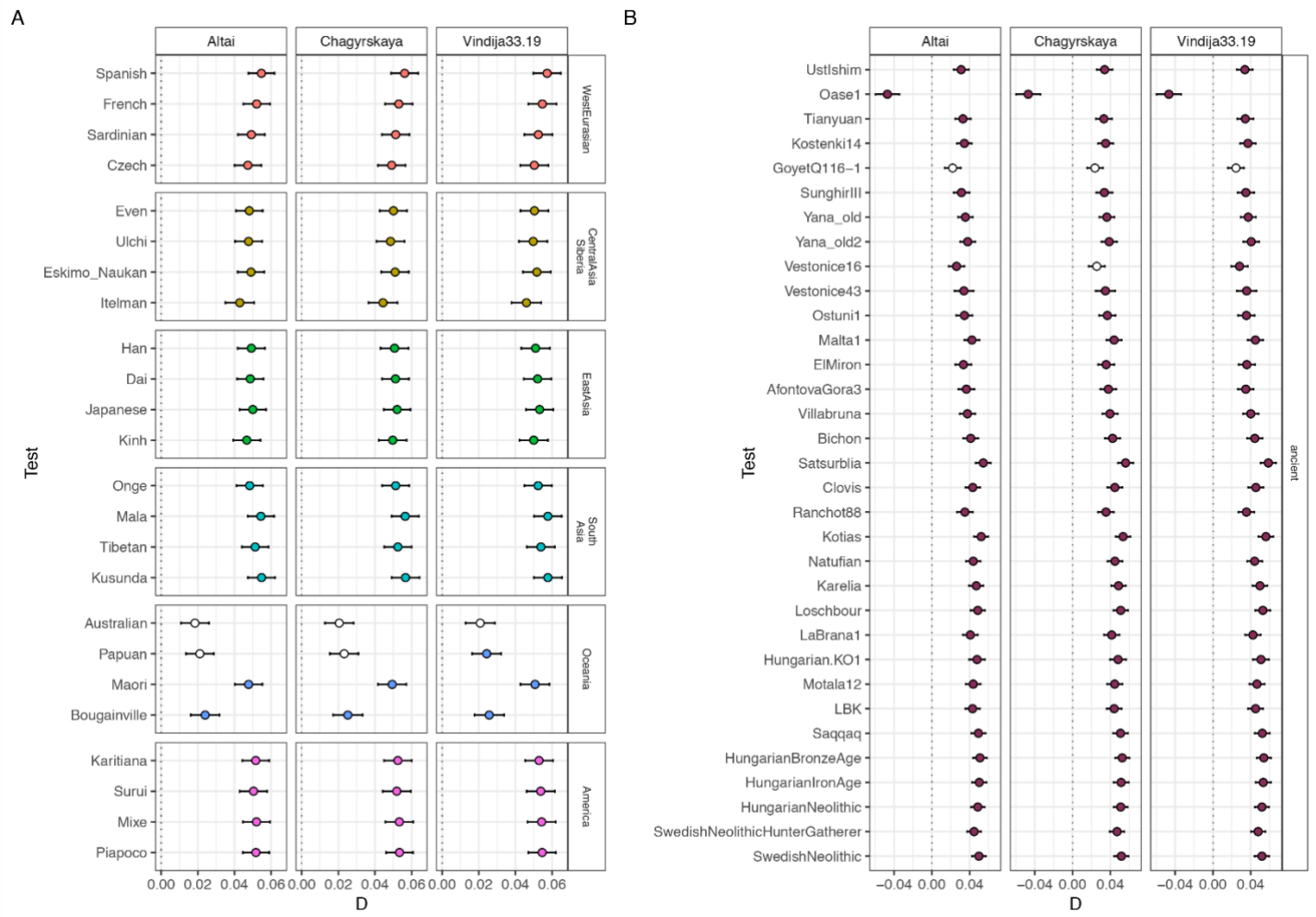

Figure S7.1 D-statistics comparing derived allele sharing with an archaic genome between IUP Bacho Kiro *F6-620* and a range of present-day and ancient modern humans. Values for *D(Bacho Kiro F6-620, Test; Archaic, Mbuti)* denoted as circles are plotted on the *x*-axes where *Archaic* is a high-coverage Neandertal genome[2,3,11] and *Test* is either a present-day population from SGDP[8] (panel A) or an ancient individual (panel B). Three Mbuti individuals from SGDP[8] were used as outgroup. *D* statistics were calculated using ADMIXTOOLS[5] as implemented in *admixr*[6]. Filled-in circles indicate a significant Z-score or $|Z| \geq 3$, and open circles indicate a non-significant Z-score or $|Z| < 3$. Whiskers on each side of the plotted *D* values correspond to one standard error calculated with a Weighted Block Jackknife[5,7] and a block size of 5 Mb across all autosomes on the "2200k" Panel (nsnps (*Bacho Kiro F6-620*) = 1,779,883).

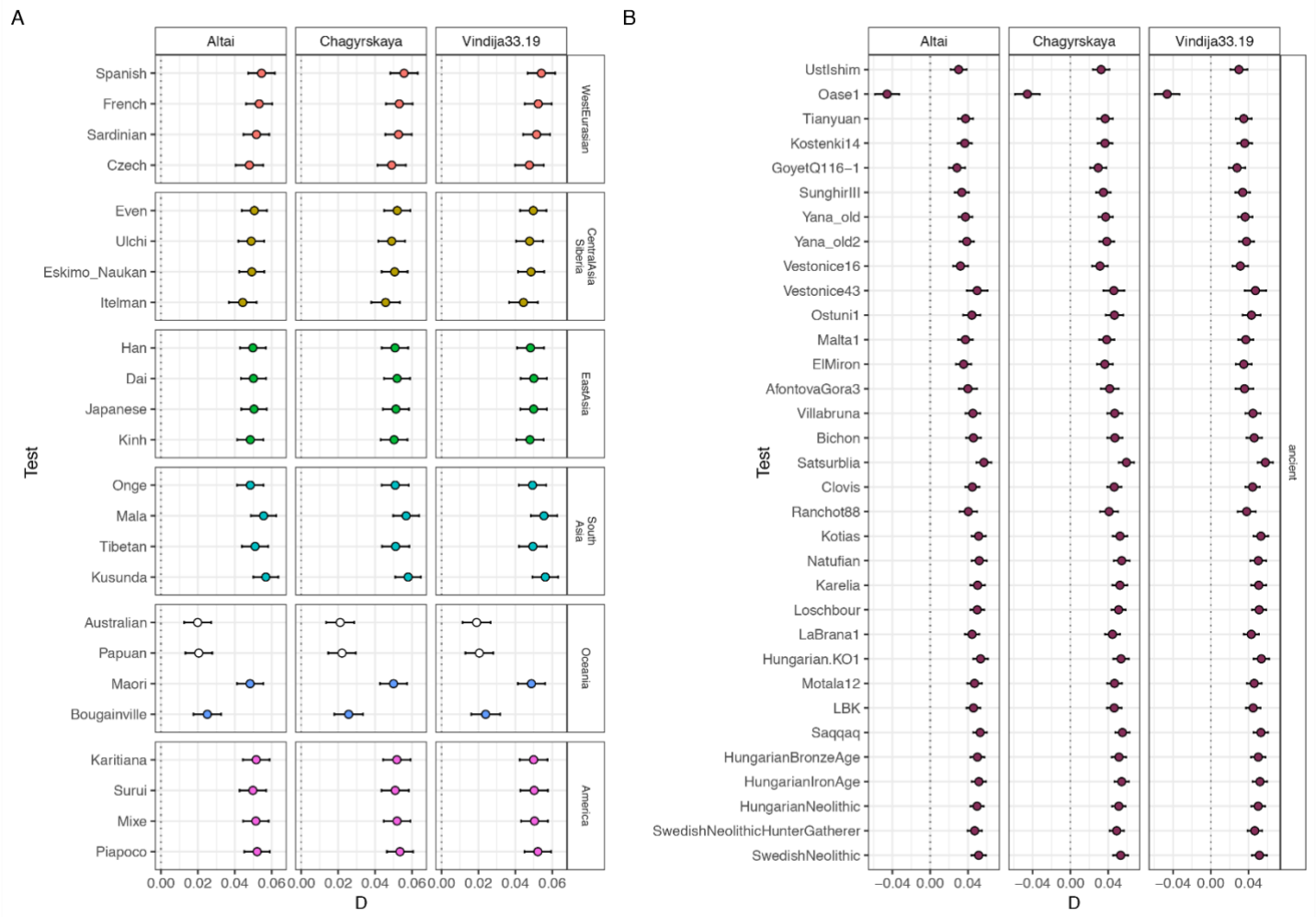

Figure S7.2 D-statistics comparing derived allele sharing with an archaic genome between IUP Bacho Kiro *BB7-240* and a range of present-day and ancient modern humans. Values for *D(Bacho Kiro BB7-240, Test; Archaic, Mbuti)* denoted as circles are plotted on the *x*-axes where *Archaic* is a high-coverage Neandertal genome[2,3,11] and *Test* is either a present-day population from SGDP[8] (panel A) or an ancient individual (panel B). Three Mbuti individuals from SGDP[8] were used as outgroup. *D* statistics were calculated using ADMIXTOOLS[5] as implemented in *admixr*[6]. Filled-in circles indicate a significant Z-score or $|Z| \geq 3$, and open circles indicate a non-significant Z-score or $|Z| < 3$. Whiskers on each side of the plotted *D* values correspond to standard errors calculated with a Weighted Block Jackknife[5,7] and a block size of 5 Mb across all autosomes on the "2200k" Panel (nsnps (*Bacho Kiro BB7-240*) = 787,706).

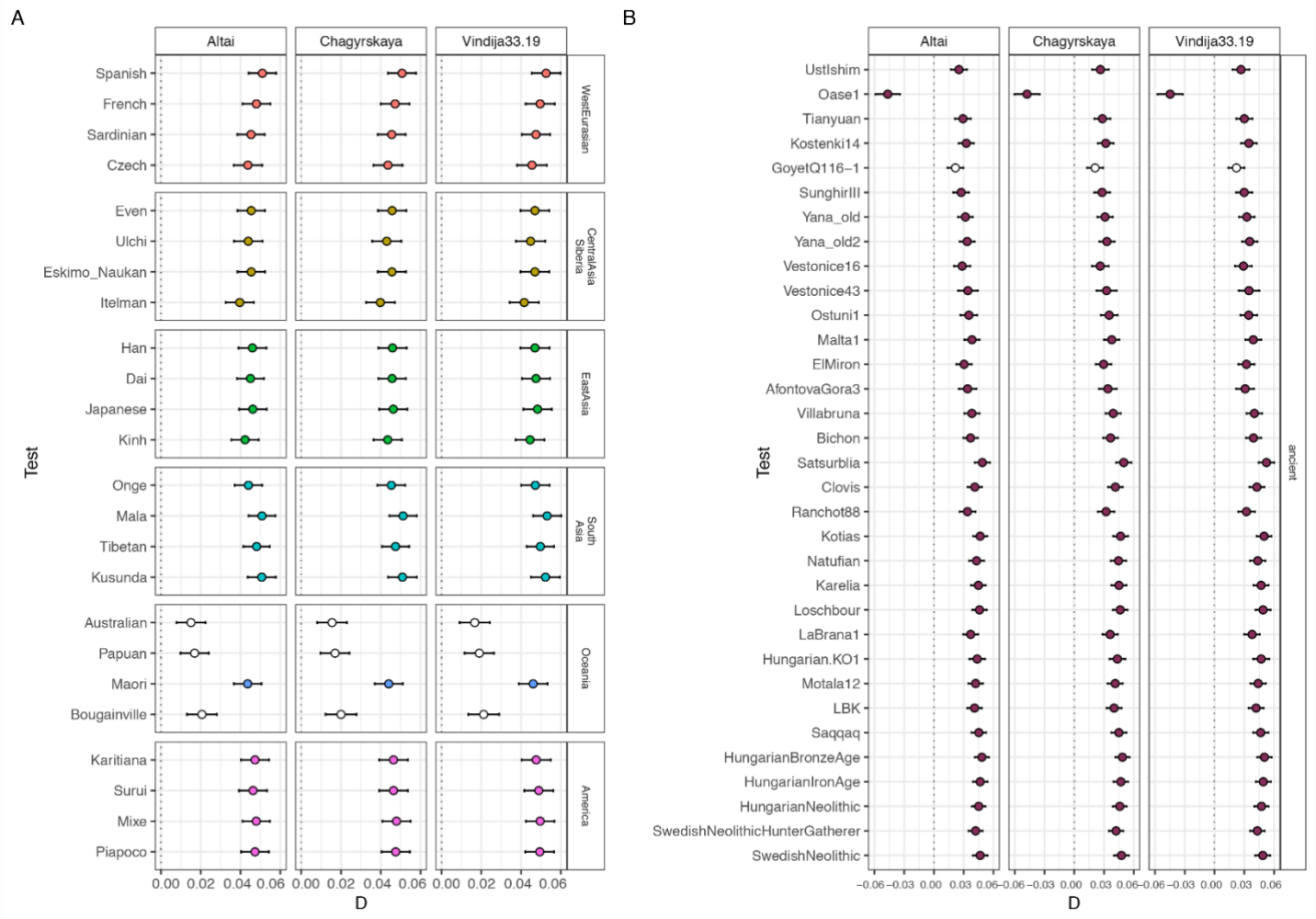

Figure S7.3 D-statistics comparing derived allele sharing with an archaic genome between IUP Bacho Kiro CC7-335 and a range of present-day and ancient modern humans. Values for *D(Bacho Kiro CC7-335, Test; Archaic, Mbuti)* denoted as circles are plotted on the *x*-axes where *Archaic* is a high-coverage Neandertal[2,3,11] genome and *Test* is either a present-day population from SGDP[8] (panel A) or an ancient individual (panel B). Three Mbuti individuals from SGDP[8] were used as outgroup. *D* statistics were calculated using ADMIXTOOLS[5] as implemented in *admixr*[6]. Filled-in circles indicate a significant Z-score or $|Z| \geq 3$, and open circles indicate a non-significant Z-score or $|Z| < 3$. Whiskers on each side of the plotted *D* values correspond to one standard error calculated using a Weighted Block Jackknife[5,7] and a block size of 5 Mb across all autosomes on the "2200k" Panel (nsnps (*Bacho Kiro CC7-335*) = 723,129).

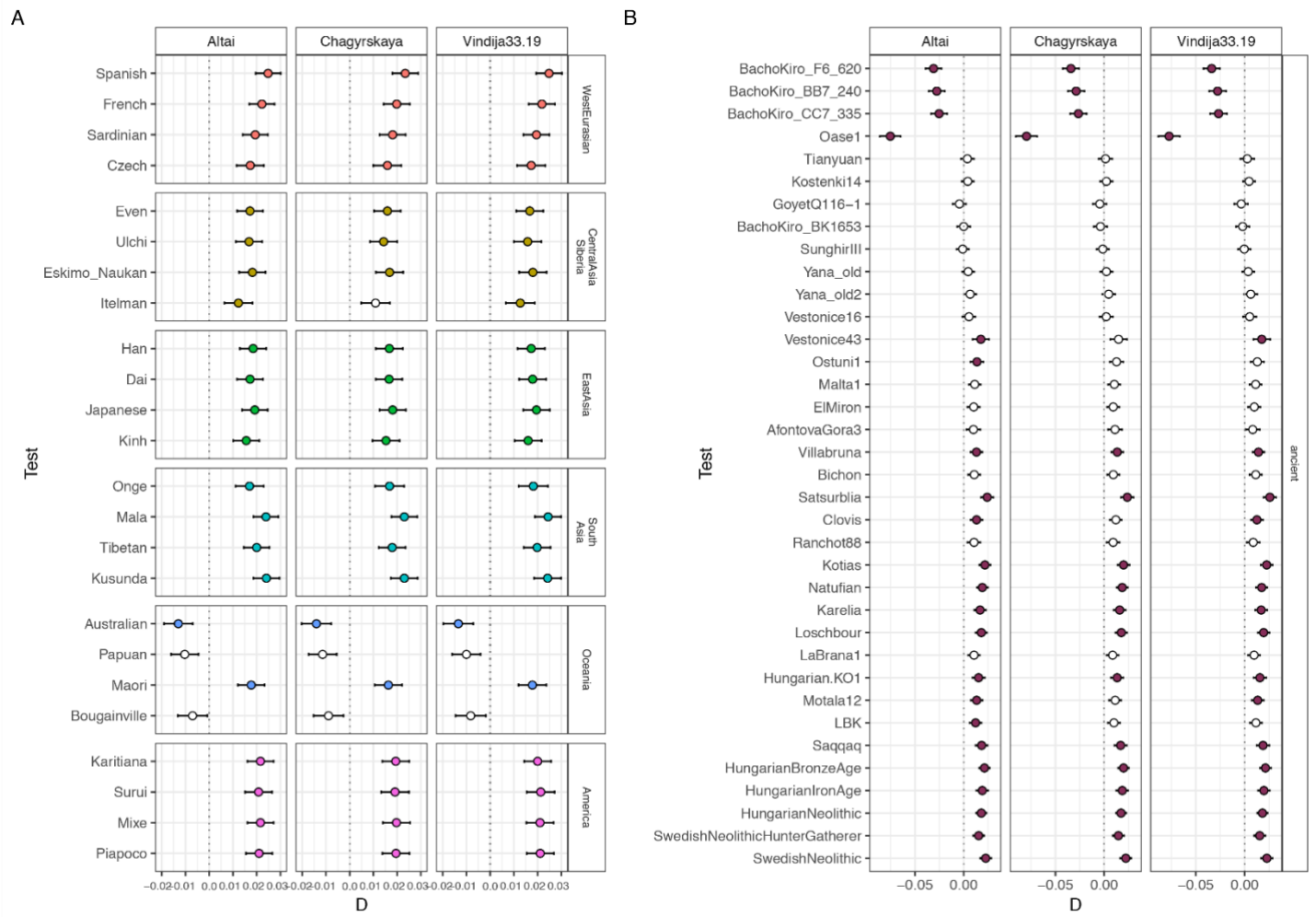

Figure S7.4 D-statistics comparing derived allele sharing with an archaic genome between ~45,000-year-old *Ust'Ishim* from Siberia and a range of present-day and ancient modern humans. Values for *D(Ust'Ishim, Test; Archaic, Mbuti)* denoted as circles are plotted on the *x*-axes where *Archaic* is a high-coverage Neandertal[2,3,11] genome and *Test* is either a present-day population from SGDP[8] (panel A) or an ancient individual (panel B). Three Mbuti individuals from SGDP[8] were used as outgroup. *D* statistics were calculated using ADMIXTOOLS[5] as implemented in *admixr*[6]. Filled-in circles indicate a significant Z-score or $|Z| \geq 3$, and open circles indicate a non-significant Z-score or $|Z| < 3$. Whiskers on each side of the plotted *D* values correspond to one standard error calculated using a Weighted Block Jackknife[5,7] and a block size of 5 Mb across all autosomes on the "2200k" Panel (nsnps (*Ust'Ishim*) = 1,951,462).

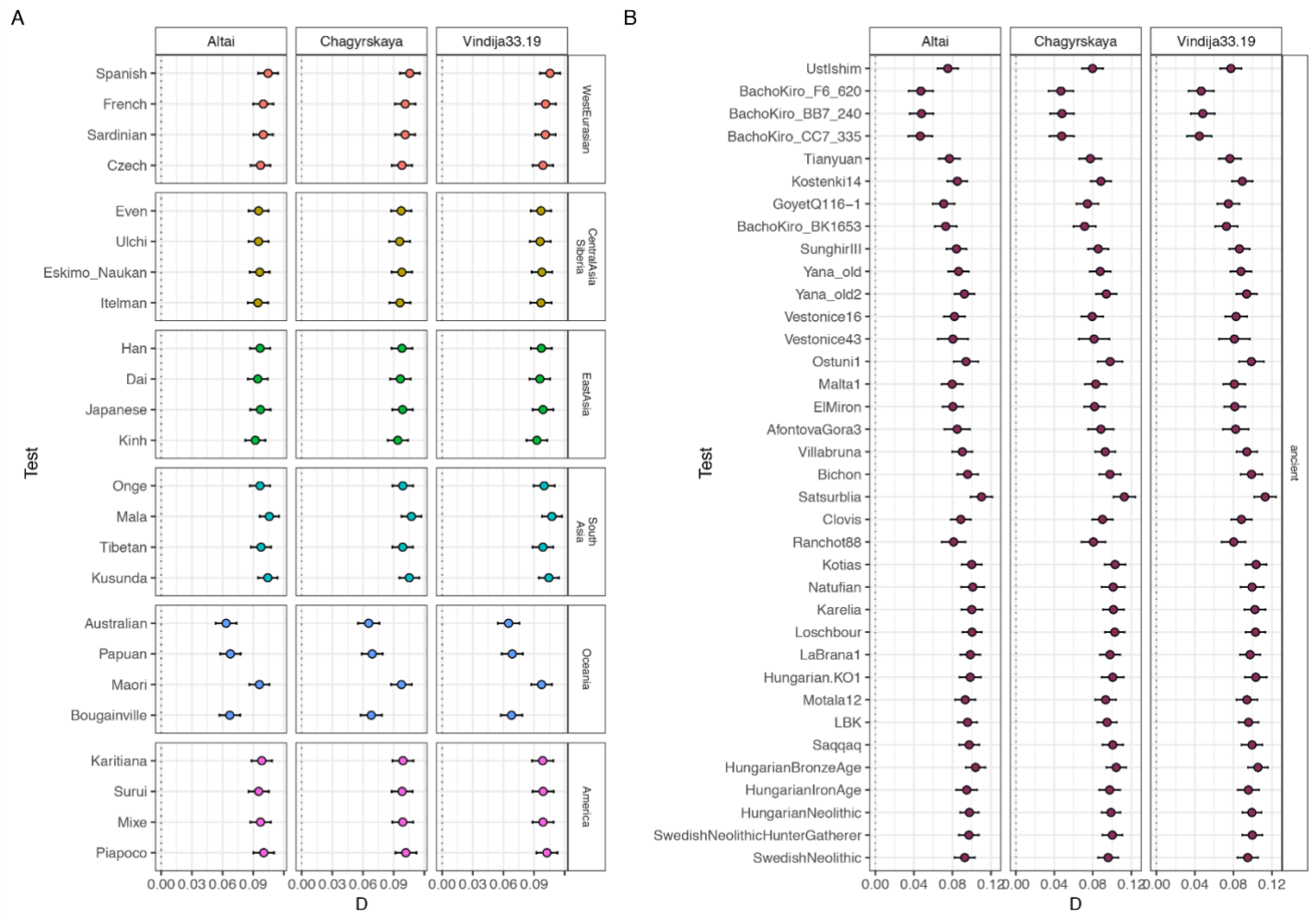

Figure S7.5 D-statistics comparing derived allele sharing with an archaic genome between *Oase1* and a range of present-day and ancient modern humans. Values for *D(Oase1, Test; Archaic, Mbuti)* denoted as circles are plotted on the *x*-axes where *Archaic* is a high-coverage Neandertal[2,3,11] genome and *Test* is either a present-day population from SGDP[8] (panel A) or an ancient individual (panel B). Three Mbuti individuals from SGDP[8] were used as outgroup. *D* statistics were calculated using ADMIXTOOLS[5] as implemented in *admixr*[6]. We used a merged dataset of *Oase1* from this and the previous study. Filled-in circles indicate a significant Z-score or $|Z| \geq 3$, and open circles indicate a non-significant Z-score or $|Z| < 3$. Whiskers on each side of the plotted *D* values correspond to one standard error calculated using a Weighted Block Jackknife[5,7] and a block size of 5 Mb across all autosomes on the "2200k" Panel (nsnps (*Oase 1*) = 402,526).

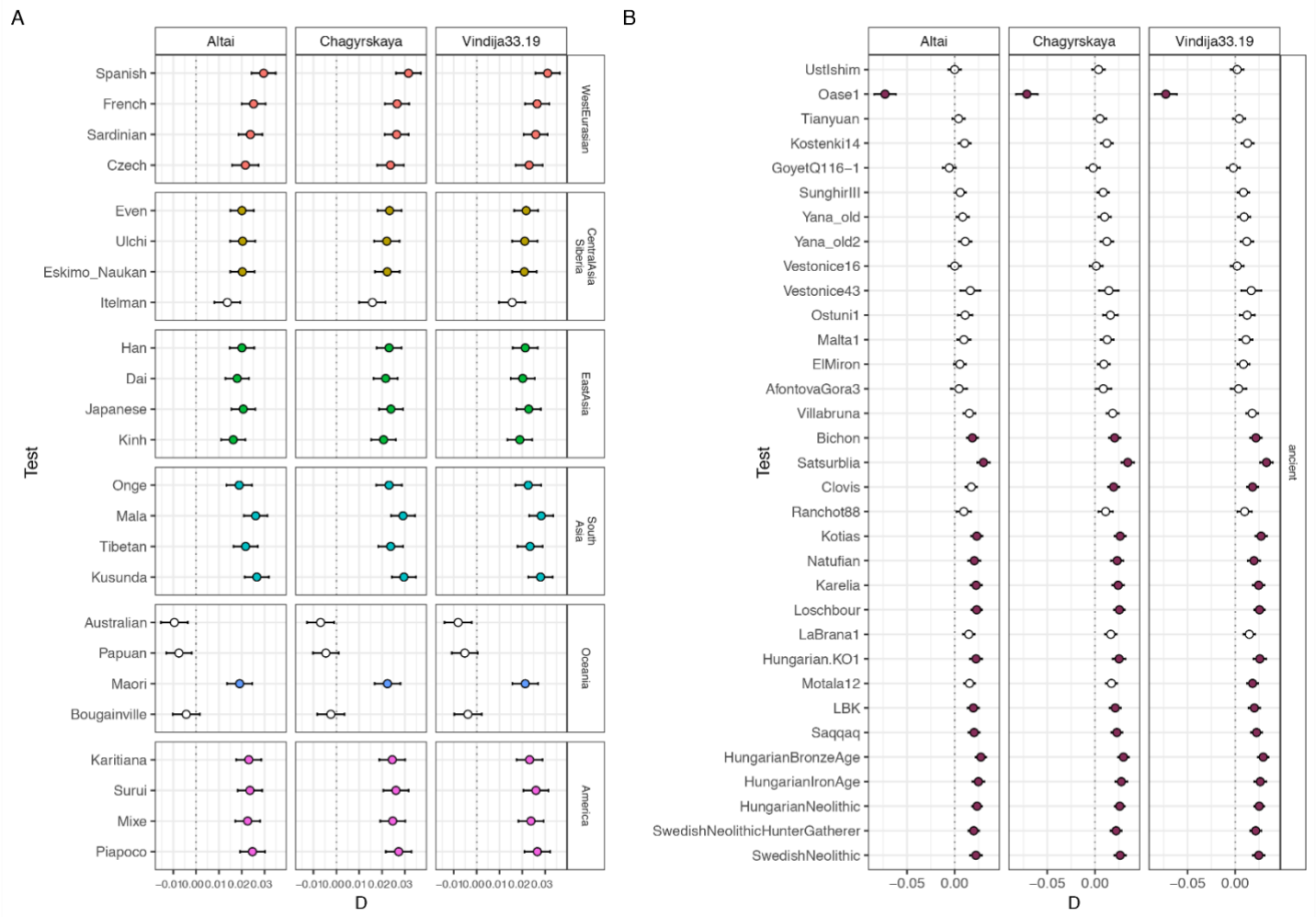

Figure S7.6 D-statistics comparing derived allele sharing with an archaic genome between Bacho Kiro BK1653 and a range of present-day and ancient modern humans. Values for *D(Bacho Kiro BK1653, Test; Archaic, Mbuti)* denoted as circles are plotted on the *x*-axes where *Archaic* is a high-coverage Neandertal[2,3,11] genome and *Test* is either a present-day population from SGDP[8] (panel A) or an ancient individual (panel B).Three Mbuti individuals from SGDP[8] were used as outgroup. *D* statistics were calculated using ADMIXTOOLS[5] as implemented in *admixr*[6]. Filled-in circles indicate a significant Z-score or $|Z| \geq 3$, and open circles indicate a non-significant Z-score or $|Z| < 3$. Whiskers on each side of the plotted *D* values correspond to one standard error calculated using a Weighted Block Jackknife[5,7] and a block size of 5 Mb across all autosomes on the "2200k" Panel (nsnps (*Bacho Kiro BK1653*) = 825,379).

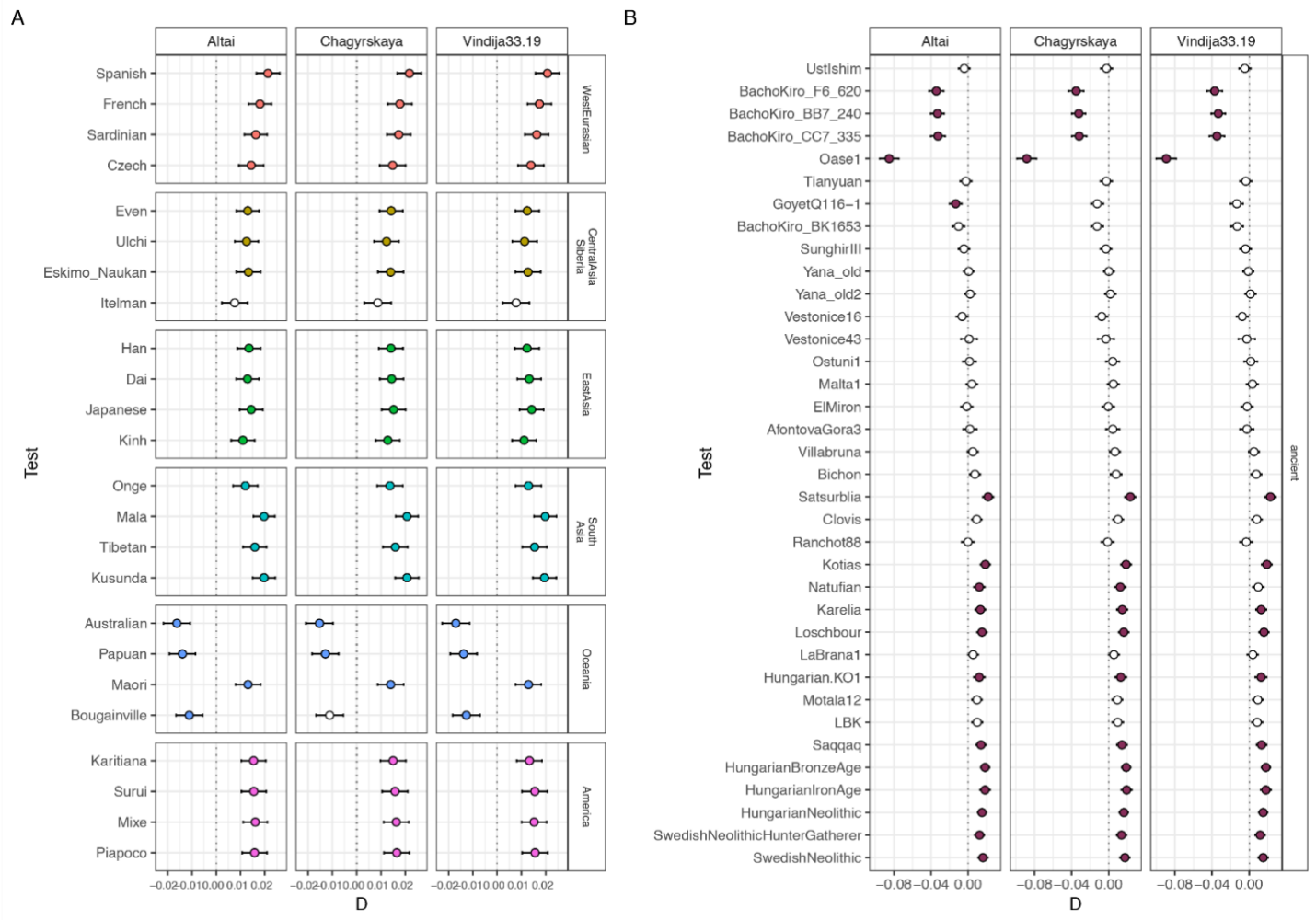

Figure S7.7 D-statistics comparing derived allele sharing with an archaic genome between ~38,000-year-old *Kostenki14*[19] from Russia and a range of present-day and ancient modern humans. Values for *D(Kostenki14, Test; Archaic, Mbuti)* denoted as circles are plotted on the *x*-axes where *Archaic* is a high-coverage Neandertal[2,3,11] genome and *Test* is either a present-day population from SGDP[8] (panel A) or an ancient individual (panel B). Three Mbuti individuals from SGDP[8] were used as outgroup. *D* statistics were calculated using ADMIXTOOLS[5] as implemented in *admixr*[6]. Filled-in circles indicate a significant Z-score or $|Z| \geq 3$, and open circles indicate a non-significant Z-score or $|Z| < 3$. Whiskers on each side of the plotted *D* values correspond to one standard error calculated using a Weighted Block Jackknife[5,7] and a block size of 5 Mb across all autosomes on the "2200k" Panel (nsnps (*Kostenki 14*) = 1,676,430).

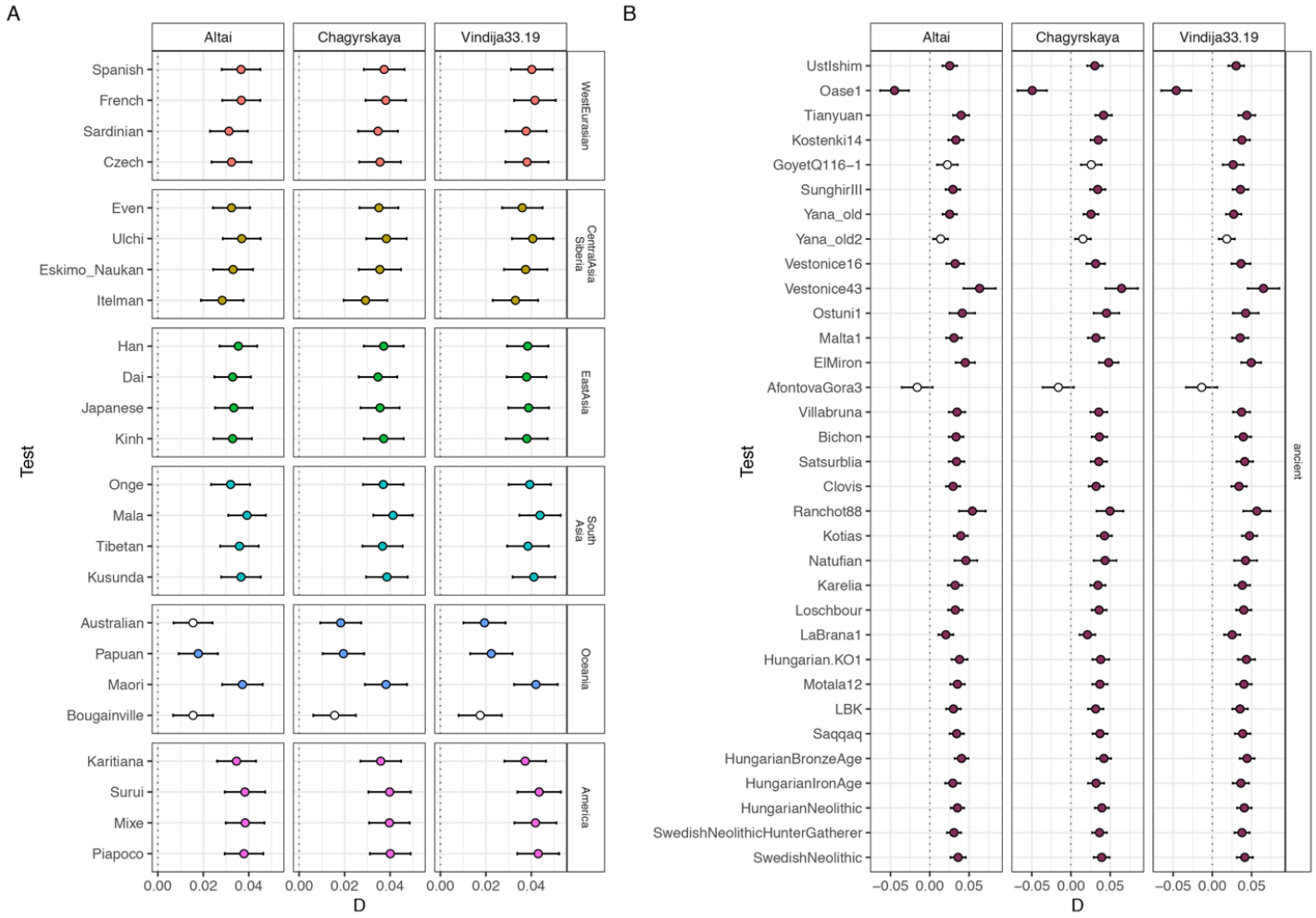

Figure S7.8 D-statistics comparing derived allele sharing with an archaic genome between IUP Bacho Kiro F6-620 and a range of present-day and ancient modern humans. Values for *D(Bacho Kiro F6-620, Test; Archaic, Chimpanzee)* denoted as circles are plotted on the *x*-axes where *Archaic* is a high-coverage Neandertal[2,3,11] genome and *Test* is either a present-day population from SGDP[8] (panel A) or an ancient individual (panel B). These analyses are restricted to transversion polymorphisms to mitigate the effect of ancient DNA damage. The genome of *panTro2* was used as an outgroup. *D* statistics were calculated using ADMIXTOOLS[5] as implemented in *admixr*[6]. Filled-in circles indicate a significant Z-score or $|Z| \geq 3$, and open circles indicate a non-significant Z-score or $|Z| < 3$. Whiskers on each side of the plotted *D* values correspond to one standard error calculated using a Weighted Block Jackknife[5,7] and a block size of 5 Mb across all autosomes on the "2200k" Panel (nsnps (*Bacho Kiro F6-620*) = 922,946).

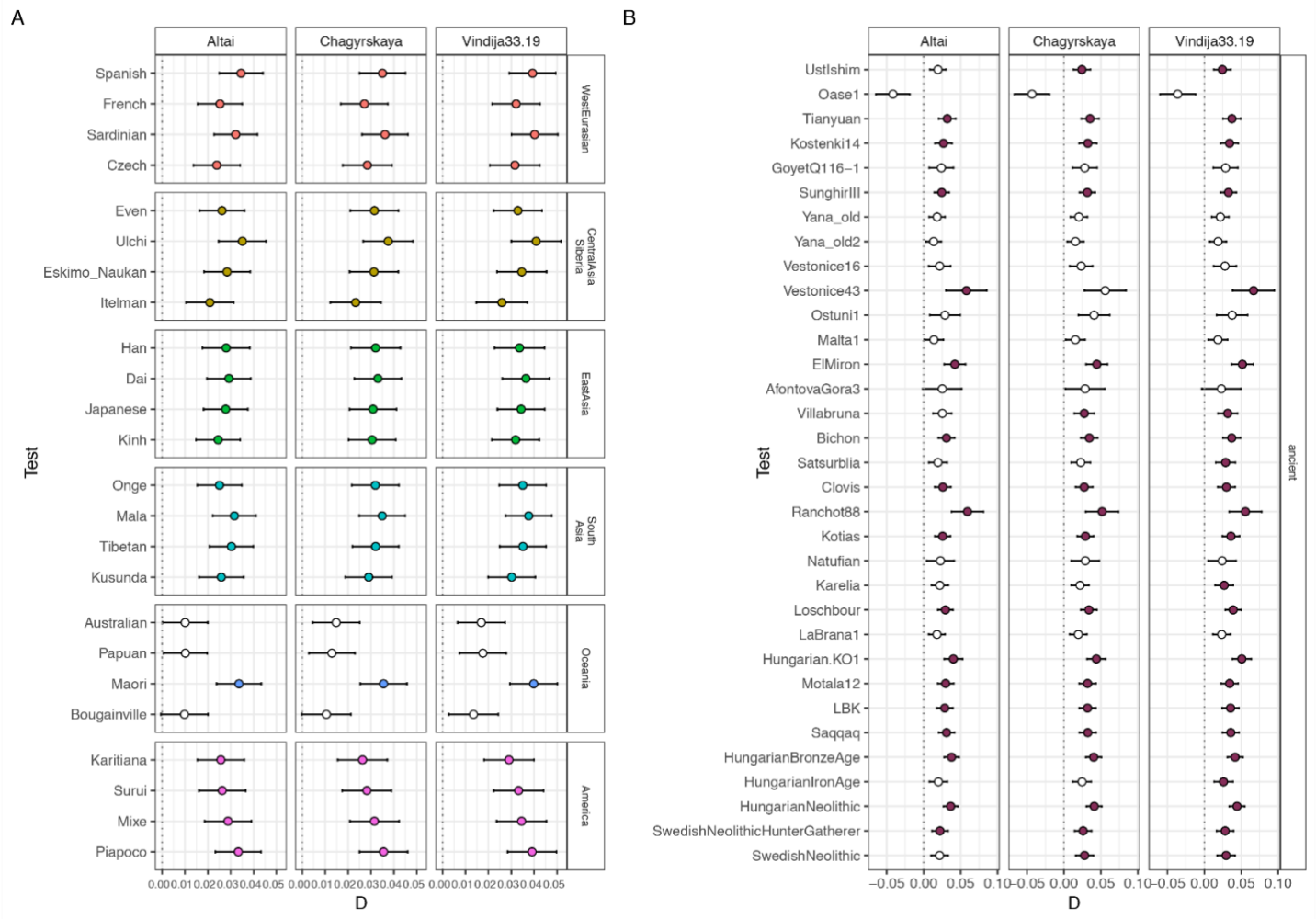

Figure S7.9 D-statistics comparing derived allele sharing with an archaic genome between IUP Bacho Kiro CC7-335 and a range of present-day and ancient modern humans. Values for *D(Bacho Kiro CC7-335, Test; Archaic, Chimpanzee)* denoted as circles are plotted on the *x*-axes where *Archaic* is a high-coverage Neandertal[2,3,11] genome and *Test* is either a present-day population from SGDP[8] (panel A) or an ancient individual (panel B). These analyses are restricted to transversion polymorphisms to mitigate the effect of ancient DNA damage. The genome of *panTro2* was used as an outgroup. *D* statistics were calculated using ADMIXTOOLS[5] as implemented in *admixr*[6]. Filled-in circles indicate a significant Z-score or $|Z| \geq 3$, and open circles indicate a non-significant Z-score or $|Z| < 3$. Whiskers on each side of the plotted *D* values correspond to one standard error calculated using a Weighted Block Jackknife[5,7] and a block size of 5 Mb across all autosomes on the "2200k" Panel (nsnps (*Bacho Kiro CC7-335*) = 340,010).

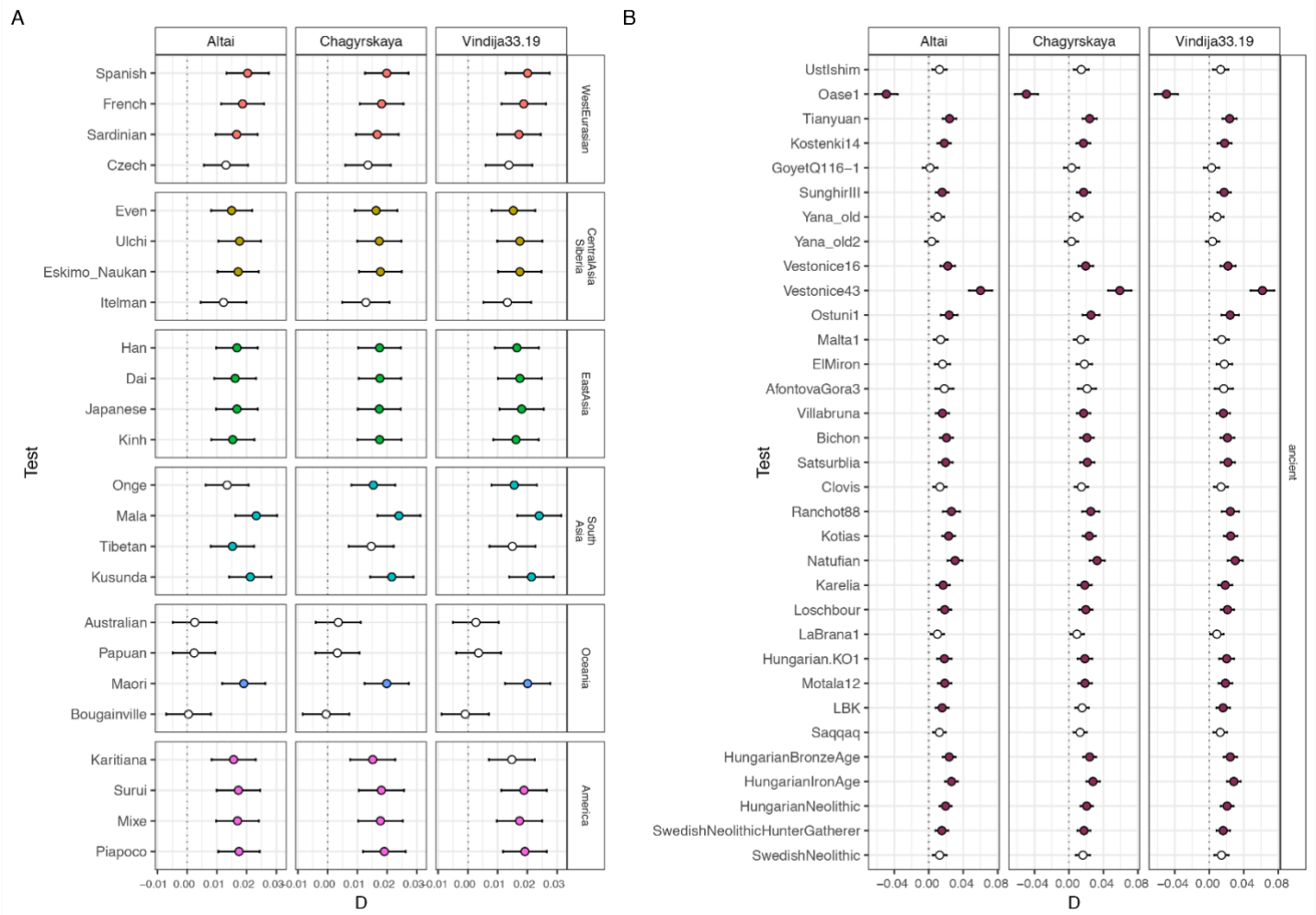

Figure S7.10 D-statistics comparing derived allele sharing with an archaic genome between IUP Bacho Kiro BB7-240 and a range of present-day and ancient modern humans. Values for *D(Bacho Kiro BB7-240, Test; Archaic, Chimpanzee)* denoted as circles are plotted on the *x*-axes where *Archaic* is a high-coverage Neandertal[2,3,11] genome and *Test* is either a present-day population from SGDP[8] (panel A) or an ancient individual (panel B). These analyses are restricted to transversion polymorphisms to mitigate the effect of ancient DNA damage. The genome of *panTro2* was used as an outgroup. *D* statistics were calculated using ADMIXTOOLS[5] as implemented in *admixr*[6]. Filled-in circles indicate a significant Z-score or $|Z| \geq 3$, and open circles indicate a non-significant Z-score or $|Z| < 3$. Whiskers on each side of the plotted *D* values correspond to one standard error calculated using a Weighted Block Jackknife[5,7] and a block size of 5 Mb across all autosomes on the "2200k" Panel (nsnps (*Bacho Kiro BB7-240*) = 362,545).

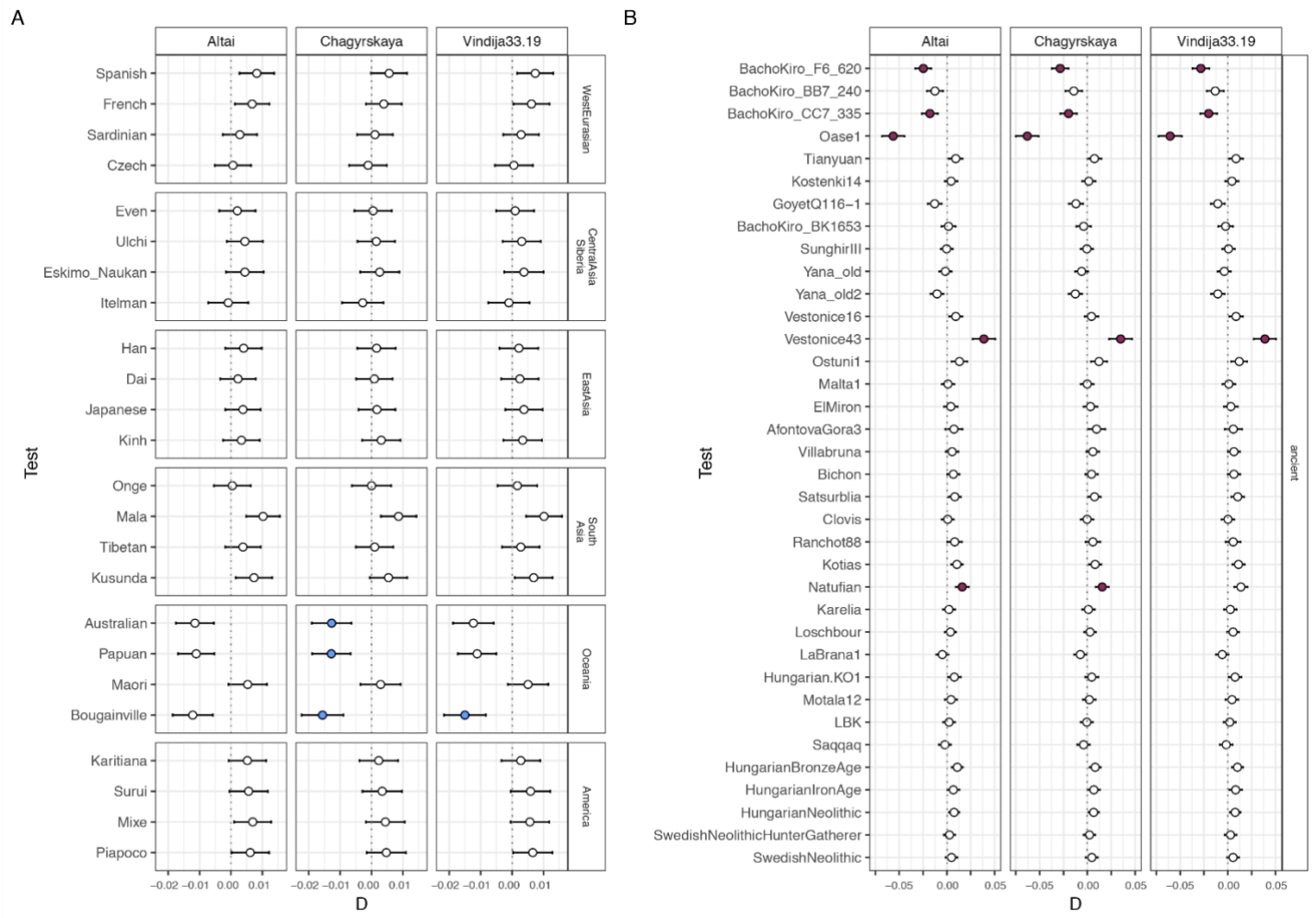

Figure S7.11 D-statistics comparing derived allele sharing with an archaic genome between ~45,000-year-old *Ust'Ishim* from Siberia and a range of present-day and ancient modern humans. Values for *D(Ust'Ishim, Test; Archaic, Chimpanzee)* denoted as circles are plotted on the *x*-axes where *Archaic* is a high-coverage Neandertal[2,3,11] genome and *Test* is either a present-day population from SGDP[8] (panel A) or an ancient individual (panel B). These analyses are restricted to transversion polymorphisms to mitigate the effect of ancient DNA damage. The genome of *panTro2* was used as an outgroup. *D* statistics were calculated using ADMIXTOOLS[5] as implemented in *admixr*[6]. Filled-in circles indicate a significant Z-score or $|Z| \geq 3$, and open circles indicate a non-significant Z-score or $|Z| < 3$. Whiskers on each side of the plotted *D* values correspond to one standard error calculated using a Weighted Block Jackknife[5,7] and a block size of 5 Mb across all autosomes on the "2200k" Panel (nsnps (*Ust'Ishim*) = 1,095,471).

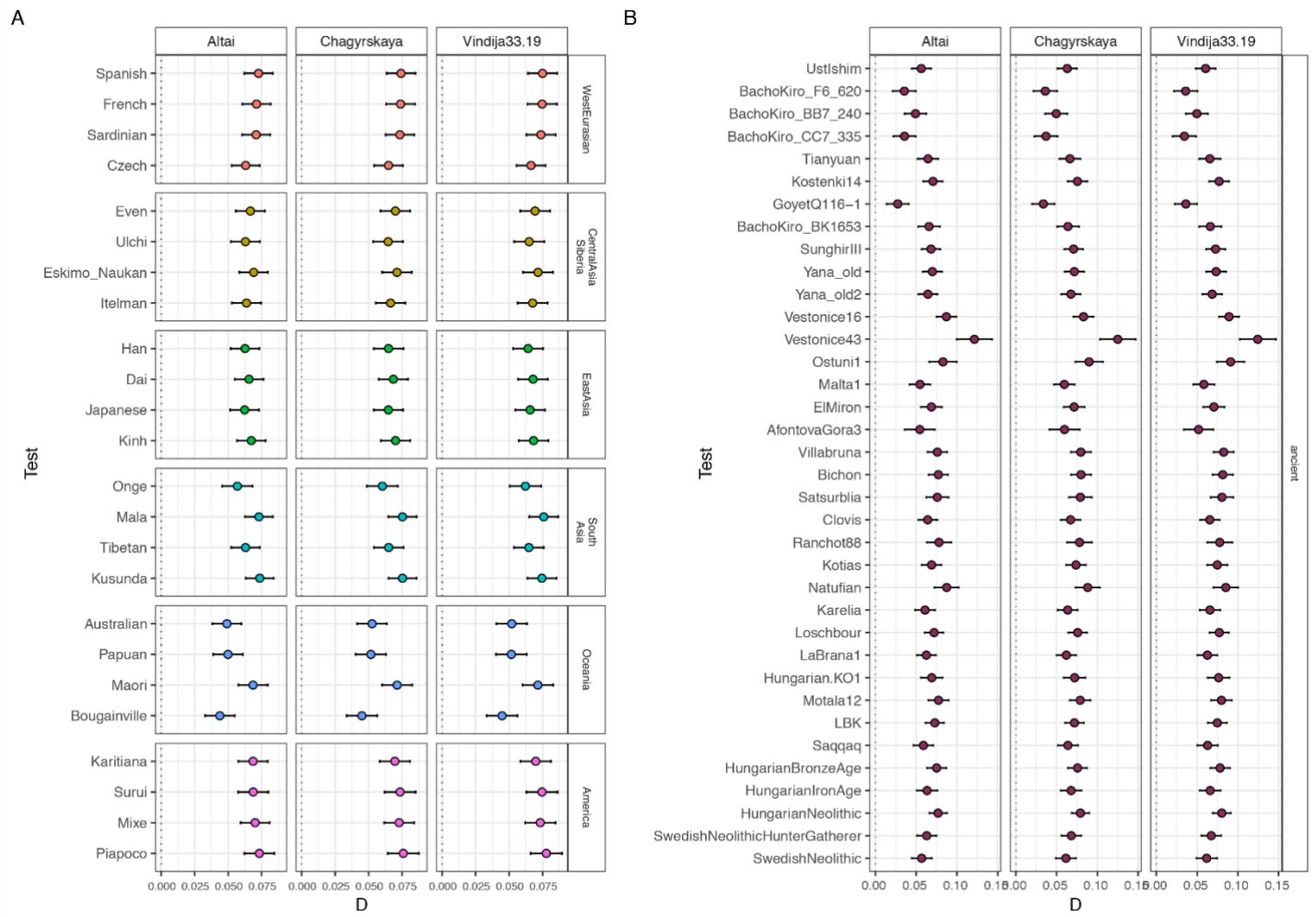

Figure S7.12 D-statistics comparing derived allele sharing with an archaic genome between *Oase1* and a range of present-day and ancient modern humans. Values for *D(Oase1, Test; Archaic, Chimpanzee)* denoted as circles are plotted on the *x*-axes where *Archaic* is a high-coverage Neandertal[2,3,11] genome and *Test* is either a present-day population from SGDP[8] (panel A) or an ancient individual (panel B). These analyses are restricted to transversion polymorphisms to mitigate the effect of ancient DNA damage. The genome of *panTro2* was used as an outgroup. *D* statistics were calculated using ADMIXTOOLS[5] as implemented in *admixr*[6]. Filled-in circles indicate a significant Z-score or $|Z| \geq 3$, and open circles indicate a non-significant Z-score or $|Z| < 3$. Whiskers on each side of the plotted *D* values correspond to one standard error calculated using a Weighted Block Jackknife[5,7] and a block size of 5 Mb across all autosomes on the "2200k" Panel (nsnps (*Oase 1*) = 180,040).

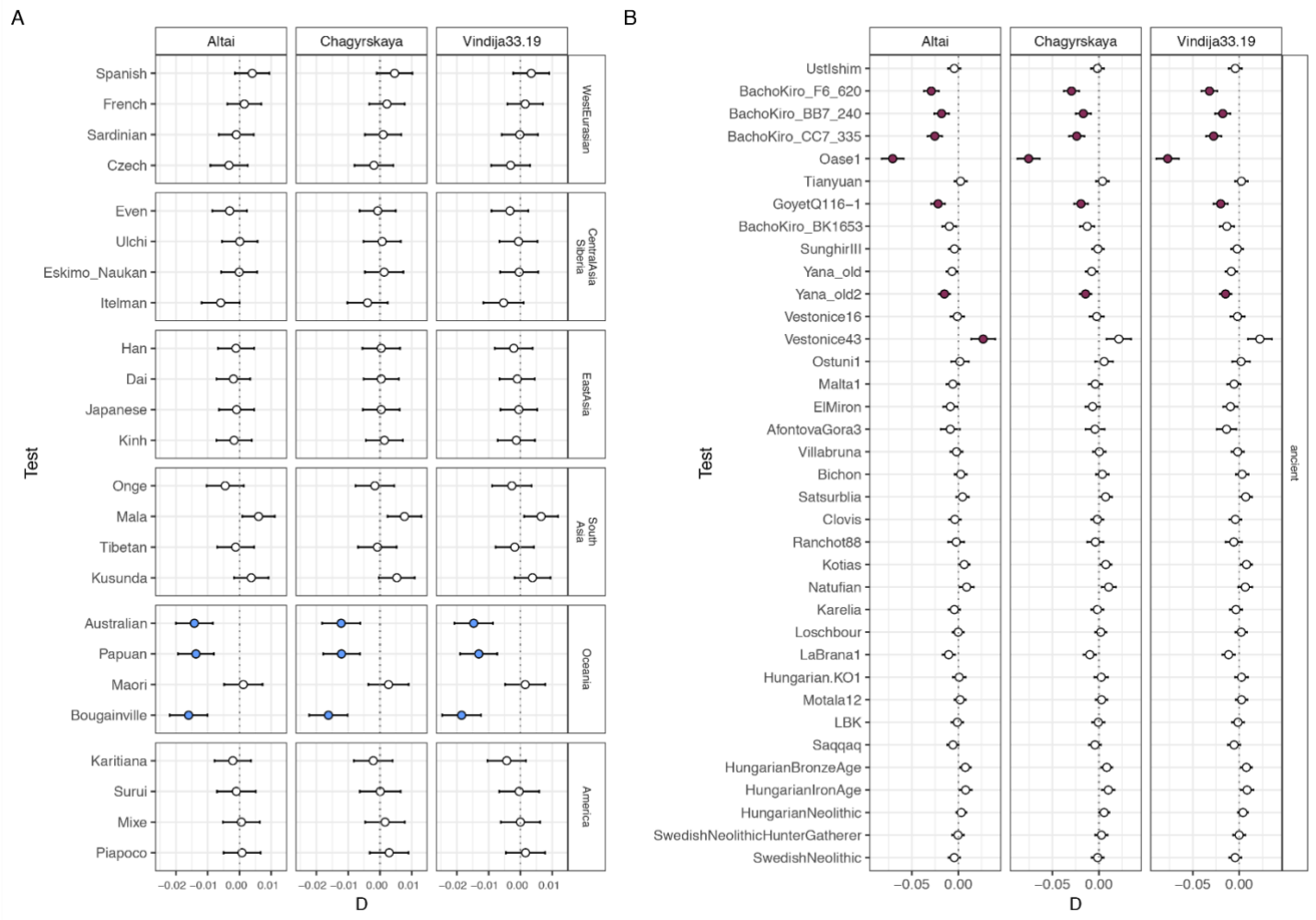

Figure S7.13 D-statistics comparing derived allele sharing with an archaic genome between ~38,000-year-old *Kostenki14*[19] from Russia and a range of present-day and ancient modern humans. Values for *D(Kostenki14, Test; Archaic, Chimpanzee)* denoted as circles are plotted on the *x*-axes where *Archaic* is a high-coverage Neandertal[2,3,11] genome and *Test* is either a present-day population from SGDP[8] (panel A) or an ancient individual (panel B). These analyses are restricted to transversion polymorphisms to mitigate the effect of ancient DNA damage. The genome of *panTro2* was used as an outgroup. *D* statistics were calculated using ADMIXTOOLS[5] as implemented in *admixr*[6]. Filled-in circles indicate a significant Z-score or $|Z| \geq 3$, and open circles indicate a non-significant Z-score or $|Z| < 3$. Whiskers on each side of the plotted *D* values correspond to one standard error calculated using a Weighted Block Jackknife[5,7] and a block size of 5 Mb across all autosomes on the "2200k" Panel (nsnps (*Kostenki 14*) = 814,133).

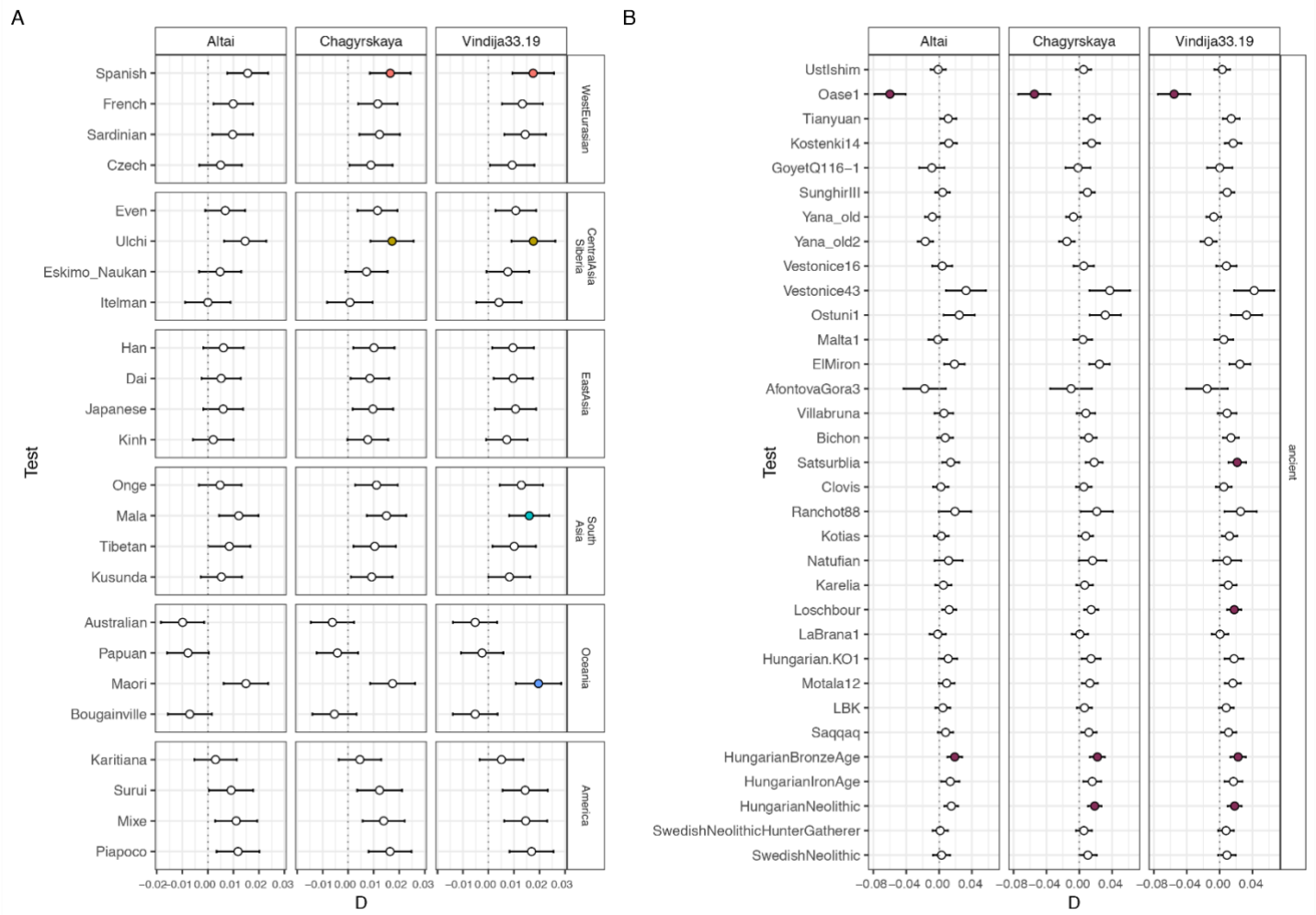

Figure S7.14 D-statistics comparing derived allele sharing with an archaic genome between Bacho Kiro BK1653 and a range of present-day and ancient modern humans. Values for *D(Bacho Kiro BK1653, Test; Archaic, Chimpanzee)* denoted as circles are plotted on the *x*-axes where *Archaic* is a high-coverage Neandertal[2,3,11] genome and *Test* is either a present-day population from SGDP[8] (panel A) or an ancient individual (panel B). These analyses are restricted to transversion polymorphisms to mitigate the effect of ancient DNA damage. The genome of *panTro2* was used as an outgroup. *D* statistics were calculated using ADMIXTOOLS[5] as implemented in *admixr*[6]. Filled-in circles indicate a significant Z-score or $|Z| \geq 3$, and open circles indicate a non-significant Z-score or $|Z| < 3$. Whiskers on each side of the plotted *D* values correspond to one standard error calculated using a Weighted Block Jackknife[5,7] and a block size of 5 Mb across all autosomes on the "2200k" Panel (nsnps (*Bacho Kiro BK1653*) = 382,191).

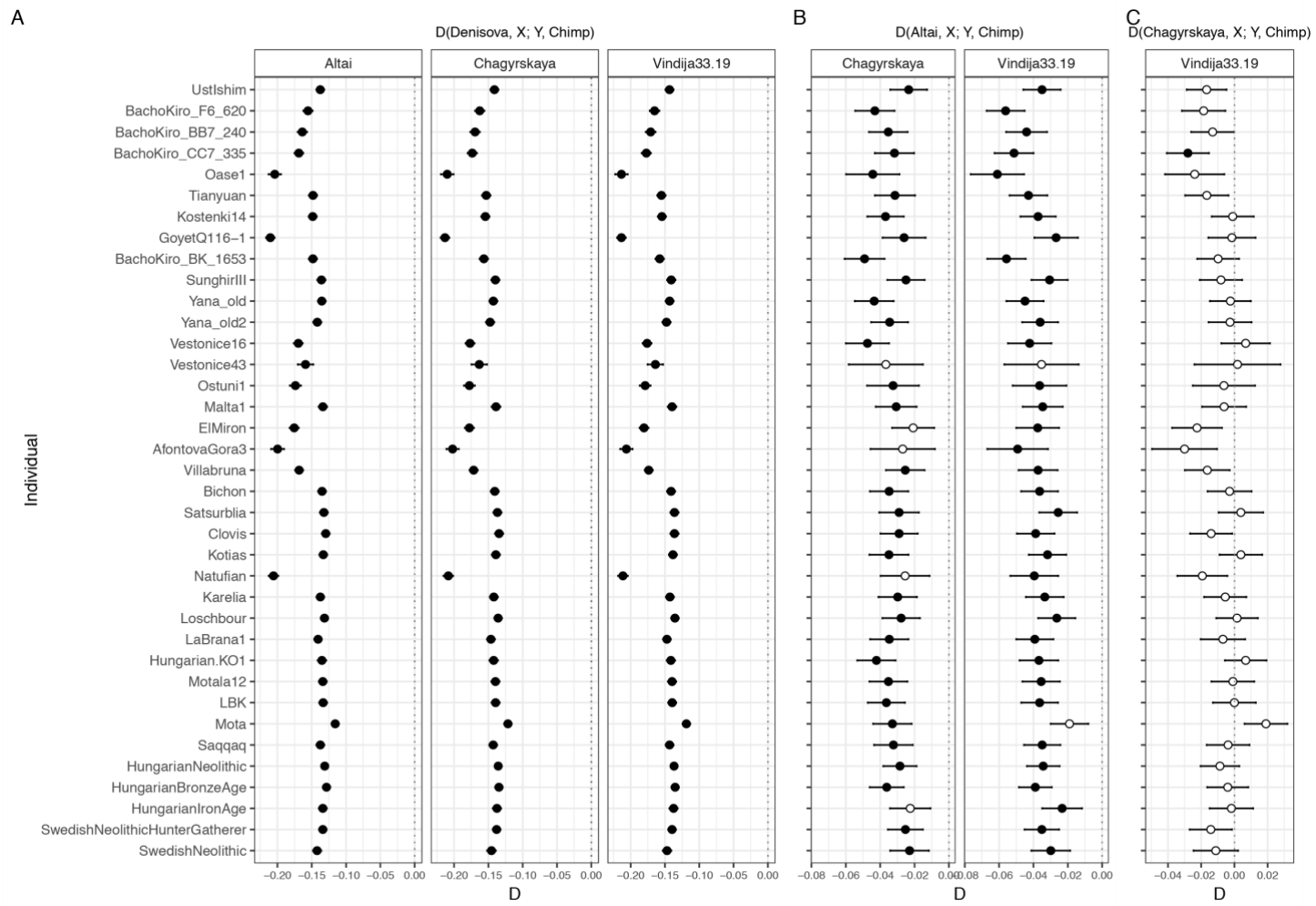

Figure S7.15 Proximity to the introgressing archaic population in ancient humans calculated as *D(Archaic$_1$, Archaic$_2$; ancient human, Chimp).* A) All ancient modern humans are significantly closer to Neandertals[2,3,11] than to *Denisova3*, *D(Denisova3, Neandertal; ancient human, Chimp)*, B) introgressing Neandertals are significantly closer to *Chagyrskaya 8* and *Vindija 33.19* than to the *Altai* Neandertal in most ancient modern humans, *D(Altai Neandertal, Neandertal$_2$; ancient human, Chimp)*, C) no significant difference in the introgressing Neandertal proximity to *Chagyrskaya 8* and *Vindija 33.19*, *D(Chagyrskaya 8, Vindija 33.19; ancient human, Chimp). D* values denoted as circles plotted on the *x*-axes were calculated using ADMIXTOOLS[5] as implemented in *admixr*[6]. The genome of *panTro2* was used as an outgroup. Filled-in circles indicate a significant Z-score or $|Z| \geq 3$, and open circles indicate a non-significant Z-score or $|Z| < 3$. Whiskers on each side of the plotted *D* values correspond to one standard error calculated using a Weighted Block Jackknife[5,7] and a block size of 5 Mb across all autosomes on the "2200k" Panel (nsnps = 2,056,573).

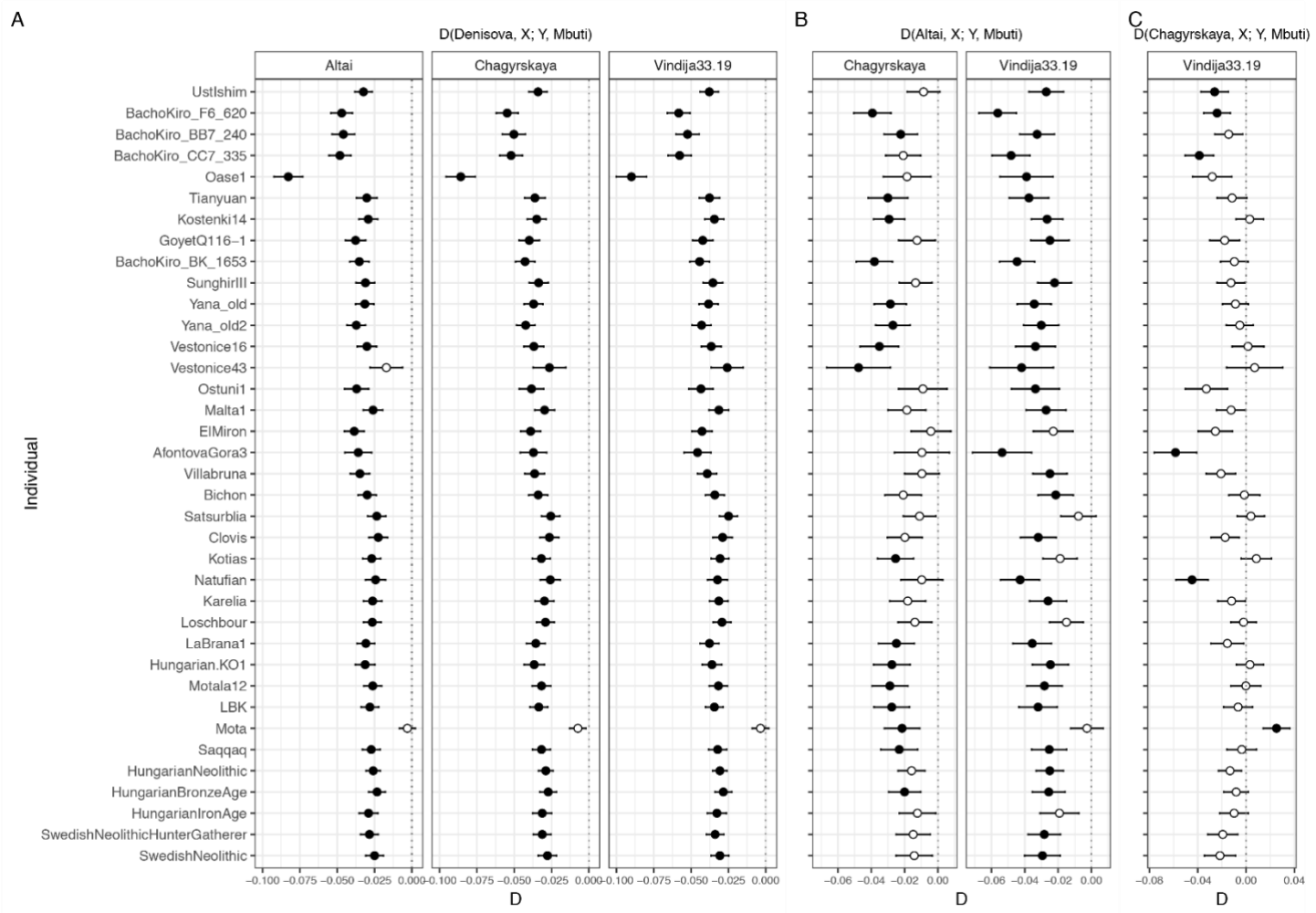

Figure S7.16 Proximity to the introgressing archaic population in ancient humans calculated as *D(Archaic$_1$, Archaic$_2$; ancient human, Mbuti).* A) All ancient modern humans are significantly closer to Neandertals than to *Denisova3*[18], *D(Denisova3, Neandertal; ancient human, Mbuti)*, B) introgressing Neandertals are significantly closer to *Chagyrskaya 8*[11] and *Vindija 33.19*[3] than to the *Altai* Neandertal[2] in most ancient modern humans, *D(Altai Neandertal, Neandertal$_2$; ancient human, Mbuti)*, C) no significant difference in the introgressing Neandertal proximity to *Chagyrskaya 8*[11] and *Vindija 33.19*[3] for most ancient modern humans, *D(Chagyrskaya 8, Vindija 33.19; ancient human, Mbuti). D* values denoted as circles plotted on the *x*-axes were calculated using ADMIXTOOLS[5] as implemented in *admixr*[6]. Genomes of three Mbuti individuals from SGDP[8] are used as an outgroup. Filled-in circles indicate a significant Z-score or $|Z| \geq 3$, and open circles indicate a non-significant Z-score or $|Z| < 3$. Whiskers on each side of the plotted *D* values correspond to one standard error calculated using a Weighted Block Jackknife[5,7] and a block size of 5 Mb across all autosomes on the "2200k" Panel (nsnps = 2,056,573).

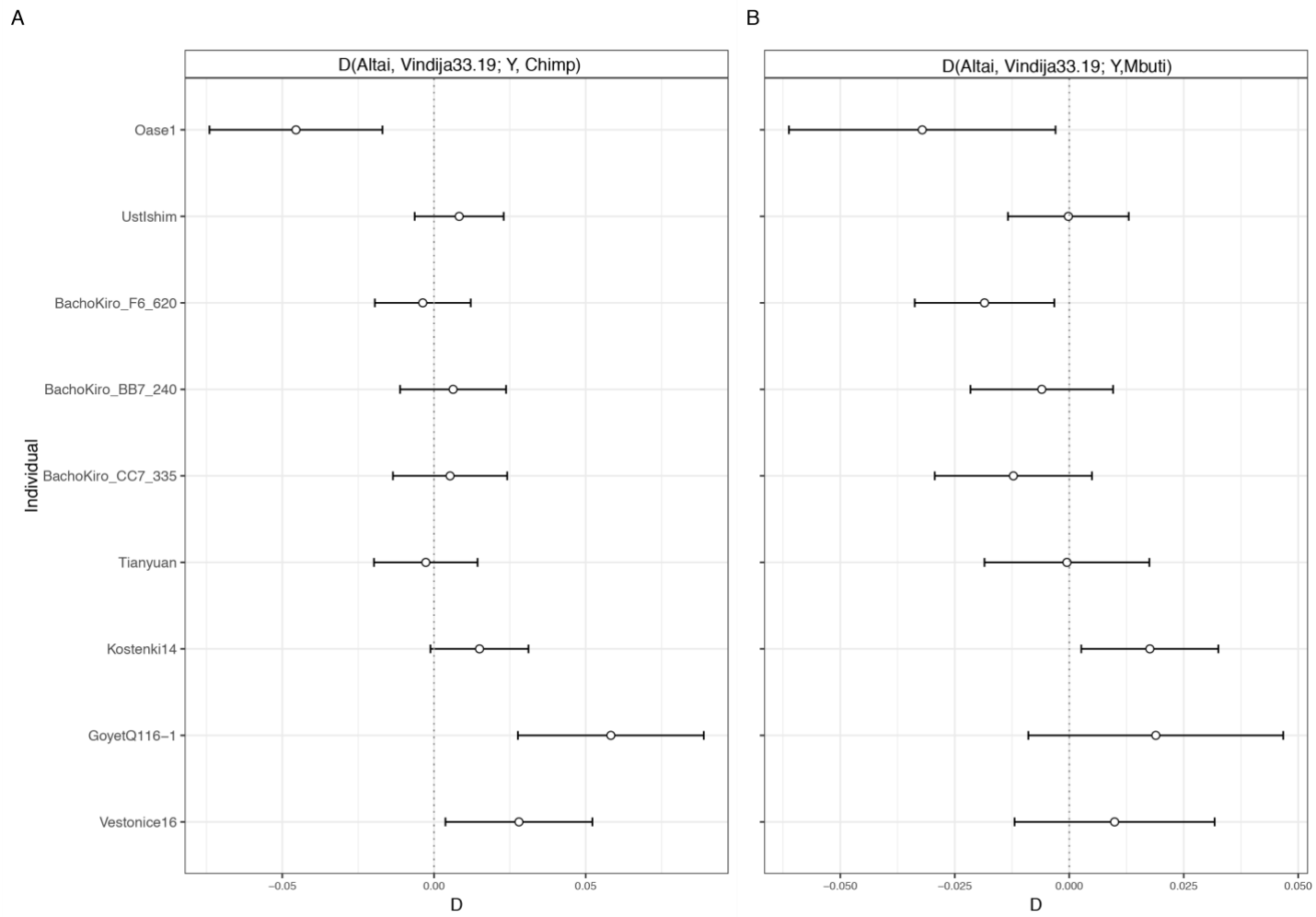

Figure S7.17 The effect of down-sampling high-coverage genomes of the *Altai* Neandertal[2] and *Vindija 33.19*[3] on *D(Altai Neandertal, Vindija 33.19; ancient human, Outgroup)*. Down-sampling high-coverage Neandertal genomes to the same coverage as in late Neandertals[17] (number of SNPs reported in the Tab. S7.1) on "2200k" Panel and restricting the analyses to transversion polymorphisms causes the statistics that are otherwise significant (see Fig. S7.15 and S7.16) to become not significantly different from 0. *D* values denoted as circles plotted on the *x*-axes were calculated using ADMIXTOOLS[5] as implemented in *admixr*[6]. Genomes of *panTro2* (panel A) and three Mbuti individuals from SGDP[8] (panel B) are used as outgroups. Open circles indicate a non-significant Z-score or $|Z| < 3$. Whiskers on each side of the plotted *D* values correspond to one standard error computed with a Weighted Block Jackknife[5,7] and a block size of 5 Mb across all autosomes on the "2200k" Panel.

Supplementary Information 8

Neandertal introgressed segments in Bacho Kiro individuals and dating of Neandertal admixture

Distribution of Neandertal introgressed tracks in the genomes of Bacho Kiro and other ancient modern humans

We used *admixfrog*[1] (version 0.5.6, https://github.com/BenjaminPeter/admixfrog/) for detecting archaic introgressed segments in the genomes of Bacho Kiro Cave individuals, as well as in 32 ancient modern humans[2-12] and 254 present-day non-Africans from the Simons Genome Diversity Project (SGDP)[13] as a direct comparison. *Admixfrog* allows the reliable detection of introgressed segments in low-coverage ancient genomes even in the presence of substantial levels of present-day human DNA contamination[1]. In short, *admixfrog* models each individual (*Target*) as a mixture of at least two different *Sources*. As potential *Sources* we used three high-coverage Neandertal genomes[14-16] (abbreviated as NEA), the high-coverage *Denisova 3* genome[17] (abbreviated as DEN) and 44 genomes of present-day Sub-Saharan Africans from SGDP[13] (abbreviated as AFR). We used the genome of a chimpanzee (*panTro4*, abbreviated as PAN) to infer the ancestral state at each position in the "Archaic admixture" panel.

We used BAM files of 21 ancient modern humans[2-4], including six Bacho Kiro Cave specimens and *Oase 1*, that were enriched for ~1.7 million SNPs informative of Neandertal and Denisovan ancestry ("Archaic admixture"[3] panel, Supplementary Information 3). All BAM files were filtered as described in Supplementary Information 2. Briefly, all files were aligned to the human reference genome containing the decoy sequences (GRCh37/1000 Genomes release) and we used *samtools*[18] to filter for fragments equal or longer than 35 base pairs (bp) that had a mapping quality of 25 or greater (MQ≥25). We also used 16 ancient modern humans from different points in time and different geographical regions for which whole-genome shotgun data are available[5-12] as a comparison. Their respective BAM files were intersected with ~1.7 million SNPs of the "Archaic admixture" panel using *BEDTools*[19] (version: 2.24.0) after alignment to the GRCh37 and filtering for fragments of at least 35 bp with a mapping quality of at least 25. For *GoyetQ116-1*, we did not have "Archaic admixture" panel data and we therefore used "2200k" SNP Panel for inferring Neandertal introgressed segments in this individual.

For each ancient modern human (*Target*) we generated input files directly from the respective BAM files using the following command:

```
admixfrog-bam --bamfile {individual}.bam --out {individual}.in.xz --ref {ref_archaicadmixture.csv.xz}
```

To further identify archaic introgressed segments in a genome of a given *Target*, we run:

```
admixfrog --infile {individual}.in.xz --ref {ref_archaicadmixture.csv.xz} --out {out_individual} --states AFR NEA DEN --cont-id AFR --ll-tol 0.01 --bin-size 5000 --est-F --est-tau --freq-F 3 --freq-contamination 3 --e0 0.01 --ancestral PAN --run-penalty 0.4 --max-iter 250 --n-post-replicates 200 --filter-pos 50 --filter-map 0 –{female/male}
```

where --states AFR NEA DEN correspond to potential *Sources*, --cont-id AFR is a potential contaminant and --ancestral PAN indicates that *panTro4* is used to infer a putative ancestral allele. The window size (--bin-size) is set to 5,000 base pairs (bp) for all individuals except Bacho Kiro *CC7-2289*, where a window size is increased to 100,000 bp due to the sparse coverage of informative sites for this individual (a total of 19,703 SNPs covered by at least one fragment, see Supplementary Information 2, Tab. S2.6). The African American genetic map[20] (build hg19) was used for re-scaling physical distances (in base pairs) into genetic distances (in centimorgans [cM]). For all downstream analyses we only consider archaic fragments longer than 0.2 cM in ancient modern humans, as these are can be confidently inferred with high accuracy using *admixfrog*[1].

With the additional data produced in this study we identify a total of 496.56 cM of Neandertal segments in *Oase1*, with ten segments longer than five cM and three of them longer than 50 cM (Fig. 3 and Extended Data Fig. 8A). Interestingly, we also identify large stretches of Neandertal ancestry across autosomes of IUP Bacho Kiro *F6-620, AA7-738, CC7-335, BB7-240* and *CC7-2289* (Fig. 3, Extended Data Fig. 8A, Fig. S8.1), *i.e.* all Initial Upper Palaeolithic specimens from Bacho Kiro Cave. In total, we detect 279.59 cM of Neandertal introgressed segments *in F6-620*, 251.63 cM in *CC7-335* and 220.86 cM in *BB7-240*, with seven, six and nine of those segments longer than five cM (Tab. S8.1). The longest introgressed segment of Neandertal ancestry in *F6-620* is located on chromosome 5 (chr5:5,207,757-53,693,820) and has a recombination length of 54.26 cM (48.49 Mb). The inferred Neandertal introgressed

segment boundaries in *F6-620* and *AA7-738* are nearly identical (Fig. 3, Extended Data Fig. 8A, Fig. S8.1A), which is not expected even for the first-degree relatives, thus further supporting our conclusion based on the pairwise mismatch rate (see Supplementary Information 4) that these two specimens originate from the same individual.

The longest Neandertal segments that we identify are 25.61 cM on chromosome 19 (chr19:41,743,126-53,982,102) in *CC7-335* and 17.42 cM on chromosome 20 (chr20:39,121,854-49,228,176) in *BB7-240*. We also detect three Neandertal segments longer than 6 cM in Bacho Kiro *CC7-2289* on chromosomes 12 (chr12:71,475,600-80,845,047 and chr12:89,691,728-97,676,702) and chromosome 9 (chr9:110,903,519-115,770,224), albeit with lower confidence in the boundaries of the introgressed segments due to the limited amount of data for this individual (Fig. S8.1B). As a comparison, using *admixfrog* we identify 143.42 cM of Neandertal segments in a ~45,000-year-old *Ust'Ishim* from Siberia, with the longest segments of 6.12 cM and 5.92 cM on chromosomes 13 (chr13: 22,719,662-24,676,454) and 21 (chr21:31,552,179-35,448,101), respectively (Extended Data Fig. 7).

Neandertal ancestry is distributed in smaller segments across the genome of the ~34,000-year-old Bacho Kiro *BK1653*, with the longest segment of 2.49 cM on chromosome 6 (chr6:37,721,776- 40,410,185), an average segment length of 0.49 cM, and a total of 121.74 cM of Neandertal ancestry (Fig. 3). These numbers are similar to other Upper Palaeolithic modern humans, such as the ~38,000-year-old *Kostenki14* from Russia with an average segment length of 0.59 cM and a total of 118.62 cM of Neandertal introgressed segments, and the ~35,000-year-old *Goyet Q116-1* from Belgium with an average segment length of 0.51 cM and a total of 134.18 cM of Neandertal introgressed segments. Fig. 3 and the Extended Data Fig. 7 show the physical distribution of the inferred Neandertal introgressed segments across all autosomes in IUP Bacho Kiro individuals, *Ust'Ishim*, *Oase1*, *Tianyuan*, *Kostenki 14*, *Goyet Q116-1* and Bacho Kiro *BK1653*.

Neandertal introgressed segments on the X chromosome

Since the "Archaic admixture" panel does not contain SNPs of the sex chromosomes, we investigated 55,248 SNPs on the X chromosome from the "2200k" Panel for inferring the distribution of Neandertal introgressed segments on the X chromosome in Bacho Kiro Cave individuals, *Oase1*, and other ancient modern humans for which we have both panels available. We created the input files for admixfrog directly from BAM files as detailed above, with the difference of using `--ref ref_A3700k.csv.xz`.

Interestingly, we identify two long segments of Neandertal ancestry on the X chromosome of *Oase 1,* with the recombination length of 4.00 cM (chrX:12,535,839-13,850,789) and 7.37 cM (chrX:30,969,935-32,771,678) (Extended Data Fig. 8A). We also detect one Neandertal segment of ~2 cM on each of the X chromosomes of *F6-620, CC7-335* and *BB7-240* (Extended Data Fig. 8A).

Dating of the Neandertal admixture

In order to estimate the timing of the most recent Neandertal introgression in the Bacho Kiro individuals, we applied three different methods to the Neandertal fragments identified with *admixfrog*[1]. For all methods we calculate the genetic length of the tracts using the African-American recombination map[20] and we compare the estimates with those obtained for *Oase1*[2].

First, we calculated the likelihood of the observed Neandertal tract lengths under the assumption of an exponential decay of fragment length due to recombination, with rate of decay *recombination rate* x *number of generations since introgression*. In order to isolate fragments of recent origin and specific to Bacho Kiro Cave individuals from those introgressed in modern humans and common to all out-of-Africa human populations, we considered only fragments longer than 10cM, for which the probability of having introgressed more recently than 50 generations prior is 96% assuming an exponential decay. Uncertainty, represented in Extended Data Fig. 8B as 96% confidence intervals, is estimated assuming an asymptotic gaussian approximation of the likelihood function. Our point estimates indicate that most Bacho Kiro Cave individuals had Neandertal ancestors ~7 generations before they lived. Only the *F6-620* shows a lower point estimate, 5 generations, however the confidence intervals overlap. The point estimate for *Oase1* is 4 generations, with uncertainty between 4 and 10 generations, comparably to what was estimated previously[2]. Note that three tracts identified previously in *Oase 1*[2] are estimated by *admixfrog* to be composed of different fragments, possibly explaining the slightly higher point estimate. Despite this, our estimates of timing of introgressions are comparable to those of Fu *et al.*[2].

We then modelled the lengths of the fragments as a mixture of two exponential distributions. Specifically, we co-estimated the number of generations since a more recent and an older introgression, as well as the proportion *p* of the fragments > 0.1cM originating from the more recent introgression event. For all genomes we performed a likelihood ratio test (degrees of freedom=2) comparing the likelihood of a simple exponential model with only one introgression event, and the model with two events. In Figure S8.2 we show the proportion of fragments originating from the different introgression events for different genetic lengths. We

find support for two introgression events for both *Oase 1* and several Bacho Kiro Cave specimens (S8.5). Estimates for models with one or two introgression events are reported in Tab. S8.1.

We then fitted the complementary cumulative distribution (CCD) of the lengths of Neandertal tracts , i.e. the proportion of tracts with length equal or higher than a given length X, as in Fu *et al.*[2]. Briefly, because of the exponential relationship between timing of introgression and length of the introgressed tracts, the logarithm of the cumulative distribution of tract length is expected to the depend linearly on the tract length, i.e. ln(CCD) ~ -(n – 1) x tract_length. We thus fitted the slope of this relationship separating introgressed tracts in older (≤ 5cM) and more recent (>5cM). The threshold of 5cM (96% of a tract to be introgressed <100 generations earlier), that is lower than 10cM used for the previous method, is used here to obtain enough data points to estimate accurately the slope. Fig. S8.3 shows both the slopes for older and more recent fragments, while the estimated values and uncertainties are shown in Tab. S8.2. For all genomes, except for the *F6-620* and *Oase 1*, the point estimates appear as slightly older, although the confidence intervals overlap. Therefore, consistent with our maximum likelihood estimates we infer that the *F6-620*, like *Oase 1*, had a Neandertal ancestor less than 6 generations before he lived.

Finally, we co-estimated the number of generations since introgression and the proportion of Neandertal admixture into the ancestors of the Bacho Kiro Cave individuals via simulations, using a similar approach used in Fu *et al.*[2]. Specifically, we computed full genome simulations of introgressing events contributing on average to 0.01-12.5% of the genome, and occurring 3 to 250 generations before the Bacho Kiro Cave individuals lived, in addition to an earlier introgression occurring 350 generations earlier (~10,000 years assuming a generation time of 29 years). For each of 10,000 simulations for each parameter combination, we calculated the mean of the longest 2, 5 or 10 Neandertal tracts, obtaining an expected distribution of average length of the longest Neandertal tracts. Then, for each sample, we compared the observed values with this distribution. In Fig. S8.5 we show combinations of parameters for which the observed means fall between the 5% and the 95% of the simulations (coloured squares). Combinations of parameters for which the observed values fall out of this expected distribution are marked in grey. Proportions of admixtures corresponding to the introgression of a single Neandertal ancestor are marked as black dots for each number of generations. We can see that while estimates are consistent with the other two methods assuming a single recent Neandertal ancestors (5-10 generations for all individuals), a higher proportion of Neandertal admixture – hence more recent Neandertal ancestors than a single one

– would better explain the average length of the longest fragments for a number of generations higher than ~8, for all Bacho-Kiro genomes (Fig.S8.5 and S8.6).

References SI8:

1 Peter, B. M. 100,000 years of gene flow between Neandertals and Denisovans in the Altai mountains. *bioRxiv* (2020).

2 Fu, Q. *et al.* An early modern human from Romania with a recent Neanderthal ancestor. *Nature* **524**, 216-219, doi:10.1038/nature14558 (2015).

3 Fu, Q. *et al.* The genetic history of Ice Age Europe. *Nature* **534**, 200-205, doi:10.1038/nature17993 (2016).

4 Yang, M. A. *et al.* 40,000-Year-Old Individual from Asia Provides Insight into Early Population Structure in Eurasia. *Curr. Biol.* **27**, 3202-3208.e9, doi: 10.1016/j.cub.2017.09.030 (2017).

5 Fu, Q. *et al.* Genome sequence of a 45,000-year-old modern human from western Siberia. *Nature* **514**, 445-449, doi:10.1038/nature13810 (2014).

6 Sikora, M. *et al.* Ancient genomes show social and reproductive behavior of early Upper Paleolithic foragers. *Science* **358**, 659-662, doi: 10.1126/science.aao1807 (2017).

7 Sikora, M. *et al.* The population history of northeastern Siberia since the Pleistocene. *Nature* **570**, 182-188, doi: 10.1038/s41586-019-1279-z (2019).

8 Raghavan, M. *et al.* Upper Palaeolithic Siberian genome reveals dual ancestry of Native Americans. *Nature* **505**, 87-91, doi:10.1038/nature12736 (2014).

9 Lazaridis, I. *et al.* Ancient human genomes suggest three ancestral populations for present-day Europeans. *Nature* **513**, 409-413, doi:10.1038/nature13673 (2014).

10 Olalde, I. *et al.* Derived immune and ancestral pigmentation alleles in a 7,000-year-old Mesolithic European. *Nature* **507**, 225-228, doi:10.1038/nature12960 (2014).

11 Gallego Llorente, M. *et al.* Ancient Ethiopian genome reveals extensive Eurasian admixture throughout the African continent. *Science* **350**, 820-822, doi:10.1126/science.aad2879 (2015).

12 Rasmussen, M. *et al.* The genome of a Late Pleistocene human from a Clovis burial site in western Montana. *Nature* **506**, 225-229, doi:10.1038/nature13025 (2014).

13 Mallick, S. *et al.* The Simons Genome Diversity Project: 300 genomes from 142 diverse populations. *Nature* **538**, 201-206, doi:10.1038/nature18964 (2016).

14 Prüfer, K. *et al.* The complete genome sequence of a Neanderthal from the Altai Mountains. *Nature* **505**, 43-49, doi:10.1038/nature12886 (2014).

15 Prüfer, K. *et al.* A high-coverage Neandertal genome from Vindija Cave in Croatia. *Science* **358**, 655-658, doi: 10.1126/science.aao1887 (2017).
16 Mafessoni, F. *et al.* A high-coverage Neandertal genome from Chagyrskaya Cave. *Proc. Natl. Acad. Sci. U.S.A.* **117**, 15132-15136, doi:10.1073/pnas.2004944117 (2020).
17 Meyer, M. *et al.* A high-coverage genome sequence from an archaic Denisovan individual. *Science* **338**, 222-226, doi:10.1126/science.1224344 (2012).
18 Li, H. *et al.* The Sequence Alignment/Map format and SAMtools. *Bioinformatics* **25**, 2078-2079, doi:10.1093/bioinformatics/btp352 (2009).
19 Quinlan, A. R. & Hall, I. M. BEDTools: a flexible suite of utilities for comparing genomic features. *Bioinformatics* **26**, 841-842 (2010).
20 Hinch, A. G. *et al.* The landscape of recombination in African Americans. *Nature* **476**, 170-175, doi: 10.1038/nature10336 (2011).

Table S8.1 Estimates of the number of generations before the ancient (*n.anc*) and more recent (*n.rec*) Neandertal introgression in Bacho Kiro Cave individuals and other ancient modern humans, and the proportion of Neandertal fragments originating from the most recent introgression event (*p*). p-values obtained with a likelihood ratio tests comparing an exponential model with only one introgression occurred *n.gen1* generations before the birth of the individual and that with two events are reported as *LR*, and as LR Bonferroni after a multiple testing Bonferroni correction for the number of tested specimens (n=22). Specimens for which a model with two admixture events is supported (LR Bonferroni<0.05) are highlited in gray and an asterisk. Two-tailed 95% asymptotic confidence intervals (+/-CI) are calculated from the Hessian of the likelihood profile. Confidence intervals for the more recent introgression event are not calculated when this is not supported (n.a.).

Specimen	n.rec	-CI	+CI	n.anc	-CI	+CI	p	-CI	+CI	n.gen 1	LR	LR Bonferroni
BK AA7_738	5.1	0.7	9.5	47.5	38.8	56.2	0.04	0.00	0.09	34.63	9.83E-09*	2.16E-07*
BK BB7_240	13.0	5.0	21.1	76.5	66.9	86.2	0.05	0.01	0.08	62.73	5.20E-07*	1.14E-05*
BK 1653	9.9	n.a.	n.a.	201.4	185.9	216.8	0.00	0.00	0.07	201.36	1	1
BK CC7_2289	12.0	5.6	18.5	393.6	286.2	500.9	0.17	0.09	0.26	60.44	0*	0*
BK CC7_335	11.5	6.9	16.1	91.3	79.0	103.6	0.10	0.06	0.15	53.58	0*	0*
BK F6-620	6.3	2.3	10.4	82.0	72.5	91.5	0.04	0.01	0.06	57.49	0*	0*
GoyetQ116-1	6.5	n.a.	n.a.	235.7	207.3	264.1	0.00	0.00	0.12	235.67	1	1
Kostenki 14	7.1	n.a.	n.a.	197.4	172.7	222.1	0.00	0.00	0.02	197.43	1	1
LBK	5.1	n.a.	n.a.	428.8	367.8	489.8	0.00	0.00	0.12	428.79	1	1
Loschbour	5.2	n.a.	n.a.	385.7	337.9	433.5	0.00	0.00	0.06	385.68	1	1
Malta 1	5.2	n.a.	n.a.	347.0	301.1	392.8	0.00	0.00	0.14	346.96	1	1
Oase1	4.0	1.4	6.7	82.8	69.8	95.7	0.06	0.02	0.09	39.78	0*	0*
Sunghir III	6.3	n.a.	n.a.	248.0	218.7	277.2	0.00	0.00	0.12	247.99	1	1
Sunghir II	6.0	n.a.	n.a.	248.9	218.0	279.7	0.00	0.00	0.13	248.86	1	1
Sunghir I	5.8	n.a.	n.a.	247.0	211.8	282.1	0.00	0.00	0.12	246.96	1	1
Sunghir IV	6.3	n.a.	n.a.	242.0	213.3	270.7	0.00	0.00	0.09	241.98	1	1
Tianyuan	6.3	n.a.	n.a.	215.2	186.2	244.2	0.00	0.00	0.14	215.19	1	1
Ust'Ishim	10.0	n.a.	n.a.	104.3	87.7	120.9	0.00	0.00	0.04	104.29	1	1

Vestonice 16	5.4	n.a.	n.a.	301.1	264.1	338.1	0.00	0.00	0.13	301.08	1	1
Yana_old	5.9	n.a.	n.a.	261.0	229.9	292.1	0.00	0.00	0.09	260.99	1	1
Yana_old2	43.5	0.0	90.2	255.4	223.5	287.4	0.02	0.00	0.04	236.74	8.31E-03*	1.83E-01

1936

Figure S8.1 Neandertal introgressed segments in the genomes of Bacho Kiro *AA7-738* and Bacho Kiro *CC7-2289* as inferred by admixfrog. Neandertal segments are highlighted in blue and Denisovan segments are highlighted in orange. The height of the segment on each autosome is denoted on the y-axis and corresponds to the probability of the inferred segment.

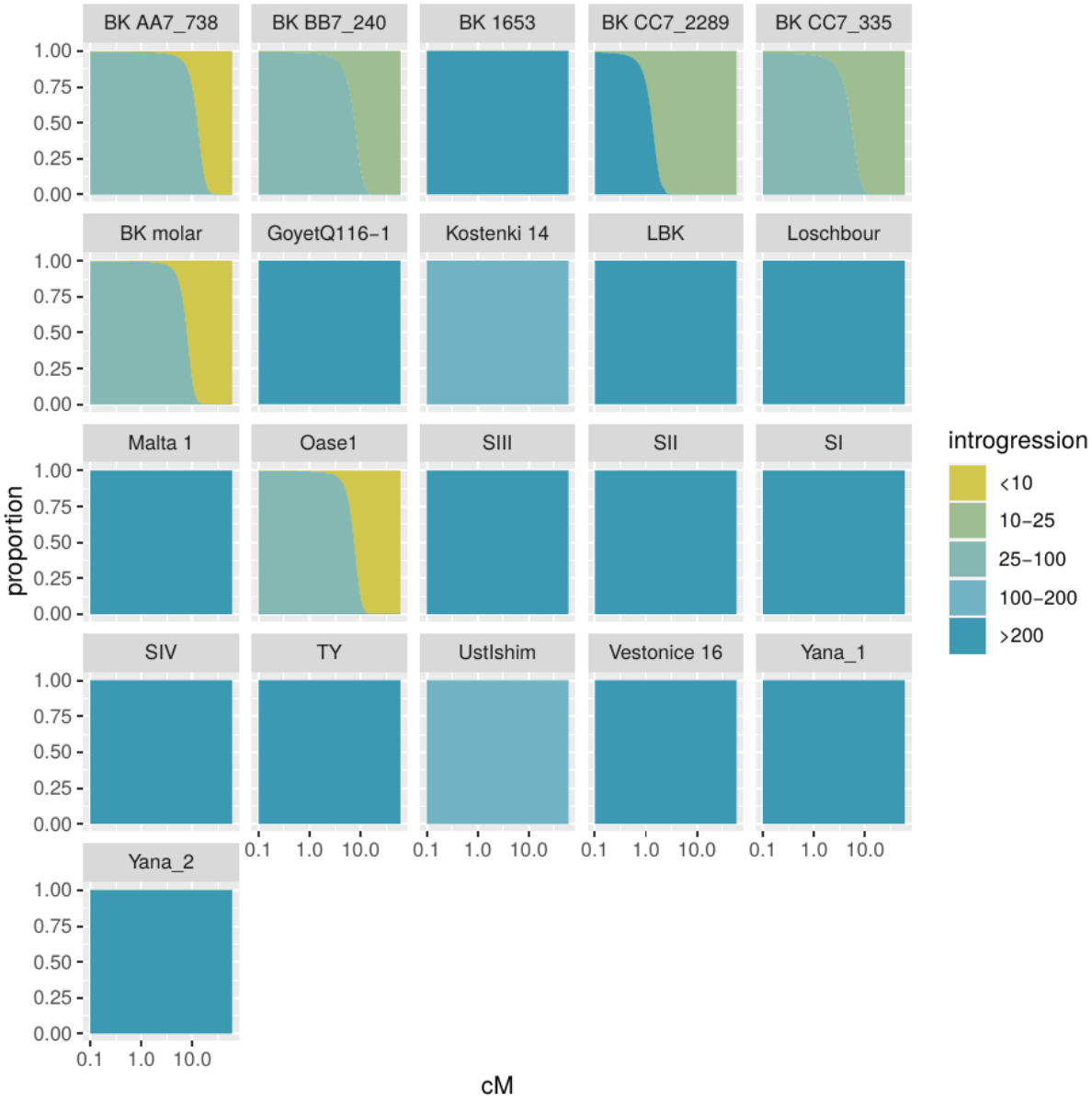

1942 **Figure S8.2 Proportion of fragments (y-axis) originating from different introgression**
1943 **events (number of generation indicated by the colors in the legend).** Models with two
1944 different introgression events were plotted if supported by a likelihood ratio test <0.001 over
1945 models with only one introgression event (Table S8.1).

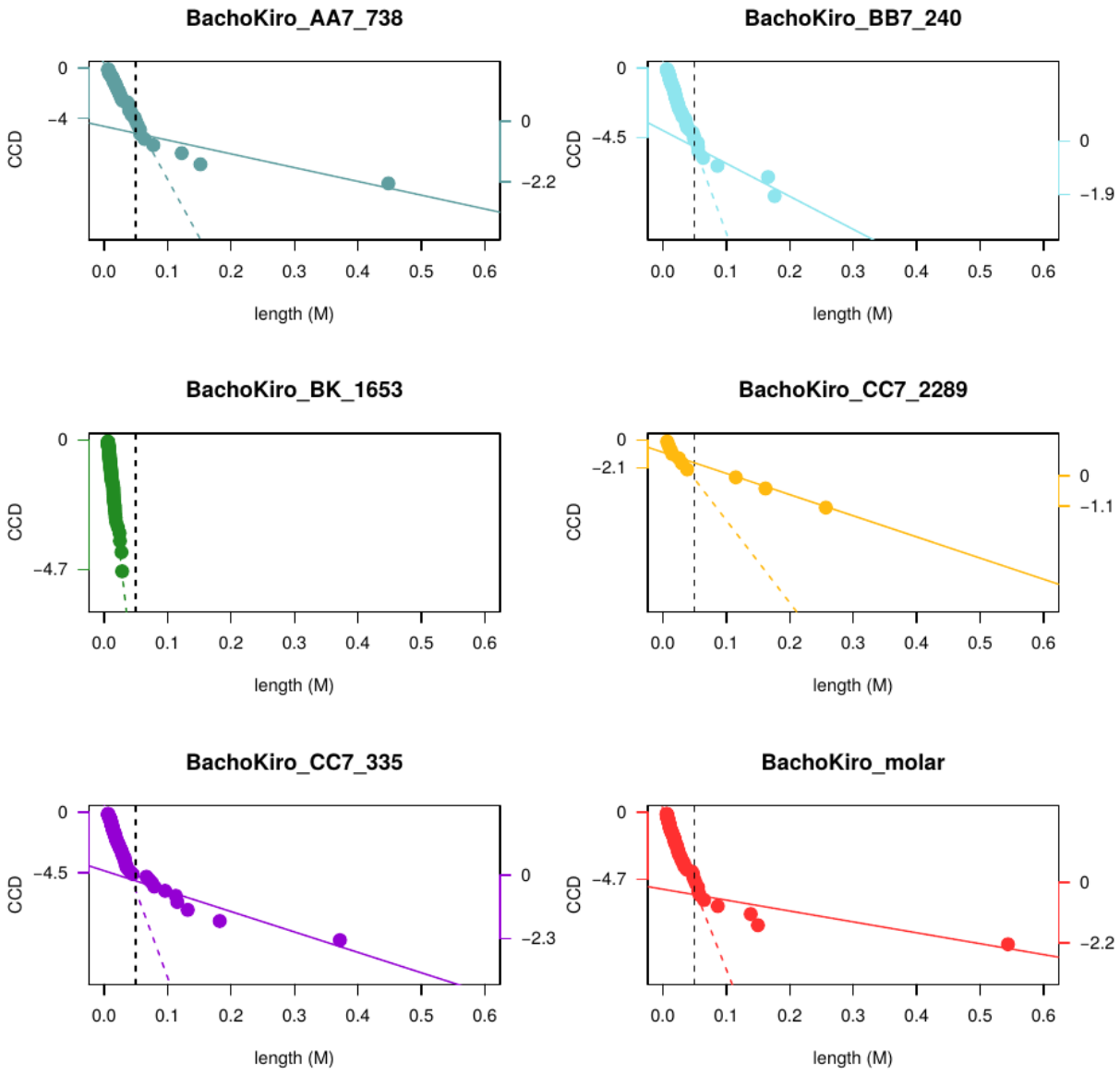

Figure S8.3 Graphical representation of the relationship between CCD of tracts and tract lengths. Slopes corresponding to the estimates of the number of generations before the most recent Neandertal introgression in Bacho Kiro (tracts >5cM) and older introgression events, here modelled as a single pulse (tracts ≤ 5cM), are shown as continuous and dashed colored lines, respectively. In order to visualize both slopes in the same plot, the CCD of all fragments with length >0.5cM is used as y-axis. The corresponding CCD for tracts lower and higher than 5cM are shown as coloured axes on the left and right of the plots, respectively. The 5cM threshold is indicated by a vertical dashed line. The x-axis represent the genetic length of the tracts in Morgans.

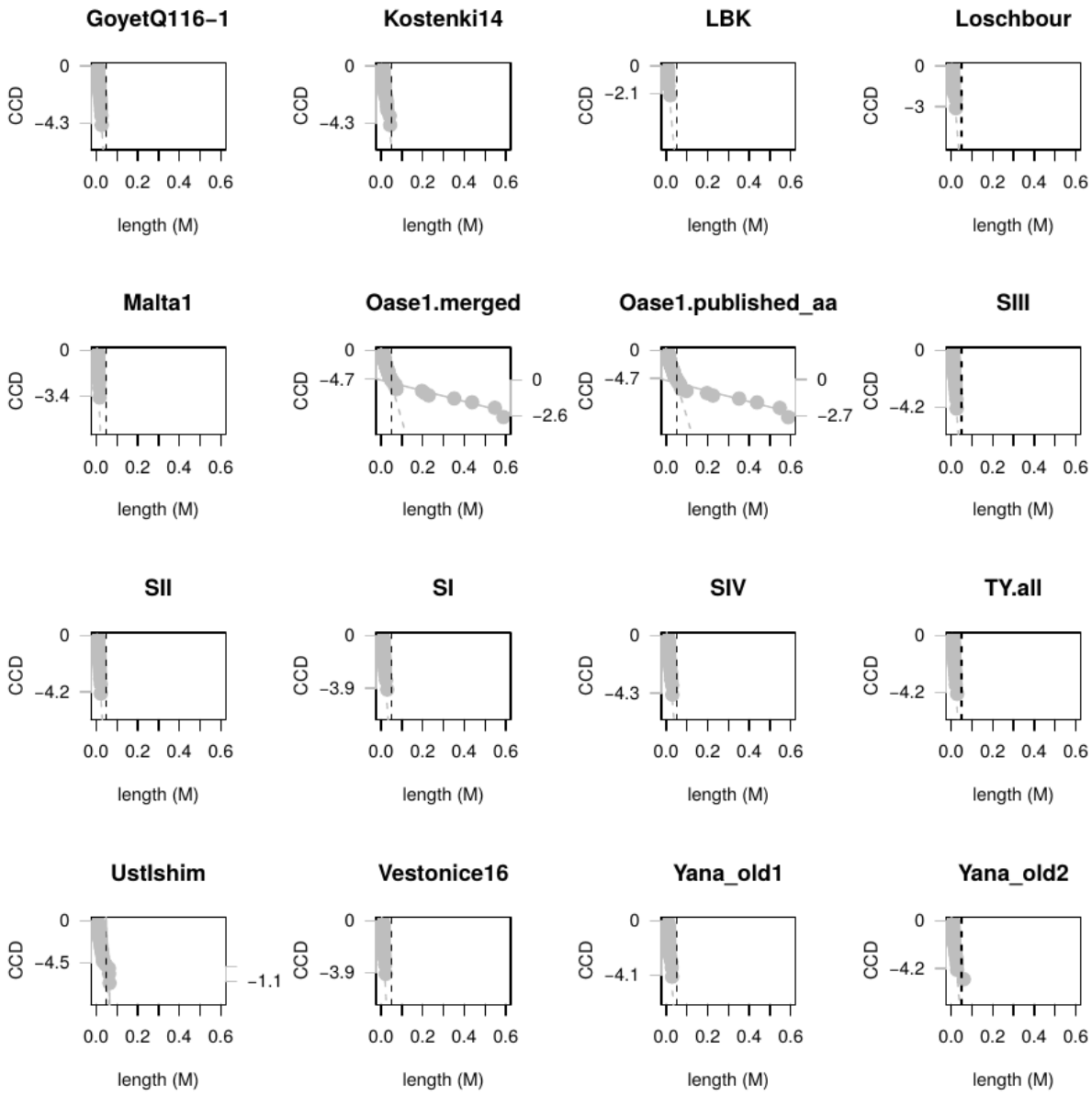

Figure S8.4 Graphical representation of the relationship between CCD of tracts and tract lengths in other ancient modern humans.

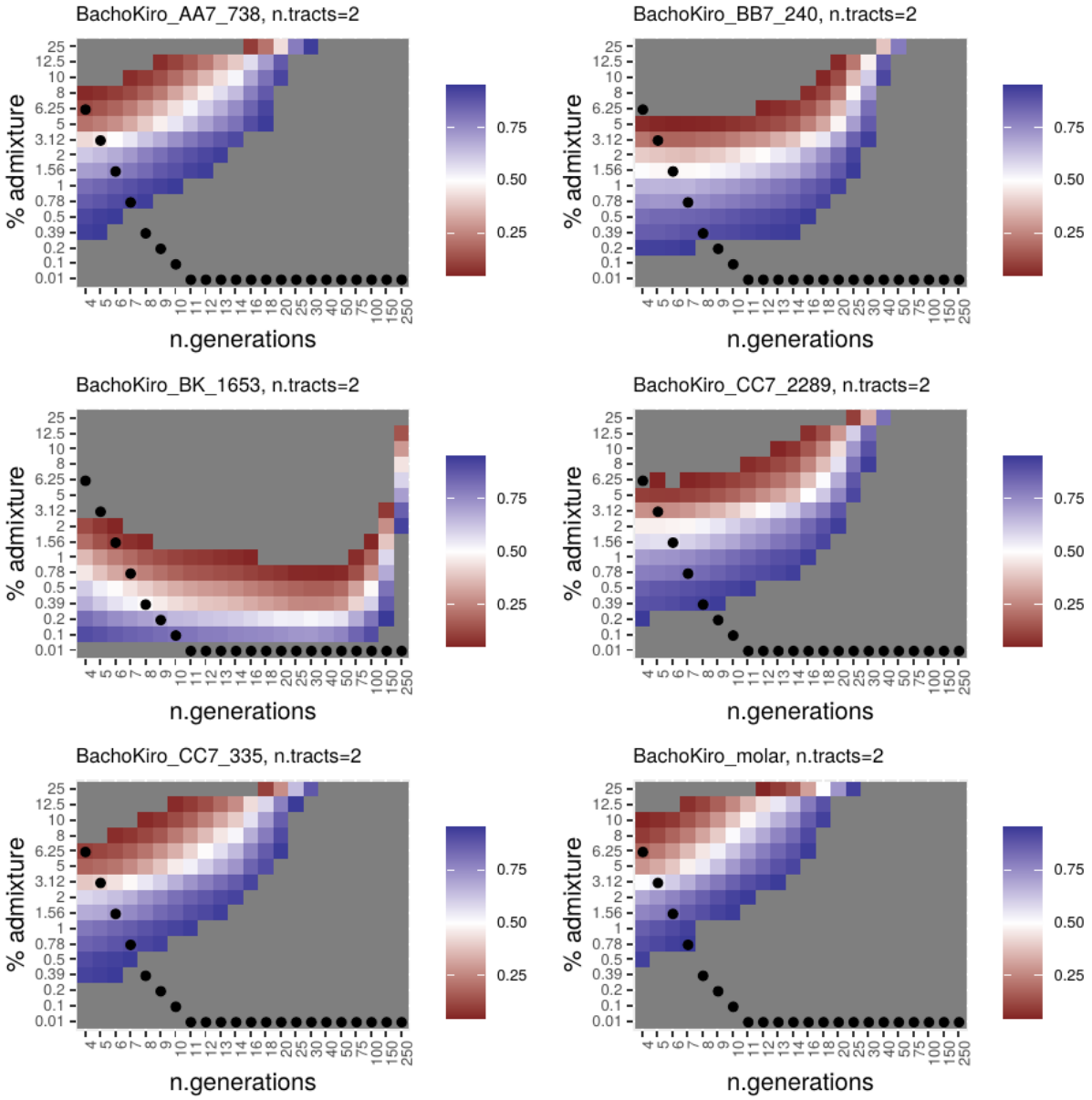

1959 **Figure S8.5 Proportions of the simulations (q) where the two longest Neandertal tracts**
1960 **are shorter than for the observed tracts.** White indicates the best fitting combinations of
1961 parameters, i.e. combinations of parameters for which the observed data fall at the 50%
1962 percentile of the simulations. Combinations of parameters for which the observed data fall out
1963 of the 5 and 95 percentiles are shown in grey. Proportions of admixtures corresponding to the
1964 introgression of a single Neandertal ancestor are marked as black dots for each number of
1965 generations.

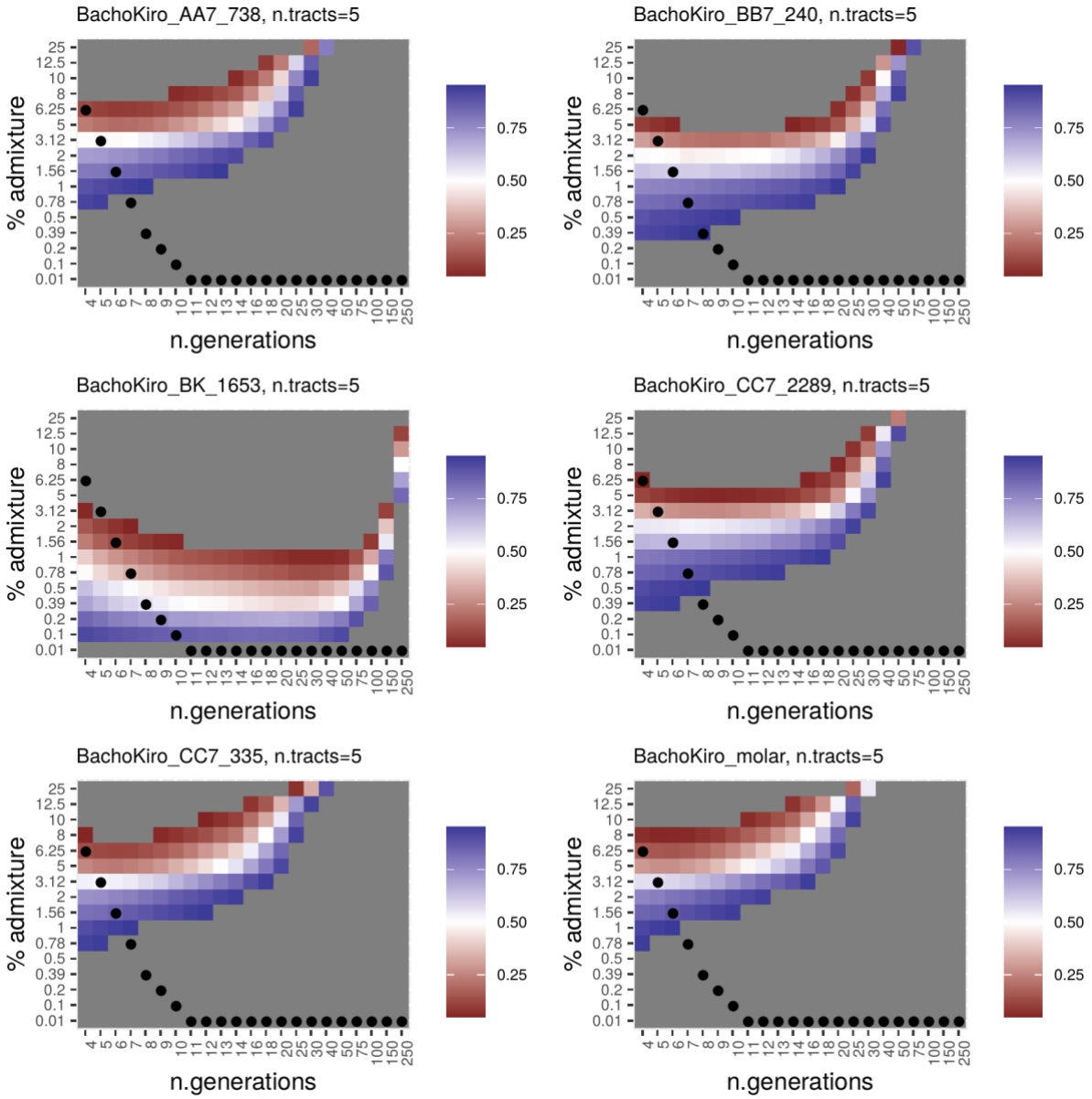

Figure S8.6 Proportions of the simulations (q) where the five longest Neandertal tracts are shorter than for the observed tracts. Figure description follows as Fig.S8.5.

Supplementary information 9

Sharing of Neandertal introgressed segments between Bacho Kiro and present-day individuals

We wanted to investigate if the Neandertal fragments we detect in Bacho Kiro individuals are shared with other ancient and present-day individuals. For ancient individuals (n=32) we consider segments longer than 0.2 cM and for modern day non-African individuals (n=229)[1] we consider segments longer than 0.05 cM[2] (see Supplementary Information 8). Furthermore, we group present-day individuals[1] by population (n=109) to increase the number of segments for comparisons. To evaluate the sharing we calculate how well the genomic positions of Neandertal segments correlate between Bacho Kiro Cave individuals vs ancient and present-day individuals, using the Pearson correlation coefficient, which we calculate in the following way:

p(X,Y) = (observed_overlap – expected_overlap)/(standard deviation of X * standard deviation of Y)

observed = overlapping sequence / callable genome length

expected_overlap = (sequence in X) / callable genome length * (sequence in Y) / callable genome length

standard deviation of X (or Y) = sqrt(overlapping sequence / callable genome length - (overlapping sequence / callable genome length)^2)

If there is a perfect overlap, the correlation coefficient will be equal to 1 and if there is no correlation the coefficient will be equal to 0. This allows us to ask the question: “do Neandertal segments in Bacho Kiro individuals overlap more with other present-day and ancient individuals then expected by chance?”. If they do, this suggests that the fragments are shared because of shared ancestry. In addition, we can evaluate the strength of the correlation to different populations. Introgressed Neandertal segments will be subject to drift the same way that allele frequencies are. Thus, populations that share more Neandertal segments share more drift.

In order to investigate if the fragment sets between Bacho Kiro individuals and other genomes overlap more than by chance we performed 500 bootstrap iterations where we randomly place the same number of archaic fragments of the same saize as in the analyzed genomes in the genomes of the Bacho Kiro individuals. If fragments overlap more than this, we conclude that the two genomes share ancestry. Furthermore, the magnitude of the correlation

coefficient will show if archaic segments in Bacho Kiro individuals are shared more with some present-day human populations than others.

Note that the amount of Neandertal segments in the genome is positively correlated with local recombination rate (Spearmans rank correlation coefficient = 0.15, pval < 4.46e-54)[3,4]. However, because recombination maps between different populations differ[5] and have changed over 35-45,000 years, we used homogeneous recombination rates for the tests.

Table S8.1 shows the mean correlation coefficient for each Bacho Kiro individual vs each "Super population", *i.e*. America, CentralAsia/Siberia, EastAsia, Oceania, SouthAsia, WestEurasia. The segments in the later Bacho Kiro Cave individual *BK1653* correlate more with Neandertal segments in West Eurasia than the Neandertal segments in IUP Bacho Kiro Cave individuals do. In contrast, the Neandertal segments in the IUP Bacho Kiro Cave individuals correlate more with Neandertal segments in present-day East Asian individuals (Fig. S9.1). The correlation coefficients when comparing Bacho Kiro individuals (segments shorter than 5 cM) with each individual SGDP population and 32 ancient individuals are shown in Fig. S9.2.

Segments longer than 5 cM found in IUP Bacho Kiro Cave individuals show very low correlation with present-day individuals (see Fig. S9.3). In fact, in all Bacho Kiro Cave individuals, except *CC7-2289* where we have little data, the genomic position of segments shorter than 5cM correlates significantly more with segments in present-day populations than segments which are longer than 5 cM (see Fig. S9.4).

References SI9:

1 Mallick, S. *et al.* The Simons Genome Diversity Project: 300 genomes from 142 diverse populations. *Nature* **538**, 201-206, doi:10.1038/nature18964 (2016).

2 Peter, B. M. 100,000 years of gene flow between Neandertals and Denisovans in the Altai mountains. *bioRxiv* (2020).

3 Skov, L. *et al.* The nature of Neanderthal introgression revealed by 27,566 Icelandic genomes. Nature 582, 78-83, doi: 0.1038/s41586-020-2225-9 (2020).

4 Schumer, M. *et al.* Natural selection interacts with recombination to shape the evolution of hybrid genomes. *Science* **360**, 656-660, doi: 10.1126/science.aar3684 (2018).

5 Kong, A. *et al.* Fine-scale recombination rate differences between sexes, populations and individuals. *Nature* **467**, 1099-1103, doi: 10.1038/nature09525 (2010).

Table S9.1 Correlation coefficient of overlapping segments between Bacho Kiro Cave individuals and present-day super populations groups from SGDP[1]. The mean correlation coefficient for each super population are reported along with the 95% confidence intervals in brackets. Here we use tracts ≤ 5cM, thus representative of older introgression events. Bacho Kiro *CC7-2289* is highlighted in grey due to low amounts of data.

Individual	America	CentralAsiaSiberia	EastAsia	Oceania	SouthAsia	WestEurasia
BachoKiro_AA7_738	0.08 (0.07-0.09)	0.08 (0.07-0.09)	0.09 (0.08-0.1)	0.08 (0.05-0.11)	0.06 (0.05-0.07)	0.04 (0.04-0.04)
BachoKiro_BB7_240	0.09 (0.08-0.1)	0.08 (0.07-0.09)	0.1 (0.09-0.11)	0.08 (0.06-0.1)	0.07 (0.06-0.08)	0.04 (0.04-0.04)
BachoKiro_BK_1653	0.08 (0.08-0.08)	0.08 (0.07-0.09)	0.07 (0.06-0.08)	0.06 (0.04-0.08)	0.08 (0.07-0.09)	0.11 (0.1-0.12)
BachoKiro_CC7_2289	0 (-0.01-0.01)	0.01 (0.01-0.01)	0.03 (0.02-0.04)	0.02 (0.01-0.03)	0.03 (0.02-0.04)	0.02 (0.02-0.02)
BachoKiro_CC7_335	0.09 (0.08-0.1)	0.09 (0.08-0.1)	0.12 (0.11-0.13)	0.1 (0.08-0.12)	0.08 (0.07-0.09)	0.04 (0.04-0.04)
BachoKiro_F6_620	0.1 (0.09-0.11)	0.09 (0.08-0.1)	0.1 (0.09-0.11)	0.09 (0.06-0.12)	0.06 (0.05-0.07)	0.05 (0.05-0.05)

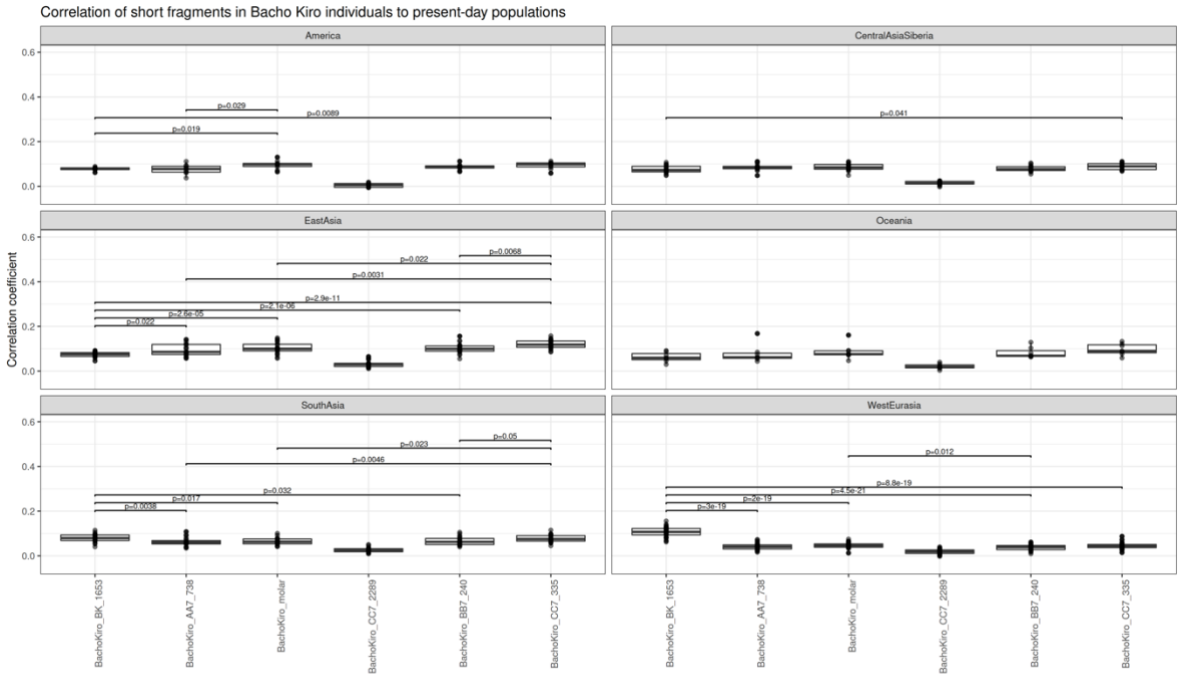

Figure S9.1 Correlation coefficient of overlapping segments between Bacho Kiro Cave individuals and present-day super populations. The mean correlation coefficient for each super population is reported for each Bacho Kiro Cave individual (black horizontal bar). Each point is a population from the super population (n=10 for America, n=15 for CentralAsiaSiberia, n=22 for EastAsia, n=7 for Oceania, n = 19 for SouthAsia, n = 36 for WestEurasia). The top and bottom part of the box indicates the 75% and 25% quantile respectively. We use tracts ≤ 5cM. The pvalues for each Wilcoxon signed-rank two-sided test are reported if significant (<0.05). We do not use the individual Bacho Kiro *CC7-2289* due to the low amounts of data.

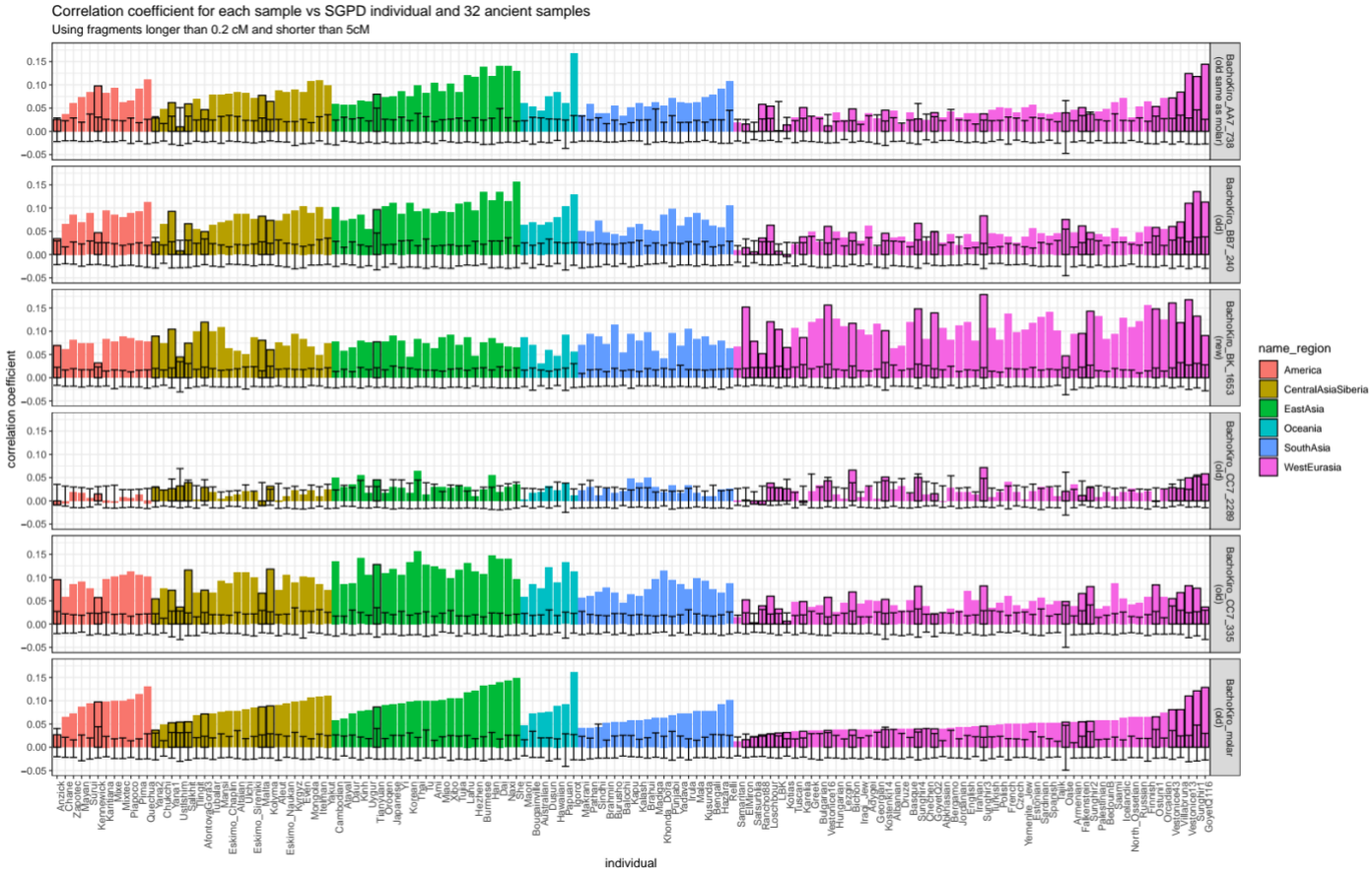

Figure S9.2 Correlation coefficient of overlapping segments between Bacho Kiro Cave individuals and present-day population and ancient individuals. The mean correlation coefficient between tracts ≤ 5cM in BachoKiro individuals, thus representative of older introgression events (n=138 for BachoKiro_BB7_240, n=66 for BachoKiro_AA7_738, n=153 for BachoKiro_molar, n=137 for BachoKiro_CC7_335, n=11 for BachoKiro_CC7_2289, n=257 for BachoKiro_BK_1653) and all tracts in present day populations and ancient individuals (mean n=1038, min n = 385, max n = 7535) is shown as a bar. The color of the bar indicates the super population. The black error bars show the 95% confidence intervals when we randomly place fragments in the genome (500 iterations) with the middle of the error bar being the mean correlation coefficient. Ancient individuals are highlighted with a black outline.

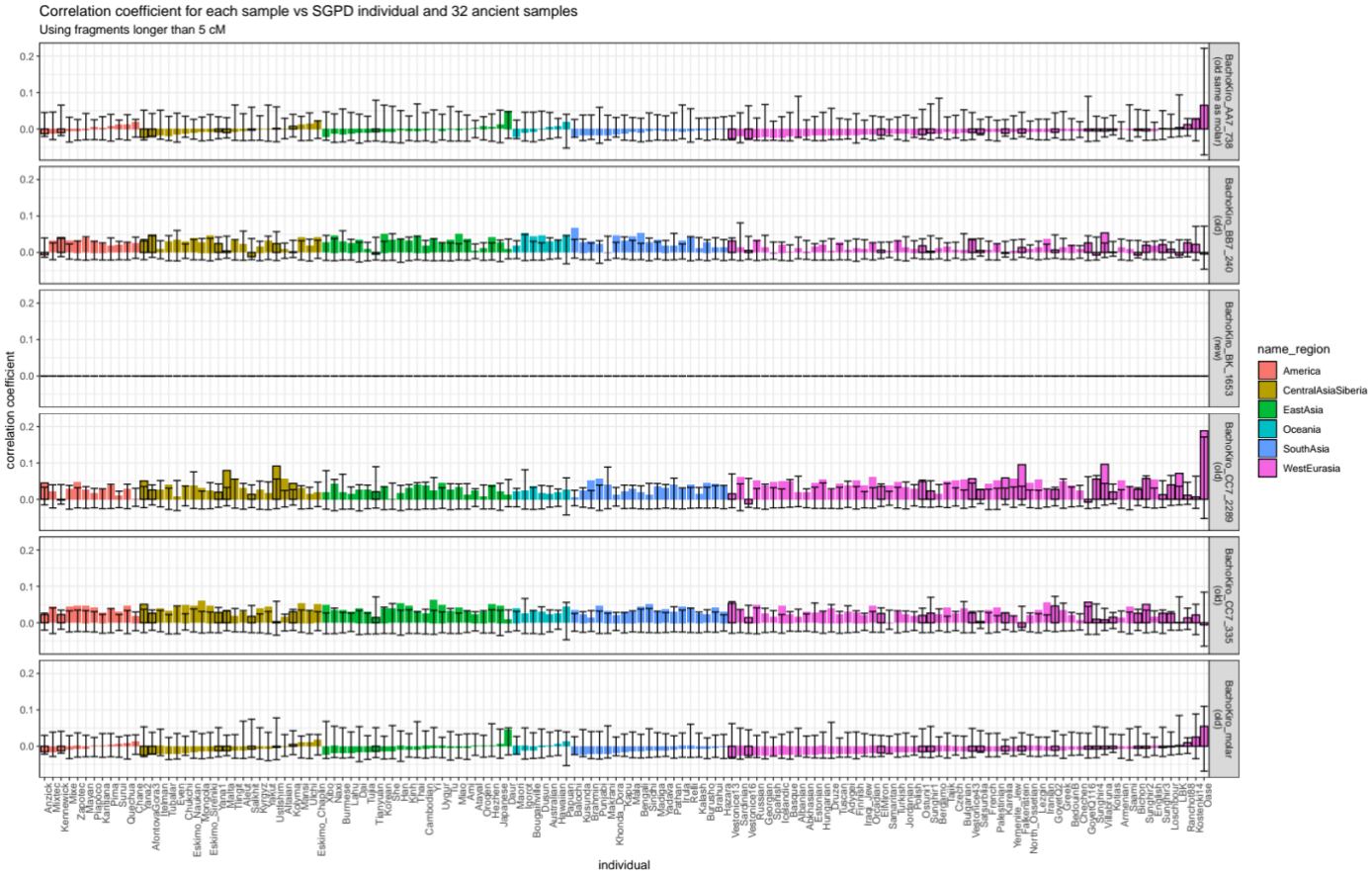

Figure S9.3 Correlation coefficient of overlapping segments between Bacho Kiro Cave individuals and present-day population and ancient individuals. The mean correlation coefficient between tracts ≥ 5cM in BachoKiro individuals, thus representative of more recent introgression events (n=8 for BachoKiro_BB7_240, n=7 for BachoKiro_AA7_738, n=9 for BachoKiro_molar, n=10 for BachoKiro_CC7_335, n=3 for BachoKiro_CC7_2289, n=0 for BachoKiro_BK_1653) and all tracts in present day populations and ancient individuals (mean n=1038, min n = 385, max n = 7535) is shown as a bar. The color of the bar indicates the super population. The black error bars show the 95% confidence intervals when we randomly place fragments in the genome (500 iterations) with the middle of the error bar being the mean correlation coefficient. Ancient individuals are highlighted with a black outline.

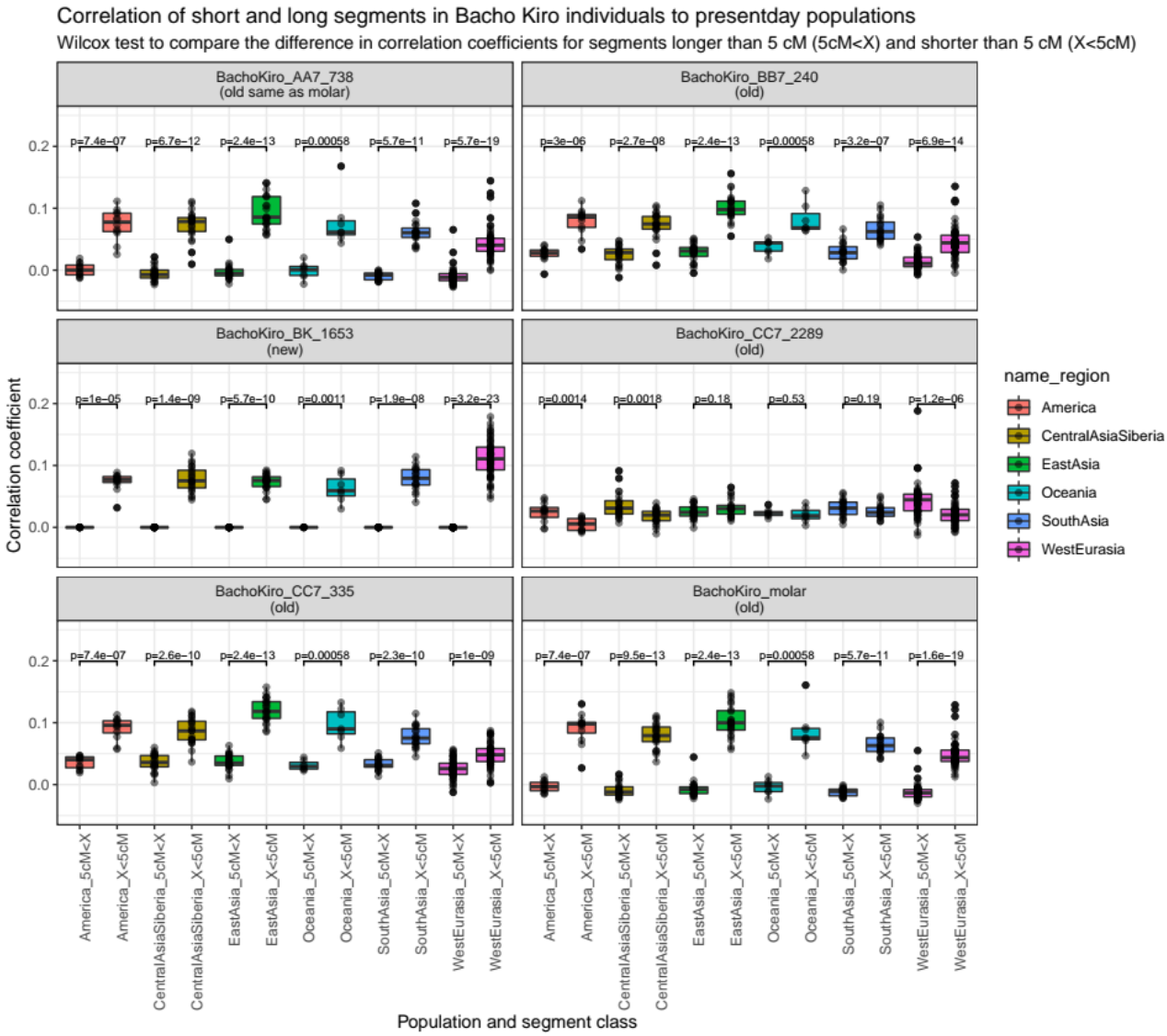

Figure S9.4 Correlation coefficient of overlapping segments between Bacho Kiro Cave individuals and present-day population for segments longer and shorter than 5cM. For each super population we compare the correlation coefficient of segments from Bacho Kiro individuals longer than 5cM vs the correlation coefficient of segments from Bacho Kiro individuals shorter than 5cM (n=10 for America, n=15 for CentralAsiaSiberia, n=22 for EastAsia, n=7 for Oceania, n = 19 for SouthAsia, n = 36 for WestEurasia). The top and bottom part of the box plot indicates the 75% and 25% quantile respectively. The pvalues for each Wilcoxon signed-rank two-sided test are reported if significant (<0.05).

Supplementary Information 10

Neandertal deserts

Previous studies of Neandertal introgression concluded that Neandertal introgressed fragments are heterogeneously distributed throughout the genome in modern day non-African populations[1,2]. Strikingly, this heterogeneity includes large regions that are nearly devoid of any Neandertal introgressed DNA. These so-called "Neandertal deserts" have been speculated to be regions where Neandertal DNA was removed by selection after introgression occurred, and thus may represent regions with important functional differences or even incompatibilities between Neandertals and modern humans. A subsequent analysis of 35 Melanesian individuals found that several of these deserts are also significantly depleted of Denisovan introgression, suggesting archaic DNA has been removed from the human genome in at least two events[3,4].

However, these analyses were performed on contemporary populations, making it difficult to resolve the timing of the formation of these Neandertal deserts; an important characteristic for considering models of selection. Genome-wide data from early modern humans may help to resolve this timing - e.g., we can ask the question "were these deserts present within 10,000 years following introgression?" In addition, the existence of very recent introgression events into such early modern humans may allow us to investigate the dynamics of desert formation on very short time scales, as little as a few generations. We therefore examined the overlap of Neandertal introgressed fragments in the three IUP Bacho Kiro Cave individuals, plus *Oase1*, with six previously identified Neandertal deserts[3]. Strikingly, these individuals carry almost no Neandertal DNA in the deserts (249 Kb out of 898 Mb of introgressed sequence). To determine if this lack of overlap could have occurred by chance, we calculated an empirical p-value by shifting the location of the deserts along the genome, eventually covering the entire genome. In 1 out of 251 such permutations, the overlap of Neandertal fragments and deserts was greater than the observed overlap, leading to an adjusted empirical p-value of 0.0079. Assuming an introgression date of 55,000 years ago[5,6] we can determine that the Neandertal deserts had already been established by approximately 10,000 years after introgression.

To examine desert formation in the more recent introgression event, we performed the same analysis on all introgressed fragments larger than 5cM. We use this threshold as described in Supplementary Information 8, since fragments longer than 5cM are unlikely to originate in the older introgression event. To maximize power, we also included fragments from the *Oase1*

individual, which experienced a similar recent introgression event. Strikingly, none of these large fragments overlap with previously identified deserts. However, when performing our permutation test, a substantial proportion of permutations (36 out of 251) also yielded no overlap, giving an adjusted empirical p-value of 0.147. Therefore, although we have no evidence of Neandertal DNA in the deserts as recently as 6-10 generations post-admixture, we also cannot reject that this occurs by chance. It is likely that the discovery of even a few additional individuals with recent introgression will allow the resolution of this question.

References SI10:

1 Vernot, B. & Akey, J. M. Resurrecting surviving Neandertal lineages from modern human genomes. *Science* **343**, 1017-1021, doi:10.1126/science.1245938 (2014).

2 Sankararaman, S. *et al.* The genomic landscape of Neanderthal ancestry in present-day humans. *Nature* **507**, 354-357, doi: 10.1038/nature12961 (2014).

3 Vernot, B. *et al.* Excavating Neandertal and Denisovan DNA from the genomes of Melanesian individuals. *Science* **352**, 235-239, doi:10.1126/science.aad9416 (2016).

4 Sankararaman, S., Mallick, S., Patterson, N. & Reich, D. The Combined Landscape of Denisovan and Neanderthal Ancestry in Present-Day Humans. *Curr. Biol.* **26**, 1241-1247, doi:10.1016/j.cub.2016.03.037 (2016).

5 Sankararaman, S., Patterson, N., Li, H., Paabo, S. & Reich, D. The date of interbreeding between Neandertals and modern humans. *PLoS Genet* **8**, e1002947, doi:10.1371/journal.pgen.1002947 (2012).

6 Fu, Q. *et al.* Genome sequence of a 45,000-year-old modern human from western Siberia. *Nature* **514**, 445-449, doi:10.1038/nature13810 (2014).